DTU Library

Efficient Operation of Energy Grids

Banis, Frederik

Publication date:
2020

Document Version
Publisher's PDF, also known as Version of record

EFFICIENT OPERATION OF ENERGY GRIDS

FREDERIK BANIS

PhD Thesis

Department of Applied Mathematics and Computer Science
DTU Compute
Technical University of Denmark (DTU)

April 2020

Technical University of Denmark (DTU)
Department of Applied Mathematics and Computer Science
(DTU Compute)

EFFICIENT OPERATION OF ENERGY GRIDS

FREDERIK BANIS

Supervisors:

Niels Kjølstad Poulsen
Daniela Guericke
Henrik Madsen

Frederik Banis: *Efficient Operation of Energy Grids,* PHD Thesis

SUPERVISORS:
Niels Kjølstad Poulsen
Daniela Guericke
Henrik Madsen

LOCATION:
DTU Compute
Richard Petersens Plads
Building 324
DK-2800 Kgs. Lyngby

TIME FRAME: December 2016– April 2020 (with 4 months leave)
ORCID: 0000-0003-1807-7009
ISSN: 0909-3192

Our Leaders of today need the philosophy of the past, paired with the scientific knowledge and technology of tomorrow.

— Anders Indset

SUMMARY (ENGLISH)

This thesis deals with the investigation and application of optimization routines for the efficient operation of energy grids.

The uncoordinated penetration of fluctuating generation units and consumers in the power system leads to increased variability and uncertainty. This poses challenges for stable grid operation. Introduction and lifting of flexibility potentials may alleviate these issues. For example, grid operation can be stabilized by investments in infrastructure, such as energy storage systems. While this can be a solution, this is also associated with substantial economical costs.

Other flexibility potentials are available. It has been shown that fluctuating distributed energy resources do not have to be part of the problem, but can be part of the solution. The concept of microgrids facilitates the integration of such flexibility concepts.

The power system is a complex and expensive infrastructure. The return of investment may, therefore, be higher when considering improvements into system controls that address existing infrastructure in a more efficient manner, rather than to invest into additional power system infrastructure.

In order to leverage the flexibility potentials of distributed energy resources, automatic generation control in microgrids can be addressed by model predictive control (MPC) principles. Proactive action of the microgrid can then lead to optimized frequency stability. Automatic generation control is, therefore, a first topic addressed by this thesis and tested within a case study.

Furthermore, flexibility potentials can be addressed through price–based control. Hereby, the flexible electricity consumers and prosumers are rewarded by an economical incentive to achieve the desired response. The integration of price–based controls is, therefore, another topic addressed by this thesis.

RESUMÉ (DANISH)

Denne afhandling omhandler undersøgelser og anvendelser af optimeringsrutiner for effektiv drift af elnet.

Den ukoordinerede penetration af svingende produktionsenheder og forbrugere i kraftsystemet fører til øget variation og usikkerhed. Dette medfører udfordringer med hensyn til stabil drift af nettet. Introduktion og udnyttelse af fleksibilitetspotentialer kan afhjælpe disse problemer. For eksempel kan netdrift stabiliseres ved investeringer i infrastruktur, såsom energilagringssystemer. Selvom dette kan være en løsning, er dette også forbundet med betydelige økonomiske omkostninger.

Den ukoordinerede penetration af varierende elproduktion og -forbrug fra forskelige produktionsenheder og forbrugere i elsystemet fører til en øget variation og usikkerhed. Dette medfører udfordringer med hensyn til stabil drift af nettet. Introduktion og udnyttelse af fleksibilitetspotentialer kan afhjælpe disse problemer. For eksempel kan netdrift stabiliseres ved investeringer i infrastruktur, såsom energilagringssystemer. Selvom dette kan være en løsning, er dette også forbundet med betydelige økonomiske omkostninger.

Andre fleksibilitetspotentialer er tilgængelige. Det har vist sig at varierende distribuerede energiressourcer ikke behøver at være en del af problemet, men kan være en del af løsningen. Mikro-grid konceptet letter integrationen af sådanne fleksibilitetskoncepter.

Elnettet er en kompleks og dyr infrastruktur. Afkastet af investeringer kan derfor være højere, når man overvejer forbedringer af systemkontroller, der adresserer optimal drift af eksisterende infrastruktur på en mere effektiv måde, snarere end at investere i yderligere infrastruktur.

For at udnytte fleksiblitetspotentialerne af distribuerede energiressourcer, automatisk genereringskontrol i mikro-grids kan adresseres med model prædiktive kontrolprincipper (MPC). Proaktiv styring af mikro-grids kan derved føre til optimeret frekvensstabilitet. Automatisk generationskontrol er derfor det første emne, der behandles i denne afhandling og testet ved et case-studie.

Yderligere kan fleksibilitetspotentialer opnås ved prisbaseret kontrol. Herved belønnes fleksible elforbrugere og -producenter via et økonomisk incitament til at opnå den ønsket respons. Integrationen af prisbaserede kontroller er derfor det andet og sidste emne, der behandles i denne afhandling.

PREFACE

This thesis was carried out at the Department of Applied Mathematics and Computer Science at the Technical University of Denmark (DTU Compute) in partial fulfillment of the requirements for acquiring a Ph.D. degree. This thesis funded by the Horizon 2020 ERA Net Smart Grids+ project "microGRId Positioning – uGRIP" (77731) and the "CITIES" project (1035-00027B).

This thesis addresses real–time control of Microgrids by means of Model Predictive Control.

This thesis consists of a summary report, one technical report and six papers, two of which are of secondary authorship.

ACKNOWLEDGMENTS

First and foremost I would like to thank Professor Niels Kjølstad Poulsen for his supervision throughout this thesis, his support and his patience. I have benefited from your substantial knowledge in the areas of dynamical systems modeling and control. To Professor Henrik Madsen I want to thank in similar respect, especially for his positive attitude and his valuable feedback. Furthermore I would to thank you both for granting me the chance to conduct this PhD. Assistant Professor Daniela Guericke I would like to also thank for her valuable reviews and comments.

My sincere thank–you to Doctor Yelena Vardanyan for her highly useful comments, feedback and discussions. They have been a tremendous help. My appreciation to Doctor Goran Goranovic for his humor and interesting philosophical talks.

I would like to express my gratitude to Prof. Dr. Hrvoje Pandziĉ and Mateo Beus for the great hospitality at the hosting institution during my research exchange — the Faculty of Electrical Engineering at the University of Zagreb (FER-UNIZG). I would also like to thank the staff in Zagreb for their warm welcome.

Furthermore, I would like to thank all my colleagues at the Dynamical Systems group for all the interesting discussions we have had. My thankfulness also to Hanne Marie Maar Jensen, Anette Iversen and Janne Kofod Lassen for their support.

Also, I want to thank all people producing and maintaining great pieces of software free for everyone to use. This demonstrates that we can achieve a lot by means of collaboration.

I want to express my gratitude to my parents, Monika Tucht and Reimar Banis, as well as to my brother, David Banis. Last but not least I would like to thank Anthea Ŝtor for her support.

LIST OF PUBLICATIONS IN THIS THESIS

Paper	
A	Frederik Banis, Daniela Guericke, Henrik Madsen, and Niels Kjølstad Poulsen. „Load Frequency Control in Microgrids Using Target Adjusted Model Predictive Control.“ English. In: *IET Renewable Power Generation* (2019). ISSN: 17521424 and 17521416. DOI: 10.1049/iet-rpg.2019.0487
B	Frederik Banis, Daniela Guericke, Henrik Madsen, and Niels Kjølstad Poulsen. „Utilizing Flexibility in Microgrids Using Model Predictive Control.“ In: *Proceedings of Mediterranean Conference on Power Generation, Transmission, Distribution and Energy Conversion*. IET Control Theory and Applications. Croatia: Institution of Engineering and Technology, Nov. 2018. ISBN: 978-1-83953-133-0. DOI: 10.1049/cp.2018.1856
C	Frederik Banis, Daniela Guericke, Henrik Madsen, and Niels Kjølstad Poulsen. „Supporting Power Balance in Microgrids with Uncertain Production Using Electric Vehicles and Indirect Control.“ English. In: *IFAC-PapersOnLine* 52.4 (2019), pp. 371–376. ISSN: 2405-8963. DOI: 10.1016/j.ifacol.2019.08.238
D	Frederik Banis, Henrik Madsen, Niels Kjølstad Poulsen, and Daniela Guericke. „Prosumer Response Estimation Using SINDYc in Conjunction with Markov-Chain Monte-Carlo Sampling.“ In: *ENERGIES (submitted for review)*. Smart Grids and Microgrids (2020)
E	Mateo Beus, Frederik Banis, Hrvoje Pandzic, and Niels Kjølstad Poulsen. „Three Level Hierarchical Microgrid Control — Model Development and Laboratory Implementation.“ In: *21st Power Systems Computation Conference*. Porto, Portugal, June 2020
F	Yelena Vardanyan, Frederik Banis, S. Ali Pourmousavi, and Henrik Madsen. „Optimal Coordinated Bidding of a Profit-Maximizing EV Aggregator under Uncertainty.“ In: *Proceedings of the 2018 IEEE International Energy Conference (ENERGYCON)*. United States: IEEE, June 2018, pp. 1–6. ISBN: 978-1-5386-1283-5. DOI: 10.1109/ENERGYCON.2018.8398821
G	Frederik Banis, Kamal Jafarian Dehkordi, Henrik Madsen, and Niels Kjølstad Poulsen. „Reactive Power Control in Microgrids Using Target Adjusted Model Predictive Control.“ In: *Unpublished Technical Report*. Apr. 2020

DISSEMINATION AT CONFERENCES

Title	Conference/Workshop/Meeting
"Aggregated Optimized System Controls for Microgrids"	OpenMod Workshop, January 2020, Berlin (Germany)
"Handling Uncertainty in Sector Coupled Systems using Dynamic Programming and Model Predictive Control"	Smart Energy System International Conference (SESIC), September 2019, Copenhagen (Denmark)
"Operating Microgrids with High Penetration of Renewable Energy Units"	European Conference on Operational Research (EURO), June 2019, Dublin (Ireland)
"Supporting power balance in Microgrids with Uncertain Production using Electric Vehicles and Indirect Control"	IFAC workshop on Control of Smart Grid and Renewable Energy Systems (CSGRES), June 2019, Jeju Island (South Korea)
"Model Predictive Control in connection with district heating networks"	CITIES District Heating workshop, April 2019, Zagreb (Croatia)
"Control hierarchy for the improved operation of Microgrids with high shares of Renewable Energy Sources"	Power and Energy Summit (PES), November 2019, Dubai (UAE)
-	ERA-NET Smart Energy Systems Meeting Fraunhofer IFF, September 2018, Magdeburg (Germany)
"The uGRIP project"	ERA-Net SES at the Nordic Clean Energy Week, May 2018, Malmö (Sweden)

continued →

→ continued

Title	Conference/Workshop/Meeting
"Utilizing flexibility in Microgrids using Model Predictive Control"	Young Energy Economists and Engineers Seminar (YEEES), April 2018, Delft (Netherlands)
"Utilizing flexibility in Microgrids using Model Predictive Control"	Mediterranean Power Conference (MedPower), November 2018, Dubrovnik (Croatia)
-	SmartNet workshop, March 2017, Brussels (Belgium)

CONTENTS

LIST OF FIGURES

LIST OF TABLES

ACRONYMS

AC	alternating current
AC-PF	alternating current power flow
AC-OPF	alternating current optimal power flow
AD	algorithmic differentiation
ADN	active distribution network
AGC	automatic generation control
ADRC	active disturbance rejection
AVR	automatic voltage regulation
BB	black–box
BESS	battery energy storage system
CG	computational graph
CHP	combined heat and power plant
CL	closed loop
CT	continuous time
DA	day–ahead
DARE	discrete time algebraic riccati equation
DC	direct current
DCf	direct control for frequency stabilization
DCo	direct control
DER	distributed energy resource
DG	distributed generation
DH	district heating
DLQR	discrete time linear quadratic regulator
DR	demand response
DT	discrete time
EMS	energy management system
ESS	energy storage system
ESO	extended state observer
EV	electric vehicle
GAMS	general algebraic modeling system
GB	grey–box
GCM	grid-connected mode

ID	system identification
IM	islanded mode
ICo	indirect control
ICU	indirectly controllable unit
IEC	international electrotechnical commission
IP	internet protocol
IRC	impulse response coefficient
ISE	integrated squared error
LASSO	least absolute shrinkage and selection operator
LMPC	linear model predictive control
LCF	local control Lyapunov function
LFC	load frequency control
LLM	local linear model
LTI	linear time invariant system
LV	low voltage
LVDC	low voltage direct current
LQG	linear quadratic regulator
MG	microgrid
MCMC	markov chain monte carlo
MPC	model predictive control
MPP	maximum power point
MIMO	multiple input multiple output
MILP	mixed integer linear problem
MINLP	mixed integer nonlinear optimization problem
MISO	multiple input single output
MLE	maximum likelihood estimation
MV	medium voltage
NMPC	nonlinear model predictive control
NN	neural network
OC	optimal control
OL	open loop
ODE	ordinary differential equation
OPC	open platform communication
OPF	optimal power flow
PCC	point of common coupling
PD	positive definite

PDF	probability density function
PI	proportional integral
PID	proportional integral derivative
PMU	Phasor Measuring Unit
PSD	positive semi–definite
PV	photovoltaic
RD	redispatch
PR	prosumer response
QP	quadratic programming
RES	renewable energy source
ROM	reduced order model
RT	real time
RTU	remote terminal unit
SCADA	supervisory control and data acquisition
SDE	stochastic differential equation
SG	synchronous generator
SINDyc	sparse system identification of nonlinear dynamics with control
SMPC	stochastic model predictive controller
SO	state observer
SUC	stochastic unit commitment
SVD	singular–value decomposition
Sys-ID	system identification
SP	stochastic programming
TCP	transmission control protocol
UA	unified architecture
UC	unit commitment
VPP	virtual power plant
V2G	vehicle to grid
WB	white–box

NOMENCLATURE

Functions

$\mathcal{N}$	Normal distribution
ω	Standard Wiener process
σ	CT nonlinear diffusion coefficient function
Θ	Candidate model structure
f	Nonlinear dynamical function
f_p	Prediction function
h	Nonlinear function
J	Cost function
Pr	Probability function
S_m	Measurement noise variance map

Matrices

$\bar{F}$	State constraints left–hand–side coefficients
$\bar{H}$	Input constraints left–hand–side coefficients
$\bar{U}$	Dispatch schedule generated from a UC or SUC
$\epsilon_{\Delta y}$	Trajectory planning output precision
Γ_d	Forced response IRC (uncontrolled)
Γ_u	Forced response IRC (controlled)
$\mathcal{O}$	Operating polytope of an LLM
Φ_x	Free response IRC
Φ_ω	Free response IRC (state noise)
Σ	Filter covariance matrix
$\tilde{U}$	Dispatch schedule feasible for the RT system
$\tilde{X}$	State trajectory feasible for the RT system
Ξ	Model coefficients
A	Free system dynamics

A_o	Augmented free system dynamics
B	Forced system dynamics (controlled)
C	Output space mapping
G	Forced system dynamics (uncontrolled)
I	Identity matrix of suitable dimensions
K	Kalman gain
M	Lumped model matrix
$P_{\Delta\bar{u}}$	Prices associated with deviations from $\bar{U}$
$P_{\Delta y}$	Prices associated with absolute deviations from $\bar{Y}$
Q	State noise variance matrix
R	Measurement noise variance matrix
s	Slack variables
$W_{\Delta u}$	Control variation regularization coefficients
W_s	Target problem weights
W_T	Terminal regularization coefficients
W_u	Control effort regularization coefficients
W_y	Output regularization coefficients

Scalars

α	Output space tracking switch
β	Input space tracking switch
Δf	Frequency excursion
$\hat{d}_r$	Residual disturbance estimate
θ_{PCC}	Phasor angle at PCC
θ_{ref}	Reference phasor angle
θ_l	Phasor angle at node l
θ_m	Phasor angle at node m
B_d	Residual disturbance associated filter dynamics
b_{lm}	Susceptance over line lm
$b_{sh,i}$	Shunt susceptance of line i

C_d Residual disturbance feedthrough

D_a Load damping factor

d_r Residual disturbance

g_{lm} Conductance of line lm

G_r Residual disturbance associated dynamics

$g_{sh,i}$ Shunt conductance of line i

$H(t)$ Time dependend inertia based supply time

k Sampling iterate

n_s Number of considered scenarios

p_i Active power balance of line i

P_{mech} Active effective power balance

p_{lm} Real power flow from node l to m

q_i Reactive power balance of line i

q_{lm} Reactive power flow from node l to m

t Time variable

t_k DT sampling time

v_l Voltage over line l

v_m Voltage over line m

Vectors

$\bar{f}$ State constraints right–hand–side values

$\bar{h}$ Input constraints right–hand–side values

$\bar{u}$ Input space MPC reference

$\bar{y}$ Output space MPC reference

$\bar{y}$ Output target

$\epsilon_{\bar{u}}$ Target input tracking precision

γ_j Chance–constraint overshoot probability for scenario j

$\hat{d}$ Disturbance estimate

$\hat{x}$ State estimate

$\hat{x}_0$ Initial state estimate

$\hat{y}$	Output prediction
θ	Model parameter vector
θ_f	Prediction function parameterization
$\underline{\mathrm{u}}$	Inferred system equilibrium input
$\underline{\mathrm{x}}$	Inferred system equilibrium state
ξ_x	Hyperstate of x
ξ_y	Hyperstate of y
B_o	Augmented forced system dynamics
C_o	Augmented output mapping
d_0	Initial disturbance
d_k	DT disturbance
d_t	CT disturbance
I	Information vector
K_∞	Target adjustment feedback gain
$K_{u,\infty}$	Target adjustment input feedback gain
$K_{x,\infty}$	Target adjustment state feedback gain
L_o	Augmented static Kalman gain
L_u	Static disturbance Kalman gain
L_x	Static state Kalman gain
$u^\star$	Optimal system input
u_k	DT system input
u_t	CT system input
u_s	Steady state system input
v_k	White noise process samples (measurement noise)
x_0	Initial state
x_k	DT system state
x_t	CT system state
x_o	Augmented state
x_s	Steady state system state

y_k DT system observation

y_m Output measurement

Sets

$\bar{e}_0$ Reference trajectory

$\hat{D}$ Set of disturbance predictions

$\mathcal{D}_0$ Set of initial system disturbances

$\mathcal{L}$ Set of lines

$\mathcal{T}$ Operating trajectory

$\mathcal{X}_0$ Set of initial system states

$\underline{\mathrm{P}}$ Inferred system equilibrium

e_0 Point of linearization (system equilibrium)

X General set

X_N Terminal set

Part I

SUMMARY REPORT

This summary report documents the context and background of this thesis, relevant methods and basic models and key findings.

1 INTRODUCTION

This chapter shall give an introductory overview of this thesis. Therefore, Section 1.1 describes the context and motivation of this thesis, whereas objectives and contributions are stated in Section 1.2. The chapter closes with an outline in Section 1.3.

1.1 CONTEXT AND MOTIVATION

The increasing and partly uncoordinated penetration of fluctuating generation units and consumers in the power system leads to increased variability and uncertainty [BGL10; Kat+08]. Accordingly and in order to achieve a stable system operation in this situation, the flexibility within the system must be addressed [Mei+13; Mar16]. A high share of renewable energy systems (RESs), such as wind or photovoltaics (PVs), is desirable by economic means [Mor+14] and reduction of, amongst others, carbon dioxide emissions [OED15].

Small sized and locally dispersed RESs are distributed energy resources (DERs). Generation capacity of such units and their inertia is reduced in comparison to conventional power plants [UBA14; DM16]. Furthermore, such units are often connected via inverters [GP07; Sch+16a]. Operational properties of these units are, therefore, different than conventional synchronous generators (SGs) [BH07].

However, DERs at the medium voltage (MV) and low voltage (LV) levels can increase power quality and reliability [Hat+07; Han17] and reduce transmission losses [Han17]. They reduce the stress of transmission and distribution systems [Jus+13].

Coordination of DER and/or distributed generation (DG) within a spatially confined cluster at LV level can utilize their associated flexibility potentials [Han17]. A network in which DERs are enabled to participate in power flow regulation is in literature denoted an active distribution network (ADN) [HAJ10; Bor+10]. Along these lines we can identify the MG concept, which can be defined as follows:

"The microgrid encompasses a portion of an electric power distribution system that is located downstream of the distribution substation, and it includes a variety of DER units and different types of end users of electricity and/or heat" [Kat+08].

The history of MGs hereby goes back to the birth years of power systems itself [Asm10].

MGs are ADNs, that is, networks with potentially bidirectional power flows. In such systems, DERs become active components in the grid when properly actuated, such that reliable generation and consumption are feasible in close spatial perimeters. MGs are, therefore, a concept facilitating the reduction of stress in the transmission system [Han17].

We can increase flexibility also using additional actuators such as energy storage systems (ESSs) or additional distribution system components such as lines. However, measures as the latter are cost–intensive, especially when considering the low number of full–load hours during peak load operation. Another approach is to use existing infrastructure, and possibly additional infrastructure, in a more efficient way. This includes adapted controls that act proactively and with higher degrees of system knowledge. Application of such control strategies to energy systems is only satisfactory with well–defined control area boundaries, that is, considering the underlying system structure and system requirements as well as the modeling capabilities used to describe the system.

1.2 OBJECTIVES AND CONTRIBUTIONS

The main objective of this Ph.D. thesis is the development and application of model predictive controllers (MPCs) for the operation of energy systems including flexibility activation, with a focus on power system operations in context of microgrids. We tested a selection of these controllers throughout a case study. This objective encompasses the modeling of grid components, the application of system identification approaches and the formulation of uncertainty representations.

Resulting from these objectives, we propose the following contributions:

- An alternative solution to the load frequency control (LFC) problem (Paper A) based on the related conference contribution (Paper B). The outlined LMPCs can be used as master controllers or subordinate controllers.

- A solution to the problem of controlling electric vehicles (EVs) using indirect control (ICo) approaches (Paper C). Hereby, the ICo generates price offers for price–sensitive EVs such that they support grid frequency stability by adjusting their interaction behavior.

- The *Sparsity Promoting System Identification of Nonlinear Dynamics with control* algorithm (SINDyc) in combination with *Markov chain Monte Carlo* (MCMC) (Paper D). This setup yields sparse and potentially nonlinear probabilistic system models. Such models can be used within stochastic model predictive controllers (SMPCs).

- A case study including a temporal control hierarchy concept presenting the coupling of multiple optimization routines for the automatic generation control (AGC) problem using the co–simulation framework MOSAIK [SSS12] (Paper E).
- Alternative solutions to the coordinated voltage control problem (Paper G).

1.3 OUTLINE

This thesis is structured as follows.

Part i is a summary report outlining the main contributions of this thesis. Chapter 2 reviews the context and background. Chapter 3 states methods utilized throughout this thesis. Chapter 4 discusses the key findings of this thesis. Chapter 5 summarizes the thesis and outlines possible future work.

Part ii consists of the publications contributing to this thesis.

2 CONTEXT AND BACKGROUND

This chapter covers the context and background of this thesis. In particular, the following topics are discussed:

- Relevant microgrid (MG) components. See Section 2.1.
- Automatic Generation Control (AGC) in MGs. See Section 2.2.
- Aspects of energy grids and in this context, flexibility and efficiency. See Section 2.4.

2.1 COMPONENTS OF A MICROGRID

We can distinguish the following technological component groups within an microgrid (MG):

- Distributed Energy Resources (DER)
  - Production side
    - Dispatchable production (e. g. combined heat and power plants (CHPs), diesel generators, battery energy storage system (BESS))
    - Stochastic production (e. g. PV, wind turbines)
  - Dispatchable storage capacities (e. g. BESSs, fuel cells, supercapacitors)
- Load side
  - Free loads (e. g. households, industrial loads)
  - Flexible loads (e. g. EVs)
  - Controllable (dispatchable) loads (e. g. BESSs)
  - Base load
- Distribution system components

We cannot influence the *free loads* apart from curtailment. In contrast, we can direct *flexible loads* towards the desired behavior using incentives. Flexible loads can, therefore, act as a form of storage, in the sense of shifting consumption temporally rather than removing this consumption altogether. Controllable loads can act as a degree of freedom, similarly to flexible loads. Contrary to the latter, we may dispatch controllable loads assuming zero associated uncertainty.

Electric boilers interfacing the power system with a district heating system are an example of controllable loads [MT18; MP16]. Further notions in relation to loads are "residential, commercial and industrial loads" [Sch+16b], see also [Kat+08]. Storage capacities enable temporal shifting similarly to flexible loads. Stochastic production units act as if they have been scheduled by an uncertain dispatch schedule. They are controllable to a lesser degree, however we may curtail such units if necessary. Curtailments may be associated with economic losses. Such losses do not apply if the marginal cost of a production unit is zero [Mor+14].

As an MG in grid-connected mode (GCM) connects to the utility distribution system via the point of common coupling (PCC), the distribution system may be considered as an "electric slack bus" [Kat+08].

Most DERs within the grid include some local controller(s), such as maximum power point (MPP) trackers in PV systems [AA10]. The design of such controllers is hereby tailored to a specific operational mode. Such modes encompass the *grid–following mode* and the *grid–forming mode* and DERs can potentially operate in both modes [Sch+16b; Kat+08]. Classically, sufficiently large units operate in grid–forming mode [Kat+08]. Coupled DERs may however also perform this task, especially in modern MGs with a high penetration of DERs (ibid). RESs, constituted as DERs driven by stochastic processes, can also contribute to the operational objectives, by exploiting the operational system properties associated with the individual plant and its technological type. [Im+17] show the emulation of virtual inertia using PVs to support the operation of MGs in islanded mode (IM). See [UEJ13] as an example. Overlapping all mentioned cases is the potential of improving the operational performance using model–based and predictive control approaches. See [Gey17] for related examples.

Distribution system infrastructure includes components such as transformers, lines, switches or circuit breakers and AC/DC converters. Inverters are a core component in the modern power system [Sch+16b], contrary to power systems dominated by SGs. This is due to that a majority of DGs are inverter–based, consequently such units must provide system services (ibid).

2.1.1 Inverter Based Microgrids

Inverter interfaced units enable faster response and, therefore, potentially improved operation of the system [GP07]. A fast actuator response is especially relevant in IM with its reduced available inertia [KIL07; Im+17].

As a large number of components in future MGs will interface the network through inverters [Sch+16a; Sch+16b], properties of the formerly SG–centered power system are going to change. Reference [GP07] reports such operational properties.

Inverters are complex systems with internal control loops and filters. As a result, encapsulation principles are relevant also when working with inverters in the context of MGs [LD14]. While inherently different from the SG–focused power system, inverters are flexible and can mimic SG based production units [BH07]. Inverters can and should participate in grid–forming applications in order to provide system services and support the system stability [Sch+16b].

High–frequency harmonics distortions resulting from inverter switching is an issue, potentially causing power quality problems [GP07]. Filtering may alleviate it (ibid), as well as an increase in the switching frequency [TTL16]. When using the former, a filter absorbs the harmonics. When increasing the switching frequency, harmonics caused by switching are also moved to higher frequencies. Both approaches can be combined (ibid). Also, model predictive control (MPC) control has been both proposed and applied in this context [Gey17].

2.1.2 Direct Current Microgrids

Direct current (DC) networks have not been a focus in this thesis, therefore, they are mentioned here only in brief.

DC–based MGs are commonly named *low voltage direct current* (LVDC) distribution networks [Jus+13]. Such LVDCs can improve the efficiency of power distribution by removal of the need of the DC–AC–DC conversion in inverter–based alternating current (AC) distribution networks [Jus+13; LH11]. Furthermore, improvements to the reliability of the distribution system in comparison to conventional AC systems have been reported [LH11; SS07].

2.2 AUTOMATIC GENERATION CONTROL IN MICRO-GRIDS

Automatic Generation Control (AGC) aims to achieve the power balance of generation and load such that the grid frequency stabilizes to the nominal frequency. This is commonly referred to as secondary control [Gom+18].

Apart from this balancing task, production units should share the load. This is traditionally addressed by means of droop control [Sta+16; Pla+13; KI06; DSB16; DM16; Han17], sometimes denoted as *power sharing*. Droop control regulates the frequency by adjusting the unit's output active power. I can also track setpoints provided by the dispatch schedule, while rejecting disturbances by means of proportional action. Droop control however, as a purely feedback based strategy, leaves room for improvements.

We can improve AGC with droop by addition of a predictive optimized control layer at aggregation level acting as reference governor to plant–level controllers [Kat+08]. Given the reduced inertia in IM of an MG (see [UBA14] in this context), increasing numbers of DERs [Bas+12], aggregation schemes in development [Mor+14] or integration of prosumers [Str08] — optimized control strategies facilitate innovations and provide solutions to operational challenges.

We can distinguish AGC in MGs from AGC in classical distribution systems by the feature of disconnecting from the overall grid at the so–called PCC [Kat+08]. The disconnected MG operation — denoted *islanded mode* (IM) — has distinctive properties and associated operational challenges in contrast to *grid-connected mode* (GCM) [KIL07]. In IM, available inertia is drastically reduced [DM16; UBA14]. It follows that these types of operations differ fundamentally. Stable system operation in IM requires sufficiently short controller response times in combination with sufficiently fast actors actuating the controller decisions. See for example [Bas+12]. Such a fast system may be a so–called BESS, for example, allowing for the provision of steep ramps. BESSs may furthermore provide damping of high–frequency oscillations [BGL10; Mae+07].

Aside from IM, operational challenges in tendency become more stringent, as the share of intermittent units such as RESs and EVs increases. For example, lines and cables may operate close to physical limitations in such scenario. Intensified requirements in such scenario then result in heightened requirements for controllers and associated routines, such as, model accuracy and sensor coverage.

In consequence, MPC based strategies for the AGC problem have been proposed, in order to account for operational constraints optimally and incorporate predictions, see for example [EIU16; Ven+08; SRA13; SS16]. Applied on the aggregated system level, these approaches enable the overall system to respond to disturbances in a coordinated and more optimal manner.

2.3 AUTOMATIC VOLTAGE REGULATION IN MICRO–GRIDS

Voltages are sensitive to reactive power provided to or absorbed from the grid. Using automatic voltage regulation (AVR), voltages are maintained within desired boundaries [Kun94].

As for AGC, droop controllers have been proposed also for the primary AVR problem [CDA93]. As stated in [Sch+16a], droop control in AVR suffers from that "it does in general not guarantee a desired reactive power sharing". Similarly to AGC, secondary control by means of integrative action can remove this offset. LMPC has been successfully applied for this task, for example in [VC13; JR18].

2.4 ENERGY GRIDS, FLEXIBILITY AND EFFICIENCY

Energy grids are a backbone technology of every modern society. The electric power system, district heating (DH) or gas distribution networks are examples of such. Every energy grid is a complex system comprising sensors and actuators, monitoring, optimization and control routines. Interlinking of such domains offers additional degrees of freedom. For example, DH systems in Denmark facilitate the integration of RES, predominantly wind power, at large scale [MP16; MT18]. Hereby, additional degrees of freedom in the distribution system is a spatial source of flexibility whereas the high inertia of the DH system is a temporal source of flexibility.

Integrated energy system optimization considers multiple energy carriers [Gei07], contrary to single–domain optimization methods. Co–optimization of physically linked multi–energy domains increases the available degrees of freedom of operating the system. As a consequence, synergies of the different energy domains lead to higher overall system performance, with increased economic performances. [OED15; Gei+07; GA07] are typical examples. The cost of unlocking such synergies appears through an increase in system complexity and computational burden.

The former affects the modeling process, as the engineer has to understand relevant aspects of the multi–domain energy system. This is commonly addressed by means of encapsulation, such that complexity reduces to a desirable level for the given modeling task.

A larger computational burden results from the larger operational space available to the system operator. Similarly to the modeling problem, the encapsulation of the optimization problem is a method to address complexity in the operational problem.

Efficiency denotes the performance of a system with respect to some performance metric. In energy systems operation, different performance metrics are relevant:

TECHNICAL METRICS such as electric energy transformed into thermal energy within the distribution network of a power system.

ECONOMIC METRICS such as a price on an energy commodity.

ENVIRONMENTAL METRICS such as CO_2 release.

In rare situations, different metrics may lead to a equivalent outcome. More often, a trade–off in–between these metrics must be searched.

2.5 MICROGRIDS: ORGANIZING AND OPTIMIZING SUBSYSTEMS

The definition of a microgrid (MG) differs in literature. Historically, MGs were operated solely in islanded mode (IM): "In fact, Thomas Edison's first power plant [...] was essentially a microgrid" [Asm10].

The definitions below are valid for this thesis:

"A microgrid gathers a combination of generation units, loads and energy storage elements at distribution or sub-transmission level into a locally controllable system, which can be operated either in grid-connected mode or in islanded mode, i.e., in a completely isolated manner from the main transmission system. The microgrid concept has been identified as a key component in future electrical networks." [Sch+16b] (consider citations therein).

A formal definition of the AC MG is given as [Sch+16b]:

> "An AC electrical network is said to be an AC microgrid if it satisfies the following conditions.
>
> 1. It is a connected subset of the LV or MV distribution system of an AC electrical power system.
> 2. It possesses a single point of connection to the remaining electrical power system. This point of connection is called point of common coupling (PCC).
> 3. It gathers a combination of generation units, loads and energy storage elements.
> 4. It possesses enough generation and storage capacity to supply most of its loads autonomously during at least some period of time.
> 5. It can be operated either connected to the remaining electrical network or as an independent island network. The first operation mode is called grid-connected mode and the second operation mode is called islanded, stand-alone or autonomous mode.
> 6. In grid-connected mode, it behaves as a single controllable generator or load from the viewpoint of the remaining electrical system.
> 7. In islanded mode, frequency, voltage and power can be actively controlled within the microgrid."

Virtual Power Plant, Market Participation and Commitments

As a result of bullet 6, we may consider a coordinated MG as a power plant. Then, the MG is commonly labeled as a virtual power plant (VPP).

"Formally, a VPP, also referred to as Virtual Utility, can be defined as a cluster of dispersed generating units, flexible loads, and storage systems that are grouped in order to operate as a single entity" [Mor+14, P. 243].

A VPP may by design outperform a conventional power plant in terms of flexibility [Mol+10; Jus+13] and efficiency [Jus+13].

By aggregating DERs the VPP can participate in energy markets and provide system services in response to market requests in order to obtain economic profit [Mor+14; VM19; Jus+13]. Such market designs can also be formulated for the local system, such that peer–to–peer trading is established [Men+17]. Peer–to–peer trading is an approach to leverage flexibility potentials, as a single consumer, producer or prosumer can gain a monetary revenue for hers system service provision. Local market design can hereby benefit from agent–based simulation studies [RKF16].

Commitment to services may be binding [Mor+14]. Failing to provide the contracted service may then constitute penalties. The market interaction is, therefore, both desirable as well as constraining. This tendency furthers beneficial investments for a particularly attractive operational mode. Conclusively, an MG operator can and will as consequence to economic considerations tend to exploit the specific strengths of the MG. Technical limitations are partly dynamic, and consequently so are services that the MG can provide. Therefore, we should not consider the control structure used to operate the MG as a static construct, but rather such that the time–varying system can be optimally operated as desired.

3 METHODOLOGIES

This chapter provides an overview of central methods in this thesis.

Section 3.1 discusses modeling related aspects. Section 3.2 introduces the unit commitment (UC). Section 3.3 considers model predictive control (MPC) techniques. Section 3.4 introduces estimations and predictions in context with real–time (RT) system operation. Section 3.5 discusses the topic of control hierarchies.

3.1 MODELS

3.1.1 Dynamical Systems

Dynamical systems can be solely based on knowledge of the governing physical equations (white–box (WB) models) or solely based on data (black–box (BB) models). We may combine both approaches in order to obtain grey–box (GB) models [Lju99].

3.1.1.1 Differential Equations

We can describe dynamical systems by ordinary differential equations (ODEs):

$$\frac{dx_t}{dt} = f(x_t, u_t, t, \theta) \tag{3.1a}$$

$$y_k = h(x_k, u_k, t_k, \theta) \tag{3.1b}$$

Equation (3.1a) denotes the continuous time (CT) system dynamics, Equation (3.1b) describes discrete time (DT) system measurements. x_t is the system state, u_t the system input, t the time variable, θ is the system parameterization. The latter is here assumed static but may be time–varying. In correspondence, we denote the DT system variables. f and h are in general nonlinear functions.

By inclusion of stochastic processes into the system we obtain the stochastic differential equations (SDEs) below, as given in [KMJ04]:

$$dx_t = f(x_t, u_t, t, \theta)\; dt + \sigma(u_t, t, \theta)\; d\omega_t \tag{3.2a}$$

$$y_k = h(x_k, u_k, t_k, \theta) + v_k \quad | \; v_k \sim \mathcal{N}_{iid}(0, S_m(u_k, t_k, \theta)) \tag{3.2b}$$

σ is a nonlinear function and ω is a standard Wiener process. v_k is a random normal process with zero mean and independent individual samples, that is, white noise. u_t and u_k may include controlled and uncontrolled system inputs. From here on, we denote uncontrolled system inputs as disturbances d_t (CT) and d_k (DT) respectively. Consequently, (3.2a) and (3.2b) become:

$$dx_t = f(x_t, u_t, d_t, t, \theta)\ dt + \sigma(u_t, d_t, t, \theta)\ d\omega_t \tag{3.3a}$$

$$\begin{aligned} y_k = h(x_k, u_k, d_k, t_k, \theta) + \\ v_k \quad | \ v_k \sim \mathcal{N}_{iid}(0, S(u_k, d_k, t_k, \theta)) \end{aligned} \tag{3.3b}$$

3.1.1.2 *Linear System Approximation*

Linear system models reduce the computational burden compared to nonlinear system representations stated previously and enable the application of the broad range of tools available within linear control theory. As a result, the linear model approximates the nonlinear system well within an operating polytope $\mathcal{O}$ and with respect to some objective. $\mathcal{O}$ depends on the sampling rate of the controller. A higher sampling rate results in a reduction of the nonlinearity of the problem.

In the following, we describe the linearization with respect to an operating point (see Section 3.1.1.2) and with respect to a operating trajectory (see Section 3.1.1.2). We refer to these two cases as *operating reference* from here on.

We also briefly discuss the linearization over an operating polytope (see Section 3.1.2.2) and the treatment of uncertainty (see Section 3.1.1.2).

OPERATING POINT: We can obtain the linear perturbation model at an approximated stable system equilibrium e_0:

$$A = \frac{\partial f}{\partial x}|_{e_0} \tag{3.4a}$$

$$B = \frac{\partial f}{\partial u}|_{e_0} \tag{3.4b}$$

$$G = \frac{\partial f}{\partial d}|_{e_0} \tag{3.4c}$$

$$C = \frac{\partial h}{\partial x}|_{e_0} \tag{3.4d}$$

We hereby neglect the feedthrough coefficients D. f and h refer to Equation (3.1), the deterministic nonlinear system model. The stable system equilibrium is hereby a set of linearization coordinates:

$$e_0 = \{x^{e_0}, \quad u^{e_0}, \quad d^{e_0}\} \tag{3.5}$$

The model $\{A, B, G, C\}$ is a local linear model (LLM), locally valid at e_0 [Nel01]. When deviating from e_0 the mismatch of this linear system approximation to the true dynamics increases. See Figure 3.1 as an example.

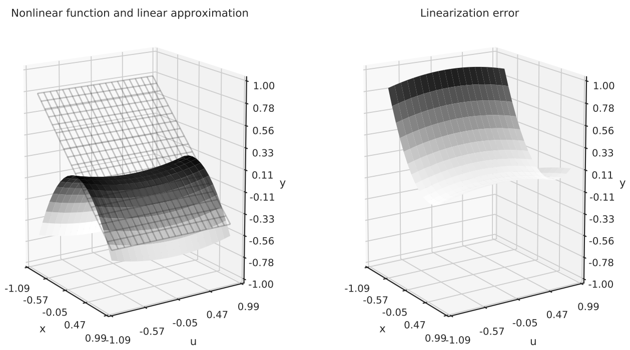

Figure 3.1: Linearization example: Approximation at an operating point. The linear approximation illustrated as a plane in the left plot approximates the nonlinear function illustrated as solid manifold. The approximation error when deviating from the point of linearization increases when deviating from the latter, illustrated as a manifold in the right plot.

In the case of a single operating point, we can denote the time–invariant discrete–time deterministic linear system model:

$$\Delta x_{k+1}^{e_0} = A\Delta x_k^{e_0} + B\Delta u_k^{e_0} + G\Delta d_k^{e_0} \tag{3.6a}$$
$$\Delta y_k^{e_0} = C\Delta x_k^{e_0} \tag{3.6b}$$

This is a linear on–step prediction model in perturbation form evaluated at sampling instance k. If Equation (3.3) on the facing page is considered, we may use instead:

$$\Delta x_{k+1}^{e_0} = A\Delta x_k^{e_0} + B\Delta u_k^{e_0} + G\Delta d_k^{e_0} + \Delta w_k^{e_0} \tag{3.7a}$$
$$\Delta y_k = C\Delta x_k^{e_0} + \Delta v_k \tag{3.7b}$$

Δw_k and Δv_k are zero–mean normal distributed white noise processes, reflecting the impact of the noise processes σ and v in Equation (3.3) on the preceding page.

The state, input, disturbance, and output of the overall model are:

$$x_k^{e_0} = x^{e_0} + \Delta x_k^{e_0} \tag{3.8a}$$
$$u_k^{e_0} = u^{e_0} + \Delta u_k^{e_0} \tag{3.8b}$$
$$d_k^{e_0} = d^{e_0} + \Delta d_k^{e_0} \tag{3.8c}$$
$$y_k^{e_0} = y^{e_0} + \Delta y_k^{e_0} \tag{3.8d}$$

x^{e_0}, u^{e_0}, d^{e_0} denote state, controlled system input and disturbance system input at the point of linearization e_0.

The overall system output is then

$$y_k = h(e_0, k, \theta) + \Delta y_{k,e_0} \tag{3.9}$$

The discrete system dynamics A, B, G and C are valid in $\mathcal{O}$ until some routine triggers the update of the linear model. This may, for instance, be some local model error evaluation or an update of a disturbance prediction.

A, B, and G are impulse response coefficients (IRC) [1] matrices with state x, input u and disturbance d related elements, respectively. C is a linear mapping from state space to output space. Potentially, the output Equation (3.11b) includes a feed–forward term from control decisions to the system output. This term is omitted here. Consider an exemplary linearization in Figure 3.1

The model $\{A, B, G, C\}$ is a local linear model (LLM), locally valid with respect to the nonlinear system model at e_0. For simplicity, we drop the Δ notation and the subscript e_0 from here on and consequently yield the deterministic system:

$$x_{k+1} = Ax_k + Bu_k + Gd_k \tag{3.10a}$$
$$y_k = Cx_k \tag{3.10b}$$

And, respectively, the stochastic system:

$$x_{k+1} = Ax_k + Bu_k + Gd_k + w_k \tag{3.11a}$$
$$y_k = Cx_k + v_t \tag{3.11b}$$

PREDICTION MODEL: Impulse response coefficients obtained from Equations (3.10a) or (3.11) enable the iteration of the model forward in time, subject to the states and exogenous inputs. Based on the principle of superposition, we may decompose the linearized system with respect to states and exogenous inputs. See for example [CB04]. The uncontrolled and undisturbed system portion is commonly denoted

1 Also known as *Markov parameters*.

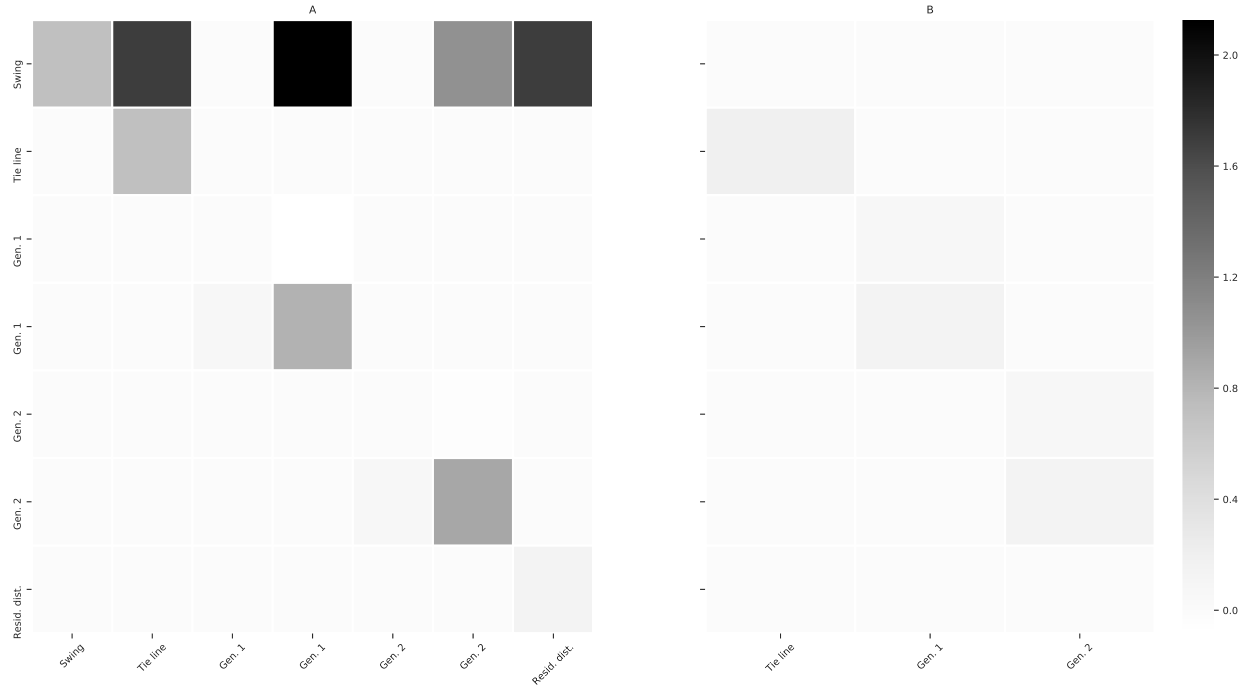

Figure 3.2: Heatmap of an exemplary LTI system. The exploitation of the sparsity structure of the system can be relevant for larger models or explicit MPC.

as *free–response* and the forced system portion as *forced–response*. For the free–response, we denote the corresponding IRC as Φ_x and Φ_w, following the notation given in [JHR11]. Φ_x are then IRC relating to the states x, Φ_w are IRC relating to the state noise w. Due to that most systems are subject to disturbances, we may decompose the forced–response into exogenous forcing portions. Following the notation ibid, we denote the corresponding IRC as Γ_u and Γ_d in relation to controlled system input u and uncontrolled system input d, respectively.

As stated in for example [Mac02; CB04], we can derive the IRC with respect to the free system response and forced system response as a consequence of the principle of superposition:

$$\begin{aligned} y = & \begin{matrix} CA \\ CA^2 \\ \vdots \\ CA^N \end{matrix} x_k + \begin{matrix} CB \\ CA^2B \\ \vdots \\ \sum_{i=0}^{N-1} CA^iB \end{matrix} \quad u_{k-1} \\ & + \begin{bmatrix} B & \dots & 0 \\ C(AB+B) & \dots & 0 \\ \vdots & \ddots & \vdots \\ \sum_{i=0}^{N-1} CA^iB & \dots & \sum_{i=0}^{N} CA^iB \end{bmatrix} u \end{aligned} \tag{3.12}$$

N is hereby the prediction horizon. In contrast to the formulation given in [CB04, P. 29], we neglect a dedicated control horizon N_u for simplicity. Using the latter approach offers an additional degree of freedom for tuning. The prediction horizon should at least encompass 80-90% of the open loop (OL) rise time of the system, as stated for example in [Mau+88].

Let the IRC with respect to the states from here on be Φ_x, IRC with respect to the controlled inputs be Γ_u, IRC with respect to the uncontrolled inputs be Γ_d. Φ_w denotes the IRC with respect to the state noise w. The N–step system output prediction $\hat{y}$ using the linear model and considering both controlled and uncontrolled system inputs, u and d respectively, is then

$$\hat{y}_k = \Phi_x x_{k|k} + \Gamma_u u_k + \Gamma_d d_{k|k} + \Phi_w w_{k|k} + v_{k|k} \tag{3.13}$$

UNCERTAINTY TREATMENT: States and disturbances may be uncertain. We can then infer the initial state value by the evaluation of its probability conditioned on available information at present time I:

$$x_0 = P(x_0|I_{t-1}) \tag{3.14}$$

where:

$$I_{t-1} = [y_{t-1}, \ldots, y_0, u_{t-2}, \ldots, u_0] \tag{3.15}$$

and, by means of applying the Bayesian estimation principle

$$Pr(x_{t-1}|I_{t-1}) = \frac{Pr(y_{t-1}|x_{t-1})Pr(x_{t-1}|I_{t-2})}{Pr(y_{t-1}|I_{t-2})} \tag{3.16}$$

as formulated in [RL19, P. 76].

Similarly, we may consider the conditional probability:

$$d_0 = Pr(d_0|f_p(\theta_f, t-1)) \tag{3.17}$$

f_p hereby may be a prediction function with some arguments θ_f that provides us with a guess on d. Such function may furthermore provide the expectation $\mathbb{E}(\hat{d})$ of the predicted disturbance trajectory $\hat{d}$.

Contrary to assuming an *expected* initial state x_0, disturbance d_0 or disturbance trajectory $\hat{d}$, we may consider sets of such quantities and associated realization probabilities. Then, we may consider $\mathcal{X}_0$, $\mathcal{D}_0$ and $\hat{\mathcal{D}}$ as such sets.

ADDITIONAL METHODS:

ADAPTIVE LINEARIZATION: For certain dynamical systems, we may consider adaptive linearization techniques. This may apply when robustness can be certified also with the adaptive linearization approach. See Section 3.1.2.2 on adaptive linearization in context of static system models.

OPERATING TRAJECTORY: The linearization procedure described in Section 3.1.1.2 is hereby performed over a time–varying reference trajectory $\bar{e}_0 = \{x^{\text{ref}}, u^{\text{ref}}, d^{\text{ref}}\}$. When considering the SDE Equation (3.3) on page 16, this results in:

$$\frac{d\Delta x_t^{\bar{e}_0}}{dt} = A_t \Delta x_t^{\bar{e}_0} + B_t \Delta u_t^{\bar{e}_0} + G_t \Delta d_t^{\bar{e}_0} + \Delta w_t^{\bar{e}_0} \tag{3.18a}$$

$$\Delta y_t^{\bar{e}_0} = C_t \Delta x_t^{\bar{e}_0} + \Delta v_t^{\bar{e}_0} \tag{3.18b}$$

Where the perturbation model relates to the reference trajectory:

$$x_t = x_t^{\bar{e}_0} + \Delta x_t^{\bar{e}_0} \tag{3.19a}$$

$$u_t = u_t^{\bar{e}_0} + \Delta u_t^{\bar{e}_0} \tag{3.19b}$$

$$d_t = d_t^{\bar{e}_0} + \Delta d_t^{\bar{e}_0} \tag{3.19c}$$

$$y_t = y_t^{\bar{e}_0} + \Delta y_t^{\bar{e}_0} \tag{3.19d}$$

Notice that we may potentially interpolate linear models [Nel01, P. 610].

3.1.1.3 Computational Graphs, Algorithmic Differentiation

Computational graphs (CGs) capture the causality structure in mathematical operations and enable the optimized exploitation of the latter. We can apply algorithmic differentiation (AD) [2] to a computational graph (CG) in order to obtain linear system approximations as outlined in Section 3.1.1.2. AD is commonly used within nonlinear model predictive control (NMPC) schemes in order to obtain the linear approximation implicitly in the optimization step.

Grouping within CGs enables us to apply operations on sub–CGs. This aspect is relevant in aggregated system models, see Section 3.1.1.4. Recall that an aggregated system model is heterogeneous. Subsystems operate within distinct operational domains. Consequently, accuracy requirements within these domains differ. CG facilitate the evaluation of local error metrics which can be used to trigger updates of the corresponding linear model. Such a model is commonly denoted an LLM [Nel01].

In automatic generation control (AGC), we aim to coordinate a portfolio of such heterogeneous plants, leading to frequent need to perform AD for some subsystems in order to retain accuracy. This also depends on the operational mode. In IM, accuracy requirements may be higher. See also Section 2.2 on AGC.

Independent of the MG constitution, the organization of subsequent models using CG is an important aspect in optimized MG operation.

3.1.1.4 Unit Models, Aggregation and Graphs

We can characterize system units within energy systems as a collection of properties. Dynamics, confined operating polytopes and switching, measurements and more, are relevant during RT operation. As such, we can describe system units as objects with properties. Aggregation of system units closely relates to encapsulation. When aiming to optimize the system at a chosen aggregation level, we can inform the assembly of the required aggregated system model by means of graphs. Graphs encode the causality structure and are a fundamental ingredient of efficient energy system's operations. See Figure 3.3 on the next page as an example.

Aggregation and dimensionality reduction techniques relate to each other. As an example, units 2 and 3 in Figure 3.3 may be accurately represented as lumped system model. An example of a model reduction technique is the application of the singular–value decomposition (SVD) to linear time invariant systems (LTIs) in combination with rank truncation. See for example [BK19] and Figure 3.4.

2 Also called *Automatic Differentiation*.

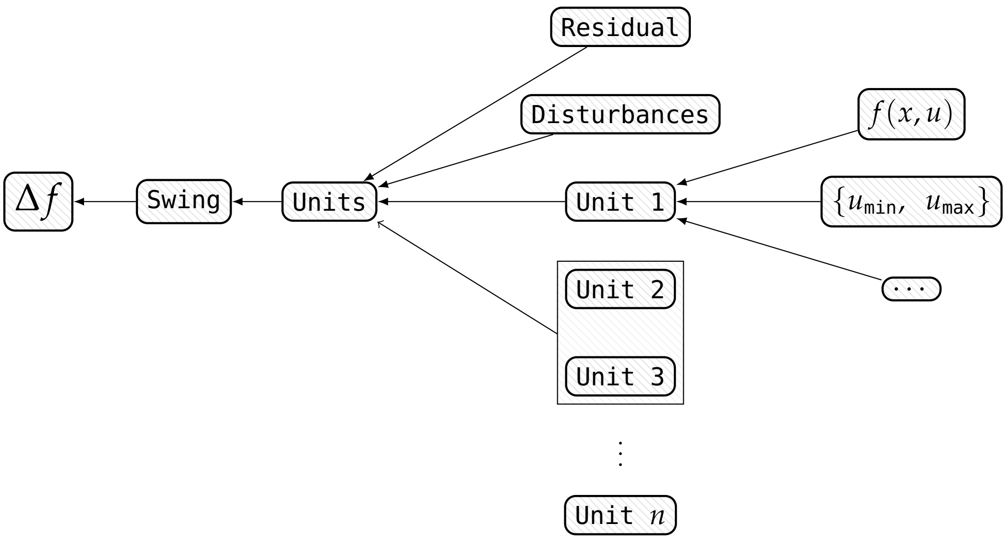

Figure 3.3: Exemplary aggregated system graph.

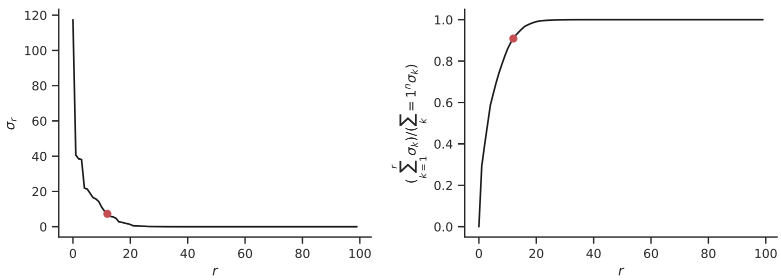

Figure 3.4: Model order reduction example. Around 20 modes capture around 90% of the input–output energy. See [See BK19, P. 334].

By design, state space models enable efficient indexing and sparse forms which we can relate to computational graphs. The combination of both state space models and graphs leverages mutual benefits.

ADDITIONAL METHODS: Here we state methods that have not been explicitly covered within the publications in this thesis, however do pose reasonable additions.

MODEL ORDER REDUCTION: A simplified model can reduce computational load while retaining a high degree of accuracy. Such a model is typically referred to as reduced order model (ROM). Some techniques such as sparse Sys-ID aim to directly obtain a balance of model complexity and accuracy. Other techniques, such as neural networks (NNs), may yield a high dimensional model. Reduction of such model can then be a prerequisite to the usefulness of the model itself.

[LD14], for example, propose ROM for inverter–based MGs in IM. They perform both temporal and spatial model order reduction. The latter leads to isolation of the inverter interactions, an aspect that can be used in controller design.

ERROR PROPAGATION IN AGGREGATED SYSTEM MODELS: A controller shall compensate for uncertainty with respect to the dynamics and uncertainty with respect to the measurements. An example for such uncertainty is the linear approximation error. As a plant deviates from the point of linearization, the linearized model loses its accuracy in comparison to the nonlinear model. The linearization error propagates to the model output and contributes to its uncertainty. The growth rate of the linearization error is hereby individual for each plant, depending on their dynamics magnitude. In fast plants, such error may require more frequent compensation as in slow plants.

An aggregated system typically consists of multiple causally connected plants as described in Section 3.1.1.4. In this situation, the evaluation of uncertainty measures at a plant level enables the prevention of error propagation by assigning feasible countermeasures. This may entail to specify the relinearization frequency on a plant level for a given operating point.

Consider Figure Figure 3.3 on the preceding page for example. Compensating for uncertainty at the plant level improves the decision making for the aggregated system.

3.1.1.5 System Identification

While system identification (Sys-ID) has always been part of control and systems operation, ongoing technological transitions change how we can use these technologies. The abundant availability of sensor data at high sampling rates and low noise levels or the long term data–storage in combination with improvements of existing Sys-ID approaches result in the trend to conduct system modeling and control based on *data–driven* principles [BK19; Tu13]. The modern power system "will be a combination of both power system and information and communication system networks" [Jus+13].

While this has been the case for some time, this trend to cyber–physical systems is going to prevail. Along these lines, data–driven techniques are relevant for system operation [Cre+19].

Given sufficiently informative experimental Sys-ID data, sparsity promoting algorithms aim to derive a model explaining this data with the fewest active terms [Nel01]. We can state such model as [Nel01, Pp. 219], describing the relation of model output $\hat{y}$ to the data X by regressors Θ:

$$\hat{y} = \Theta X \tag{3.20}$$

With change in the notation, such as to reflect the notation used in Paper D, as well as extension of X to both model states and inputs x and u, we can write

$$\dot{x} = \Xi \Theta^T(x,\ u) \tag{3.21}$$

We may infer Ξ using least–squares methods [Lju99]. Furthermore, we may estimate the probability density function (PDF) associated with Ξ using maximum likelihood estimation (MLE) or markov chain monte carlo (MCMC) methods. See [MZM16; Mad07; KMJ04].

3.1.2 Stationary System Models

Stationary system models aim to approximate the system in steady–state. Such point of view on the system is useful and appropriate when operating around a system equilibrium, alongside a range of assumptions. In the context of Microgrid operation, see [Sch+16b] for a discussion on these assumptions. A stationary system model is — as modeling approaches in general — an approximation. This simplification may be desirable when the trade–off of accuracy in representing the system dynamics versus reduced computational load is in favor for the latter. This typically is the case when considering large timesteps and large scale models. Notice that large scale models here can refer also to high model complexity.

As a result from these considerations, stationary system models are commonly used to determine feasible operating points of the system.

3.1.2.1 The AC Power Flow equations

Using the notation and formulation given in [MMD18], the real power flow in a line (l, m) modeled as symmetrical π –model is given by

$$p_{lm} = g_{lm}v_l^2 - g_{lm}v_l v_m \cos(\theta_l - \theta_m) - b_{lm}v_l v_m \\ \sin(\theta_l - \theta_m) \tag{3.22a}$$

and the reactive power flow

$$q_{lm} = -(b_{lm} + b_{sh,lm}/2)v_l^2 + b_{lm}v_l v_m \cos(\theta_l - \theta_m) - \\ g_{lm}v_l v_m \sin(\theta_l - \theta_m) \tag{3.22b}$$

The set of model spaces consists of the buses $i \in \mathcal{B}$ and the lines $(l, m) \in \mathcal{L}$. Real and reactive power injections and extractions are denoted p_i and q_i respectively, voltages and phasor angles v_i and θ_i respectively. We may assume that the angle reference for the MG is set at PCC and is, therefore, $\theta_{\text{ref}} = \theta_{\text{PCC}} = 0°$. See [MMD18] further details upon notation.

Power balance is achieved by restricting feasible states at each bus, see 3.23.

$$p_i = \sum_{(l,m)\in\mathcal{L}|l=i} p_{lm} + \sum_{(l,m)\in\mathcal{L}|m=i} p_{ml} + g_{sh,i}v_i^2 \tag{3.23a}$$

$$q_i = \sum_{(l,m)\in\mathcal{L}|l=i} q_{lm} + \sum_{(l,m)\in\mathcal{L}|m=i} q_{ml} + b_{sh,i}v_i^2 \tag{3.23b}$$

Notice that unbalanced and unsymmetrical systems are common in MGs, depending on their topology [Sch+16b].

3.1.2.2 *Additional Methods: Adaptive Linearization*

In contrast to the linearization with respect to one nominal operating point or an operating trajectory (see Section 3.1.1.2) in context of dynamical systems, we may optimize the approximation over a chosen operating polytope $\mathcal{O}$ as suggested in [MMD18]. They obtain a linearization minimizing the worst–case error of this approximation over a specified operational range, see an implementation of their in algorithm in Listing 1. See also an exemplary result in Figure 3.5.

This may be reasonable for dynamical system models as well, if the closed loop (CL) is robust enough to compensate for the resulting inaccuracies. Further, $\mathcal{O}$ should be chosen sufficiently small, such that the linearization error remains bounded in some range associated with robust controller performance. It can then lead to an LLM approximating the nonlinear system sufficiently well over a broader operating range.

Algorithmus 1 : `FindOptLin` algorithm, see [MMD18]

Input : f, $\mathcal{S}$, $\mathcal{O}$
Output : l

`// Minimize worst-case error`

for $\mathcal{S}$ **do**

$$\min_{l} \quad || \quad \max_{x,u} \quad || \quad f_l(x,u,l) - f(x,u) \quad ||^2||^2$$

if *optimal* **then**

return l

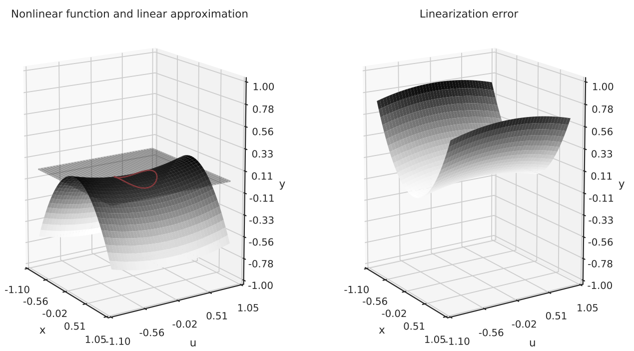

Figure 3.5: Approximation over an operating polytope $\mathcal{O}$, highlighted by a red circle in the left plot.

3.2 UNIT COMMITMENT

The unit commitment (UC) problem considers stationary system models (see Section 3.1.2). For the scope of application of such model and its optimization, dynamics are of inferior importance. The scope of UC is consequently the static system behavior. As result of this, UC enables the solution of large problem sizes using mixed integer linear problems (MILPs). Examples of static UC problems in context with MGs are given in [Bor+10; PRG16; Han+14; Com+16; NX17; KS12].

An UC considering stochasticity in steady state operation is denoted as stochastic unit commitment (SUC). This variation of the UC enables the treatment of uncertainty, for example, by application of stochastic programming (SP) approaches [CCM10a].

The UC or SUC may generate a new dispatch schedule $\bar{u}$ every 15 minutes, for example, as in [PRG14]. For an MG with moderate number of DERs, this provides sufficient time to apply scenario based optimization approaches [PRG16; ZG13].

The sampling rate and optimization horizon in general depend on the addressed problem. Typical problems are day–ahead (DA) market and balancing market dispatch, for which different variations of problem formulations exist [CCM10b; CCM10c; CCM10d; Mor+14].

Such approaches may include guarantees for a distinct security threshold, see [BKV13, Pp. 70-83].

3.3 CONTROL

In model based control, the model is the central component and affects the controller performance. Linear model predictive control (LMPC) provides sufficient performance in presence of mild nonlinearity, or over well chosen dynamics approximations. Furthermore, deriving control solutions based on linear models may reduce computational load compared to optimizing based on nonlinear models. By solving underlying nonlinear equations, we can warm–start linear model predictive control (LMPC) at well–chosen initial conditions [PRW11]. Such conditions are, therefore, candidate operating points for LMPC, see [HJS08; RMD17; CB04] for examples. Transients in the system dynamics are then treated for example by means of relinearization with respect to a given operating point.

3.3.1 Trajectory Planning

We need to translate the dispatch schedule $\bar{U}$, obtained using steady state optimization methods (see the SUC in Section 3.2), into a trajectory $\mathcal{T} = \{\tilde{X}, \tilde{U}\}$ feasible for the real–time (RT) system.

We may define the temporal period during which $\bar{U}$ is constant as *operating period*. A subsequent operating period is, then, associated with an updated $\bar{U}$.

We can state this problem as open loop (OL)–optimal control (OC) problem, involving the nonlinear dynamical system (Equation (3.1b) on page 15 or Equation (3.3b) on page 16), the dispatch schedule $\bar{U}$ and the set of constraints active in the corresponding operating period. Notice that $\bar{U}$ is optimal with respect to the objective considered by the generating routine. This typically is a minimum economic cost objective. Furthermore, $\bar{U}$ must satisfy system constraints in order to be well–posed.

Therefore, it may be redundant to consider the same objective already treated in the commitment problem. Yet, $\bar{U}$ is typically available at a lower temporal resolution, resulting from the properties of the generating routine and its scope, see Section 3.2. Additional differences in the problem parameterization apply, which further justify the dedicated treatment RT trajectory planning problem. Application of the same objective, or an alternative objective, in the trajectory planning problem is, therefore, reasonable.

Typical objectives are:

- Minimum time of converging to $\bar{U}$
- Minimum economic cost

Additional objectives may encompass the minimization of CO_2 or other emissions. Commonly, combinations of such objectives are reasonable, due to that:

- The minimum time objective may lead to intense wear and tear of the actuators.
- The minimum economic cost objective may lead to inadequate system performance.

Furthermore, we may consider constraints that enforce convergence to the dispatch schedule. Then, the main scope of the trajectory planning problem is to optimize for an interpolated target trajectory informed by the chosen objective. We can solve this OC problem using shooting or collocation methods [NW06].

As an example of a simple planning problem, assume the ODE Equation (3.1b) on page 15 is used, and furthermore, that $\bar{U}$ is derived by minimizing economic cost. We may then consider the planning objective:

$$\min_{u,x,s} = ||u - \bar{u}||^2_{P_{\Delta\bar{u}}} + ||s||^2_{P_{\Delta y}} \tag{3.24}$$

$$\text{s.t.} \tag{3.25}$$

$$y - \bar{y} + \epsilon_{\Delta y} + s = 0 \tag{3.26}$$

$$s \geq 0 \tag{3.27}$$

$$y = h(x, u, t, \theta) \tag{3.28}$$

$$\bar{H}\ u \leq \bar{h} \tag{3.29}$$

$$\bar{F}\ x \leq \bar{f} \tag{3.30}$$

Here, we account for the dispatch schedule $\bar{U}$ by transforming it to vector form using a suitable transformation. We then consequently consider $\bar{u}$. Furthermore, we may account for an output reference $\bar{y}$ in a similar manner. Here, we assume $\bar{y} = 0$. We may yield $y = 0$ for an inactive slack bound where $s = 0$ and consequently resolve this constraint up to computational precision. A defined precision $\epsilon_{\Delta y}$ may relax the precision in this equality constraint up to a prescribed value. $P_{\Delta y}$ are economic costs of deviating from the reference to the controlled variable $\bar{y}$, associated with the slack variables s. We must transform $P_{\Delta y}$ in order to reflect the proper cost terms per slack variable s_j.

Equation (3.24) minimizes the sum of squared errors of the RT input trajectory u from its reference $\bar{u}$ weighted by deviation prices $P_{\Delta\bar{u}}$. These are economic costs arising from deviating from the economically optimal schedule $\bar{u}$. s ensures feasibility. $P_{\Delta y}$ may relate to the cost of activating backup capacities in the case when $\bar{y}$ denotes the power balance within the grid. Equation (3.29) on the preceding page are general input constraints, Equation (3.30) on the previous page are general state constraints. These constraints may represent both limits on the absolute magnitude of $\{u, x, y\}$, as well as ramp–rate limitations.

The system dynamics Equation (3.28) on the preceding page and constraints (3.29), (3.30) model the system. This entails the alternating current power flow (AC-PF) Equation (3.22) on page 25 and bus power balance equations Equation (3.23) on page 26.

The solution set $\mathcal{T} = \{U,\ X\}$, transformed to matrix form, is then denoted as operating trajectory for linear model predictive controls (LMPCs) described in Section 3.3.2.

See also [ST14] and [Moh+18].

3.3.2 Linear Model Predictive Control

3.3.2.1 *Constraints*

INPUT CONSTRAINTS: In general, we may formulate input constraints as inequality constraints:

$$\bar{H}_{k+i|k}\, u_{k+i|k} \leq \bar{h}_{k+i|k} \tag{3.31}$$

Equation (3.31) may specify limitations on the magnitude of u and associated ramp rate:

$$u_{\min,k+i|k} \leq u_{k+i|k} \leq u_{\max,k+i|k} \tag{3.32}$$

$$\Delta u_{\min,k+i|k} \leq \Delta u_{k+i|k} \leq \Delta u_{\max,k+i|k} \tag{3.33}$$

A broad range of quadratic programming (QP) solvers support specialized and/or optimized handling of (3.32). Both Equation (3.32) and Equation (3.33) can be dynamic, as indicated by the subscript k.

STATE AND OUTPUT CONSTRAINTS: In general, we may formulate state and output constraints as inequality constraints:

$$\bar{F}_{k+i+1|k}\, x_{k+i+1|k} \leq \bar{f}_{k+i+1|k} \tag{3.34}$$

In conjunction with augmentation of the considered regulator objective by slack variables associated with soft output limits, we may formulate so–called soft constraints. See for example [RMD17, P. 8].

GENERAL SET: Constraints (3.35) below restrict the state x to lie in the set X:

$$x \in X \tag{3.35}$$

Similarly, we can formulate constraints for the output space y. These constraint types can lead to infeasibility and are therefore commonly reformulated to soft constraints, see for example [GJ09].

TERMINAL SET: For robustness considerations in deterministic MPC, we may enforce the terminal set constraint, requiring that the state at optimization horizon instant $k = N$ lies in X_N associated with a stable system operation [May+00]:

$$x_N \in X_N \tag{3.36}$$

As discussed in, for example, [RMD17, P. 248], this does not suffice in enforcing stability in context of SMPC.

CHANCE CONSTRAINTS: We may consider the probabilistic constraints on the states, using the formulation given in [Hei+18a]:

$$Pr_k\left[\bar{H}_j x_{k+i+1|k} \leq \bar{h}_j\right] \geq 1 - \gamma \tag{3.37}$$

where:

$$j = 1, 2, \ldots, n_s \tag{3.38}$$

n_s is the number of considered scenarios.

3.3.2.2 Target Problem

The RT system status may differ from the system status anticipated by the SUC problem (see Section 3.2) or the trajectory planning problem (see Section 3.3.1).

Convergence to the dispatch schedule $\bar{U}$ is then circumvented. Notice that here, $\bar{U}$ is the input reference feasible for the RT system, see Section 3.3.1 on trajectory planning.

We can test feasibility of $\bar{U}$ given the RT system status using the steady state target problem, modified from [RMD17, P. 48]:

$$\min_{x_s,u_s} \frac{1}{2}||u_s - \bar{u}||^2_{W_s} \tag{3.39a}$$

s.t.

$$\begin{bmatrix} I-A & -B \\ C & 0 \end{bmatrix} \begin{bmatrix} x_s \\ u_s \end{bmatrix} = \begin{bmatrix} G\bar{d} \\ \bar{y} \end{bmatrix} \tag{3.39b}$$

$$\bar{u} - \epsilon_{\bar{u}} \leq u_s \leq \bar{u} + \epsilon_{\bar{u}} \tag{3.39c}$$

$$Cx_s \leq \bar{f} \tag{3.39d}$$

Notice that we here assume Equation (3.39b) to satisfy the requirement of linear independence. This holds when the number of system outputs is less than the number of system inputs (ibid). Furthermore, notice that $\bar{u}$ is a transformation of $\bar{U}$ to a suitable vector representation. Equation (3.39c) states the required precision of convergence with respect to $\bar{u}$. The tuning weights matrix W_s is positive definite (PD).

If Equation (3.39) is infeasible, we trigger the recalculation of the trajectory planning problem with the currently observed lumped disturbance $\hat{d}_l$.

3.3.2.3 Setpoint Tracking

The quadratic control cost J in (3.40) below denotes the accumulated squared output errors in relation to the control effort and control rate of movement, weighed by the weights W_y, W_u, W_Δ and W_T:

$$J = \frac{1}{2} \sum_{i=0}^{N-1} [y^T_{k+i+1|k} W_y \; y_{k+i+1|k} + u^T_{k+i|k} W_u \; u_{k+i|k} + \\ \Delta u^T_{k+i|k} W_{\Delta u} \; \Delta u_{k+i|k}] + \frac{1}{2} y^T_{k+N|k} W_T \; y_{k+N|k} \tag{3.40}$$

Weights W_y and W_T are positive semi–definite (PSD), W_u and $W_{\Delta u}$ are positive definite (PD) [RMD17]. By minimizing Equation (3.40) subject to operational constraints, we obtain the associated deterministic optimal control input sequence $u^\star$:

$$\min_{u} \quad (3.40) \tag{3.41}$$

s.t.

$$x_{k+i+1} = Ax_{k+i|k} + Bu_{k+i|k} + Gd_{k+i|k} \tag{3.42}$$

$$y_{k+i+1} = Cx_{k+i|k} \tag{3.43}$$

$$\bar{H}_{k+i|k} \; u_{k+i|k} \leq \bar{h}_{k+i|k} \tag{3.44}$$

$$\bar{F}_{k+i+1|k} \; x_{k+i+1|k} \leq \bar{f}_{k+i+1|k} \tag{3.45}$$

$u^\star$ is the minimizing argument to this constrained QP:

$$u^\star = \arg\min(3.41) \tag{3.46}$$

In general receding horizon control, the inputs associated with the first control horizon iterate $k = 0$ are actuated in the plant.

In order to generalize this controller to the constrained linear quadratic regulator (LQG) form, we combine (3.41) with an augmented state observer (SO) in form of a Kalman filter. This generalization includes the assumption of normally distributed state noise and measurement noise. We drop the assumption of exact state knowledge and replace the state x with its estimate $\hat{x}$. Furthermore, we add the disturbance residual estimate $\hat{d}_r$, in order to enable for residual disturbance rejection[3] in conjunction with the estimation of $\hat{x}$. See Section 3.3.2.3 below.

Instead of considering only the first moment of x, the mean μ_x, we may propagate the hyper–state $\xi = P(\mu_x, \sigma_x^2)$ through the corresponding LLM. This linear projection provides an approximation of the uncertainty associated with future states. In conjunction with probabilistic constraints on the states or the outputs, this enables the implementation of stochastic model predictive controllers (SMPCs). See Section 3.3.2.5 on SMPC.

RESIDUAL DISTURBANCE REJECTION: Unknown disturbances lead to offset in steady state, if the regulator cannot infer such disturbance by means of a state observer (SO). We may denote the residual disturbance causing such offset as d_r and its estimate $\hat{d}_r$.

We can account for d_r by using the estimate $\hat{d}_r$, alongside the state estimate $\hat{x}$, within the constrained regulator Equation (3.41) on the preceding page. This includes the assumption of observability and is also referred to as offset–free control. The considered system model is then an extension of Equation (3.11) on page 18, the stochastic LTI model:

$$\hat{x}_{k+i+1|k} = A\hat{x}_{k+i|k} + Bu_{k+i|k} + G\hat{d}_{k+i|k} + G_r\hat{d}_{r,k+i|k} \tag{3.47a}$$

$$y_{k+i+1|k} = C\hat{x}_{k+i+1|k} \tag{3.47b}$$

Notice that the residual disturbance associated dynamics G_r are unknown. We have to estimate G_r, or choose them similarly as controller tuning parameters (see Section 3.3.3). See also [PGA15; PR03; RMD17].

We then consider the minimization of the following constrained objective:

3 Also referred to as offset–free control.

$$\begin{aligned}
\min_{u} \quad & J = \frac{1}{2}\sum_{i=0}^{N-1}[\hat{y}^T_{k+i+1|k} W_y \ \hat{y}_{k+i+1|k} + \\
& u^T_{k+i|k} W_u \ u_{k+i|k} + \Delta u^T_{k+i|k} W_{\Delta u} \ \Delta u_{k+i|k}] + \\
& \frac{1}{2} y^T_{k+N|k} W_T \ y_{k+N|k} && (3.48) \\
\text{s.t.} \quad & \\
& (3.47a) && (3.49) \\
& (3.47b) && (3.50) \\
& \bar{H}_{k+i|k} \ u_{k+i|k} \le \bar{h}_{k+i|k} && (3.51) \\
& \bar{F}_{k+i+1|k} \ x_{k+i+1|k} \le \bar{f}_{k+i+1|k} && (3.52)
\end{aligned}$$

Alternatively, we can search a combination of states and inputs compensating $\hat{d}_r$, as described in [PR03]. For each system model M, we can hereby formulate the following system of equations. Notice that here, I is a $n_x \times n_x$ identify matrix.

$$\overbrace{\begin{bmatrix} A - I & B \\ C & 0 \end{bmatrix}}^{M} \overbrace{\begin{bmatrix} \underline{x} \\ \underline{u} \end{bmatrix}}^{\underline{P}} = \begin{bmatrix} B_d d_r \\ \bar{y} \end{bmatrix} \tag{3.53}$$

A feedback gain K_∞ from the residual disturbance d_r balances the system:

$$\begin{bmatrix} A - I & B \\ C & 0 \end{bmatrix} \underbrace{\begin{bmatrix} K_{x,\infty} \\ K_{u,\infty} \end{bmatrix}}_{K_\infty} = \begin{bmatrix} B_d \\ \bar{y} \end{bmatrix} \tag{3.54}$$

Then, we can determine the couple $\underline{x}$, $\underline{u}$ compensating for $\hat{d}_r$ by:

$$\underline{P} = \{\underline{x} \, , \underline{u}\} = K_\infty \hat{d}_r \tag{3.55}$$

The minimizer of the constrained target adjusted residual disturbance rejection output error objective, using an augmented SO, is then given by:

$$\begin{aligned}
\min_{u} \quad & J = \frac{1}{2}\sum_{i=0}^{N-1}[(\hat{x}_{k+i+1|k} - \underline{x})^T W_x\ (\hat{x}_{k+i+1|k} - \underline{x}) + \\
& (u_{k+i|k} - \underline{u})^T W_u (u_{k+i|k} - \underline{u})] + G\hat{d}_{k|k} + \\
& \frac{1}{2} x^T_{k+N|k} W_T\ x_{k+N|k} && (3.56) \\
\text{s.t.} \quad & \\
& \hat{x}_{k+i+1|k} = A\hat{x}_{k+i|k} + Bu_{k+i|k} + G\hat{d}_{k+i|k} + G_r\hat{d}_{r,k+i|k} && (3.57) \\
& y_{k+i+1|k} = C\hat{x}_{k+i+1|k} && (3.58) \\
& \bar{H}_{k+i|k}\ u_{k+i|k} \leq \bar{h}_{k+i|k} && (3.59) \\
& \bar{F}_{k+i+1|k}\ x_{k+i+1|k} \leq \bar{f}_{k+i+1|k} && (3.60)
\end{aligned}$$

Notice that contrary to considering a single target adjustment within the prediction horizon $\underline{x}$ (and $\underline{u}$), we may consider targets at sampling resolution $\underline{x}_{k+i+1}$ (and $\underline{u}_{k+1}$).

3.3.2.4 *Trajectory Tracking*

The objective in Equation (3.61) includes both input–reference and output–reference tracking. See [MR93] or [CB04; GFH88; RMD17]. Equation (3.40) on page 32 is hereby augmented with the output reference $\bar{y}$ and the input reference $\bar{u}$:

$$\begin{aligned}
J = & \frac{1}{2}\sum_{i=0}^{N-1}[(y_{k+i+1|k} - \alpha\bar{y}_{k+i+1|k})^T W_y\ (y_{k+i+1|k} - \alpha\bar{y}_{k+i+1|k}) + \\
& (u_{k+i|k} - \beta\bar{u}_{k+i|k})^T W_u\ (u_{k+i|k} - \beta\bar{u}_{k+i|k}) + \\
& \Delta(u_{k+i|k} - \beta\bar{u}_{k+i|k})^T W_{\Delta u}\ \Delta(u_{k+i|k} - \beta\bar{u}_{k+i|k})] + \\
& \frac{1}{2} y^T_{k+N|k} W_T\ y_{k+N|k} && (3.61)
\end{aligned}$$

In contrast to the setpoint tracking problem described in Section 3.3.2.3, the tracking error minimization problem enables the direct modification of controller goals in the output and input spaces.

α and β switch the tracking in the output space and input space respectively:

$$\alpha \in \{0,\ 1\} \qquad (3.62)$$

$$\beta \in \{0,\ 1\} \qquad (3.63)$$

We obtain the deterministic optimal control input sequence similar as for the setpoint tracking regulator by minimization of Equation (3.61) subject to a deterministic system representation:

$$\min_{u} \quad (3.61) \tag{3.64}$$

s.t.

$$x_{k+i+1} = Ax_{k+i|k} + Bu_{k+i|k} + Gd_{k+i|k} \tag{3.65}$$
$$y_{k+i+1} = Cx_{k+i|k} \tag{3.66}$$
$$\bar{H}_{k+i|k}\, u_{k+i|k} \leq \bar{h}_{k+i|k} \tag{3.67}$$
$$\bar{F}_{k+i+1|k}\, x_{k+i+1|k} \leq \bar{f}_{k+i+1|k} \tag{3.68}$$

With $\alpha = 1$ and $\beta = 0$, (3.61) is a convex combination of output space tracking and input space tracking. The challenge in using this objective is the increased complexity of the associated tuning problem, compared to the setpoint tracking objective Equation (3.40) on page 32. We have to choose $W_{\bar{u}}$ such that we obtain balance in output tracking and input tracking precision while retaining sufficient stability. If $\bar{u}$ is ill–posed and $W_{\bar{u}}$ is too restrictive, we may face operational issues. As for general MPC, tuning is the main issue associated with this regulator form. Tuning must respect stability and robustness, see related citations in Section 3.3.2.3.

Similarly as in the previous Section 3.3.2.3, we can state this objective as SMPC, see Section 3.3.2.5.

RESIDUAL DISTURBANCE REJECTION: In tracking error minimization regulator form, we can achieve residual disturbance rejection[4] similarly as described in relation to the setpoint tracking regulator (see Section 3.3.2.3) by using an augmented SO. We then minimize Equation (3.61) subject to the stochastic system representation:

$$\min_{u} \quad (3.61) \tag{3.69}$$

s.t.

$$\hat{x}_{k+i+1|k} = A\hat{x}_{k+i|k} + Bu_{k+i|k} + G\hat{d}_{k+i|k} + G_r\hat{d}_{r,k+i|k} \tag{3.70}$$
$$y_{k+i+1|k} = C\hat{x}_{k+i+1|k} \tag{3.71}$$
$$\bar{H}_{k+i|k}\, u_{k+i|k} \leq \bar{h}_{k+i|k} \tag{3.72}$$
$$\bar{F}_{k+i+1|k}\, x_{k+i+1|k} \leq \bar{f}_{k+i+1|k} \tag{3.73}$$

Using the target adjusted approach described in Section 3.3.2.3, we can formulate the following objective in tracking error minimization regulator form:

4 Also referred to as offset–free control.

$$
\begin{aligned}
J = & \frac{1}{2} \sum_{i=0}^{N-1} \left[(\hat{x}_{k+i|k} - \underline{x})^T W_x \; (\hat{x}_{k+i|k} - \underline{x}) + \right. \\
& \beta (u_{k+i|k} - u_{k+i|k-1})^T W_u (u_{k+i|k} - u_{k+i|k-1}) + \\
& \left. (1-\beta)(u_{k+i|k} - \bar{u})^T W_{\bar{u}} (u_{k+i|k} - \bar{u}) + G\hat{d}_{k+i|k} \right] + \\
& \frac{1}{2} x_{k+N|k}^T W_T \; x_{k+N|k}
\end{aligned} \tag{3.74}
$$

Again, we here use the system model Equation (3.70) and Equation (3.71) in conjunction with this objective.

3.3.2.5 *Stochastic Control*

If the disturbance acting on the system is bounded, we can apply stochastic control principles to the system [RMD17, P. 248].

The residual disturbance rejection regulators discussed in Section 3.3.2.3 and Section 3.3.2.4 consider stochastic linear system models such as Equation (3.11) on page 18. We can cast them as stochastic controllers when considering probabilistic state constraints, in literature often referred to as *chance-constraints*.

The general state constraint (or output constraint) we can formulate as:

$$
\bar{H}_j x_{k+i+1|k} \leq \bar{h}_j \tag{3.75}
$$

We can then state the chance–constraint [Hei+18a]:

$$
\mathrm{Pr}_k[(3.75)] \geq 1 - \gamma_j, \quad j = 1, 2, \ldots, n_s \tag{3.76}
$$

The left–hand–side here states the probability of satisfying (3.75) with a prescribed lower bound $1 - \gamma_j$, where j is the scenario index. n_s is the number of considered scenarios.

The main challenge associated with this constraint formulation is to achieve the desired trade–off between robustness and cost. See for example [Hei+18a; SGM13; PRG16; Can+10; RMD17]. In context of the optimal power flow (OPF) problem, see for example [Old+15; Sum+14; Roa+13; RA17].

Sampling based stochastic formulations for LMPC may be prohibitive for RT application due to their elevated computational complexity [Kou+10].

These issues may be alleviated when making assumptions about the disturbance. An example is [DBK06], in which they assume a norm–bounded disturbance and computation of control decisions for the worst–case realization. They approximate this worst–case linearly and can guarantee the worst–case feasibility.

3.3.3 Tuning and Stability

While tuning is a key aspect in controller design in general, this applies specifically to model based controllers:

"The first act of 'tuning' is to develop an appropriate process model. If the model is accurate enough, then the rest of the tuning is straight-forward. And if the controller exhibits poor performance, then one should consider the model poor (inaccurate) unless proven otherwise" [GS10].

Tuning entails a multitude of aspects, some of which compete in the considered objectives. Then, balancing measures are required. Multi–objective optimization can facilitate the determination of well balanced adjustments, see for example [YZO16].

While some tuning aspects apply in general, some are highly specific to the operational situation. In relation to control related topics, a selection of tuning aspects is discussed below.

3.3.3.1 *Trajectory Planning*

We must solve this nonlinear OC problem intermittently, hereby the RT–supervisory control and data acquisition (SCADA) system triggers the solver calls. The call frequency depends, in general, on the operating situation. In relation to performance, tuning of this problem may therefore be more relevant for specific operating situations. Tuning of the call frequency can lead to sufficient accuracy in the control decisions while reducing the computational load.

A related tuning problem is the selection of the temporal resolution. For example, in [RMD17, P. 513], an example of efficiency tuning of NMPC is given by the "adaptive stepsize selection". They underline the importance of this measure for the efficiency of NMPC.

The parameterization of this problem entails process models of both the system and uncertain disturbance processes driving the former. Depending on the process models and available data, tuning may then entail adjustment of the associated data analysis routines or the model used within the optimization problem. For example, uncertain disturbance process prediction models may generate prohibitively large number of scenarios to be efficiently treated with RT controls. Scenario reduction techniques can then provide a reduced set of scenario clusters. Along those lines we can also optimize the models for RT controls. We may first transform a complex process model to a ROM representation prior to using it during RT operation.

3.3.3.2 *Linear MPC*

The linearization approach utilized to derive the local linear model (LLM) used in linear model predictive control (LMPC) is a starting point for tuning. When we obtain the LLM through Sys-ID experiments, we must consider tuning of the candidate Sys-ID method [Lju99].

The underlying system model may be precise in vicinity of the system's operating point but generalize poorly when leaving it. Active learning techniques such as [Hei+18b; HSM19] or adaptive control [Ngu17] techniques can support the reduction of uncertainty during online operation. Along these lines, [MDG17; Sir+10; DE18; Vaj+85] are publications in relation to energy– and power systems.

The evaluation of the stability of the LLM is a prerequisite to its utilization in MPC. Stability evaluation must hereby include the derivation of stability margins defining the operating region $\mathcal{O}$.

Regularization of the objective is commonly achieved by tuning of the control decision related penalization matrices:

CONTROL MAGNITUDE PENALIZATION coefficients W_u must be adjusted in both absolute magnitude and in relative magnitude.

CONTROL EFFORT PENALIZATION coefficients $W_{\Delta u}$ must be adjusted, similarly as the control magnitude penalization.

See Equation (3.40) on page 32 for a utilization of these penalization coefficients.

We can simplify the tuning problem by removing the control effort penalization term while retaining the control magnitude penalization. This highlights the typical balancing issue associated with tuning. Additional complexity in the control objective may lead to desired controller performance but complicates the tuning problem.

Other tuning approaches involve specification of a surrogate problem for which tuning is easier. An example is [DB09], in which they tune MPC such that the unconstrained controller obtains equal properties as a discrete time linear quadratic regulator (DLQR) with desired static gain K.

By using soft constraints we can modify the objective function such that we penalize overshoot of state– or output soft–limits, as exemplified in [GJ09], while retaining feasibility. This comes at expense of elevated computational load, depending on the number of slack variables and added constraints in the augmented objective.

We can treat stochasticity in LMPC using chance-constraints. The controller is then cast as SMPC. See Section 3.3.2.5. The accuracy of the estimated back–off depends on the knowledge of the disturbance, for which reason the quality of the disturbance model is central in SMPC. [Hei+18a] provide a related discussion.

3.3.3.3 *Stability*

Stability in MPC we can assess by Lyapunov stability theory. As stated in [RMD17, P. 164, 165], a local control Lyapunov function (LCF) enhances the performance of MPC. A *terminal cost* is such LCF (ibid,

P. 165). In order for such terminal cost to take its desired effect, one can add a *terminal constraint*, requiring the state to lie in a desired set in which the terminal cost is an LCF (ibid). This terminal constraint must be control invariant (ibid), we briefly state it in Equation (3.36) on page 31.

Dual mode control is a related approach that uses the beneficial stability properties associated with infinite horizon control. See for example [KC16, Pp. 28]. Sufficiently large optimization horizons[5] enforce robust asymptotic stability [Tee04], [RMD17, P. 169]. In the limit, an MPC with theoretical infinite optimization horizon approaches an infinite horizon optimal controller and then inherits its stability properties (ibid). The optimization horizon should hereby at least encompass 80-90% of the OL rise time of the system, as stated in [Mau+88], for example.

A seminal paper in context of stability is [May+00], where they identify stability ingredients appearing in MPC, so–called *stability axioms* [RMD17, P. 169]. For additional requirements, assumptions and variations see for example [KC16, P. 13 and following] or [RMD17; CB04; Mac02].

In this thesis we consider the principle of long horizons. Reduction of the optimization horizon may reduce computational load, but may require the consideration of terminal constraints. The latter however add to the computational load, which in return is undesirable. Furthermore, terminal constraints complicate the MPC design process, as it may require constraint tightening as employed in [Tee04]. [PRW11] underline the importance of *feasibility resolution* whenever state or output constraints are considered.

They furthermore stress the importance of a "well–defined set of initial conditions" (ibid). This initial value problem entails the requirement of a *guarantee of feasibility* [Kou+10].

[PRW11] "conclude that there is no qualitative change in robustness when shifting from optimal MPC to suboptimal MPC for the class of models considered here". In consequence, they show that we can achieve robustness also when using suboptimal MPC.

3.3.4 Additional Methods

Here we state methods that have not been explicitly covered within the publications in this thesis, however do pose reasonable additions.

3.3.4.1 Economic Model Predictive Control

While tracking of economic operating references $\bar{U}$ inherently accounts for economic considerations, economic MPC treats economics implicitly within the optimization step. The dynamic problem is then informed

5 Here, equivalent to *prediction horizons*.

by, for example, per–unit excursion prices. Deviations from this operating reference $\bar{U}$ are in LMPC informed by the control effort matrix $W_{\Delta u}$ and the model as such. [OM16] propose a tuning method for conventional MPC such that similar economic performance as when using economic MPC is achieved. Consider also [EDC14; DAR11].

3.3.4.2 *Nonlinear Model Predictive Control*

Modern algorithms used in NMPC may converge to the optimal solution in similar time as LMPC, depending on the problem at–hand [Gro+20]. As NMPC can directly handle the nonlinear model and nonlinear constraints it may simplify the control pipeline by removal of the distinction into trajectory planning (see Section 3.3.1) and online control (see Section 3.3.2). Robust NMPC implementations are also reported to provide comparable performance as LMPC schemes [KAM19; Koh+].

3.3.4.3 *Explicit Model Predictive Control*

Lookup tables are commonly used in control. Explicit MPC uses such principles [Bem+00; AB09] by precomputing the control law and storing it within a lookup table. For some applications, this can improve performance as the problem reduces to applying the correct gain for a given operational situation. Such approaches have been also applied to stochastic nonlinear problems [GKJ07; GJ12].

3.3.4.4 *Adaptive Control and Active Learning*

Adaptive control enables online–reformulation of the control law for a given system uncertainty. We may consider it, therefore, as an online tuning approach:

"An adaptive control system can be broadly described as any control system that has the ability to adjust control design parameters such as control gains online based on inputs received by the plant in order to accommodate the system uncertainty [...]" [Ngu17, P. 2].

Active learning on the other hand aims to augment the control law such that uncertainty in the system can be identified by making it observable [Mes18; HSM19; Hei+18b].

3.4 ESTIMATION AND PREDICTION

3.4.1 State Observer

For linear systems and Gaussian noise, the Kalman filter [Kal60] is the optimal SO. In this thesis, we assume this setting and refer to the large body of literature in context with nonlinear system estimation and non–normal distributions.

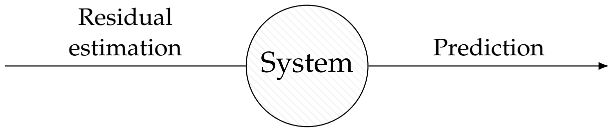

Figure 3.6: Residual estimation and prediction in a dynamical system: We can infer the approximated residual error using an augmented SO. The residual error may partly result from suboptimal predictions.

The Kalman filter consists of the *prediction step*[6]:

$$\hat{x}_{k|k-1} = A\hat{x}_{k-1|k-1} + Bu_{k-1} \tag{3.77}$$
$$\Sigma_{k|k-1} = A\Sigma_{k-1|k-1}A^T + Q_k \tag{3.78}$$

and following update step:

$$K_k = \Sigma_{k|k-1}C^T(C\Sigma_{k|k-1}C^T + R_k)^{-1} \tag{3.79}$$
$$\Sigma_{k|k} = (I - K_kC)\Sigma_{k|k-1} \tag{3.80}$$
$$\hat{x}_{k|k} = \hat{x}_{k|k-1} + K_k(y_k - C\hat{x}_{k|k-1}) \tag{3.81}$$

Notice I is here an identify matrix of suitable dimension. Σ is the state precision or state covariance matrix. Q denotes the variance of the state noise, R denotes the variance of the measurement.

Both the state estimate $\hat{x}$ and the precision P characterize a Gaussian distribution ξ_x [7]:

$$\xi_{x,k|k} = \mathcal{N}(\hat{x}_{k|k}, \Sigma_{k|k}) \tag{3.82}$$

See also [KMJ04].

By mapping the distribution ξ_x into the system output, we obtain the estimated output distribution:

$$\xi_{y,k|k} = C\xi_{k|k} \tag{3.83}$$

We may augment the considered system in order to estimate additional system states as described in the following Section 3.4.2 on disturbance rejection.

Tuning of such state observer is equally important for the regulator performance as tuning of the controller. See also [RMD17] for further discussions, for example on the unscented Kalman filter (ibid, Pp. 310).

6 Also referred to as *time–update*.
7 In literature sometimes referred to as *hyperstate of* x.

3.4.2 Disturbance Rejection

Model–plant mismatch always occurs, due to that the model is merely an approximation of the true system. Disturbance rejection, therefore, is a central aspect in control. See for example [PR03].

3.4.2.1 *Augmented State Observer*

We estimate the system state x alongside a residual disturbance d_r in order to enable system controllers to account for the latter.

STATIC FILTER: As described for example in [PR01; PR03], we may consider the augmented system dynamics:

$$A_o = \begin{bmatrix} A & B_d \\ 0 & I \end{bmatrix} \tag{3.84a}$$

$$B_o = \begin{bmatrix} B \\ 0 \end{bmatrix} \tag{3.84b}$$

$$C_o = \begin{bmatrix} C & C_d \end{bmatrix} \tag{3.84c}$$

I here is an identity matrix of dimensions corresponding to the residual disturbance d_r, that is, a unity scalar. B_d are hereby model residual disturbance $\hat{d}_r$ associated dynamics. When neglecting feedthrough of the residual disturbance d_r to the output, we let $C_d = 0$. Due to that B_d are commonly unknown we have to approximate them. Resulting from that this models the residual disturbance acting on the model input space, this is in literature referred to as input–disturbance model.

Furthermore, we consider the augmented states:

$$x_o = \begin{bmatrix} x \\ d_r \end{bmatrix} \tag{3.85}$$

and the augmented static Kalman gain:

$$L_o = \begin{bmatrix} L_x \\ L_d \end{bmatrix} \tag{3.86}$$

The filter gains $L_o = \{L_x \quad L_d\}$ are result of solving the discrete time algebraic riccati equation (DARE), see [Van81; Lau78]. The static input disturbance residual filter equations are then given by:

$$\hat{x}_{o,k|k} = A_o \hat{x}_{o,k|k-1} + B_o u_k + L_o (y_{m,k|k-1} - C_o \hat{x}_{o,k|k-1}) \tag{3.87}$$

In relation to Equation (3.85), $\hat{x}_o$ then denotes the estimate of the augmented state x_o. $\hat{x}$ and $\hat{d}_r$ are consequently estimates of the system state and the residual disturbance. y_m is the output measurement.

DYNAMIC FILTER: Using the augmented system equations stated in Equation (3.84) in the previous section, we can state the augmented dynamic filter equations as:

$$\hat{x}_{o,k|k-1} = A_o\hat{x}_{o,k-1|k-1} + B_o u_{k-1} \tag{3.88}$$

$$\Sigma_{k|k-1} = A_o\Sigma_{k-1|k-1}A_o^T + Q_k \tag{3.89}$$

and following update step:

$$K_k = \Sigma_{k|k-1}C_o^T(C_o\Sigma_{k|k-1}C_o^T + R_k)^{-1} \tag{3.90}$$

$$\Sigma_{k|k} = (I - K_k C_o)\Sigma_{k|k-1} \tag{3.91}$$

$$\hat{x}_{o,k|k} = \hat{x}_{o,k|k-1} + K_k(y_{m,k|k-1} - C\hat{x}_{k|k-1}) \tag{3.92}$$

3.4.3 Predictions

Predictive capabilities are at the core of modern energy system control approaches. Disturbances acting on the system, switching actions or other events affect the system and its performance. Predicting such events within the operational routines enables anticipatory action, thereby improving the systems actual performance. See an example of proactive action of an MPC in Figure 3.7.

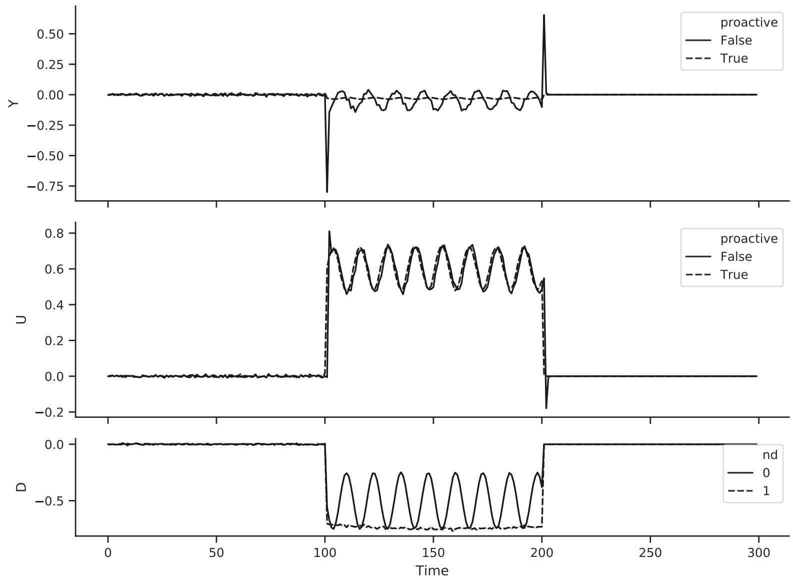

Figure 3.7: Predictive MPC/ reactive MPC example. The control horizon is chosen as $N = 10$. Perfect knowledge of the disturbance trajectories is assumed.

Forecasting services may provide probabilistic forecasts of stochastic processes, such as wind speed. See [Mor+14, Pp.26] and [BKV13] for examples. See [ZL16] in context of load forecasting.

Apart from central drivers of power conversion, forecasts for ramp detection [BKV13, Pp. 40-54] may provide valuable information for preparing the system for such events.

In the real setting associated with limited information, we can only anticipate a share of upcoming RT system disturbances. Even when aiming to predict a substantial share of such potential disturbances, we cannot remove the stochasticity arising, amongst others, from human behavior. Announcement of switching may, therefore, improve the system operation. For example, EV owners may provide information on an upcoming trip some minutes ahead of time. The RT controls can then prepare the system by means of proactive action.

3.4.3.1 Combining Process Estimates and Predictions: Probabilistic Weighting

Multiple sources of information of a process can be available for system operation. Probabilistic approaches enable informed weighting of such information for improved decision making. See for example [Sim06; Sco15]. Erroneous predictions are not only uninformative, but moreover can harm the system performance and its stability. Considering the uncertainty associated with the prediction using Bayes' theorem is one approach to deciding which source of information is to be trusted.

3.5 CONTROL HIERARCHIES

Control hierarchies[8] are layered constructs of controllers. We may refer to subsequent controllers as *superordinate* for a relative superior hierarchy position and *subordinate* for a relative inferior position. These enable the design of controllers tailored to the requirements corresponding to a given *layer*[9]. Such requirements can include, for example, the complexity for the derivation of appropriate control decisions.

More specifically, such requirements are:

- associated with the calculation of well–posed control signals at a desired sampling rate
- associated with the precision in the control decisions

We may address these potentially contradictory requirements by identification of the problem structure. Consider the following examples:

8 In literature also referred to as *control cascades*.
9 In literature also referred to as *level*.

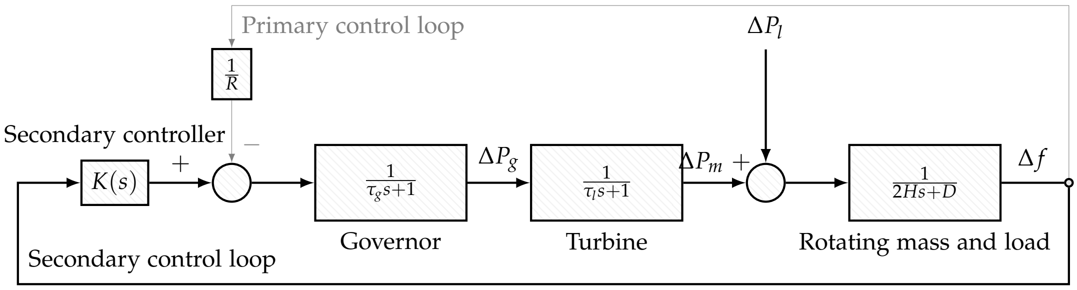

Figure 3.8: Exemplary block diagram of a turbine with governor system and approximated influence on the system frequency. The primary control loop here is a proportional factor (droop), the secondary control loop may be an optimized controller with integral action. See for example [Bev14; Kla17; Bem].

- In the load frequency control (LFC) problem the primary, secondary and tertiary frequency controls act on different dynamics and have different properties, see Figure 3.8. The main task of primary controls is to reject fast disturbances. The main task of secondary controls is to restore the grid frequency to the nominal frequency using integral action. See [Kun94; Bev14].
- Lower layers derive control decisions for potentially fast actuators. If such unit is to participate to its full capability, the controller formulation must be accordingly. See [Gey17] for examples along these lines. Precision with respect to the remaining system is then accounted for by tracking references from a superordinate layer that takes the overall system into account. Such layer naturally considers problems only solvable with considerable computational effort. Therefore, accurate references from the global system perspective are available at comparable lower sampling rates.

Analysis of subsequent layer requirements and integration within the control hierarchy enables us to exploit the causality of the problem. Consequently, we can treat computationally demanding tasks in superordinate layers while focusing on the requirements at subsequent subordinate layers.

A hierarchy of controllers arranged for different magnitudes of dynamics is, therefore, denoted a *temporal control hierarchy*.

Aside from generating control references, superordinate controllers may generate additional information relevant to subordinate controllers. For example, these may be risk values or economic prices. Such information may then be available at the subordinate level without additional computational expense.

Consider along these lines Figure 3.10. This control hierarchy comprises an energy management system (EMS) layer, optimized aggregated layer and basic layer. This hierarchy consists of two main layer groups:

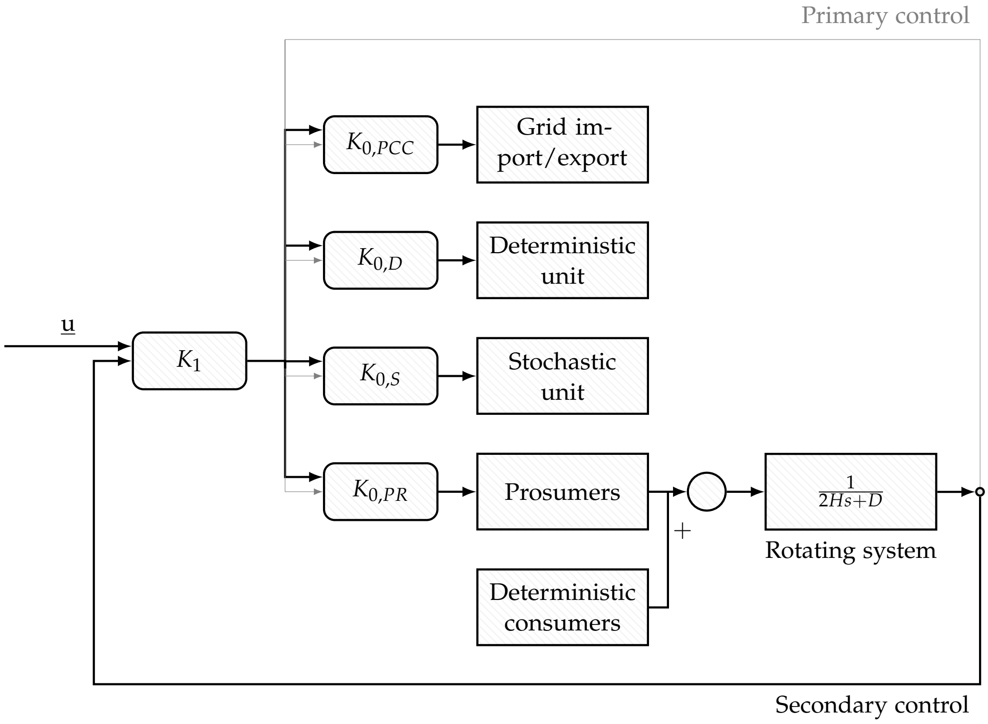

Figure 3.9: Exemplary block diagram of aggregated system controls for the AGC problem with a secondary controller.

STATIC PROBLEM which we may formulate as stochastic programming (SP) (see Section 3.2). This layer focuses on the long–term optimization, the treatment of forecasts of stochastic processes and a detailed system description in steady state. This layer generates a dispatch schedule $\bar{U}$. The dispatch schedule is passed to subordinate layers.

DYNAMIC PROBLEM for the RT system operation, hereby consisting of an aggregated optimized control layer and basic controllers at subsequent plants.

- **OPTIMIZED AGGREGATED CONTROL** coordinates the RT system, such that the overall system can participate in, amongst others, disturbance rejection, tracking of the dispatch schedule $\bar{U}$ or activation of additional flexibility when needed.

- **BASIC CONTROLLERS** actuate the plants for fast RT control objectives, such as compensation of fast frequency fluctuations.

Both EMS and RT are relevant in context of this thesis and are, therefore, highlighted in Figure 3.10. For an energy system with considerable uncertainty, the operating points specified in the dispatch schedule $\bar{U}$ must be feasible during real–time operation.

Related to the control hierarchy concept are associated tuning tasks. For example, the trajectory tracking controller discussed in Section 3.3.2.4 must be parameterized such that it tracks the input reference

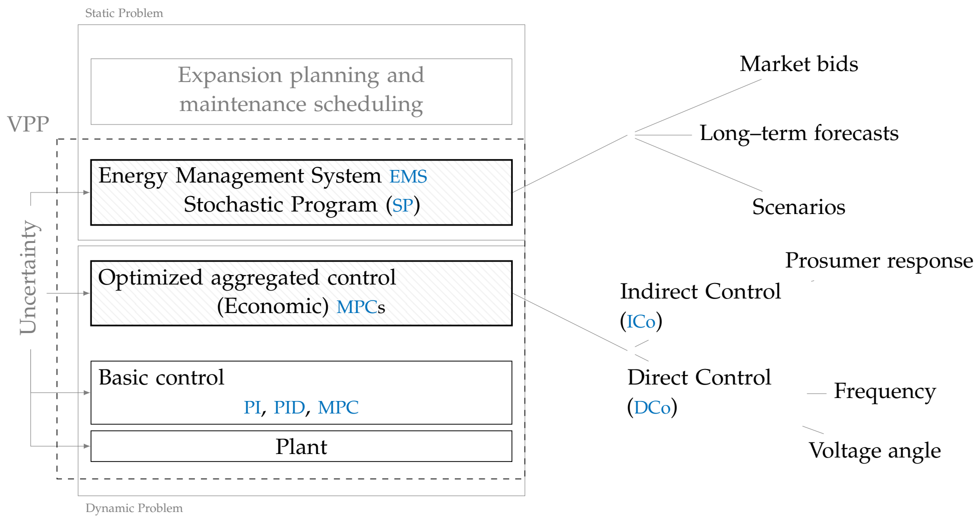

Figure 3.10: A temporal control hierarchy and associated scopes.

provided by a superordinate layer with sufficient precision. Furthermore, such parameterization should also provide sufficient degrees of freedom for such RT controller in order to compensate for excessive fluctuations and disturbance events. An example is the loss of a plant, where the RT controller can orchestrate the overall system to compensate for this loss in a coordinated manner. A sufficient decoupling of layers within the hierarchy therefore improves robustness, as subordinate controllers can deviate from provided control references.

4 BASIC MODELS AND KEY FINDINGS

This chapter summarizes models and key findings in this thesis.

Section 4.1 discusses the real–time Supervisory Control And Data Acquisition (RT–SCADA) system. Section 4.2 considers control scopes. Section 4.3 discusses automatic generation control (AGC) in context of microgrids (MGs). Section 4.4 gives a brief discussion on automatic voltage regulation (AVR) in context of MGs. Section 4.5 considers the activation of prosumers.

4.1 REAL–TIME SUPERVISORY CONTROL AND DATA ACQUISITION

The real–time (RT) supervisory control and data acquisition (SCADA) system organizes the optimized controls associated with the aggregated real–time (RT) layer. It is, therefore, a central component of the RT MG layer.

As mentioned in Section 2.5 on MG operations, operational requirements of an MG are most likely time–varying. This may involve:

TARGET TRAJECTORY type to be optimized for, such as a minimum time or a minimum economic cost trajectory (See Section 3.3.1 on trajectory planning).

CONTROLLER formulation, involving a selection of the controller type and its parameterization.

- **TYPE** selection. (See Section 3.3.2 on LMPC).
- **PARAMETERIZATION** of the controller, involving the controller model and treatment of the tuning problem.
  - **TUNING PROBLEM** involving the specification of the control effort penalization (See Section 3.3.3 on tuning).
  - **MODEL** composition. This involves the selection of active units during the upcoming operation period.
  - **PROBING CONSTRAINTS** formulation. Such constraints may trigger the execution of a backup routine should the controller fail. Equation (3.35) on page 31 is an example. Instead of provoking controller failures, we may instead examine slack variable values s_j active when well–define boundaries are violated. This can allow us

to call a backup routine while actuating the currently valid control decision in the plant.

This list can may be extended given the operational requirements. Two characteristic operational scenarios are:

SYSTEM STABILIZATION Hereby the system operates with a constant operating point, see Section 3.1.1.2.

TRAJECTORY TRACKING Hereby the system operates with respect to an operating trajectory, see Section 3.1.1.2.

4.2 CONTROL SCOPES

We aim to operate the RT system with respect to a given dynamic system trajectory set $\mathcal{T}$, obtained by solving the trajectory planning problem (see Section 3.3.1). We can derive local linear models (LLMs) in perturbation form with respect to $\mathcal{T}$. Consequently, we state such LLMs in a local coordinate system[1].

The temporal resolution in $\mathcal{T}$ is a relevant metric defining the RT system performance. While a coarsely meshed $\mathcal{T}$ may be well–posed, it translates to more dominant discontinuities in the RT trajectory. Higher sampling rate in the trajectory planning problem alleviates undesirable magnitudes in such discontinuities, while resulting in elevated computational load. A suboptimal workaround is naive interpolation.

We can operate along $\mathcal{T}$ by either using the setpoint tracking regulator (see Section 3.3.2.3) or the trajectory tracking regulator (see Section 3.3.2.4). In Sections 4.2.1 and 4.2.2 below we discuss the differences to consider when using either regulator formulation.

4.2.1 Setpoint Tracking

An optimized predictive setpoint tracking regulator can drive the system to the origin in a local coordinate system, when conditions for residual disturbance rejection apply. See Section 3.3.2.3 on setpoint tracking.

The local coordinate system is defined by the operating point and approximated system dynamics within the local coordinate system by the LLM using by the controller. See Section 3.1.1.2.

Due to that disturbances in the considered control situations always occur, we formulate this regulator with the goal of residual disturbance rejection. See Section 3.3.2.3. We may consider such regulator as SMPC formulation in order to stabilize the system states or outputs within a chosen set with chosen probability.

1 Also referred to as *local reference frame*.

In either regulator formulation, the single reference of this regulator is the local coordinate system. Discontinuities of the RT trajectory $\mathcal{T}$ translate into discontinuities in the objective of such regulator. Therefore, the quality of $\mathcal{T}$ determines a large share of the overall control performance. In consequence, we need to solve the nonlinear trajectory planning problem with a smaller timestep in order to improve RT performance. Due to being a nonlinear problem, computational limitations arise to this effect.

We can partly improve on this issue by considering the trajectory tracking regulator formulations, as discussed in Section 3.3.2.4 below.

4.2.2 Trajectory Tracking

Contrary to the setpoint tracking regulator formulations, the trajectory tracking regulator formulations can consider interpolations of the input and output references $\bar{u}$ and $\bar{y}$. See Section 3.3.2.4. While still considering a local coordinate system, this enables smoothing of the trajectory tracking problem informed by the local LMPC law. Naive interpolation of $\mathcal{T}$ is suboptimal. However, when interpolating using LMPC we retain some optimality. We can state such regulators similarly as discussed in the previous section 3.3.2.3.

4.3 AUTOMATIC GENERATION CONTROL IN MICROGRIDS

By augmenting the temporal control hierarchy depicted in Figure 4.1 on the next page with an aggregated RT layer we can optimize the power sharing problem. For brevity, we denote the *aggregated real–time* (RT) controllers as *real–time* (RT) controller and the *temporal control hierarchy* as *control hierarchy*, from here on.

The swing equation is the main model component in this control problem and describes the approximated inertia of the rotating system:

$$\frac{d}{dt}\Delta f(t) = -\frac{D_a}{2H(t)}\Delta f(t) + \frac{1}{2H(t)}\Delta P_{\text{mech}}(t) \tag{4.1}$$

Δf is the frequency excursion in relation to the nominal frequency, D is the load damping factor, $H(t)$ the inertia based supply time. ΔP_{mech} denotes the power balance. Notice that we here state H as function of time as suggested in [UBA14].

By combining plant models with Equation (4.1) we obtain an approximated mapping of active power injections and extractions to frequency excursions. We use this model in the RT controller(s) to the drive frequency excursion to zero and, therefore, the frequency towards the nominal frequency.

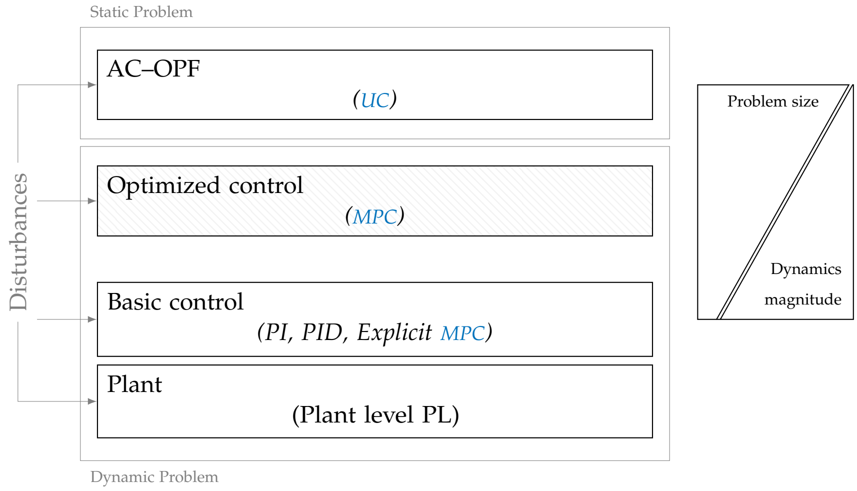

Figure 4.1: Control hierarchy for AGC with optimized aggregated RT controller. The alternating current optimal power flow (AC-OPF) is the problem with highest complexity, magnitude of dynamics increase when descending the hierarchy.

We can address efficiency considerations and uncertainty treatment at distinct layers in a control hierarchy as depicted in Figure 4.1.

We may denote efficiency metrics at a layer–level as local efficiency metrics and system efficiency metrics as global efficiency metrics. While we may optimize the local efficiency at a distinct layer, this may have adverse impacts on the overall system efficiency. This observation follows from that the control hierarchy is coupled. Consequently, global system efficiency in this setting is a multi–objective problem. A well–balanced trade–off of this problem depends, among others, on the MG, its current composition and operational goals of the system operator. The chosen efficiency metric is therefore also time–varying.

Disturbances act on the system at the subsequent layers and associated magnitudes of dynamics. Feasibility of the system operation therefore depends on uncertainty treatment at least on the upper layers. Performance can then be further improved by treating uncertainty also in subsequent lower layers.

We may improve RT system performance further by exploiting additional degrees of freedom. See along these lines Section 4.5 on prosumer response activation.

Papers Paper A, Paper B, Paper C and Paper E are related to the AGC problem.

4.3.1 AGC Combining Nonlinear and Linear Model Predictive Control

The optimized control layer depicted in Figure 4.1 may consist of an RT–SCADA system (see Section 4.1), including:

- The trajectory planning problem (see Section 3.3.1).
- The target problem (see Section 3.3.2.2).
- At least one optimized aggregated system controller (see Section 3.3.2.3)[2].
- A set of models (see Section 3.1).

For the upcoming operation period, the main task of the RT–SCADA system is then:

SOLVE THE TRAJECTORY PLANNING PROBLEM as a single objective or a multi–objective problem in order to obtain a feasible convergence trajectory to $\mathcal{T}$. See Section 3.3.1. This entails the treatment of disturbance forecasts when useful. This is the case, for example, when disturbance forecasts are available with higher temporal granularity than the sampling rate of the dispatch problem. In this case, we can then consider such residual disturbance forecasts in the RT layer. See Section 3.4.3.

SELECT THE RT CONTROLLER(S) given the system type and its status. More specifically, dynamics within the system may be heterogeneous to a degree where dedicated RT controllers per dynamics cluster are reasonable. For example, BESSs and diesel generators are two groups of heterogeneous dispatchable production units.

PARAMETERIZE THE AGGREGATED RT CONTROLLER(S) for the AGC problem, including the following tasks:

SELECT THE RT CONTROLLER MODEL based on the current system status. Only the active set of controllable units available as actuators throughout the operation period is relevant. See Section 3.1. This may involve:

ASSIGNMENT OF LOCAL ERROR EVALUATION FUNCTIONS to each model. Such a function should observe the linearization error and trigger recurrent linearization when required. See Section 3.1.1.4.

RESIDUAL ERROR ASSOCIATED DYNAMICS which we need to approximate. Evaluation of the uncertainty associated with subsequent systems (for example, heterogeneous loads) can inform the modeling of this quantity and provide an initial guess. We may in this way improve convergence of the estimation routine to the global minimum of this problem.

2 We can apply aggregated controllers to distinct groups of actors. For example, one controller may operate fast actuators (e. g. BESS), another slower actuators (e. g. conventional generators).

CONSTRAINT preparation. Subsets of constraints may be time–varying and based on system observations. This aspect, therefore, includes the data acquisition for these constraint groups.

Additional inputs to this RT control problem may apply in different settings.

Operational scenarios associated with islanded mode (IM) and grid-connected mode (GCM) differ fundamentally:

- In GCM, the MG has no ability to steer the grid–frequency f. In GCM, priorities are in consequence tracking and predictive action with respect to input references $\bar{\mathcal{U}}$ provided by the higher control layer, constraint satisfaction, residual disturbance rejection and provision of resilience.

- In IM, we can steer the grid–frequency to the nominal frequency. The local grid is less inert, dynamics are in consequence faster. In order to account for this, we need sufficiently fast controllers and actuators. The operating condition is more stringent.

Notice that switching in between these two modes is another relevant mode that is not considered in this thesis.

We can identify two characteristic operational situations, the *balanced operation* and the *imbalanced operation*. See Section 4.3.3.

4.3.2 AGC with Linear Model Predictive Control

With aggregated optimized RT controls using solely LMPC, the optimized control layer depicted in Figure 4.1 may consist of an RT–SCADA system (see Section 4.1), including:

- The target problem (see Section 3.3.2.2).

- At least one optimized aggregated system controller (see Section 3.3.2.3)[2].

- A set of models (see Section 3.1).

This control setup is used in the publications Paper A, Paper B and Paper E.

Notice that this requires the operational trajectory $\mathcal{T}$ to be feasible during RT operation. Due to disturbances acting on the system, convergence to $\mathcal{T}$ may be prohibited. This infeasibility then requires consideration of the nonlinear trajectory planning problem and consequently the employment of a control hierarchy as described in the previous Section 4.3.1.

4.3.3 Operational Scopes

IN BALANCED OPERATION we can account for the expected disturbance $\bar{d}$. This is characterized by feasibility of the target problem Equation (3.39) on page 31 (see Section 3.3.2.2) up to some accuracy in the control decisions $\epsilon_{\tilde{u}}$. Then, convergence to the dynamic dispatch schedule $\tilde{u}$ subject to the disturbance $\bar{d}$ is possible.

IN IMBALANCED OPERATION convergence to the dynamic dispatch schedule $\tilde{u}$ within the accuracy thresholds $\pm\epsilon_{\tilde{u}}$ is not possible. Recalculation of the trajectory planning problem (see Section 3.3.1) is then required. The result of this call is the updated dynamic dispatch schedule $\tilde{u}$ that should result in feasibility of the target problem Equation (3.39) on page 31.

4.4 AUTOMATIC VOLTAGE REGULATION

The control approaches described in the previous section 4.3 on AGC can be applied to the AVR problem as well. In Paper G we examine an alternative controller formulation for the AVR problem, similar to the one examined in Paper A. This controller we may use similarly as the approach provided in [VC13].

4.5 PROSUMER RESPONSE ACTIVATION

Related to the AGC problem discussed in Section 4.3, the prosumer response activation addresses the prosumer–associated flexibility potential. Posed as problem at the aggregated system level, at minimum a single price signal provides the incentive to prosumers to perform either up–regulation or down–regulation. The approach of using a price signal to incentivize a desired response in the operational domain is denoted as ICo, see for example [Mad+14; OH11].

Multiple price signals — up to prosumer–individual prices — can more effectively activate prosumers. With multiple price signals, ICo can support congestion management.

We can generate such price signals at different stages in the temporal control hierarchy. The stage to consider for the type of price–responsive unit depends on its dynamic properties:

FAST UNITS such as small ESSs, we may address by lower levels in the control hierarchy.

SLOW UNTIS such as large ESSs we may address by higher levels in the control hierarchy. If dynamics are irrelevant for system performance, we can generate such price–signal in the stationary dispatch problem.

See Figure 4.2 as an example.

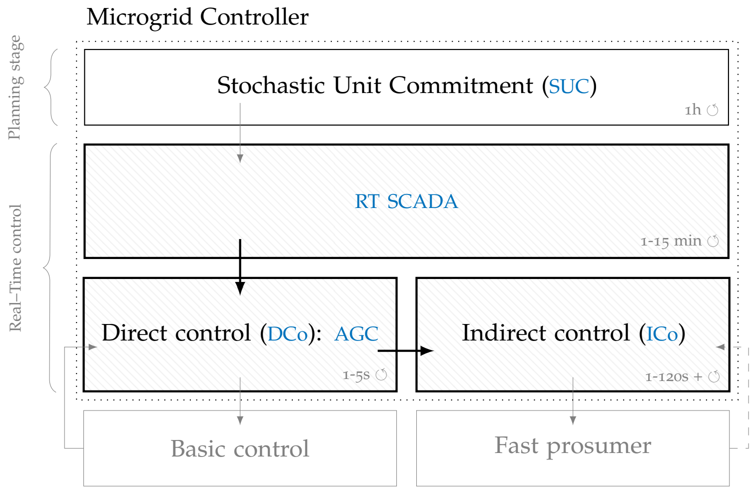

Figure 4.2: Temporal control hierarchy with focus on the highlighted control routines for flexibility activation of fast prosumers, such as EVs. The aggregator entity, employs the SUC to derive a dispatch schedule, here on an hourly basis. direct control (DCo) is sampled in the magnitude of a few seconds. ICo is sampled depending on the desired magnitudes of dynamics to be activated regarding fast prosumers.

In Paper C, we propose such temporal control hierarchy arrangement for the inclusion of fast ESSs such as EVs. EVs with vehicle to grid (V2G) functionality can support the AGC problem as fast price–responsive prosumers. See Section 4.5.2.

A price–response model is the main component of the ICo and is both time–varying and uncertain [MVA13]. In a general case, we may observe price–response dynamics through grid measurement units[3] when the prosumers are subject to the price signal p. By means of Sys-ID approaches, we can then infer the price–response dynamics. In Paper D we consider the sparse system identification of nonlinear dynamics with control (SINDyc) algorithm alongside markov chain monte carlo (MCMC) for identification of prosumer dynamics and model uncertainty. See Section 4.5.1 below. Such a model we can then utilize within stochastic ICo–MPCs (See Section 3.3.2.5).

4.5.1 Prosumer Response Estimation

We can obtain the price–response relationship using Sys-ID approaches, see Section 3.1.1.5.

3 Such as Phasor Measuring Units (PMUs).

In Paper C we use linear Sys-ID approaches and aggregate identified systems in temporal clusters. Given a sufficiently large number of observations, the evaluation of the response characteristics in these clusters can yield an approximation of their associated uncertainty. Using ICo and activation of EVs, we improve LFC in the examined scenario.

In Paper D we treat this problem by combining the sparse system identification of nonlinear dynamics with control (SINDyc) algorithm [BPK16] with markov chain monte carlo (MCMC). For MCMC, we use the software package Stan [Car+17].

This combination lifts synergies in the following manner:

- SINDyc yields a sparse system model.
- MCMC as computationally demanding algorithm can benefit from a well–chosen prior, such that the sampling space is bounded in some feasible set.

Furthermore, it enables the incorporation of system knowledge:

- We can incorporate knowledge on the system dynamics by adapting the candidate model of the SINDyc algorithm.
- We can modify the model priors in MCMC

This setup yields a detailed posterior distribution which we can utilize to inform stochastic ICo–MPCs. The potentially high computational load associated with MCMC algorithms is a drawback of this setup for RT operation [Fri+13]. The RT–SCADA may schedule computational demanding calculations such as MCMC in computational low–load times. Then, the updated system uncertainty representation derived by MCMC is available only at a later time, potentially lacking in the ongoing system operation. We may combine properties of different Sys-ID algorithms and approaches in an efficient manner, such as to circumvent such situations.

Furthermore, we may aim to obtain information of a dynamic system during ongoing system operation. In the setting of ICo, this entails that the activation of prosumer flexibility should be possible while executing an Sys-ID experiment. We can augment the controller for this purpose with active learning strategies, see Section 3.3.4.4.

4.5.2 Indirect Control and Prosumer Activation

As mentioned previously, we can associate an ICo with different layers in the control hierarchy. The association of an ICo with lower layers enables the actuation of faster prosumers as a result of the faster sampling rates at such layers.

Furthermore, we can take the causality structure within the control hierarchy into account, as highlighted in Figure 4.2 on page 56. Here, it is highlighted that the ICo in this situation is subordinate to the DCo for the AGC problem. In an event such as the loss of a production unit, this DCo can send the request to reduce the consumption (and potentially increase injection) of fast prosumer units by means of ICo.

The ICo can use constrained LQG regulator formulations such as described in Sections 3.3.2.3 and 3.3.2.4. When the aim is to achieve a desired response with approximated probability level, such regulators may be cast as SMPCs as described in Section 3.3.2.5.

5 SUMMARY

5.1 CONCLUSIONS AND FUTURE RESEARCH

Think like a man of action, act like a man of thought.

— Henri Bergson

In this thesis we proposed model predictive control (MPC) for the optimized real–time (RT) operation of microgrids (MGs) in combination with flexibility estimation and flexibility activation. We investigated some of these approaches throughout a case study in grid-connected mode (GCM) operation of an MG.

5.1.1 Contributions

Paper A and Paper B consider the automatic generation control (AGC) problem by means of optimized load frequency control (LFC) for the aggregated system. Compared to non–proactive control approaches, optimized and predictive control can improve the system performance in the AGC problem by coordinating the power production of subsequent units based on additional system knowledge. While MPC approaches for this problem exist, we formulate alternative control approaches including input reference tracking. By tracking input references, we facilitate the integration of these controllers into existing control hierarchies while retaining benefits of optimized and predictive control. These benefits include constraint satisfaction, consideration of process predictions and coordination of dynamics using multiple–inputs single–output (MISO) and multiple–input multiple–output (MIMO) system models. Due to that MPC approaches center around such models, updates to the latter given updated system knowledge result in improved control performance while facilitating the tuning problem compared to, for example, proportional integral derivative (PID)–based control schemes. The proposed controllers have been tested in a MG test facility[1]. Paper G considers related control approaches for the AVR problem.

Paper C proposes a control hierarchy for the AGC problem that includes the activation of electric vehicles (EVs) as fast prosumers using price–based indirect control (ICo). Prices generated by such ICo approach stimulate a desired reaction. By integrating such ICo into the optimized AGC controller, fast prosumers can support frequency

1 See Section 12.7.

stability. Stochasticity is a central aspect associated with EVs, due to that human behavior drives such prosumer units. We consider a modeled scenario with behavioral clusters in order to highlight the importance of considering clustering approaches when addressing such units. Uncertainty in the prosumer response is an important metric that influences a grid operator's decision to consider ICo of such units for a given operating period or operating regime. Only given manageable uncertainty of the prosumer's price–response the benefits of flexibility activation do prevail. Paper C considers linear models of the prosumer response and estimates response' uncertainty through aggregation.

Paper D considers the prosumer response estimation problem using sparse and potentially nonlinear dynamic models in conjunction with probabilistic parameter estimation techniques. For the latter, we here use markov chain monte carlo (MCMC). By providing the computationally intensive MCMC algorithm with a sparse candidate model structure, we bound the sampling space in MCMC to a feasible region. This results in an optimized Sys-ID pipeline yielding sparse and potentially nonlinear dynamic probabilistic models. We can integrate such models similarly as described in Paper C.

An RT–SCADA can use this information to decide whether the unit(s) may be supportive during a given operation period. It can also decide which RT controller may best treat the underlying system, for example an MPC considering the parametric uncertainty by means of stochastic model predictive controller (SMPC) principles.

Paper E presents a case study in which a co–simulation framework triggers the execution of operational routines and establishes the information exchange in–between the latter. This case study considers grid-connected mode (GCM) of a MG test facility[2].

5.1.2 Limitations and Future Research

Limitations

In context of microgrids (MGs) as systems with administrative and technical limits we considered centralized MPC schemes in this thesis. Prospects to address prohibitively complex problem sizes resulting from large numbers of individual units do exist in form of aggregation schemes and model order reduction techniques. Yet, decentralized approaches may improve the overall performance over the more centralized approaches discussed in this thesis for large problem sizes.

We consider the Kalman filter in the classical form in context of this thesis (see Section 3.4.1) assuming linear models and Gaussian distributions in the estimation problem.

Related to both aspects above are operational situations with active critical constraints. Likewise, in such situations, the performance of

2 See Section 12.7.

the overall control architecture is critical. This entails, amongst others, the accuracy of the assumed models, quality of process predictions and quality in the estimation problem.

Due to that MGs are heterogeneous technical systems, case studies for individual systems must examine such critical operating regimes in order to optimize all relevant aspects accordingly. In context of this thesis, solely Paper E documents a case study, which does not focus on such critical operating regime.

Future Research

The case study considered in Paper E may be extended to islanded mode (IM). In IM, the RT becomes more demanding and associated issues should be addressed.

Along these lines we can identify the computationally efficient orchestration of control layers within MG operation as a future research problem. A related and important research question is to consider MG control hierarchies as time–varying modular constructs, such that varying operational conditions can be addressed in an optimal manner. Such time–varying constructs may encompass all layers in the control hierarchy — from different treatments of the SUC considering the AC-OPF problem over distinct controllers tailored to the specific RT problem(s) at a given time.

Explicit MPC formulations should be considered, both in context of LMPC and NMPC. Offline computations should be exploited as far as possible in order to reduce computational load throughout real–time system operation.

Tuning of all control hierarchy layers using global efficiency metrics and multi–objective optimization may enable to determine beneficial controller parameterizations for different MGs and distinct operational conditions.

An improved RT–SCADA should treat the problem of flexibility activation to greater detail. Distinct flexibility sources may exist within an MG. The tailored activation of such flexibility by means of distinct ICos can further improve the leveraging of flexibility potentials. This results in flexibility–group' specific prices. Furthermore — as for all modules in MG control hierarchies — these controllers and associated routines must function in an automatized and robust manner. While underlying algorithms are well–developed, reliability must be proved and potential issues associated with recipes to circumvent undesired outcome.

The controllers proposed in Paper A and Paper B could be tested as stochastic formulations in disturbance scenarios of varying degree of severity. This could build on the co–simulation approaches outlined in Paper E. Tube based MPC may be applied to IM operation, such that robustness can be improved.

Paper D may be extended to consider alternative candidate model structures. Additionally, the derivation of probabilistic models from the generated posterior distributions may be further investigated.

Finally, and most importantly, we must provide stability certificates for all controllers in order to use them beyond test systems.

BIBLIOGRAPHY

[BGL10] H. Bevrani, A. Ghosh, and G. Ledwich. „Renewable Energy Sources and Frequency Regulation: Survey and New Perspectives.“ en. In: *IET Renewable Power Generation* 4.5 (2010), p. 438. ISSN: 17521416. DOI: 10.1049/iet-rpg.2009.0049. URL: https://digital-library.theiet.org/content/journals/10.1049/iet-rpg.2009.0049 (visited on 03/17/2020).

[Kat+08] Farid Katiraei et al. „Microgrids Management.“ In: *IEEE Power and Energy Magazine* 6.3 (May 2008), pp. 54–65. ISSN: 1558-4216. DOI: 10.1109/MPE.2008.918702.

[Mei+13] P. Meibom et al. „Energy Comes Together in Denmark: The Key to a Future Fossil-Free Danish Power System.“ In: *IEEE Power and Energy Magazine* 11.5 (Sept. 2013), pp. 46–55. ISSN: 1540-7977. DOI: 10.1109/MPE.2013.2268751.

[Mar16] Bonnie Marini. „The Duck Pond - A Look at Non-Renewable Generation on Grids with A Lot of Renewable Resources.“ In: *POWER Engineering* (2016), p. 7. URL: https://www.energy.siemens.com/ru/pool/hq/power-generation/power-plants/gas-fired-power-plants/The-duck-pond.pdf (visited on 05/09/2017).

[Mor+14] Juan M. Morales et al. *Integrating Renewables in Electricity Markets*. Vol. 205. International Series in Operations Research & Management Science. Boston, MA: Springer US, 2014. ISBN: 978-1-4614-9410-2 978-1-4614-9411-9. DOI: 10.1007/978-1-4614-9411-9. URL: http://link.springer.com/10.1007/978-1-4614-9411-9 (visited on 02/08/2018).

[OED15] Kristina Orehounig, Ralph Evins, and Viktor Dorer. „Integration of Decentralized Energy Systems in Neighbourhoods Using the Energy Hub Approach.“ In: *Applied Energy* 154 (Sept. 2015), pp. 277–289. ISSN: 0306-2619. DOI: 10.1016/j.apenergy.2015.04.114. URL: http://www.sciencedirect.com/science/article/pii/S0306261915005772 (visited on 01/02/2017).

[UBA14] Andreas Ulbig, Theodor S. Borsche, and Göran Andersson. „Impact of Low Rotational Inertia on Power System Stability and Operation.“ In: *IFAC Proceedings Volumes*. 19th IFAC World Congress 47.3 (Jan. 2014), pp. 7290–7297. ISSN: 1474-6670. DOI: 10.3182/20140824-6-ZA-

1003.02615. URL: http://www.sciencedirect.com/science/article/pii/S1474667016427618 (visited on 12/27/2018).

[DM16] O. Dag and B. Mirafzal. „On Stability of Islanded Low-Inertia Microgrids." In: *2016 Clemson University Power Systems Conference (PSC)*. Mar. 2016, pp. 1–7. DOI: 10.1109/PSC.2016.7462854.

[GP07] T. C. Green and M. Prodanović. „Control of Inverter-Based Micro-Grids." en. In: *Electric Power Systems Research*. Distributed Generation 77.9 (July 2007), pp. 1204–1213. ISSN: 0378-7796. DOI: 10.1016/j.epsr.2006.08.017. URL: http://www.sciencedirect.com/science/article/pii/S037877960600191X (visited on 03/14/2020).

[Sch+16a] Johannes Schiffer et al. „Voltage Stability and Reactive Power Sharing in Inverter-Based Microgrids With Consensus-Based Distributed Voltage Control." en. In: *IEEE Transactions on Control Systems Technology* 24.1 (Jan. 2016), pp. 96–109. ISSN: 1063-6536, 1558-0865. DOI: 10.1109/TCST.2015.2420622. URL: http://ieeexplore.ieee.org/document/7097655/ (visited on 03/05/2020).

[BH07] Hans-Peter Beck and Ralf Hesse. „Virtual Synchronous Machine." In: *2007 9th International Conference on Electrical Power Quality and Utilisation*. Oct. 2007, pp. 1–6. DOI: 10.1109/EPQU.2007.4424220.

[Hat+07] Nikos Hatziargyriou et al. „Microgrids." In: *IEEE Power and Energy Magazine* 5.4 (July 2007), pp. 78–94. ISSN: 1558-4216. DOI: 10.1109/MPAE.2007.376583.

[Han17] Yang Han. „Review of Active and Reactive Power Sharing Strategies in Hierarchical Controlled Microgrids." In: *Ieee Transactions on Power Electronics* 32.3 (2017), pp. 2427–2451. ISSN: 08858993. DOI: 10.1109/TPEL.2016.2569597.

[Jus+13] Jackson John Justo et al. „AC-Microgrids versus DC-Microgrids with Distributed Energy Resources: A Review." en. In: *Renewable and Sustainable Energy Reviews* 24 (Aug. 2013), pp. 387–405. ISSN: 1364-0321. DOI: 10.1016/j.rser.2013.03.067. URL: http://www.sciencedirect.com/science/article/pii/S1364032113002268 (visited on 03/14/2020).

[HAJ10] Rodrigo Hidalgo, Chad Abbey, and Géza Joós. „A Review of Active Distribution Networks Enabling Technologies." In: *IEEE PES General Meeting*. July 2010, pp. 1–9. DOI: 10.1109/PES.2010.5590051.

[Bor+10] A. Borghetti et al. „Short-Term Scheduling and Control of Active Distribution Systems With High Penetration of Renewable Resources.“ In: *IEEE Systems Journal* 4.3 (Sept. 2010), pp. 313–322. ISSN: 1932-8184. DOI: 10.1109/JSYST.2010.2059171.

[Asm10] Peter Asmus. „Microgrids, Virtual Power Plants and Our Distributed Energy Future.“ en. In: *The Electricity Journal* 23.10 (Dec. 2010), pp. 72–82. ISSN: 10406190. DOI: 10.1016/j.tej.2010.11.001. URL: https://linkinghub.elsevier.com/retrieve/pii/S1040619010002873 (visited on 04/01/2020).

[SSS12] Steffen Schütte, Stefan Scherfke, and Michael Sonnenschein. „Mosaik-Smart Grid Simulation API.“ In: *Proceedings of SMARTGREENS* (2012), pp. 14–24. URL: https://mosaik.offis.de/downloads/mosaik_SimAPI_SmartGreens2012.pdf (visited on 12/31/2016).

[MT18] Lesia Mitridati and Josh A. Taylor. „Power Systems Flexibility from District Heating Networks.“ In: *2018 Power Systems Computation Conference (PSCC)*. June 2018, pp. 1–7. DOI: 10.23919/PSCC.2018.8442617.

[MP16] L. Mitridati and P. Pinson. „Optimal Coupling of Heat and Electricity Systems: A Stochastic Hierarchical Approach.“ In: *2016 International Conference on Probabilistic Methods Applied to Power Systems (PMAPS)*. Oct. 2016, pp. 1–6. DOI: 10.1109/PMAPS.2016.7764188.

[Sch+16b] Johannes Schiffer et al. „A Survey on Modeling of Microgrids—From Fundamental Physics to Phasors and Voltage Sources.“ In: *Automatica* 74 (Dec. 2016), pp. 135–150. ISSN: 0005-1098. DOI: 10.1016/j.automatica.2016.07.036. URL: http://www.sciencedirect.com/science/article/pii/S0005109816303041 (visited on 01/02/2017).

[AA10] Mohammad Saad Alam and Ali T. Alouani. „Dynamic Modeling of Photovoltaic Module for Real-Time Maximum Power Tracking.“ en. In: *Journal of Renewable and Sustainable Energy* 2.4 (July 2010), p. 043102. ISSN: 1941-7012. DOI: 10.1063/1.3435338. URL: http://aip.scitation.org/doi/10.1063/1.3435338 (visited on 03/28/2018).

[Im+17] W. S. Im et al. „Distributed Virtual Inertia Based Control of Multiple Photovoltaic Systems in Autonomous Microgrid.“ In: *IEEE/CAA Journal of Automatica Sinica* 4.3 (2017), pp. 512–519. ISSN: 2329-9266. DOI: 10.1109/JAS.2016.7510031.

[UEJ13] Carlos E. Ugalde-Loo, Janaka B. Ekanayake, and Nicholas Jenkins. „State-Space Modeling of Wind Turbine Generators for Power System Studies." en. In: *IEEE Transactions on Industry Applications* 49.1 (Jan. 2013), pp. 223–232. ISSN: 0093-9994, 1939-9367. DOI: 10.1109/TIA.2012.2228836. URL: http://ieeexplore.ieee.org/document/6359908/ (visited on 03/09/2020).

[Gey17] Tobias Geyer. *Model Predictive Control of High Power Converters and Industrial Drives*. eng. First edition. Chichester, West Sussex, United Kingdom: Wiley, 2017. ISBN: 978-1-119-01086-9 978-1-119-01090-6 978-1-119-01089-0.

[KIL07] F. Katiraei, M.R. Iravani, and P.W. Lehn. „Small-Signal Dynamic Model of a Micro-Grid Including Conventional and Electronically Interfaced Distributed Resources." In: *Transmission Distribution IET Generation* 1.3 (May 2007), pp. 369–378. ISSN: 1751-8695. DOI: 10.1049/iet-gtd:20045207.

[LD14] Ling Luo and Sairaj V. Dhople. „Spatiotemporal Model Reduction of Inverter-Based Islanded Microgrids." In: *IEEE Transactions on Energy Conversion* 29.4 (Dec. 2014), pp. 823–832. ISSN: 1558-0059. DOI: 10.1109/TEC.2014.2348716.

[TTL16] Quang-Tho Tran, Anh Viet Truong, and Phuong Minh Le. „Reduction of Harmonics in Grid-Connected Inverters Using Variable Switching Frequency." en. In: *International Journal of Electrical Power & Energy Systems* 82 (Nov. 2016), pp. 242–251. ISSN: 01420615. DOI: 10.1016/j.ijepes.2016.03.027. URL: https://linkinghub.elsevier.com/retrieve/pii/S0142061516304409 (visited on 04/01/2020).

[LH11] Jackson Lago and Marcelo Lobo Heldwein. „Operation and Control-Oriented Modeling of a Power Converter for Current Balancing and Stability Improvement of DC Active Distribution Networks." In: *IEEE Transactions on Power Electronics* 26.3 (Mar. 2011), pp. 877–885. ISSN: 1941-0107. DOI: 10.1109/TPEL.2011.2105284.

[SS07] Daniel Salomonsson and Ambra Sannino. „Low-Voltage DC Distribution System for Commercial Power Systems With Sensitive Electronic Loads." In: *IEEE Transactions on Power Delivery* 22.3 (July 2007), pp. 1620–1627. ISSN: 1937-4208. DOI: 10.1109/TPWRD.2006.883024.

[Gom+18] Antonio Gomez-Exposito et al. *Electric Energy Systems : Analysis and Operation*. en. CRC Press, June 2018. ISBN: 978-1-315-19224-6. DOI: 10.1201/9781315192246. URL: h ttps://www.taylorfrancis.com/books/9781315192246 (visited on 08/26/2019).

[Sta+16] M. Stanojević et al. „Analysis of Generalized Droop Control in Medium and Low Voltage Power Electric Grids.“ In: *2016 International Symposium on Industrial Electronics (INDEL)*. Nov. 2016, pp. 1–6. DOI: 10.1109/INDEL.2016.7797817.

[Pla+13] Estefanía Planas et al. „General Aspects, Hierarchical Controls and Droop Methods in Microgrids: A Review.“ en. In: *Renewable and Sustainable Energy Reviews* 17 (Jan. 2013), pp. 147–159. ISSN: 1364-0321. DOI: 10.1016/j.rser.2012.09.032. URL: http://www.sciencedirect.com/science/article/pii/S1364032112005333 (visited on 03/14/2020).

[KI06] F. Katiraei and M.R. Iravani. „Power Management Strategies for a Microgrid With Multiple Distributed Generation Units.“ In: *IEEE Transactions on Power Systems* 21.4 (Nov. 2006), pp. 1821–1831. ISSN: 1558-0679. DOI: 10.1109/TPWRS.2006.879260.

[DSB16] Florian Dörfler, John W. Simpson-Porco, and Francesco Bullo. „Breaking the Hierarchy: Distributed Control and Economic Optimality in Microgrids.“ In: *IEEE Transactions on Control of Network Systems* 3.3 (Sept. 2016), pp. 241–253. ISSN: 2372-2533. DOI: 10.1109/TCNS.2015.2459391.

[Bas+12] Prasenjit Basak et al. „A Literature Review on Integration of Distributed Energy Resources in the Perspective of Control, Protection and Stability of Microgrid.“ In: *Renewable and Sustainable Energy Reviews* 16.8 (Oct. 2012), pp. 5545–5556. ISSN: 1364-0321. DOI: 10.1016/j.rser.2012.05.043. URL: http://www.sciencedirect.com/science/article/pii/S1364032112003772 (visited on 08/01/2017).

[Str08] Goran Strbac. „Demand Side Management: Benefits and Challenges.“ en. In: *Energy Policy* 36.12 (Dec. 2008), pp. 4419–4426. ISSN: 03014215. DOI: 10.1016/j.enpol.2008.09.030. URL: http://linkinghub.elsevier.com/retrieve/pii/S0301421508004606 (visited on 11/22/2017).

[Mae+07] H. Maejima et al. „Structures of Small Power Supply Networks and a Practical Example with Renewable Energy Resources.“ In: *2007 IEEE Power Engineering Society General Meeting*. June 2007, pp. 1–7. DOI: 10.1109/PES.2007.386088.

[EIU16] A. M. Ersdal, L. Imsland, and K. Uhlen. „Model Predictive Load-Frequency Control." In: *IEEE Transactions on Power Systems* 31.1 (Jan. 2016), pp. 777–785. ISSN: 0885-8950. DOI: 10.1109/TPWRS.2015.2412614.

[Ven+08] A. N. Venkat et al. „Distributed MPC Strategies With Application to Power System Automatic Generation Control." In: *IEEE Transactions on Control Systems Technology* 16.6 (Nov. 2008), pp. 1192–1206. ISSN: 1063-6536. DOI: 10.1109/TCST.2008.919414.

[SRA13] Mojtaba Shiroei, Ali Mohammad Ranjbar, and Toraj Amraee. „A Functional Model Predictive Control Approach for Power System Load Frequency Control Considering Generation Rate Constraint: Functional MPC Approach For Power System LFC." en. In: *International Transactions on Electrical Energy Systems* 23.2 (Mar. 2013), pp. 214–229. ISSN: 20507038. DOI: 10.1002/etep.653. URL: http://doi.wiley.com/10.1002/etep.653 (visited on 10/02/2017).

[SS16] P. S. V. Sagar and K. S. Swarup. „Load Frequency Control in Isolated Micro-Grids Using Centralized Model Predictive Control." In: *2016 IEEE International Conference on Power Electronics, Drives and Energy Systems (PEDES)*. Dec. 2016, pp. 1–6. DOI: 10.1109/PEDES.2016.7914478.

[Kun94] Kundur. *Power System Stability And Control*. en. The Epri Power System Engineering. India: McGraw-Hill, 1994. ISBN: 978-0-07-063515-9.

[CDA93] M.C. Chandorkar, D.M. Divan, and R. Adapa. „Control of Parallel Connected Inverters in Standalone AC Supply Systems." In: *IEEE Transactions on Industry Applications* 29.1 (Jan. 1993), pp. 136–143. ISSN: 1939-9367. DOI: 10.1109/28.195899.

[VC13] G. Valverde and T. Van Cutsem. „Model Predictive Control of Voltages in Active Distribution Networks." In: *IEEE Transactions on Smart Grid* 4.4 (Dec. 2013), pp. 2152–2161. ISSN: 1949-3053. DOI: 10.1109/TSG.2013.2246199.

[JR18] M Jayachandran and G Ravi. „MPC Based Secondary Control Strategy for an Islanded AC Microgrid under Linear Loads." In: *2018 4th International Conference on Electrical Energy Systems (ICEES)*. Feb. 2018, pp. 644–651. DOI: 10.1109/ICEES.2018.8443273.

[Gei07] Martin Geidl. „Integrated Modeling and Optimization of Multi-Carrier Energy Systems." PhD thesis. TU Graz, 2007. URL: http://0-bibing.us.es.fama.us.es/proyectos/abreproy/4503/fichero/2.+Documentacion%5C%252FEnergy_Hubs.pdf (visited on 01/25/2017).

[Gei+07] M. Geidl et al. „Energy Hubs for the Future." In: *IEEE Power and Energy Magazine* 5.1 (Jan. 2007), pp. 24–30. ISSN: 1540-7977. DOI: 10.1109/MPAE.2007.264850.

[GA07] M. Geidl and G. Andersson. „Optimal Coupling of Energy Infrastructures." In: *2007 IEEE Lausanne Power Tech*. July 2007, pp. 1398–1403. DOI: 10.1109/PCT.2007.4538520.

[Mol+10] A. Molderink et al. „Management and Control of Domestic Smart Grid Technology." In: *IEEE Transactions on Smart Grid* 1.2 (Sept. 2010), pp. 109–119. ISSN: 1949-3053. DOI: 10.1109/TSG.2010.2055904.

[VM19] Yelena Vardanyan and Henrik Madsen. „Optimal Coordinated Bidding of a Profit Maximizing, Risk-Averse EV Aggregator in Three-Settlement Markets Under Uncertainty." en. In: *Energies* 12.9 (Jan. 2019), p. 1755. DOI: 10.3390/en12091755. URL: https://www.mdpi.com/1996-1073/12/9/1755 (visited on 07/15/2019).

[Men+17] Esther Mengelkamp et al. „Designing Microgrid Energy Markets." In: *Applied Energy* (June 2017). ISSN: 0306-2619. DOI: 10.1016/j.apenergy.2017.06.054. URL: http://www.sciencedirect.com/science/article/pii/S030626191730805X (visited on 08/01/2017).

[RKF16] Philipp Ringler, Dogan Keles, and Wolf Fichtner. „Agent-Based Modelling and Simulation of Smart Electricity Grids and Markets – A Literature Review." In: *Renewable and Sustainable Energy Reviews* 57 (May 2016), pp. 205–215. ISSN: 1364-0321. DOI: 10.1016/j.rser.2015.12.169. URL: http://www.sciencedirect.com/science/article/pii/S136403211501552X (visited on 12/04/2016).

[Lju99] L. Ljung. *System Identification: Theory for the User*. Prentice Hall Information and System Sciences Series. Prentice Hall PTR, 1999. ISBN: 978-0-13-656695-3. URL: https://books.google.dk/books?id=nHFoQgAACAAJ.

[KMJ04] Niels Rode Kristensen, Henrik Madsen, and Sten Bay Jørgensen. „Parameter Estimation in Stochastic Grey-Box Models." en. In: *Automatica* 40.2 (Feb. 2004), pp. 225–237. ISSN: 00051098. DOI: 10.1016/j.automatica.2003.10.001. URL: https://linkinghub.elsevier.com/retrieve/pii/S0005109803002985X (visited on 08/06/2019).

[Nel01] Oliver Nelles. *Nonlinear System Identification*. en. Berlin, Heidelberg: Springer Berlin Heidelberg, 2001. ISBN: 978-3-642-08674-8 978-3-662-04323-3. DOI: 10.1007/978-3-662-04323-3. URL: http://link.springer.com/10.1007/978-3-662-04323-3 (visited on 03/06/2020).

[CB04] E. F. Camacho and C. Bordons. *Model Predictive Control*. Advanced Textbooks in Control and Signal Processing. London ; New York: Springer, 2004. ISBN: 978-1-85233-694-3.

[JHR11] John Bagterp Jørgensen, Jakob K. Huusom, and James B. Rawlings. „Finite Horizon MPC for Systems in Innovation Form." In: *Decision and Control and European Control Conference (CDC-ECC), 2011 50th IEEE Conference*. Orlando, USA: IEEE, 2011, pp. 1896–1903.

[Mac02] J.M. Maciejowski. *Predictive Control: With Constraints*. Prentice Hall, 2002. ISBN: 978-0-201-39823-6. URL: https://books.google.dk/books?id=HV_Y58c7KiwC.

[Mau+88] Paul R. Maurath et al. „Predictive Controller Design by Principal Components Analysis." en. In: *Industrial & Engineering Chemistry Research* 27.7 (July 1988), pp. 1204–1212. ISSN: 0888-5885, 1520-5045. DOI: 10.1021/ie00079a020. URL: https://pubs.acs.org/doi/abs/10.1021/ie00079a020 (visited on 02/18/2020).

[RL19] Saša V. Raković and William S. Levine, eds. *Handbook of Model Predictive Control*. en. Control Engineering. Cham: Springer International Publishing, 2019. ISBN: 978-3-319-77488-6 978-3-319-77489-3. DOI: 10.1007/978-3-319-77489-3. URL: http://link.springer.com/10.1007/978-3-319-77489-3 (visited on 02/26/2020).

[BK19] S.L. Brunton and J.N. Kutz. *Data-Driven Science and Engineering: Machine Learning, Dynamical Systems, and Control*. Cambridge University Press, 2019. ISBN: 978-1-108-42209-3. URL: https://books.google.dk/books?id=gNcRuQEACAAJ.

[Tu13] Jonathan H. Tu. „Dynamic Mode Decomposition: Theory and Applications." English. Dissertation. Princeton: Princeton, 2013. URL: http://cwrowley.princeton.edu/theses/tu.pdf (visited on 03/26/2020).

[Cre+19] Jochen L. Cremer et al. „Data-Driven Power System Operation: Exploring the Balance Between Cost and Risk." en. In: *IEEE Transactions on Power Systems* 34.1 (Jan. 2019), pp. 791–801. ISSN: 0885-8950, 1558-0679. DOI: 10.1109/TPWRS.2018.2867209. URL: https://ieeexplore.ieee.org/document/8447254/ (visited on 02/11/2020).

[MZM16] Jan Kloppenborg Møller, Marco Zugno, and Henrik Madsen. „Probabilistic Forecasts of Wind Power Generation by Stochastic Differential Equation Models: Probabilistic Forecasts of Wind Power Generation." en. In: *Journal of Forecasting* 35.3 (Apr. 2016), pp. 189–205. ISSN: 02776693.

DOI: 10.1002/for.2367. URL: http://doi.wiley.com/10.1002/for.2367 (visited on 02/06/2018).

[Mad07] H. Madsen. *Time Series Analysis*. Chapman & Hall/CRC Texts in Statistical Science. Taylor & Francis, 2007. ISBN: 978-1-4200-5967-0. URL: https://books.google.dk/books?id=0yFNKoIWdFkC.

[MMD18] S. Misra, D. K. Molzahn, and K. Dvijotham. „Optimal Adaptive Linearizations of the AC Power Flow Equations." In: *2018 Power Systems Computation Conference (PSCC)*. June 2018, pp. 1–7. DOI: 10.23919/PSCC.2018.8442547.

[PRG16] Alessandra Parisio, Evangelos Rikos, and Luigi Glielmo. „Stochastic Model Predictive Control for Economic/Environmental Operation Management of Microgrids: An Experimental Case Study." In: *Journal of Process Control* 43 (July 2016), pp. 24–37. ISSN: 0959-1524. DOI: 10.1016/j.jprocont.2016.04.008. URL: http://www.sciencedirect.com/science/article/pii/S0959152416300324 (visited on 01/02/2017).

[Han+14] Christian A. Hans et al. „Minimax Model Predictive Operation Control of Microgrids." In: *IFAC Proceedings Volumes*. 19th IFAC World Congress 47.3 (Jan. 2014), pp. 10287–10292. ISSN: 1474-6670. DOI: 10.3182/20140824-6-ZA-1003.00683. URL: http://www.sciencedirect.com/science/article/pii/S1474667016432465 (visited on 12/27/2018).

[Com+16] S. Raimondi Cominesi et al. „A Multi-Layer Control Scheme for Microgrid Energy Management." en. In: *IFAC-PapersOnLine* 49.27 (2016), pp. 256–261. ISSN: 24058963. DOI: 10.1016/j.ifacol.2016.10.700. URL: http://linkinghub.elsevier.com/retrieve/pii/S2405896316323199 (visited on 05/06/2018).

[NX17] Nnamdi I. Nwulu and Xiaohua Xia. „Optimal Dispatch for a Microgrid Incorporating Renewables and Demand Response." In: *Renewable Energy* 101 (Feb. 2017), pp. 16–28. ISSN: 0960-1481. DOI: 10.1016/j.renene.2016.08.026. URL: http://www.sciencedirect.com/science/article/pii/S0960148116307273 (visited on 08/01/2017).

[KS12] Phillip Oliver Kriett and Matteo Salani. „Optimal Control of a Residential Microgrid." In: *Energy*. 8th World Energy System Conference, WESC 2010 42.1 (June 2012), pp. 321–330. ISSN: 0360-5442. DOI: 10.1016/j.energy.2012.03.049. URL: http://www.sciencedirect.com/science/article/pii/S0360544212002526 (visited on 08/01/2017).

[CCM10a] Antonio J. Conejo, Miguel Carrión, and Juan M. Morales. „Stochastic Programming Fundamentals.“ en. In: *Decision Making Under Uncertainty in Electricity Markets*. International Series in Operations Research & Management Science. Springer, Boston, MA, 2010, pp. 27–62. ISBN: 978-1-4419-7420-4 978-1-4419-7421-1. URL: https://link-springer-com.proxy.findit.dtu.dk/chapter/10.1007/978-1-4419-7421-1_2 (visited on 03/14/2018).

[PRG14] Alessandra Parisio, Evangelos Rikos, and Luigi Glielmo. „A Model Predictive Control Approach to Microgrid Operation Optimization.“ In: *IEEE Transactions on Control Systems Technology* 22.5 (Sept. 2014), pp. 1813–1827. ISSN: 1558-0865. DOI: 10.1109/TCST.2013.2295737.

[ZG13] C. Zhao and Y. Guan. „Unified Stochastic and Robust Unit Commitment.“ In: *IEEE Transactions on Power Systems* 28.3 (Aug. 2013), pp. 3353–3361. ISSN: 0885-8950. DOI: 10.1109/TPWRS.2013.2251916.

[CCM10b] Antonio J. Conejo, Miguel Carrión, and Juan M. Morales. „Pool Trading for Wind Power Producers.“ en. In: *Decision Making Under Uncertainty in Electricity Markets*. International Series in Operations Research & Management Science. Springer, Boston, MA, 2010, pp. 195–251. ISBN: 978-1-4419-7420-4 978-1-4419-7421-1. DOI: 10.1007/978-1-4419-7421-1_6. URL: https://link-springer-com.proxy.findit.dtu.dk/chapter/10.1007/978-1-4419-7421-1_6 (visited on 03/14/2018).

[CCM10c] Antonio J. Conejo, Miguel Carrión, and Juan M. Morales. „Market Clearing under Uncertainty: Wind Energy.“ en. In: *Decision Making Under Uncertainty in Electricity Markets*. International Series in Operations Research & Management Science. Springer, Boston, MA, 2010, pp. 405–446. ISBN: 978-1-4419-7420-4 978-1-4419-7421-1. DOI: 10.1007/978-1-4419-7421-1_11. URL: https://link-springer-com.proxy.findit.dtu.dk/chapter/10.1007/978-1-4419-7421-1_11 (visited on 03/14/2018).

[CCM10d] Antonio J. Conejo, Miguel Carrión, and Juan M. Morales. „Market Clearing Considering Equipment Failures.“ en. In: *Decision Making Under Uncertainty in Electricity Markets*. International Series in Operations Research & Management Science. Springer, Boston, MA, 2010, pp. 357–403. ISBN: 978-1-4419-7420-4 978-1-4419-7421-1. DOI: 10.1007/978-1-4419-7421-1_10. URL: https://link-springer-com.proxy.findit.dtu.dk/chapter/10.1007/978-1-4419-7421-1_10 (visited on 03/14/2018).

[BKV13] Roy Billinton, Rajesh Karki, and Ajit Kumar Verma, eds. *Reliability and Risk Evaluation of Wind Integrated Power Systems*. en. India: Springer India, 2013. ISBN: 978-81-322-0986-7 978-81-322-0987-4. DOI: 10.1007/978-81-322-0987-4. URL: http://link.springer.com/10.1007/978-81-322-0987-4 (visited on 11/06/2019).

[PRW11] Gabriele Pannocchia, James B. Rawlings, and Stephen J. Wright. „Conditions under Which Suboptimal Nonlinear MPC Is Inherently Robust." en. In: *Systems & Control Letters* 60.9 (Sept. 2011), pp. 747–755. ISSN: 01676911. DOI: 10.1016/j.sysconle.2011.05.013. URL: https://linkinghub.elsevier.com/retrieve/pii/S0167691111001368 (visited on 04/25/2020).

[HJS08] Elbert Hendricks, O. E. Jannerup, and Paul H. Sørensen. *Linear Systems Control: Deterministic and Stochastic Methods*. OCLC: ocn298259038. Berlin: Springer, 2008. ISBN: 978-3-540-78485-2 978-3-540-78486-9.

[RMD17] James B. Rawlings, David Q. Mayne, and Moritz M. Diehl. *Model Predictive Control: Theory, Computation, and Design*. en. 2nd edition. OCLC: 1020170256. Madison, Wisconsin: Nob Hill Publishing, 2017. ISBN: 978-0-9759377-3-0.

[NW06] Jorge Nocedal and Stephen J. Wright. *Numerical Optimization*. 2nd ed. Springer Series in Operations Research. OCLC: ocm68629100. New York: Springer, 2006. ISBN: 978-0-387-30303-1.

[ST14] Paul Scott and Sylvie Thiébaux. „Dynamic Optimal Power Flow in Microgrids Using the Alternating Direction Method of Multipliers." en. In: *arXiv:1410.7868 [cs, math]* (Oct. 2014). arXiv: 1410.7868 [cs, math]. URL: http://arxiv.org/abs/1410.7868 (visited on 11/06/2019).

[Moh+18] Erfan Mohagheghi et al. „A Survey of Real-Time Optimal Power Flow." en. In: *Energies* 11.11 (Nov. 2018), p. 3142. ISSN: 1996-1073. DOI: 10.3390/en11113142. URL: http://www.mdpi.com/1996-1073/11/11/3142 (visited on 11/05/2019).

[GJ09] Guru Prasath and John Bagterp. „Soft Constraints for Robust MPC of Uncertain Systems." In: *IFAC Proceedings Volumes (ifac-papersonline)*. 1st ser. 7 (2009), pp. 225–230. URL: https://cn.inside.dtu.dk/cnnet/filesharing/download/8a3d55fe-fec4-476f-8463-f999083baf9f (visited on 11/09/2017).

[May+00] D Q Mayne et al. „Constrained Model Predictive Control: Stability and Optimality." en. In: (2000), p. 26.

[Hei+18a] Tor Aksel N. Heirung et al. „Stochastic Model Predictive Control — How Does It Work?“ en. In: *Computers & Chemical Engineering* 114 (June 2018), pp. 158–170. ISSN: 00981354. DOI: 10.1016/j.compchemeng.2017.10.026. URL: https://linkinghub.elsevier.com/retrieve/pii/S0098135417303812 (visited on 04/19/2020).

[PGA15] Gabriele Pannocchia, Marco Gabiccini, and Alessio Artoni. „Offset-Free MPC Explained: Novelties, Subtleties, and Applications.“ In: *IFAC-PapersOnLine* 48.23 (2015), pp. 342–351.

[PR03] Gabriele Pannocchia and James B. Rawlings. „Disturbance Models for Offset-Free Model-Predictive Control.“ In: *AIChE journal* 49.2 (2003), pp. 426–437.

[MR93] Kenneth R. Muske and James B. Rawlings. „Model Predictive Control with Linear Models.“ en. In: *AIChE Journal* 39.2 (1993), pp. 262–287. ISSN: 1547-5905. DOI: 10.1002/aic.690390208. URL: http://aiche.onlinelibrary.wiley.com/doi/abs/10.1002/aic.690390208 (visited on 07/30/2019).

[GFH88] P. Grosdidier, B. Froisy, and M. Hammann. „The Idocom–M Controller.“ en. In: *IFAC Proceedings Volumes* 21.4 (June 1988), pp. 31–36. ISSN: 14746670. DOI: 10.1016/B978-0-08-035735-5.50009-7. URL: https://linkinghub.elsevier.com/retrieve/pii/B9780080357355500097 (visited on 02/15/2020).

[SGM13] G. Schildbach, P. Goulart, and M. Morari. „The Linear Quadratic Regulator with Chance Constraints.“ In: *2013 European Control Conference (ECC)*. July 2013, pp. 2746–2751. DOI: 10.23919/ECC.2013.6669660.

[Can+10] Mark Cannon et al. „Stochastic Tubes in Model Predictive Control with Probabilistic Constraints.“ In: *Proceedings of the 2010 American Control Conference*. June 2010, pp. 6274–6279. DOI: 10.1109/ACC.2010.5531518.

[Old+15] Frauke Oldewurtel et al. „Adaptively Constrained Stochastic Model Predictive Control Applied to Security Constrained Optimal Power Flow.“ In: IEEE, July 2015, pp. 931–936. ISBN: 978-1-4799-8684-2. DOI: 10.1109/ACC.2015.7170853. URL: http://ieeexplore.ieee.org/document/7170853/ (visited on 02/01/2017).

[Sum+14] Tyler Summers et al. „Stochastic Optimal Power Flow Based on Convex Approximations of Chance Constraints.“ In: *Power Systems Computation Conference (PSCC), 2014*. IEEE, 2014, pp. 1–7. URL: http://ieeexplore.ieee.org/abstract/document/7038376/ (visited on 06/20/2017).

[Roa+13] Line Roald et al. *Analytical Reformulation of Security Constrained Optimal Power Flow with Probabilistic Constraints*. IEEE, 2013. URL: http://ieeexplore.ieee.org/abstract/document/6652224/ (visited on 06/20/2017).

[RA17] Line Roald and Göran Andersson. „Chance-Constrained AC Optimal Power Flow: Reformulations and Efficient Algorithms." In: *arXiv:1706.03241 [math]* (June 2017). arXiv: 1706.03241 [math]. URL: http://arxiv.org/abs/1706.03241 (visited on 03/13/2018).

[Kou+10] Basil Kouvaritakis et al. „Explicit Use of Probabilistic Distributions in Linear Predictive Control." In: *UKACC International Conference on Control 2010*. Sept. 2010, pp. 1–6. DOI: 10.1049/ic.2010.0343.

[DBK06] Moritz Diehl, Hans Georg Bock, and Ekaterina Kostina. „An Approximation Technique for Robust Nonlinear Optimization." en. In: *Mathematical Programming* 107.1-2 (June 2006), pp. 213–230. ISSN: 0025-5610, 1436-4646. DOI: 10.1007/s10107-005-0685-1. URL: http://link.springer.com/10.1007/s10107-005-0685-1 (visited on 04/25/2020).

[GS10] Jorge L. Garriga and Masoud Soroush. „Model Predictive Control Tuning Methods: A Review." en. In: *Industrial & Engineering Chemistry Research* 49.8 (Apr. 2010), pp. 3505–3515. ISSN: 0888-5885, 1520-5045. DOI: 10.1021/ie900323c. URL: https://pubs.acs.org/doi/10.1021/ie900323c (visited on 02/18/2020).

[YZO16] A. S. Yamashita, A. C. Zanin, and D. Odloak. „Tuning of Model Predictive Control with Multi-Objective Optimization." English. In: (May 2016).

[Hei+18b] Tor Aksel N. Heirung et al. „Model Predictive Control with Active Learning under Model Uncertainty: Why, When, and How." en. In: *AIChE Journal* 64.8 (2018), pp. 3071–3081. ISSN: 1547-5905. DOI: 10.1002/aic.16180. URL: http://onlinelibrary.wiley.com/doi/abs/10.1002/aic.16180 (visited on 01/04/2019).

[HSM19] Tor Aksel N. Heirung, Tito L.M. Santos, and Ali Mesbah. „Model Predictive Control with Active Learning for Stochastic Systems with Structural Model Uncertainty: Online Model Discrimination." en. In: *Computers & Chemical Engineering* 128 (Sept. 2019), pp. 128–140. ISSN: 00981354. DOI: 10.1016/j.compchemeng.2019.05.012. URL: https://linkinghub.elsevier.com/retrieve/pii/S0098135418312730 (visited on 08/27/2019).

[Ngu17] Nhan T. Nguyen. *Model-Reference Adaptive Control*. en. New York, NY: Springer Berlin Heidelberg, 2017. ISBN: 978-3-319-56392-3.

[MDG17] L. Meng, T. Dragicevic, and J. Guerrero. „Adaptive Control Design for Autonomous Operation of Multiple Energy Storage Systems in Power Smoothing Applications.“ In: *IEEE Transactions on Industrial Electronics* PP.99 (2017), pp. 1–1. ISSN: 0278-0046. DOI: 10.1109/TIE.2017.2756584.

[Sir+10] S. F. Siraj et al. „A Robust Adaptive Predictive Load Frequency Controller to Compensate for Model Mismatch.“ In: *2010 4th International Power Engineering and Optimization Conference (PEOCO)*. Malaysia, June 2010, pp. 33–37. DOI: 10.1109/PEOCO.2010.5559181.

[DE18] A. A. Z. Diab and M. A. El-Sattar. „Adaptive Model Predictive Based Load Frequency Control in an Interconnected Power System.“ In: *2018 IEEE Conference of Russian Young Researchers in Electrical and Electronic Engineering (EIConRus)*. Jan. 2018, pp. 604–610. DOI: 10.1109/EIConRus.2018.8317170.

[Vaj+85] I. Vajk et al. „Adaptive Load-Frequency Control of the Hungarian Power System.“ en. In: *Automatica* 21.2 (Mar. 1985), pp. 129–137. ISSN: 00051098. DOI: 10.1016/0005-1098(85)90108-6. URL: https://linkinghub.elsevier.com/retrieve/pii/0005109885901086 (visited on 07/26/2019).

[DB09] S. Di Cairano and A. Bemporad. „Model Predictive Controller Matching: Can MPC Enjoy Small Signal Properties of My Favorite Linear Controller?“ en. In: *2009 European Control Conference (ECC)*. Budapest: IEEE, Aug. 2009, pp. 2217–2222. ISBN: 978-3-9524173-9-3. DOI: 10.23919/ECC.2009.7074734. URL: https://ieeexplore.ieee.org/document/7074734/ (visited on 02/19/2020).

[KC16] Basil Kouvaritakis and Mark Cannon. *Model Predictive Control*. Advanced Textbooks in Control and Signal Processing. Cham: Springer International Publishing, 2016. ISBN: 978-3-319-24851-6 978-3-319-24853-0. URL: http://link.springer.com/10.1007/978-3-319-24853-0 (visited on 01/25/2017).

[Tee04] Andrew R. Teel. „Discrete Time Receding Horizon Optimal Control: Is the Stability Robust?“ en. In: *Optimal Control, Stabilization and Nonsmooth Analysis*. Ed. by Marcio S. de Queiroz, Michael Malisoff, and Peter Wolenski. Lecture Notes in Control and Information Science. Berlin, Heidelberg: Springer, 2004, pp. 3–27. ISBN: 978-3-540-39983-4. DOI: 10.1007/978-3-540-39983-4_1.

[OM16] Olumuyiwa I. Olanrewaju and Jan M. Maciejowski. „Economic Equivalence of Economic Model Predictive Control and Hierarchical Control Schemes." In: *Industrial & Engineering Chemistry Research* 55.41 (Oct. 2016), pp. 10978–10989. ISSN: 0888-5885. DOI: 10.1021/acs.iecr.6b02332. URL: http://dx.doi.org/10.1021/acs.iecr.6b02332 (visited on 12/09/2016).

[EDC14] Matthew Ellis, Helen Durand, and Panagiotis D. Christofides. „A Tutorial Review of Economic Model Predictive Control Methods." en. In: *Journal of Process Control* 24.8 (Aug. 2014), pp. 1156–1178. ISSN: 09591524. DOI: 10.1016/j.jprocont.2014.03.010. URL: http://linkinghub.elsevier.com/retrieve/pii/S0959152414000900 (visited on 01/25/2017).

[DAR11] M. Diehl, R. Amrit, and J. B. Rawlings. „A Lyapunov Function for Economic Optimizing Model Predictive Control." In: *IEEE Transactions on Automatic Control* 56.3 (Mar. 2011), pp. 703–707. ISSN: 0018-9286. DOI: 10.1109/TAC.2010.2101291.

[Gro+20] Sébastien Gros et al. „From Linear to Nonlinear MPC: Bridging the Gap via the Real-Time Iteration." en. In: *International Journal of Control* 93.1 (Jan. 2020), pp. 62–80. ISSN: 0020-7179, 1366-5820. DOI: 10.1080/00207179.2016.1222553. URL: https://www.tandfonline.com/doi/full/10.1080/00207179.2016.1222553 (visited on 03/29/2020).

[KAM19] Johannes Kohler, Frank Allgower, and Matthias A. Muller. „A Simple Framework for Nonlinear Robust Output-Feedback MPC." en. In: *2019 18th European Control Conference (ECC)*. Naples, Italy: IEEE, June 2019, pp. 793–798. ISBN: 978-3-907144-00-8. DOI: 10.23919/ECC.2019.8795965. URL: https://ieeexplore.ieee.org/document/8795965/ (visited on 02/27/2020).

[Koh+] Johannes Kohler et al. „A Computationally Efficient Robust Model Predictive Control Framework for Uncertain Nonlinear Systems." en. In: (), p. 20.

[Bem+00] A. Bemporad et al. „The Explicit Solution of Model Predictive Control via Multiparametric Quadratic Programming." en. In: *Proceedings of the 2000 American Control Conference. ACC (IEEE Cat. No.00CH36334)*. Chicago, IL, USA: IEEE, 2000, 872–876 vol.2. ISBN: 978-0-7803-5519-4. DOI: 10.1109/ACC.2000.876624. URL: http://ieeexplore.ieee.org/document/876624/ (visited on 02/26/2020).

[AB09] Alessandro Alessio and Alberto Bemporad. „A Survey on Explicit Model Predictive Control." en. In: *Nonlinear Model Predictive Control*. Lecture Notes in Control and Information Sciences. Springer, Berlin, Heidelberg, 2009, pp. 345–369. ISBN: 978-3-642-01093-4 978-3-642-01094-1. DOI: 10.1007/978-3-642-01094-1_29. URL: https://link-springer-com.proxy.findit.dtu.dk/chapter/10.1007/978-3-642-01094-1_29 (visited on 03/06/2018).

[GKJ07] Alexandra Grancharova, Jus Kocijan, and Tor A. Johansen. „Explicit Stochastic Nonlinear Predictive Control Based on Gaussian Process Models." en. In: *2007 European Control Conference (ECC)*. Kos: IEEE, July 2007, pp. 2340–2347. ISBN: 978-3-9524173-8-6. DOI: 10.23919/ECC.2007.7068422. URL: https://ieeexplore.ieee.org/document/7068422/ (visited on 03/02/2020).

[GJ12] Alexandra Grancharova and Tor Arne Johansen. *Explicit Nonlinear Model Predictive Control: Theory and Applications*. en. Lecture Notes in Control and Information Sciences 429. OCLC: ocn780478001. Heidelberg ; New York: Springer, 2012. ISBN: 978-3-642-28779-4.

[Mes18] Ali Mesbah. „Stochastic Model Predictive Control with Active Uncertainty Learning: A Survey on Dual Control." en. In: *Annual Reviews in Control* 45 (2018), pp. 107–117. ISSN: 13675788. DOI: 10.1016/j.arcontrol.2017.11.001. URL: https://linkinghub.elsevier.com/retrieve/pii/S1367578817301232 (visited on 09/05/2019).

[Kal60] R.E. Kalman. „On the General Theory of Control Systems." en. In: *IFAC Proceedings Volumes* 1.1 (Aug. 1960), pp. 491–502. ISSN: 14746670. DOI: 10.1016/S1474-6670(17)70094-8. URL: https://linkinghub.elsevier.com/retrieve/pii/S1474667017700948 (visited on 02/11/2020).

[PR01] Gabriele Pannocchia and James B. Rawlings. *Robustness of MPC and Disturbance Models for Multivariable Ill-Conditioned Processes*. English. Tech. rep. 2001-02. USA: TWMCC, Texas-Wisconsin Modeling and Control Consortium, 2001.

[Van81] P. Van Dooren. „A Generalized Eigenvalue Approach for Solving Riccati Equations." In: *SIAM Journal on Scientific and Statistical Computing* 2.2 (June 1981), pp. 121–135. ISSN: 0196-5204. DOI: 10.1137/0902010. URL: http://epubs.siam.org/doi/abs/10.1137/0902010 (visited on 07/26/2019).

[Lau78] Alan J. Laub. *A Schur Method for Solving Algebraic Riccati Equations*. eng. Tech. rep. USA: Massachusetts Institute of Technology, Laboratory for Information and Decision

Systems, 1978, pp. 44–46. URL: https://dspace.mit.edu/handle/1721.1/1301 (visited on 07/26/2019).

[ZL16] Florian Ziel and Bidong Liu. „Lasso Estimation for GEFCom2014 Probabilistic Electric Load Forecasting." In: *International Journal of Forecasting* 32.3 (July 2016), pp. 1029–1037. ISSN: 0169-2070. DOI: 10.1016/j.ijforecast.2016.01.001. URL: http://www.sciencedirect.com/science/article/pii/S0169207016000091 (visited on 08/28/2018).

[Sim06] Dan Simon. *Optimal State Estimation: Kalman, H∞, and Nonlinear Approaches*. en. Hoboken, NJ, USA: John Wiley & Sons, Inc., May 2006. ISBN: 978-0-470-04534-3 978-0-471-70858-2. DOI: 10.1002/0470045345. URL: http://doi.wiley.com/10.1002/0470045345 (visited on 02/25/2020).

[Sco15] D.W. Scott. *Multivariate Density Estimation: Theory, Practice, and Visualization*. Wiley Series in Probability and Statistics. Wiley, 2015. ISBN: 978-0-471-69755-8. URL: https://books.google.dk/books?id=pIAZBwAAQBAJ.

[Bev14] Hassan Bevrani. *Robust Power System Frequency Control*. Power Electronics and Power Systems. Cham: Springer International Publishing, 2014. ISBN: 978-3-319-07277-7 978-3-319-07278-4. DOI: 10.1007/978-3-319-07278-4. URL: http://link.springer.com/10.1007/978-3-319-07278-4 (visited on 09/27/2017).

[Kla17] Martin Klauco. *MPC-Based Reference Governors: Theory and Applications*. June 2017.

[Bem] Alberto Bemporad. „Reference Governors: On-Line Set-Point Optimization Techniques for Constraint Fulfillment." en. In: (), p. 169.

[Mad+14] Henrik Madsen et al. „Control of Electricity Loads in Future Electric Energy Systems." English. In: *Handbook of Clean Energy Systems*. Vol. 6. Denmark: Wiley, 2014, pp. 2213–2236. ISBN: 978-1-118-38858-7. URL: http://onlinelibrary.wiley.com/doi/10.1002/9781118991978.hces033/full (visited on 01/24/2017).

[OH11] Olivier Corradi and Henning Ochsenfeld. „Integration of Fluctuating Energy by Electricity Price Control." Master Thesis. Copenhagen: Technical University of Denmark, 2011.

[MVA13] Johanna L. Mathieu, Marina González Vayá, and Göran Andersson. „Uncertainty in the Flexibility of Aggregations of Demand Response Resources." In: *IECON 2013 - 39th Annual Conference of the IEEE Industrial Electronics Society*. Nov. 2013, pp. 8052–8057. DOI: 10.1109/IECON.2013.6700479.

[BPK16] Steven L. Brunton, Joshua L. Proctor, and J. Nathan Kutz. „Sparse Identification of Nonlinear Dynamics with Control (SINDYc).“ In: *arXiv:1605.06682 [math]* (May 2016). arXiv: 1605.06682 [math]. URL: http://arxiv.org/abs/1605.06682 (visited on 05/24/2019).

[Car+17] Bob Carpenter et al. „Stan: A Probabilistic Programming Language.“ In: *Journal of Statistical Software* 76.1 (Jan. 2017). DOI: 10.18637/jss.v076.i01. URL: https://www.jstatsoft.org/article/view/v076i01.

[Fri+13] Roger Frigola et al. „Bayesian Inference and Learning in Gaussian Process State-Space Models with Particle MCMC.“ en. In: *arXiv:1306.2861 [cs, stat]* (Dec. 2013). DOI: 10.1.1.766.1321. arXiv: 1306.2861 [cs, stat]. URL: http://arxiv.org/abs/1306.2861 (visited on 03/28/2020).

Part II

PUBLICATIONS

This part contains publications within this thesis:

- Paper A, Paper B: Alternative solutions to the load frequency control (LFC) problem.
- Paper C: A solution to the problem of integrating electric vehicles (EVs) into the LFC problem using indirect control (ICo).
- Paper D: Sparsity Promoting System Identification of Nonlinear Dynamics with control algorithm SINDyc in combination with MCMC in context of the identification of prosumer dynamics.
- Paper E: A case study including a hierarchical control concept combining stochastic unit dispatch and active power balancing using aggregated MPC.
- Paper G: An alternative solution to the coordinated voltage control problem.

6 PAPER A

Load Frequency Control in Microgrids using target adjusted Model Predictive Control

Abstract — *MPC has been applied in multiple ways to the Load Frequency Control problem. In this study, the authors illustrate and compare a target–adjusted MPC to a classical MPC formulation. The target–adjusted approach is also posed as optimal control law. The target–adjusted MPC is an alternative formulation that incorporates the system equilibrium into the control objective. The derived alternative controller can be used as alternative to classical MPCs.*

Authors: Frederik Banis, Daniela Guericke, Henrik Madsen, Niels Kjølstad Poulsen

Published in the *IET RPG* journal ([Ban+19]):

6.1 INTRODUCTION

The increasing share of renewable energy system (RES) in the energy production mix is associated with considerable power production uncertainty. Remedies for the issue can be categorized into improvements of infrastructure and improvements of system controls. An approach enabling for the combination of the two categories is the concept of microgrid (MG) which makes it possible to unlock the flexibility required for integrating large shares of fluctuating RES. Coordinated control of controllable units within the MG enables for leveraging of synergies in an optimized manner, due to that the limited complexity of the confined system allows for the implementation of online optimization control strategies at a high degree of precision in the controls. An example for such control strategy is model predictive control (MPC). The system operation and resilience can then be improved amongst others by inclusion of information of uncertain processes in the form of forecasts, for example with respect to the uncertainty associated

Table 6.1: Nomenclature. </> denotes unspecified units.

Symbol	Description	Unit
$u^\star$	Optimal input sequence (Control variables)	pu
$\bar{u}$	Input reference trajectory	pu
x	System state	/
$\hat{x}$	One–step prediction of x	/
$\tilde{x}$	State target	/
$\tilde{u}$	Control target	/
$\hat{d}$	Disturbance estimate	pu
$\hat{d}_e$	ϵ augmented disturbance estimate	/
y	Frequency deviation (Controlled variable)	pu
$\hat{y}$	One–step prediction of y	pu
y_m	Grid frequency measurement	Hz
ϵ	Integrated output error	Hz
$\epsilon_A, \epsilon_B, \epsilon_{B_d}$	Multiplicative model–plant errors w.r.t. corresponding model parameters	/
$\tilde{p}$	System equilibrium	/
w	State error: Wiener process	/
v	Measurement error: White noise process	Hz
θ	Model parameter vector	/
f, σ, h	Nonlinear model functions	/
ω	Standard Wiener process	/
T_s	Controller sampling time	s
N	Prediction horizon	/
$L_x,\ L_d$	Kalman gain w.r.t. states and w.r.t. disturbance	/
$A,\ B,\ B_d,\ G_s,\ C,\ D$	State Space System matrices	/
Φ_x	Free Markov parameters	/
Γ_u	Forced Markov parameters (controlled)	/
Γ_d	Forced Markov parameters (uncontrolled)	/
G, h	Objective inequality coefficients, bounds	/
K	Optimal Control feedback gain	/
K_∞	Lumped deduced disturbance gain	/
$K_{u,\infty}$	Disturbance gain to the system inputs	pu
$K_{x,\infty}$,	Disturbance gain to the system states	/
Δf	Frequency deviation with respect to nominal frequency	Hz
W_z	Output space precision penalization	/
$W_{\Delta u}$	Rate of movement penalization	/
$W_{\bar{u}}$	Input reference tracking penalization	/
β	Tuning term: Input reference tracking	/
H	Inertia based supply time	s
D	Load damping coefficient	/

with RES. Furthermore, this facilitates the use of the MG as a virtual and flexible power plant which enhances the possibilities of unlocking the flexibility required to comply with agreed market bids.

Designing controls for virtual power plants involves the setup of a control structure with consideration of complexity and system dynamics. Incorporation of predictions of stochastic processes introduce complexity due to the combinatorial explosion of manifold process outcomes. In contrary, fast system control loops require prompt decision making. Handling problem complexity in this setting and simultaneously providing sufficient sampling rates of well–posed control signals constitute two major challenges associated with the optimized control of MGs with high shares of RES. This problem complexity is usually handled by the setup of a temporal control hierarchy — the problem complexity is then managed by several specialized control routines [Sch78]. See Figure 8.2 as illustration of this principle. Control hierarchies are also considered in related areas such as ancillary services provision [De +18; Mad+14].

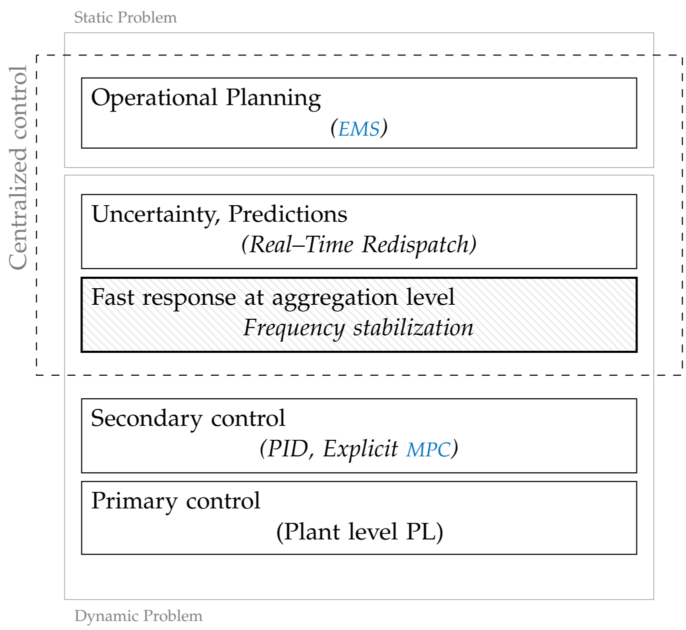

Figure 6.1: Exemplary hierarchy of controllers in the centralized control scheme and their associated dominant focus. An operational planning layer takes long–term predictions and complex system requirements in the planning stage into account. The real–time redispatch adjusts the system operation to altered requirements during operation. Scope of this paper: The frequency stabilization problem at the aggregated system level (centralized controls).

The control structure that evolved historically in the context of frequency control is split into a primary frequency control loop, a secondary frequency control loop and a tertiary frequency control loop. The primary controls hereby serve for the stabilization of the system frequency after a disturbance within delay of a few seconds. Secondary control initiates its compensation to such event in the magnitude of some seconds to minutes. Tertiary control covers a longer temporal window [Bev14; Kun94].

Table 6.3: Abbreviations.

RES	Renewable Energy Systems
LFC	Load Frequency Control
AGC	Automatic Generation Control
MG	Microgrid
MPC	Model Predictive Control
OC	Optimal Control
CL	Closed Loop
MISO	Multiple–Input Single–Output
SDE	Stochastic Differential Equation
LQG	Linear Quadratic Gaussian regulator
DLQR	Discrete–time Linear Quadratic Regulator
GUROBI	Optimizer, here used to minimize quadratic programming (QP) problems
LAPACK	Linear algebra package
GELSD	Lapack routine for solving least–squares problems
c0	Classic quadratic regulator formulation
c1	Target adjusted regulator formulation

[PML17; PRG16; Han+14] are examples where the optimization problem for the aggregated MG system is posed with a sampling rate in the magnitude of multiple minutes. Consequently, they act on the tertiary control layer. Stochastic Programming formulations are typically used for such problems, due their capability to treat uncertainty associated with process predictions. [PMK13; SSJ09; Sha+17] provide literature overview over the topic of load frequency control (LFC) and automatic generation control (AGC). For the secondary control problem many solution approaches have been proposed, including optimal control [Cal72; Bar73; FE70; ZTL13] or adaptive controllers and robust controllers [Sir+10; WZW94]. Often, these approaches are combined with state observers [YT86] and system identification techniques [HKN00]. Proactive action in the LFC can improve its performance and MPC is a control strategy enabling for it. Examples can be found in [EIU16; Ven+08; SRA13]. In this paper we illustrate an MPC formulation for LFC based on [PR03; GAM08]. To the best of our knowledge this controller has not yet been presented for the LFC problem. An optimal control (OC) using the same approach is also presented. The control problem is stated here in the context of MG LFC but can be applied to different problems alike. This paper does not consider a thorough treatment of the underlying control theory — it can be obtained by consideration of, among others, [PR03; GAM08].

6.2 MODELS

We consider the swing equation [Ben15; Bev14; Kun94] as our main state in the controller model:

$$\frac{d}{dt}\Delta f(t) = -\frac{D}{2H}\Delta f(t) + \frac{1}{2H}\Delta P_{\text{mech}}(t) \tag{6.1}$$

Δf denotes the frequency deviation from nominal frequency, D is the load damping coefficient and H the inertia based supply time. ΔP_{mech} is the power balance within the grid. The model maps the overall power imbalance to an angular frequency deviation from the nominal grid frequency by taking the approximated system inertia into account. The swing equation is a means to express the lumped system inertia and its parameters are both unknown and time–varying. Consequently adaptive estimation techniques [UBA14] should be applied in order to obtain a precise model for varying conditions.

The considered underlying processes are nonlinear and can be modeled using Stochastic Differential Equations (SDEs) such as formulated for example in [KMJ04]:

$$\mathrm{d}x_t = f(x_t, u_t, t, \theta)\mathrm{d}t + \sigma(u_t, t, \theta)\mathrm{d}\omega_t \tag{6.2}$$

$$y_k = h(x_k, u_k, t_k, \theta) + v_k \tag{6.3}$$

where t is the time variable; t_k are sampling instants; x_t is a vector of system states with the main state being the frequency deviation from nominal frequency Δf; u_t is a vector of input variables; y_k is the single output variable and equals the main state Δf; θ is a vector of parameters; f, σ and h are nonlinear functions; ω_t is a standard Wiener process and v_k is a white noise process with $v_k \in \mathcal{N}(0, S(u_k, t_k, \theta))$. See [KMJ04] for further clarifications and details of this formulation.

All used system models are linearized, enabling the application of linear control theory. The power balance is obtained by using lumped system models — groups of actors sharing dominant dynamics and requirements are hereby lumped together, resulting in a reduced order model. See in this context [EIU16; Sax19]. The accepted loss in precision of this reduced model compared to the untreated linear system model is a design choice and has to be traded against the gained reduction in computational load in the optimization step. The linearized discrete time system model can be formulated as stated in Equation 6.4, see [KMJ04].

$$
\begin{aligned}
\frac{\mathrm{d}x_{t|j}}{\mathrm{d}t} &= f_0 + A(x_t - x_j) + B(u_t - u_j) + \\
&\quad G(d_t - d_j) + w_t && (6.4a) \\
y_t &= Cx_t + e_t && (6.4b)
\end{aligned}
$$

x is the system state; u the controlled system input, d the uncontrolled system input (disturbance). w and e are process and measurement noise respectively. This is a multiple–inputs single–output (MISO) system if more than one unit in the MG are considered.

6.3 TARGET ADJUSTED DLQR

The feedback control law of the classical DLQR is commonly formulated as

$$u_k^\star = -K\hat{x}_{k|k} \tag{6.5}$$

Whereas the target adjusted DLQR can be stated as

$$u_k^\star = K(\hat{x}_{k|k} - \tilde{x}_{k|k}) - \tilde{u}_{k|k} \tag{6.6}$$

K is hereby found by solving the discrete–time algebraic Riccati equation [Van81; Lau78]. The equilibrium operating point of the system can be stated in terms of the input and state of the system $\tilde{p}$. $\tilde{p}$ can be linearly related to the filtered lumped disturbance $\hat{d}$:

$$\tilde{p}_{k|k} = \{\tilde{x}_{k|k}\,, \tilde{u}_{k|k}\} = K_\infty \hat{d}_{k|k} \tag{6.7}$$

K_∞ is a gain from a unit disturbance to one corresponding system equilibrium point. Scaling by the estimate $\hat{d}$ recovers another system equilibrium corresponding to $\hat{d}$. K_∞ can be obtained using a least–squares approximation, due to that the lumped system matrix M for the considered systems is non–symmetric in the MISO case:

$$\overbrace{\begin{bmatrix} A - I & B \\ C & 0 \end{bmatrix}}^{M} \overbrace{\begin{bmatrix} K_{x,\infty} \\ K_{u,\infty} \end{bmatrix}}^{K_\infty} = \begin{bmatrix} B_d \\ 0 \end{bmatrix} \tag{6.8}$$

This approach is outlined in [MR93; PR03] and related approaches have been applied e.g. in [Huu+10]. Notice that the system of equations denoted in Equation 6.8 has to be solved once for each model formulation. B_d hereby denotes the lumped modeled disturbance dynamics. Mismatch of B_d related to the real system dynamics lead to loss of controller performance. This loss of performance is then to be compensated for by application of appropriate robustness and adaptive control strategies which are not subject of this paper. For an ideal B_d, this regulator formulation achieves asymptotic stability in the controlled variable Δf.

6.3.1 Offset free frequency tracking

In order to drive the output $f \to \bar{f}$, where $\bar{f}$ is the goal frequency and $\bar{f} = f_{\mathrm{nom}} + \Delta f$, the control law Equation 6.5 can be augmented to include the integrated offset

$$\epsilon_{k+1|k} = \epsilon_{k|k} + \hat{y}_{k|k} - \bar{y}_k \tag{6.9}$$

$\hat{y}_{k|k}$ here is the output of the system model using the state estimate $\hat{x}_{k|k}$ and $\bar{y}_k = \Delta \bar{f}_k$, the goal frequency deviation. The target Equation 6.7 then becomes

$$\tilde{p}_{k|k} = \{\tilde{x}_{k|k}\,, \tilde{u}_{k|k}\} = K_\infty(\epsilon_{k|k} + \hat{d}_{k|k}) \tag{6.10}$$

6.4 MODEL PREDICTIVE REGULATORS

6.4.1 Classic quadratic objective

The classic quadratic reference tracking objective can be stated as such:

$$\begin{aligned} \min_{u,\ k} J_0 = {} & ||\Phi_x \hat{x}_{k|k} + \Gamma_u u_k + \Gamma_d \hat{d}_{k|k} - \tilde{y}_k||^2_{W_z} \\ & + \beta ||u_k||^2_{W_{\Delta u}} \\ & + (1-\beta)||u_k - \bar{u}_{k|k}||^2_{W_{\bar{u}}} \end{aligned} \tag{6.11}$$

Notice that we could neglect the control action regularization term $||u_k||^2_{W_{\Delta u}}$ in the case where we use a Kalman filter as smoothing component in the control loop. β is a tuning term used to gradually move the controller from regulatory behavior *without* input reference tracking ($\beta = 1$) to regulatory behavior *with* input reference tracking ($\beta = 0$). If offset–free control in the controlled variable Δf is aimed for, $\hat{d}$ can be augmented with the integrated error in the controlled variable ϵ. Then, d_e is used instead of d. In this case, $\tilde{y} = 0$. See for example [Huu+11].

$$\hat{d}_{e,k|k} = \hat{d}_{k|k} + \epsilon_k \tag{6.12}$$

$$\epsilon_{k+1|k} = \epsilon_{k|k} + \hat{y}_{k|k} - \bar{y}_k \tag{6.13}$$

Then

$$\tilde{y}_k = 0 \tag{6.14}$$

Alternatively, offset–free control can be achieved by using the following integrating term in the objective function:

$$\tilde{y}_{k+1|k} = \tilde{y}_{k|k} + \hat{y}_{k|k} - \bar{y}_k \tag{6.15}$$

A mismatch in the disturbance–associated model dynamics Γ_d can lead to loss of performance in the controlled variables.

6.4.2 Target adjusted quadratic objective

The target adjusted approach discussed in Section 6.3 can be applied in the MPC framework using

$$\begin{aligned}\min_{u,\ k} J_1 = {} & ||\Phi_x(\hat{x}_{k|k} - \tilde{x}_{k|k}) + \Gamma_u(u_k - \tilde{u}_{k|k}) - \bar{y}_k||^2_{W_z} \\ & + \beta||u_k - u^\star_{k-1}||^2_{W_{\Delta u}} \\ & + (1-\beta)||u_k - \bar{u}_{k|k}||^2_{W_{\bar{u}}}\end{aligned} \tag{6.16}$$

Again β denotes a tuning term used to switch the controller from regulatory behavior without input reference tracking to regulatory behavior with input reference tracking. Hereby, the target Equation 6.7 is used. A similar regulator implementation can be found in [Ban+18].

6.4.3 Constraints

Hard input constraints and ramp–rate constraints for both MPCs can be formulated as

$$u_{\min,k} \leq u_k \leq u_{\max,k} \tag{6.17}$$

$$\Delta u_{\min,k} \leq \Delta u_k \leq \Delta u_{\max,k} \tag{6.18}$$

$$G_k\, u_k \leq h_k \tag{6.19}$$

[JHR11] include examples of hard input constraint and ramp–rate constraint formulations.

6.5 STATE OBSERVER

We estimate the residual $\hat{d}$ using a Kalman filter following the formulations given in [PR01; PR03]. The augmented system model with integrating disturbance estimate and filter equations is then given by:

$$\begin{bmatrix} \hat{x}_{k+1|k} \\ \hat{d}_{k+1|k} \end{bmatrix} = \begin{bmatrix} A & B_d \\ 0 & I \end{bmatrix} \begin{bmatrix} \hat{x}_{k|k-1} \\ \hat{d}_{k|k-1} \end{bmatrix} + \begin{bmatrix} B \\ 0 \end{bmatrix} u_k + \begin{bmatrix} L_x \\ L_d \end{bmatrix} (y_{m,k} - C\hat{x}_{k|k-1} - C_d\hat{d}_{k|k-1}) \quad (6.20)$$

where y_m is the local grid frequency measurement. This is the one–step predictor of both estimated state $\hat{x}$ and disturbance $\hat{d}$. Notice that $\hat{d}$ hereby is a lumped disturbance capturing any mismatch between desired and effective input–output relation. As improvement to this approach an Extended Kalman Filter can be used as stated for example in [KMJ04], in order to achieve faster convergence and to estimate the uncertainty P_d of the disturbance as well.

The performance of this filter affects the control performance. See [Huu+10] for additional applications.

6.6 PREDICTIONS

The classical MPC formulation stated in Equation 6.11 incorporates the disturbance prediction sequence $\hat{d}_{k+N|k}$ via the disturbance impulse response coefficients Γ_d. The discussed target adjusted DLQR and MPC formulations, Equation 6.5 and Equation 6.16, do not have this capability. However, they can incorporate an expected future state of the disturbance process $\hat{d}_{k+j|k}$. The predictive performance of using this approach versus consideration of the full disturbance prediction sequence consequently is lower in most cases.

6.7 TUNING

For the discussed controllers — as generally for OC and MPC — a multitude of tuning opportunities do exist. Tuning is then most commonly a recursive process in which the controlled parameters are adjusted such as to comply for example with network standards [Eur13].

Soft output constraints are one means to adjust the CL performance. In the context of the LFC problem, soft output constraints allow, for example, for tailoring of the objective in order to more aggressively aim for frequency stabilization outside of the specified frequency band. For soft output constraints and a MISO system, a set of $2N$ slack variables are introduced into the optimization problem, N being the prediction horizon in the presented control objectives. This leads to a computationally more demanding formulation. See e.g. [GJ09].

Another important CL system property for the LFC problem is the capability to balance between variance in the controlled variable and variance of the control variables. The latter is often referred to as control effort. The control effort hereby is to be tuned in order to distribute the regulatory share and balance the wear and tear in the set of system actors, see e.g. [Huu+10]. As discussed in [EIU16], the control effort tuning can be augmented to include economical weights — prices which inform the control law about how to distribute the control effort. Due to the mixing of operational and economical considerations in the resulting objective, this is a sub–optimal treatment of economical aspects.

When using controllers within a control hierarchy, input reference tracking is required. The corresponding tracking precision selection is adjusted by tuning of the penalization matrix $W_{\bar{u}}$. Both $W_{\Delta u}$ and $W_{\bar{u}}$ are hereby selected by some tuning method: Genetic Algorithms (GA) [PY13] is an example for such method.

As generally in context of MPC, online system identification techniques, incorporation of adaptive measures and robustness considerations should be considered in order to compensate for unmodeled uncertainty. Such methods may be applied for the discussed target adjusted controller as well.

6.8 SIMULATIONS

Consider the test system as shown in Equation 6.21 and the constraints given in Equation 6.22. It consists of

- Swing equation parameterized with $D = 1.5$ and $H = 6.0$ as stated in Equation 7.1
- Actors (control inputs `U0, U1, U2` respectively):
  - Tie–line dynamics
  - Two generators including turbine and governor dynamics

then Control inputs are chosen based on the documented control laws. The system exposes the poles and zeroes illustrated in Figure **??**. The dynamics are selected in order to reflect a simple multi–actor system with a reasonable range of dynamics, see Table 6.4.

All systems are discretized using the zero–order hold approach with sampling rate of 2 seconds. The sampling rate here is chosen arbitrarily. The online optimization problems are solved using the GUROBI solver [Gur18]. The solution to the least-squares problem is obtained using the LAPACK GELSD driver [And+99]. Load data time–series is obtained from [18]. The classical MPC stated in Section 6.4.1 is in the following referred to as `c0`, the target adjusted MPC

$$A = \begin{bmatrix} 0.7165 & 0.0265 & 0.0165 & 0.2146 & 0.0087 & 0.1125 & 0.0775 \\ 0.0 & 0.7165 & 0.0 & 0.0 & 0.0 & 0.0 & 0.0 \\ 0.0 & 0.0 & -0.0066 & -0.0825 & 0.0 & 0.0 & 0.0 \\ 0.0 & 0.0 & 0.066 & 0.8253 & 0.0 & 0.0 & 0.0 \\ 0.0 & 0.0 & 0.0 & 0.0 & -0.0036 & -0.0454 & 0.0 \\ 0.0 & 0.0 & 0.0 & 0.0 & 0.0727 & 0.9085 & 0.0 \\ 0.0 & 0.0 & 0.0 & 0.0 & 0.0 & 0.0 & 0.1353 \end{bmatrix} \tag{6.21a}$$

$$B = \begin{bmatrix} 0.0297 & 0.0173 & 0.0089 \\ 1.7008 & 0.0 & 0.0 \\ 0.0 & 0.066 & 0.0 \\ 0.0 & 0.1397 & 0.0 \\ 0.0 & 0.0 & 0.0727 \\ 0.0 & 0.0 & 0.1464 \\ 0.0 & 0.0 & 0.0 \end{bmatrix} \tag{6.21b}$$

$$C = \begin{bmatrix} 1.0 & 0.0 & 0.0 & 0.0 & 0.0 & 0.0 & 0.0 \end{bmatrix} \tag{6.21c}$$

$$D = \begin{bmatrix} 0.0 & 0.0 & 0.0 \end{bmatrix} \tag{6.21d}$$

$$\begin{bmatrix} -0.5 \\ 0.0 \\ 0.0 \end{bmatrix} \leq u \leq \begin{bmatrix} 0.5 \\ 0.2 \\ 0.3 \end{bmatrix} \tag{6.22a}$$

$$\begin{bmatrix} -0.02 \\ -0.01 \\ -0.01 \end{bmatrix} \leq \Delta u \leq \begin{bmatrix} 0.08 \\ 0.005 \\ 0.0025 \end{bmatrix} \tag{6.22b}$$

stated in Section 6.4.2 is referred to as `c1`.

We aim to test for:

- Whether `c1` is capable of stabilizing the system frequency
- Whether constraints and penalization matrices have the desired effect on the CL system for `c1`
- How `c1` compares to `c0` in terms of sensitivity to model uncertainties

Notice that in all presented simulations no disturbance predictions are used. Given the presence of uncertainty compensated predictions, the response characteristics can be improved as a result to the proactive action of the two discussed controllers.

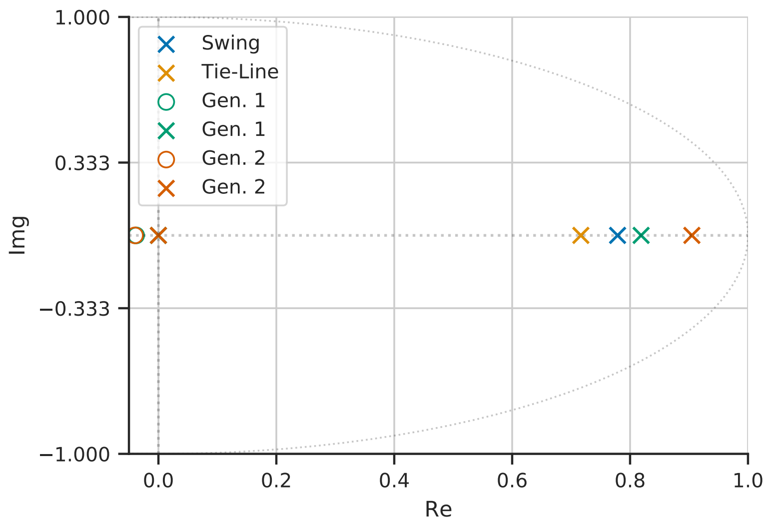

Figure 6.2: Poles–Zeroes map of the considered test system (swing equation `Swing`, tie–line dynamics `Tie-Line`, generator dynamics 1 and 2, `Gen. 1` and `Gen. 2` respectively). Both `Gen. 1` and `Gen. 2` have a pole at the origin and a zero in the left–half plane.

6.8.1 Disturbance rejection

`c1` is applied to the test system Equation 6.21 with control effort penalization $\tilde{W}_{\Delta u}$ as stated in Equation 6.23 below and without enabled input reference tracking term. $\tilde{W}_{\Delta u}$ are the first $n_u \times n_u$ elements of $W_{\Delta u}$.

$$\tilde{W}_{\Delta u} = \begin{bmatrix} 1.0 & 0.0 & 0.0 \\ 0.0 & 0.05 & 0.0 \\ 0.0 & 0.0 & 1.0 \end{bmatrix} \tag{6.23}$$

The second generator (`U1`) resulting from $W_{\Delta u}$ is penalized the least and is consequently most active in terms of control effort. See Figure 6.3. This penalization is exemplary for a real application where the operation of selected units is to be maintained mostly constant. Unit `U1` saturates in the up–ramp event on the ramp–rate constraints and partly on the hard input bounds.

6.8.2 Input reference tracking

Another important property for the LFC problem is the tracking of input–references, illustrated in Figure 6.4.

All three units receive individual input trajectories with step changes applied at two time instances throughout the experiment. As disturbance the trajectory depicted in Figure 6.3 is used. For the time–range

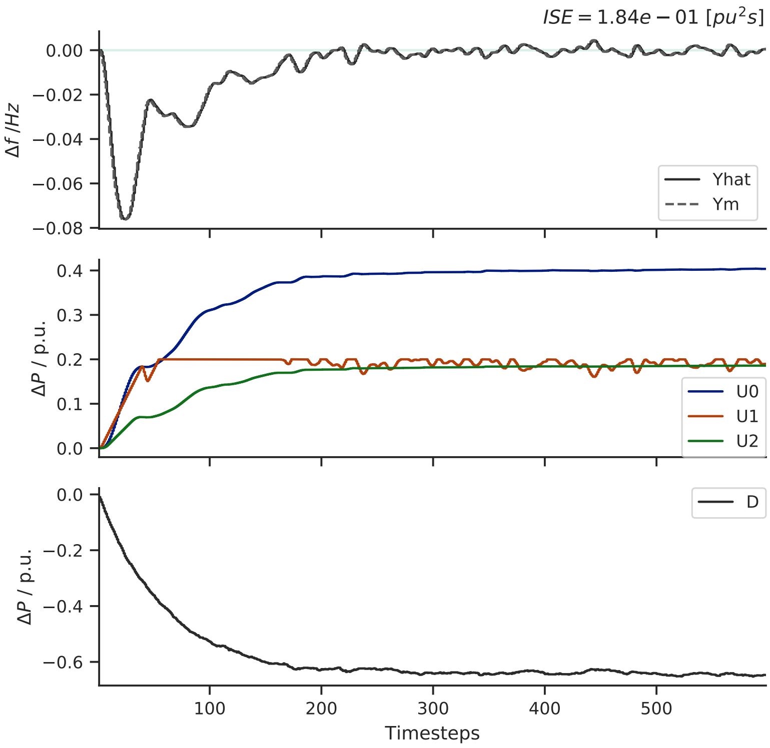

Figure 6.3: Target adjusted MPC (`c1`). Uppermost graph: Frequency deviation from reference (main state and single output), middle graph: Control input deviations from reference, lowermost graph: disturbance deviation from reference (grid load). The control effort penalization depicted in Equation 6.23 lead to the stronger utilization of `U1`. Saturation on the ramp–rate constraints and hard bounds can be observed for `U1`.

Table 6.4: Test system step–response characteristics obtained using MATLAB.

Step–response characteristic / unit	Swing	Tie–line	Gen. 1	Gen. 2
Rise time (s)	18.00	12.00	22.00	44.00
Settling time (s)	32.00	24.00	40.00	80.00
Settling min. (p.u.)	0.6119	0.9030	0.9086	0.9089
Settling max. (p.u.)	0.6667	1.00	1.00	0.9999
Overshoot (%)	0.00	0.00	0.00	0.00
Undershoot (%)	0.00	0.00	0.00	0.00
Peak (p.u.)	0.6667	1.00	1.00	0.9999
Peak time (s)	138.00	138.00	158.00	198

`350-600` an ill–posed trajectory is given to the controller: the summation of active power injection requests does not match the actual load. The controlled variable is nevertheless maintained close to its reference due to the chosen tracking penalization term $W_{\bar{u}} = 1e^{-2}$. For increasing $W_{\bar{u}}$, the tracking precision increases. Consequently, the performance in Δf deteriorates stronger for ill–posed input reference trajectories with increasing $W_{\bar{u}}$.

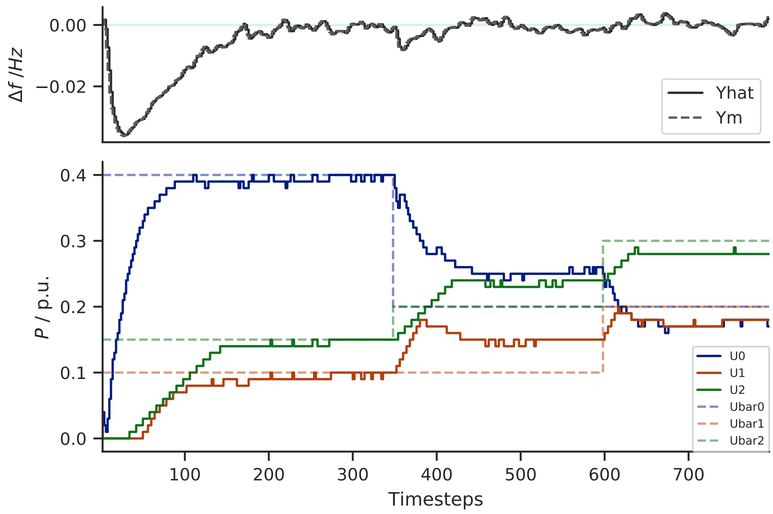

Figure 6.4: Input reference tracking with `c1` and $W_{\bar{u}} = 1e^{-2}$. The reference trajectories given from timestep `350-600` are a mismatch to the actual disturbance. As disturbance the trajectory given in Figure 6.3 is used.

6.8.3 Parametric system model mismatch

In Figure 6.5, `c0` and `c1` trajectories in Δf are compared for different multiplicative model–plant errors ϵ_A, ϵ_B, and ϵ_{B_d}. The disturbance trajectory given in Figure 6.3 without noise term is used to excite the system. It is to be noted that the sensitivity in the control effort penalization term $W_{\Delta u}$ differs for the two controllers. Additional differences in the sensitivity to available means to tuning apply. Accordingly, trajectories should be considered and compared in qualitative rather than quantitative manner. Furthermore, only a selection of lumped multiplicative parametric mismatches are considered here in order to exhibit some differences in the two considered controllers. For all considered experiments the control laws remain asymptotically stable in Δf.

For $\epsilon_A = 1.0$ the response of `c1` is less aggressive. The opposite is true for $\epsilon_A = 0.9$. `c1` oscillates for $\epsilon_A = 0.8$, the control law is then not sufficiently damped. The stabilization of `c0` is slower for most of the corresponding trajectories, see the central graph in Figure 6.5. A dedicated plot for the mismatch in G is neglected here, due to that the resulting response characteristics are similar as for the already given multiplicative mismatch in B in the central graph. For $\epsilon_{B_d} = 0.5$, `c0` overshoots. When the lumped filter disturbance dynamics B_d exceed the system disturbance dynamics G by a factor of 1.5 as shown in the lower–most graph, controller `c1` exhibits a faster response.

6.9 DISCUSSION

The target adjusted MPC `c1` based on LQG is an alternative solution to the LFC control problem. It exposes different properties compared to the classical MPC formulation `c0`. The response to perturbations in form of disturbance steps is comparatively damped; a characteristic that is non–desirable. As shown in Figure 6.5, tuning of the Kalman Filter can alter the response characteristics and lead to a more pronounced response in comparison to the classical MPC formulation `c0`. `c1` in all considered simulations stabilizes Δf unidirectional, that is, asymptotically from a single deviation direction. `c0`, at least for the non–mismatch scenario, exposes the slight overshoot typical to OC and MPC — an often desirable property.

`c1` has only predictive capabilities by using the expected disturbance considering the optimization horizon $E(\hat{d}_{k+N|k})$. `c0` in contrast evaluates a potentially available disturbance prediction sequence $\hat{d}_{k+N|k}$ directly within the objective function and consequently can achieve higher precision in the control decisions. Input reference tracking is successfully demonstrated in Figure 6.4, convergence to the imposed

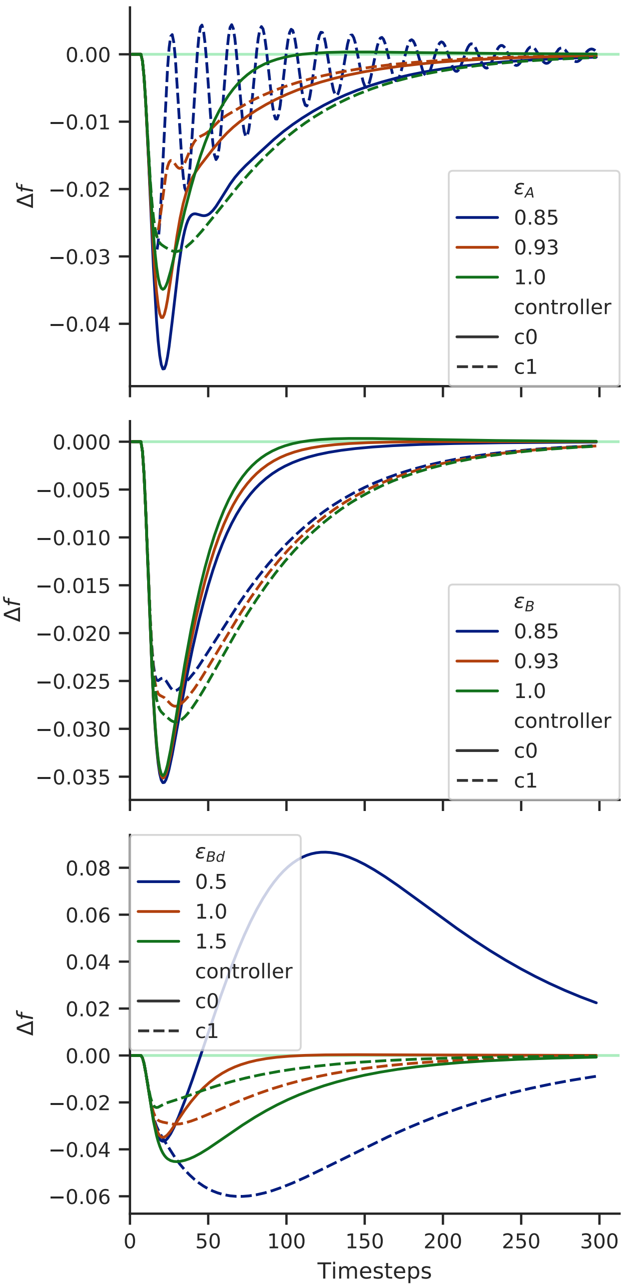

Figure 6.5: Comparison of multiplicative lumped parametric mismatches of the free system response coefficients A (ϵ_A), forced system response coefficients B (ϵ_B) and lumped filter disturbance response coefficients B_d (ϵ_{B_d}). The disturbance trajectory given in Figure 6.3 without noise term is used.

references hereby can be achieved with a chosen precision using the input reference tuning term $W_{\bar{u}}$.

6.10 CONCLUSION

We present an alternative optimal control and model predictive control formulation for the LFC problem. To the best knowledge of the author, these control law formulations are applied in this control problem for the first time. The formulation is compared to a classical MPC. The approaches incorporate an approximated system equilibrium into the controller objective and gain from an estimated lumped disturbance. We show that the derived MPC controller can be used to stabilize the frequency using a three–actor system and that it can be used to track input references. The proposed MPC formulations may be utilized within existing control hierarchy concepts.

It is shown that the proposed formulation does not expose advantages compared to the classical MPC. However, it can be considered an alternative in approaching the problem and means to comparison of different regulator formulations and associated properties.

6.11 ACKNOWLEDGMENTS

This work has been supported by *ENERGINET.DK* under the project microgrid positioning - *uGRIP* and the *CITIES* project.

REFERENCES

[Ban+19] Frederik Banis et al. „Load Frequency Control in Microgrids Using Target Adjusted Model Predictive Control.“ English. In: *IET Renewable Power Generation* (2019). ISSN: 17521424 and 17521416. DOI: 10.1049/iet-rpg.2019.0487.

[Sch78] F. C. Schweppe. „Power Systems '2000': Hierarchical Control Strategies.“ In: *IEEE Spectrum* 15.7 (July 1978), pp. 42–47. ISSN: 0018-9235. DOI: 10.1109/MSPEC.1978.6367813.

[De +18] Giulia De Zotti et al. „Ancillary Services 4.0: A Top-to-Bottom Control-Based Approach for Solving Ancillary Services Problems in Smart Grids.“ en. In: *IEEE Access* 6 (2018), pp. 11694–11706. ISSN: 2169-3536. DOI: 10.1109/ACCESS.2018.2805330. URL: http://ieeexplore.ieee.org/document/8290690/ (visited on 08/06/2019).

[Mad+14] Henrik Madsen et al. „Control of Electricity Loads in Future Electric Energy Systems." English. In: *Handbook of Clean Energy Systems*. Vol. 6. Denmark: Wiley, 2014, pp. 2213–2236. ISBN: 978-1-118-38858-7. URL: http://onlinelibrary.wiley.com/doi/10.1002/9781118991978.hces033/full (visited on 01/24/2017).

[Bev14] Hassan Bevrani. *Robust Power System Frequency Control*. Power Electronics and Power Systems. Cham: Springer International Publishing, 2014. ISBN: 978-3-319-07277-7 978-3-319-07278-4. DOI: 10.1007/978-3-319-07278-4. URL: http://link.springer.com/10.1007/978-3-319-07278-4 (visited on 09/27/2017).

[Kun94] Kundur. *Power System Stability And Control*. en. The Epri Power System Engineering. India: McGraw-Hill, 1994. ISBN: 978-0-07-063515-9.

[PML17] M. Pereira, D. Muñoz de la Peña, and D. Limon. „Robust Economic Model Predictive Control of a Community Micro-Grid." In: *Renewable Energy*. Special Issue: Control and Optimization of Renewable Energy Systems 100 (Jan. 2017), pp. 3–17. ISSN: 0960-1481. DOI: 10.1016/j.renene.2016.04.086. URL: http://www.sciencedirect.com/science/article/pii/S0960148116303883 (visited on 01/02/2017).

[PRG16] Alessandra Parisio, Evangelos Rikos, and Luigi Glielmo. „Stochastic Model Predictive Control for Economic/Environmental Operation Management of Microgrids: An Experimental Case Study." In: *Journal of Process Control* 43 (July 2016), pp. 24–37. ISSN: 0959-1524. DOI: 10.1016/j.jprocont.2016.04.008. URL: http://www.sciencedirect.com/science/article/pii/S0959152416300324 (visited on 01/02/2017).

[Han+14] Christian A. Hans et al. „Minimax Model Predictive Operation Control of Microgrids." In: *IFAC Proceedings Volumes*. 19th IFAC World Congress 47.3 (Jan. 2014), pp. 10287–10292. ISSN: 1474-6670. DOI: 10.3182/20140824-6-ZA-1003.00683. URL: http://www.sciencedirect.com/science/article/pii/S1474667016432465 (visited on 12/27/2018).

[PMK13] Shashi Kant Pandey, Soumya R. Mohanty, and Nand Kishor. „A Literature Survey on Load–Frequency Control for Conventional and Distribution Generation Power Systems." en. In: *Renewable and Sustainable Energy Reviews* 25 (Sept. 2013), pp. 318–334. ISSN: 13640321. DOI: 10.1016/j.rser.2013.04.029. URL: https://linkinghub.

elsevier.com/retrieve/pii/S1364032113002815 (visited on 07/25/2019).

[SSJ09] H. Shayeghi, H.A. Shayanfar, and A. Jalili. „Load Frequency Control Strategies: A State-of-the-Art Survey for the Researcher.“ en. In: *Energy Conversion and Management* 50.2 (Feb. 2009), pp. 344–353. ISSN: 01968904. DOI: 10.1016/j.enconman.2008.09.014. URL: https://linkinghub.elsevier.com/retrieve/pii/S0196890408003567 (visited on 07/25/2019).

[Sha+17] Ravi Shankar et al. „A Comprehensive State of the Art Literature Survey on LFC Mechanism for Power System.“ en. In: *Renewable and Sustainable Energy Reviews* 76 (Sept. 2017), pp. 1185–1207. ISSN: 13640321. DOI: 10.1016/j.rser.2017.02.064. URL: https://linkinghub.elsevier.com/retrieve/pii/S1364032117302848 (visited on 07/25/2019).

[Cal72] M. Calovic. „Linear Regulator Design for a Load and Frequency Control.“ In: *IEEE Transactions on Power Apparatus and Systems* PAS-91.6 (Nov. 1972), pp. 2271–2285. ISSN: 0018-9510. DOI: 10.1109/TPAS.1972.293383.

[Bar73] W. R. Barcelo. „Effect of Power Plant Response on Optimum Load Frequency Control System Design.“ In: *IEEE Transactions on Power Apparatus and Systems* PAS-92.1 (Jan. 1973), pp. 254–258. ISSN: 0018-9510. DOI: 10.1109/TPAS.1973.293621.

[FE70] C. E. Fosha and O. I. Elgerd. „The Megawatt-Frequency Control Problem: A New Approach Via Optimal Control Theory.“ In: *IEEE Transactions on Power Apparatus and Systems* PAS-89.4 (Apr. 1970), pp. 563–577. ISSN: 0018-9510. DOI: 10.1109/TPAS.1970.292603.

[ZTL13] C. Zhao, U. Topcu, and S. H. Low. „Optimal Load Control via Frequency Measurement and Neighborhood Area Communication.“ In: *IEEE Transactions on Power Systems* 28.4 (Nov. 2013), pp. 3576–3587. ISSN: 0885-8950. DOI: 10.1109/TPWRS.2013.2261096.

[Sir+10] S. F. Siraj et al. „A Robust Adaptive Predictive Load Frequency Controller to Compensate for Model Mismatch.“ In: *2010 4th International Power Engineering and Optimization Conference (PEOCO)*. Malaysia, June 2010, pp. 33–37. DOI: 10.1109/PEOCO.2010.5559181.

[WZW94] Y. Wang, R. Zhou, and C. Wen. „New Robust Adaptive Load-Frequency Control with System Parametric Uncertainties.“ In: *Transmission and Distribution IEE Proceedings -*

Generation 141.3 (May 1994), pp. 184–190. ISSN: 1350-2360. DOI: 10.1049/ip-gtd:19949757.

[YT86] K. Yamashita and T. Taniguchi. „Optimal Observer Design for Load-Frequency Control." en. In: *International Journal of Electrical Power & Energy Systems* 8.2 (Apr. 1986), pp. 93–100. ISSN: 01420615. DOI: 10.1016/0142-0615(86)90003-7. URL: https://linkinghub.elsevier.com/retrieve/pii/0142061586900037 (visited on 07/27/2019).

[HKN00] Y. Hain, R. Kulessky, and G. Nudelman. „Identification-Based Power Unit Model for Load-Frequency Control Purposes." In: *IEEE Transactions on Power Systems* 15.4 (Nov. 2000), pp. 1313–1321. ISSN: 0885-8950. DOI: 10.1109/59.898107.

[EIU16] A. M. Ersdal, L. Imsland, and K. Uhlen. „Model Predictive Load-Frequency Control." In: *IEEE Transactions on Power Systems* 31.1 (Jan. 2016), pp. 777–785. ISSN: 0885-8950. DOI: 10.1109/TPWRS.2015.2412614.

[Ven+08] A. N. Venkat et al. „Distributed MPC Strategies With Application to Power System Automatic Generation Control." In: *IEEE Transactions on Control Systems Technology* 16.6 (Nov. 2008), pp. 1192–1206. ISSN: 1063-6536. DOI: 10.1109/TCST.2008.919414.

[SRA13] Mojtaba Shiroei, Ali Mohammad Ranjbar, and Toraj Amraee. „A Functional Model Predictive Control Approach for Power System Load Frequency Control Considering Generation Rate Constraint: Functional MPC Approach For Power System LFC." en. In: *International Transactions on Electrical Energy Systems* 23.2 (Mar. 2013), pp. 214–229. ISSN: 20507038. DOI: 10.1002/etep.653. URL: http://doi.wiley.com/10.1002/etep.653 (visited on 10/02/2017).

[PR03] Gabriele Pannocchia and James B. Rawlings. „Disturbance Models for Offset-Free Model-Predictive Control." In: *AIChE journal* 49.2 (2003), pp. 426–437.

[GAM08] A.H. González, E.J. Adam, and J.L. Marchetti. „Conditions for Offset Elimination in State Space Receding Horizon Controllers: A Tutorial Analysis." en. In: *Chemical Engineering and Processing: Process Intensification* 47.12 (Nov. 2008), pp. 2184–2194. ISSN: 02552701. DOI: 10.1016/j.cep.2007.11.011. URL: https://linkinghub.elsevier.com/retrieve/pii/S0255270107003820 (visited on 07/29/2019).

[Ben15] Benjamin Schäfer. „Decentral Smart Grid Control." English. In: *Institute of Physics Publishing*. New Journal of Physics 17.1 (2015), p. 015002. ISSN: 13672630. DOI: 10.

1088/1367-2630/17/1/015002. URL: http://iopscience.iop.org/article/10.1088/1367-2630/17/1/015002/meta (visited on 11/17/2017).

[UBA14] Andreas Ulbig, Theodor S. Borsche, and Göran Andersson. „Impact of Low Rotational Inertia on Power System Stability and Operation." In: *IFAC Proceedings Volumes*. 19th IFAC World Congress 47.3 (Jan. 2014), pp. 7290–7297. ISSN: 1474-6670. DOI: 10.3182/20140824-6-ZA-1003.02615. URL: http://www.sciencedirect.com/science/article/pii/S1474667016427618 (visited on 12/27/2018).

[KMJ04] Niels Rode Kristensen, Henrik Madsen, and Sten Bay Jørgensen. „Parameter Estimation in Stochastic Grey-Box Models." en. In: *Automatica* 40.2 (Feb. 2004), pp. 225–237. ISSN: 00051098. DOI: 10.1016/j.automatica.2003.10.001. URL: https://linkinghub.elsevier.com/retrieve/pii/S000510980300298X (visited on 08/06/2019).

[Sax19] Sahaj Saxena. „Load Frequency Control Strategy via Fractional-Order Controller and Reduced-Order Modeling." en. In: *International Journal of Electrical Power & Energy Systems* 104 (Jan. 2019), pp. 603–614. ISSN: 01420615. DOI: 10.1016/j.ijepes.2018.07.005. URL: https://linkinghub.elsevier.com/retrieve/pii/S0142061517330727 (visited on 07/23/2019).

[Van81] P. Van Dooren. „A Generalized Eigenvalue Approach for Solving Riccati Equations." In: *SIAM Journal on Scientific and Statistical Computing* 2.2 (June 1981), pp. 121–135. ISSN: 0196-5204. DOI: 10.1137/0902010. URL: http://epubs.siam.org/doi/abs/10.1137/0902010 (visited on 07/26/2019).

[Lau78] Alan J. Laub. *A Schur Method for Solving Algebraic Riccati Equations*. eng. Tech. rep. USA: Massachusetts Institute of Technology, Laboratory for Information and Decision Systems, 1978, pp. 44–46. URL: https://dspace.mit.edu/handle/1721.1/1301 (visited on 07/26/2019).

[MR93] Kenneth R. Muske and James B. Rawlings. „Model Predictive Control with Linear Models." en. In: *AIChE Journal* 39.2 (1993), pp. 262–287. ISSN: 1547-5905. DOI: 10.1002/aic.690390208. URL: http://aiche.onlinelibrary.wiley.com/doi/abs/10.1002/aic.690390208 (visited on 07/30/2019).

[Huu+10] J. K. Huusom et al. „Tuning of Methods for Offset Free MPC Based on ARX Model Representations." In: *Proceedings of the 2010 American Control Conference*. USA, June 2010, pp. 2355–2360. DOI: 10.1109/ACC.2010.5530560.

[Huu+11] J. K. Huusom et al. „Adaptive Disturbance Estimation for Offset-Free SISO Model Predictive Control.“ In: *Proceedings of the 2011 American Control Conference*. San Francisco, CA, USA: IEEE, June 2011, pp. 2417–2422. ISBN: 978-1-4577-0081-1. DOI: 10.1109/ACC.2011.5990909.

[Ban+18] Frederik Banis et al. „Utilizing Flexibility in Microgrids Using Model Predictive Control.“ In: *Proceedings of Mediterranean Conference on Power Generation, Transmission, Distribution and Energy Conversion*. IET Control Theory and Applications. Croatia: Institution of Engineering and Technology, Nov. 2018. ISBN: 978-1-83953-133-0. DOI: 10.1049/cp.2018.1856.

[JHR11] John Bagterp Jørgensen, Jakob K. Huusom, and James B. Rawlings. „Finite Horizon MPC for Systems in Innovation Form.“ In: *Decision and Control and European Control Conference (CDC-ECC), 2011 50th IEEE Conference*. Orlando, USA: IEEE, 2011, pp. 1896–1903.

[PR01] Gabriele Pannocchia and James B. Rawlings. *Robustness of MPC and Disturbance Models for Multivariable Ill-Conditioned Processes*. English. Tech. rep. 2001-02. USA: TWMCC, Texas-Wisconsin Modeling and Control Consortium, 2001.

[Eur13] European Network of Transmission System Operators for Electricity. *The Network Code on Load-Frequency Control and Reserves*. English. June 2013. URL: https://www.acer.europa.eu/Official_documents/Acts_of_the_Agency/Annexes/The%5C%20Network%5C%20Code%5C%20on%5C%20Load-Frequency%5C%20Control%5C%20and%5C%20Reserves%5C%20submitted%5C%20on%5C%2028%5C%20June%5C%202013.pdf (visited on 07/24/2019).

[GJ09] Guru Prasath and John Bagterp. „Soft Constraints for Robust MPC of Uncertain Systems.“ In: *IFAC Proceedings Volumes (ifac-papersonline)*. 1st ser. 7 (2009), pp. 225–230. URL: https://cn.inside.dtu.dk/cnnet/filesharing/download/8a3d55fe-fec4-476f-8463-f999083baf9f (visited on 11/09/2017).

[PY13] Sidhartha Panda and Narendra Kumar Yegireddy. „Automatic Generation Control of Multi-Area Power System Using Multi-Objective Non-Dominated Sorting Genetic Algorithm-II.“ In: *International Journal of Electrical Power & Energy Systems* 53 (Dec. 2013), pp. 54–63. ISSN: 0142-0615. DOI: 10.1016/j.ijepes.2013.04.003. URL: http://www.sciencedirect.com/science/article/pii/S0142061513001622 (visited on 07/28/2019).

[Gur18] Gurobi Optimization. *Gurobi Optimizer Reference Manual*. Gurobi Optimization, LLC. 2018. URL: http://www.gurobi.com.

[And+99] E. Anderson et al. *LAPACK Users' Guide: Third Edition*. en. USA: SIAM, Jan. 1999. ISBN: 978-0-89871-960-4.

[18] *Open Power System Data, ENTSO-E Transparency Platform*. English. 2018. URL: https://data.open-power-system-data.org/time_series/2018-03-13/.

7 PAPER B

Utilizing flexibility in Microgrids using Model Predictive Control

Abstract — *We derive a control strategy for the operation of Microgrids (MGs) with high shares of Renewable Energy Sources involving MPC. By combining the MPC with an Energy Management System (EMS) utilizing stochastic programming techniques and a sufficiently large temporal optimization window we improve the point of operation of the system regarding both short and long–term operational aspects. We aim for a system operation that allows for the utilization of the MG as a Virtual Power Plant. In this work we focus on the predictive controller design and the incorporation of information derived in the EMS layer.*

Authors: Frederik Banis, Daniela Guericke, Henrik Madsen, Niels Kjølstad Poulsen

Published in the *Proceedings of Mediterranean Conference on Power Generation, Transmission, Distribution and Energy Conversion* ([Ban+18]). Presented at the *MedPower 2018* conference.

7.1 INTRODUCTION

The increasing share of renewable energy system (RES) in the energy production mix is associated with considerable power production uncertainty. Remedies for the issue can be categorized into improvement of infrastructure and improvement of system controls. An approach combining the two is the concept of Microgrids (microgrids (MGs)) representing small grid compartments at the lower voltage level. Combined control of controllable units within the MG enables utilization of this system as virtual power plant (VPP). The system operation and resilience of the VPP can be improved by inclusion of information of uncertain processes, such as uncertainties associated with RES. Designing controls for VPPs involves the setup of a control structure with respect to complexity and system dynamics. Incorporation of uncertain process predictions introduces complexity due to the combinatorial explosion of manifold process outcomes. A central system dynamics control problem is frequency stabilization. This is especially relevant considering the lower available aggregated inertia within MGs [UBA14; Ben15]. Handling problem complexity in this setting and simultaneously providing sufficient sampling rates of optimal control signals constitute two major challenges associated with the control of MGs with high shares of RES.

In this work we focus on the frequency stabilization problem while assuming an energy management system (EMS) formulated as stochastic unit commitment problem. We set up a lumped rotational system model in an model predictive control (MPC) direct control strategy balancing production and consumption. We derive the MPC in the so-called velocityform incorporating dynamic programming approaches in combination with input sequences tracking and inclusion of operational cost at MPC level. Using the input sequence tracking we take imposed input sequences u_{EMS} from an EMS into account. Input sequences hereby are power production or power consumption references for the plants in the VPP, referred to as the portfolio.

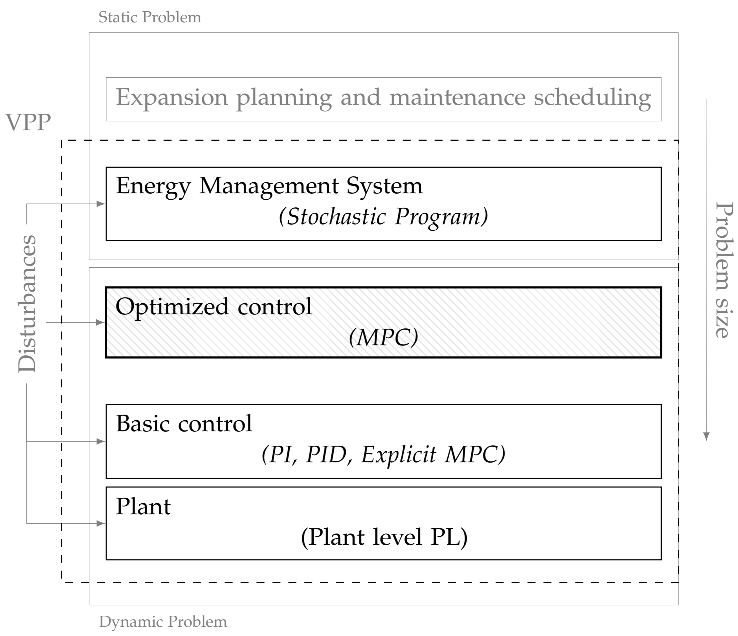

Figure 7.1: Hierarchy of controllers. We focus on the highlighted Model Predictive Control layer. This control layer optimizes the lumped system dynamics and we impose it on top of the basic controls driving each individual plant. See also [Hal+14].

Several publications related to control of MGs with emphasis on RES assume plant level controls cope with system dynamics such that aggregated system controls are left with steady state system behavior. Examples can be found in [PRG16; Han+14; Com+16; KS12]. The scope of this paper is the case where aggregated system controls are central to the overall system dynamics control problem. Related approaches in the area of Grid Frequency Control can be found in [SRA13; RAF03]. However they do neglect inclusion of long-term forecasts of uncertain system drivers.

The work [Com+16] as example does cover long-term predictions. The sampling time at aggregated control level of 15 minutes however go along with the assumption of basic controls covering essential dynamics and that these controls stabilize the system on inputs as assigned by higher level controls.

7.2 METHODOLOGY

7.2.1 Methodology

We consider two major control layers in the controller hierarchy. See Figure 8.2 on page 126.

1. Aggregated system control (VPP)
   a) EMS layer
   b) MPC layer
2. Basic control (PID, MPC, ...)

For simplicity we refer to the combined EMS+MPC controller at VPP level as the VPP controller.

The system dynamics are covered by the MPC and the basic control layer. For the MPC layer and its main objective of frequency stabilization we require sampling rates in the magnitude of a few seconds in order to capture critical dynamics. Achievable sampling rates depend on the complexity of the optimization problem.

Incorporation of forecasts is of superior importance when aiming for high shares of uncertain RES within the VPP. We consider hereby long-term and short-term forecasts of uncertain processes. Long-term forecasts are handled by the EMS layer and should yield an input sequence u_{EMS} passed to the MPC layer allowing for achievement of power balance with sufficiently high confidence. As a result from this requirement, long-term forecasts need to suffice in terms of prediction horizon, temporal resolution and considered scenarios. We assume the VPP participates in Day-Ahead market and hence considers a long-term prediction window covered by the EMS layer of minimum 24 hour with hourly granularity. The input sequence u_{EMS} is an approximation of the optimal input sequence given information available to the EMS layer. Upon realization of uncertain processes deviations from the anticipated realizations occur. This forecasting error is treated at the MPC layer by allowing for deviations from the input sequence u_{EMS}. Availability of operational costs to the MPC layer enables for informing this decision in economical means. The MPC layer handles short-term forecasts of a time span well below one minute. Short-term forecasts allow for accounting for disturbances prior to passing through the system and being visible via excelled frequency deviations.

Table 7.1: Nomenclature. </> denotes not specified units.

Symbol	Description	Unit
Variables	<40>	
$u^\star$	Optimal input sequence	pu
u_{EMS}	Optimal input sequence derived in EMS layer	pu
Φ_x	N-step free system response coefficients	/
Γ_u	N-step forced system response coefficients	/
Γ_d	N-step disturbance system response coefficients	/
G, h	Objective inequality coefficients, bounds	/
Π	Objective terms: input reference tracking and operational cost	/
x, $\hat{x}$	System state, one-step prediction	/
x_∞	Disturbance corrected system state	/
w, v	Process noise, measurement noise	/
d, $\hat{d}$	Uncontrollable inputs (disturbance), estimate	/
$y = \Delta f$, $\hat{r}$	Frequency residual, inferred residual	Hz
P_{ch}, P_{dis}	Storage charge, discharge power	kW
P_{mech}	Power balance within grid	pu
L	Kalman gain	/
c	Operational cost	Price/kW
σ^2, Σ^2	Variance	/
Parameters		
A, B, B_d, G, C, D	State Space System matrices	/
N	Controller prediction horizon	-
τ_s	Controller sampling time	s
H	Inertia based supply time	s
D	Load damping coefficient	-
R	Governor speed droop	Hz/pu
P_{nom}	Nominal grid power	kW
α, β, γ	Objective function weighing factors	-
Names		
PCC	Point Of Common Coupling	
PL	Lowest considered plant level in hierarchy	

7.2.2 Model Predictive Control layer

7.2.2.1 *Main system model*

We consider the swing equation [Ben15; Bev14]:

$$\frac{d}{dt}\Delta f(t) = -\frac{D}{2H}\Delta f(t) + \frac{1}{2H}\Delta P_{\text{mech}}(t) \tag{7.1}$$

Δf denotes the frequency deviation from nominal frequency, D is the load damping coefficient and H the inertia based supply time. ΔP_{mech} is the power balance within the grid. This is a lumped model, where we consider average and aggregated values only. The model maps the overall power miss-match to an angular frequency deviation from the nominal grid frequency taking the approximated system inertia into account. The considered underlying process is nonlinear in the sense that both the produced mechanical power and consumed power are nonlinear processes. $\Delta P_{\text{mech}}(t)$ as sum of the two consequently is nonlinear.

We model the production and consumption side as linear system models, approximating the underlying non–linear processes. For altered operational conditions we may need to relinearize the process model in order to maintain accuracy of the linearization within sufficient limits.

For deriving the regulator, we aim for a discrete time linear state space description of the process in difference form, where we consider deviations with respect to a stationary point. As we consider a discrete time simulation setup, we yield the discrete time state space description using a zero-order hold approximation. We hereby assume that this represents the process with sufficient accuracy.

$$x_{t+1} = Ax_t + Bu_t + Gd_t + w \tag{7.2a}$$
$$y_t = Cx_t + v \tag{7.2b}$$

x_t as the system state hereby includes the frequency deviation from 50 Hz as the main state.

7.2.2.2 *Storage model*

For storage components within the system we formulate time varying constraints for the regulator derived in following sections of the paper. We keep the storage process innovation separated from the main regulated system model described in Section 7.2.2.1 in order to avoid computational issues. We consider the conditional charge quantities:

$$\Delta Q_{\text{ch},k} = \begin{cases} u^{\star}_{\text{sto},k} P_{\text{nom}} \frac{T_s}{3600} & \text{if } u^{\star}_{\text{sto},k} \geq 0 \\ 0 & \text{if } u^{\star}_{\text{sto},k} < 0 \end{cases} \tag{7.3a}$$

$$\Delta Q_{\text{dis},k} = \begin{cases} 0 & \text{if } u^{\star}_{\text{sto},k} \geq 0 \\ u^{\star}_{\text{sto},k} P_{\text{nom}} \frac{T_s}{3600} & \text{if } u^{\star}_{\text{sto},k} < 0 \end{cases} \tag{7.3b}$$

Note that we formulate all optimal inputs, including the optimal sequence for the storage $u^{\star}_{\text{sto},k}$, in the per unit system in relation to the nominal grid power P_{nom}. The storage innovation is given by:

$$Q_{\text{sto},k+1} = Q_{\text{sto},k} + \eta_{\text{ch},k} \Delta Q_{\text{ch},k} + \eta_{\text{dis},k} \Delta Q_{\text{dis},k} \tag{7.4}$$

We then update the general VPP control problem constraints with the updated degrees of freedom for the storage. Both Equation (7.5) and Equation (7.6) enter the regulator objective function as part of the constraints Equation (7.11) on the next page.

$$h_{\text{sto},k} = \begin{bmatrix} \text{SoC}_{\text{max}} - Q_{\text{sto},k} \\ -\text{SoC}_{\text{min}} + Q_{\text{sto},k} \end{bmatrix} \tag{7.5}$$

With the left-hand side:

$$G_{\text{sto},k} = \begin{bmatrix} -\eta_{\text{ch},k} P_{\text{nom}} {}^{T_s}/3600 \\ \eta_{\text{dis},k} P_{\text{nom}} {}^{T_s}/3600 \end{bmatrix} \tag{7.6}$$

7.2.2.3 Regulator

We state frequency regulation as deviation minimization problem consisting of the infinite horizon terms J_{∞} and the dynamic optimization terms J_{DO}. The infinite horizon problem denotes the distance of the stabilizing couple $\{u_k,\ \hat{x}_k\}$ from the stationary point $\{u_{\infty,k},\ x_{\infty,k}\}$ mapped into the output space:

$$J_{\infty,k} = \Phi_x(\hat{x}_k - x_{\infty,k}) + \Gamma_u(u_k - u_{\infty,k}) \tag{7.7}$$

Dynamic programming terms enable offset free control also when constraints are active on parts of the VPP:

$$J_{\text{DO},k} = u_k - u^{\star}_{k-1} + \gamma W_{\Delta u} \Delta u_k \tag{7.8}$$

Including $J_{C,k}$ we modify the portfolio constitution taking both input reference sequences u_{EMS} and operational costs into account:

$$J_{C,k} = (1-\gamma)\Pi_k \tag{7.9}$$

With $W_{\Delta u}$ we introduce weights on the dynamic terms. The dynamic optimization weight $W_{\Delta u}$ is one major tuning weight for modifying the controller behavior in this setting. Increasing this weight leads to higher control effort and better performance in the controlled variable when activating the least-squares term Π_k by choosing $\gamma \neq 1$. Lowering γ results in increasingly dominant incorporation of information specified in Π_k. We then consider the objective:

$$\min_{u,k} \quad ||J_{\infty,k} + J_{\text{DO},k}||^2 + J_{C,k} \tag{7.10}$$

$$\text{s.t.} \quad G_k u_k \leq h_k \tag{7.11}$$

The inequalities Equation (7.11) are further discussed in Section 7.2.2.3.

STATIONARY POINT: We aim for retrieval of the system equilibrium incorporating both the filtered output residual $\hat{d}$ and the predicted output residual $\hat{f}_y$. The former relates to the system output in the past whereas the latter relates to the system output in the future.

We estimate the residual $\hat{d}$ using a Kalman filter following the formulations given in [PR01; PR03]. The augmented system model with integrating disturbance estimate and filter equations is then given by:

$$\begin{bmatrix} \hat{x}_{k+1|k} \\ \hat{d}_{k+1|k} \end{bmatrix} = \begin{bmatrix} A & B_d \\ 0 & I \end{bmatrix} \begin{bmatrix} \hat{x}_{k|k-1} \\ \hat{d}_{k|k-1} \end{bmatrix} + \begin{bmatrix} B \\ 0 \end{bmatrix} u_k + \overbrace{\begin{bmatrix} L_1 \\ L_2 \end{bmatrix}}^{L} (y_k - C\hat{x}_{k|k-1} - C_d \hat{d}_{k|k-1}) \tag{7.12}$$

This is the one-step predictor of both estimated state $\hat{x}$ and disturbance $\hat{d}$. Notice that $\hat{d}$ hereby is a lumped disturbance capturing any miss-match between desired and effective input-output relation. We may employ a dynamic ordinary Kalman filter in order to achieve faster convergence, resulting in L being dynamic. Aiming for stabilizing the system using the estimated disturbance we can utilize the system model to solve for the stabilizing gain g_∞ [PR01; PR03].

$$\overbrace{\begin{bmatrix} A-I & B \\ C & 0 \end{bmatrix}}^{M} \overbrace{\begin{bmatrix} g_{x,\infty} \\ g_{u,\infty} \end{bmatrix}}^{g_\infty} = \begin{bmatrix} B_d \\ 0 \end{bmatrix} \tag{7.13}$$

The lumped system matrix M for the considered system is non-symmetric, therefore we derive the solution to Equation (7.13) on the previous page using a least-squares approximation.

Using g_∞ and the filtered disturbance $\hat{d}_{k|k}$ we achieve offset free control in the unconstrained case by retrieving the stabilizing couple p_∞.

$$p_{\infty,k} = g_\infty \otimes \hat{d}_k = \begin{bmatrix} x_\infty \\ u_\infty \end{bmatrix}_k \tag{7.14}$$

This introduces feedback from the frequency measurement. Notice that the controller performance directly relies on performance of the utilized Kalman filter and availability and quality of the frequency measurement. In order to include forecasts we modify Equation (7.14) to utilize the expected frequency residual.

$$p_{\infty,k} = g_\infty \otimes \mathrm{E}(\mathrm{P}(r_k|\mathrm{Y}_k)) \tag{7.15}$$

The time varying functional Y_k takes the uncertain filtered residual $\hat{d}, \sigma_{d,k}$ alongside uncertain residual prediction $\hat{f}_{y,k}, \Sigma_{y,k}$ into account.

$$\mathrm{Y}_k = f(\hat{d}_k, \sigma_{d,k}, \hat{f}_{y,k}, \Sigma_{y,k}) \tag{7.16}$$

Y expresses our belief in the current relevance of both $\hat{d}_k$ and $\hat{f}_{y,k}$. The uncertain disturbance states $\hat{d}_{\mathrm{PL},k}, \Sigma_{\mathrm{PL},k}$ at plant level PL can be mapped to the output space at VPP level. The error introduced by this linear operation depends on the accuracy of the linearized model M. Instead of a one-step prediction we use an N–step prediction allowing the controller to utilize the information of entering fast disturbances prior to their actual impact on the system frequency.

$$\hat{f}_{y,k+N-1|k} = \Gamma_d \hat{d}_{\mathrm{PL},k} \tag{7.17}$$

$$\sigma_{y,k+N-1|k} = (\Gamma_d \Sigma_{\mathrm{PL},k})^T \Gamma_d \Sigma_{\mathrm{PL},k} \tag{7.18}$$

One approach to the formulation of Y is to infer the expected residual $\hat{r}$ by weighing both residuals taking uncertainty into account:

$$\hat{r} = \frac{\sigma^2_{y,k+N-1}}{1/\sigma^2_{y,k+N-1} + 1/\sigma^2_{d,k}} \hat{f}_{y,k+N-1} + \frac{\sigma^2_{d,k}}{1/\sigma^2_{y,k+N-1} + 1/\sigma^2_{d,k}} \hat{d}_k \tag{7.19}$$

DYNAMIC PROGRAMMING PROBLEM:

$$J_{\mathrm{DO},k} = \overbrace{u_k - u^\star_{k-1}}^{T0} + \overbrace{W_{\Delta u}\gamma\Delta(u_k - u^\star_{k-1})}^{T1} \tag{7.20}$$

As stage cost term we formulate $T0$, requiring that the minimizer $u^\star_k$ remains close to $u^\star_{k-1}$. Choosing $u^\star_{k-1}$ as the last implemented input sequence level allows for off-set free control even when hard constraints on part of the portfolio are active. Choosing $u^\star_{k-1}$ as the last solution introduces bias leading to over-compensation of the disturbance rejection behavior of the controller. This can be beneficial when the disturbance process exhibits considerable auto-correlation. The cost-to-go term $T1$ introduces ramp-rate penalization adjusted by $W_{\Delta u}$.

INPUT REFERENCE TRACKING AND OPERATIONAL COST: For $\gamma = 1$ we consider a purely operational objective from the perspective of the MPC layer, neglecting J_{C}. For $0 \leq \gamma < 1$ we consider operational modes informed by J_{C}. Π_k considers input references u_{EMS} and operational cost scaled by the relative weights α and β, see Equation (7.21). We hereby take both general operational cost and input reference deviation costs into account.

$$\begin{aligned} \Pi_k = \alpha || \overbrace{u_k - u_{\mathrm{EMS},k}}^{T2} ||^2_{W_{\Delta u}} + \\ \beta(|| \underbrace{\tilde{c}_k \tau_s u_k}_{T3} ||^2 + || \underbrace{\tilde{c}_{\Delta,k}\tau_s(u_k - u_{\mathrm{EMS},k})}_{T4} ||^2_{W_{\Delta u}}) \\ \text{where:} \quad \alpha + \beta = 1 \end{aligned} \tag{7.21}$$

$T2$ incorporates input reference tracking. $T3$ and $T4$ denote general operational cost and input reference deviation costs respectively. $\tilde{c}_k$ and $\tilde{c}_{\Delta,k}$ are hereby normalized unit production prices.

CONSTRAINTS: Hard input constraints and ramping constraints are updated based on underlying system conditions and control requirements imposed by the EMS-layer.

$$G_k u_k \leq h_k \tag{7.22}$$

We optimize over deviations encompassing the positive and negative domain. Therefore we require only the first optimal input solution to satisfy the ramping constraints. Imposing these constraints for the whole sequence $u_{k+N-1|k}$ results in numerical issues.

$$\Delta u_{\min} \leq u^\star_{k+1|k} - u^\star_{k|k} \leq \Delta u_{\max} \tag{7.23}$$

7.2.2.4 MPC supervisory system

The regulator formulation outlined in Section 7.2.2.3 as main objective aims for frequency stabilization using continuous solution spaces. Complex operational requirements such as minimum uptime or down-time for parts of the portfolio are to be handled by the EMS layer. The supervisory system constitutes a system layer executed parallel to the MPC layer. The supervisory system dynamically reformulates the MPC problem such that it enforces operational requirements. Constraints in the MPC optimization problem are as a result dynamic (see Section 7.2.2.3).

7.2.3 Energy Management System layer

For thoroughness we cover the EMS layer briefly below. It can be formulated as a stochastic program with two stages, where first stage decisions are:

- Market bidding
- Switching events

Switching events hereby may depict i.e. minimum power production level of generators.

The second stage considers the stochastic processes which may be clustered depending on the given correlation structure. We may consider the variables:

- Generated power by conventional generators
- Curtailment of RES
- Storage charging/ discharging

This optimization problem then takes the general form of a two stage stochastic problem—or stochastic unit commitment problem—see [CCM10; Pan+16]:

$$\min \quad c^T x + \sum_{\omega \in \Omega} \pi(\omega) q(\omega)^T y(\omega) \tag{7.24}$$

$$\text{s.t.} \quad Ax = b \tag{7.25}$$

$$T(\omega)x + W(\omega)y(\omega) = h(\omega) \qquad \forall \omega \in \Omega \tag{7.26}$$

$$x \geq 0 \tag{7.27}$$

$$y(\omega) \geq 0 \qquad \forall \omega \in \Omega \tag{7.28}$$

7.3 RESULTS

For an exemplifying simulation scenario we set up the components listed below. See Table 7.2.

- Thermal generator 1
- Thermal generator 2
- Storage
- Main grid interaction (PCC)
- Wind Power Plant
  - Disturbance 1: Wind speed realization
  - Input 1: Wind Power Plant curtailment

We choose $\gamma = 1/4$ and consequently allow the MPC layer to considerably deviate from imposed set points u_{EMS}. We parameterize the portfolio constitutional term with $\alpha, \beta = .2, .8$. As sampling rate we choose 2 seconds or $1/2$ Hz. The simulation is arranged using the `python` (version 3.4) programming language alongside associated packages. The `GUROBI` (version 7.0) solver is used for the solution to the quadratic programming problems.

We examine the MPC layer performance (see Figure **??**) when required to follow input references u_{EMS} from an EMS layer and observe:

- u_{ems} tracking
- Disturbance rejection
- Constraint satisfaction

The load `D0` initializes at `-0.0 p.u.` ramping up to `-0.6 p.u.`. The controlled inputs shown in the central graph adjust accordingly in order to stabilize the controlled variable in the upper graph on its reference value.

Until timestep `1500` the two thermal generators receive input reference values of `0.15 p.u.` whereas the storage receives an input reference of `0.35 p.u.`. The tie line `U3` supports frequency stabilization even though its reference of `0.0 p.u.` due to the tuning value γ chosen such that the MPC layer retains degrees of freedom for its main objective. At timestep `1000` the operational costs are adjusted and are higher from there on for the first thermal generator `U0` compared to `U1`. This results in lowered utilization. From timestep `1500` on the EMS adjusts input reference values. The storage `U2` can follow its requested reference until its charge level depletes. Consequently the MPC layer requires other plants to ramp up in order to compensate for this loss of positive power balance contribution. At timestep `2000` random

Table 7.2: :
Simulation scenario parameterization.

Component	Parameter	Value
Rotational system	H	6s
	D	1.5
Load	$P_l = N_{iid}(\mu_l, \sigma_l^2$	$\mu_l = -0.6$ pu, $\sigma_l^2 =$ 0.05 pu
Gen. Thermal 1	$Y(s)/U(s)$	$1/(.08s^2+1.08s+1)$
(U0)	u_{min}, u_{max}	0.0, 0.5
	Δu_{lower}, Δu_{upper}	$-0.005/s$, $0.0006/s$
	R	3 Hz/p.u.
Gen. Thermal 2	$Y(s)/U(s)$	$1/(.08s^2+1.08s+1)$
(U1)	u_{min}, u_{max}	0.0, 0.5
	Δu_{lower}, Δu_{upper}	$-0.005/s$, $0.005/s$
	R	3 Hz/p.u.
Storage	$Y(s)/U(s)$	$1/(6s+1)$
(U2)	u_{min}, u_{max}	-0.25, 0.25
	Δu_{lower}, Δu_{upper}	$-0.01/s$, $0.005/s$
	$\eta_{\text{stat.}}$, $\eta_{\text{ch.}}$, $\eta_{\text{dis.}}$	5%/h, 92 %, 92 %
Tie line interaction	$Y(s)/U(s)$	$1/(0.6s+1)$
(U3)	u_{min}, u_{max}	-1.0, 1.0
Wind Power Plant	$Y(s)/U(s)$	$1/(20s+1)$
(U4, D1)	u_{min}, u_{max}	.0, 10% $P_{\text{g,nom}}$
Windspeed [SP16]		$12.5 - 13.5$ m/s

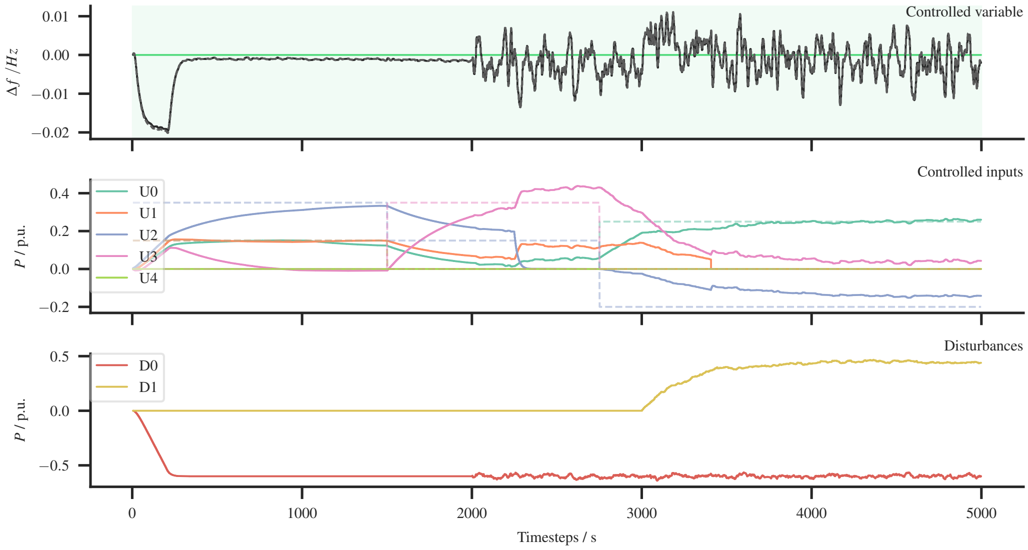

Figure 7.2: MPC controller performance: Tracking of reference on the controlled variable, disturbance rejection and tracking of input reference values u_{EMS} from an EMS layer. Inputs: Thermal Generator 1 (`U0`), Thermal Generator 2 (`U1`), Storage (`U2`), Tie line interaction (`U3`), Wind Power Plant curtailment (`U4`). Disturbances: Load (`D0`), Wind power plant production (`D1`).

noise on the disturbance `D0` is activated. From timestep `3000` on the EMS adjusts input reference values u_{EMS} anticipating the ramping up available wind power `D1`. The input reference adjustment scheduled by the EMS however comes too early at timestep `2750`, requiring the MPC layer to utilize its given degrees of freedom to drive the system such that frequency stabilizes. We can observe the satisfaction of imposed ramping constraints on the thermal generator `U0`. After the ramping up of the wind power plant `D1`, inputs convergence towards the given input reference values. The storage `U2` is request to charge with a negative power contribution of `-0.2 p.u.`. A forecasting error hereby yet again requires the MPC layer to deviate to some degree from its given input reference. Around timestep `3300` the supervisory system adjusts the constraints of the objective function such that thermal generator `U1` is shutdown.

As we observe, both tracking of the reference imposed on the controlled variables, disturbance rejection and tracking of imposed reference values on the inputs in this scenario work as intended.

7.3.1 Conclusions

In this work we outline a MPC direct control strategy for the frequency stabilization in Microgrids with high penetration of Renewable Energy Sources. We prepare the MPC covering estimated disturbance rejection and short-term disturbance forecasts. The MPC incorporates long-term probabilistic forecasts indirectly by tracking of informed input sequences u_{EMS} derived in an Energy Management System layer. We formulate the objective function such that deviations from u_{EMS} can reflect operational costs.

For future improvements the number of controlled variables may vary. Achievable sampling rates consequently can be higher when the control problem is computationally lighter, allowing for improved disturbance rejection when needed. Incorporation of indirect control approaches can leverage additional system flexibility. The EMS layer as driver of the system taking a long-term prediction horizon in account needs to be further examined with focus on critical operational conditions. Relating to this, the coupling of EMS and MPC in terms of robustness and flexibility has to be studied further. The control strategies will be extended to cover voltage angle control.

ACKNOWLEDGMENT

This work has been supported by *ENERGINET.DK* under the project microgrid positioning - *uGrip*. The work by Daniela Guericke is funded by Innovation Fund Denmark through the CITIES research center (no 1035-00027B).

REFERENCES

[Ban+18] Frederik Banis et al. „Utilizing Flexibility in Microgrids Using Model Predictive Control." In: *Proceedings of Mediterranean Conference on Power Generation, Transmission, Distribution and Energy Conversion*. IET Control Theory and Applications. Croatia: Institution of Engineering and Technology, Nov. 2018. ISBN: 978-1-83953-133-0. DOI: 10.1049/cp.2018.1856.

[UBA14] Andreas Ulbig, Theodor S. Borsche, and Göran Andersson. „Impact of Low Rotational Inertia on Power System Stability and Operation." In: *IFAC Proceedings Volumes*. 19th IFAC World Congress 47.3 (Jan. 2014), pp. 7290–7297. ISSN: 1474-6670. DOI: 10.3182/20140824-6-ZA-1003.02615. URL: http://www.sciencedirect.com/science/article/pii/S1474667016427618 (visited on 12/27/2018).

[Ben15] Benjamin Schäfer. „Decentral Smart Grid Control." English. In: *Institute of Physics Publishing*. New Journal of Physics 17.1 (2015), p. 015002. ISSN: 13672630. DOI: 10.1088/1367-2630/17/1/015002. URL: http://iopscience.

iop.org/article/10.1088/1367-2630/17/1/015002/meta (visited on 11/17/2017).

[Hal+14] Rasmus Halvgaard et al. „Model Predictive Control for Smart Energy Systems." English. PhD Thesis. Technical University of Denmark, Jan. 2014. URL: http://orbit.dtu.dk/fedora/objects/orbit:129152/datastreams/file_ec7a995a-b7f4-4eaf-9880-4e3ebed9ed4b/content (visited on 01/09/2017).

[PRG16] Alessandra Parisio, Evangelos Rikos, and Luigi Glielmo. „Stochastic Model Predictive Control for Economic/Environmental Operation Management of Microgrids: An Experimental Case Study." In: *Journal of Process Control* 43 (July 2016), pp. 24–37. ISSN: 0959-1524. DOI: 10.1016/j.jprocont.2016.04.008. URL: http://www.sciencedirect.com/science/article/pii/S0959152416300324 (visited on 01/02/2017).

[Han+14] Christian A. Hans et al. „Minimax Model Predictive Operation Control of Microgrids." In: *IFAC Proceedings Volumes*. 19th IFAC World Congress 47.3 (Jan. 2014), pp. 10287–10292. ISSN: 1474-6670. DOI: 10.3182/20140824-6-ZA-1003.00683. URL: http://www.sciencedirect.com/science/article/pii/S1474667016432465 (visited on 12/27/2018).

[Com+16] S. Raimondi Cominesi et al. „A Multi-Layer Control Scheme for Microgrid Energy Management." en. In: *IFAC-PapersOnLine* 49.27 (2016), pp. 256–261. ISSN: 24058963. DOI: 10.1016/j.ifacol.2016.10.700. URL: http://linkinghub.elsevier.com/retrieve/pii/S2405896316323199 (visited on 05/06/2018).

[KS12] Phillip Oliver Kriett and Matteo Salani. „Optimal Control of a Residential Microgrid." In: *Energy*. 8th World Energy System Conference, WESC 2010 42.1 (June 2012), pp. 321–330. ISSN: 0360-5442. DOI: 10.1016/j.energy.2012.03.049. URL: http://www.sciencedirect.com/science/article/pii/S0360544212002526 (visited on 08/01/2017).

[SRA13] Mojtaba Shiroei, Ali Mohammad Ranjbar, and Toraj Amraee. „A Functional Model Predictive Control Approach for Power System Load Frequency Control Considering Generation Rate Constraint: Functional MPC Approach For Power System LFC." en. In: *International Transactions on Electrical Energy Systems* 23.2 (Mar. 2013), pp. 214–229. ISSN: 20507038. DOI: 10.1002/etep.653. URL: http://doi.wiley.com/10.1002/etep.653 (visited on 10/02/2017).

[RAF03] D. Rerkpreedapong, N. Atic, and A. Feliachi. „Economy Oriented Model Predictive Load Frequency Control.“ In: *Large Engineering Systems Conference on Power Engineering, 2003*. May 2003, pp. 12–16. DOI: 10.1109/LESCPE.2003.1204672.

[Bev14] Hassan Bevrani. *Robust Power System Frequency Control*. Power Electronics and Power Systems. Cham: Springer International Publishing, 2014. ISBN: 978-3-319-07277-7 978-3-319-07278-4. DOI: 10.1007/978-3-319-07278-4. URL: http://link.springer.com/10.1007/978-3-319-07278-4 (visited on 09/27/2017).

[PR01] Gabriele Pannocchia and James B. Rawlings. *Robustness of MPC and Disturbance Models for Multivariable Ill-Conditioned Processes*. English. Tech. rep. 2001-02. USA: TWMCC, Texas-Wisconsin Modeling and Control Consortium, 2001.

[PR03] Gabriele Pannocchia and James B. Rawlings. „Disturbance Models for Offset-Free Model-Predictive Control.“ In: *AIChE journal* 49.2 (2003), pp. 426–437.

[CCM10] Antonio J. Conejo, Miguel Carrión, and Juan M. Morales. „Stochastic Programming Fundamentals.“ en. In: *Decision Making Under Uncertainty in Electricity Markets*. International Series in Operations Research & Management Science. Springer, Boston, MA, 2010, pp. 27–62. ISBN: 978-1-4419-7420-4 978-1-4419-7421-1. URL: https://link-springer-com.proxy.findit.dtu.dk/chapter/10.1007/978-1-4419-7421-1_2 (visited on 03/14/2018).

[Pan+16] Hrvoje Pandzic et al. „Toward Cost-Efficient and Reliable Unit Commitment Under Uncertainty.“ en. In: *IEEE Transactions on Power Systems* 31.2 (Mar. 2016), pp. 970–982. ISSN: 0885-8950, 1558-0679. DOI: 10.1109/TPWRS.2015.2434848. URL: http://ieeexplore.ieee.org/document/7115977/ (visited on 04/08/2018).

[SP16] Iain Staffell and Stefan Pfenninger. „Using Bias-Corrected Reanalysis to Simulate Current and Future Wind Power Output.“ en. In: *Energy* 114 (Nov. 2016), pp. 1224–1239. ISSN: 03605442. DOI: 10.1016/j.energy.2016.08.068. URL: http://linkinghub.elsevier.com/retrieve/pii/S0360544216311811 (visited on 03/23/2018).

8 PAPER C

Supporting power balance in Microgrids with Uncertain Production using Electric Vehicles and Indirect Control

Abstract — *In Microgrids with uncertain production storages are valuable assets to facilitate system stabilization. Consequently, EV are promising for providing prosumer services. EV are assets driven by human behavior, consequently they can rarely be directly controlled. However, indirect control approaches are considered promising regarding their integration into system controls. In this paper we consider a hierarchy of optimized system controls including indirect control approaches in order to leverage flexibility potential associated with EV.*

Authors: Frederik Banis, Daniela Guericke, Henrik Madsen, Niels Kjølstad Poulsen

Published in *IFAC-PapersOnLine* ([Ban+19]), submitted for review to *IJCAS* journal. Presented at the *CSGRES 2019* conference.

8.1 INTRODUCTION

Small grid compartments referred to as microgrids (MGs) combined with higher shares of renewable energy system (RES) require sufficient operational flexibility when aiming for the participation in energy markets. Energy market participation can be achieved when considering aggregation of distributed energy resources (DERs) by the *Aggregator* entity ([Mor+14]). Failure to meet accepted market commitments lead to the application of penalties; accordingly, avoiding such costs is beneficial from the Aggregator perspective. This is one of several motivations for the integration of additional flexibility.

Storage capacities acting as Prosumers offer degrees of freedom and are consequently valuable assets in the operational scheme. We hereby consider electric vehicles (EVs) as uncertain storage capacities. In order to leverage flexibility in conjunction with EVs, indirect control (ICo) enables the MG controller to activate this flexibility by means of economical incentives offered to the EV owners. Doing so is advantageous in terms of applicability, due to that direct control (DCo) requires bi–directional communication and reduces flexibility for the

EV owner compared to ICo ([Mad+14]). ICo however is associated with drawbacks due to that the response of the activated prosumer side is both uncertain by means of dynamics and magnitude ([OH11]). The introduction of appropriate models that enable the estimation of the consumptive response behavior is therefore central to the ICo approach.

Examples of alternative solution approaches are methods involving dual decomposition approaches and game theory based methods. Problem solutions differ not only regarding implementation, but also regarding the degree of knowledge required to achieve a near–optimal solution with respect to the considered objective. In decomposition based approaches part of the optimization problem is solved locally. As such, these methods share the property of allowing for honoring privacy concerns with ICo. [Flo+16] outline such a decomposition based approach aiming at load shaping. This is an alternative to centralized approaches such as [Sor+11; CHD09]. An example for game theory based approaches is [NX17]. This paper considers an optimal control theory based approach. [SLL13; Jin+17] are examples for multi–objective approaches in this context. [KR15] utilize a two–stage model predictive control (MPC) approach combining two DR schemes: event–based DR and price–based DR.

In contrast to the mentioned approaches we focus in this publication on the utilization of EVs for the rejection of disturbances that may lead to critical frequency deviations. We derive a control hierarchy for the integration of EVs for the support of power balance in MG using ICo. A temporal clustering approach of estimated price–sensitivity models is used, enabling the ongoing improvement of model accuracy and consideration of temporal variability of the system. Aforementioned references formulating unit commitment problems can consequently be used to provide the dispatch schedule for the discussed real–time (RT) control layers.

The rest of the paper is organized as follows. Section 7.2 introduces the considered control structure and indirect control approach. In Section 8.3 we present numerical results. We close with Section 8.4 discussing the findings and future improvements.

8.2 METHODOLOGY

Consider the structure of optimization routines and controllers as depicted in Figure 8.1.

At the highest level in the control hierarchy an optimization problem derives a dispatch schedule for the MG several hours ahead of time. This optimization problem incorporates the largest share of information available to the MG controller. This optimization problem is stated by the aggregator entity and is in literature commonly denoted as energy management system (EMS). The solution to this problem can be used to offer bids in energy markets. When bids are accepted the agreed quantities are binding and result in commitments of the aggregator and its actor, the MG. Disability to fulfill the commitment lead to application of penalties. Consequently, the solution u_{EMS} is treated as reference in subsequent layers in the control hierarchy.

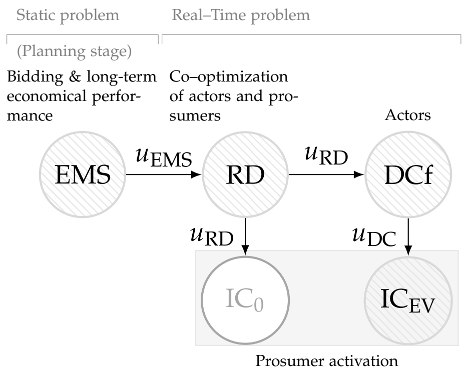

Figure 8.1: Dataflow overview: The control decision u_{EMS} by the EMS is passed to the RT control routines: The redispatch (RD) co–optimizes both directly and indirectly controllable units. The control decision u_{RD} is passed to the DCo routine. The ICo (IC_{EV}) layer for the EVs receives its input from the Direct Control routine. The ICo layer for other units (IC_0) is not scope of this paper.

RD of actors based on updated predictions is required during RT operation if considerable uncertainty is to be accounted for. Furthermore, both directly and indirectly controllable unit (ICU) are to be co–optimized such that ICU can be activated by both operational and economical means.

Notice that the IC_{EV} layer receives its control reference from the DCf layer.

As DC control problem example we choose in this paper frequency stabilization, this layer is sampled in the magnitude of a few seconds — depending on the system dynamics and disturbance characteristics.

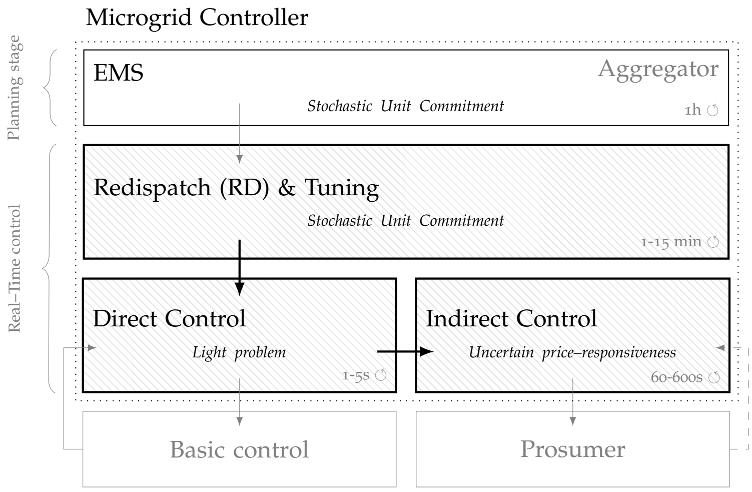

Figure 8.2: Control hierarchy. We focus on the highlighted control routines. The Redispatch problem derives economically optimal input sequences taking the estimated price–sensitivity of the EVs for the currently active cluster into account.

ENERGY MANAGEMENT SYSTEM can be formulated as stochastic programming (SP) and consequently treats uncertainty using a scenario based approach. It derives optimal bids to various electricity markets and derives a dispatch schedule for the next 24 hours ahead of time. Uncertain production quantities, uncertain consumption quantities and market prices are examples of stochastic processes.

REDISPTACH derives control decisions based on RT operational requirements, considering economical measures and/or risk based measures. Again it can be formulated as SP.

DIRECT CONTROL we consider applicable for fast dynamics ([Mad+14]), such as frequency stabilization. We formulate it as MPC problem. See Section 8.2.2.

INDIRECT CONTROL we consider for the activation of flexibility in the MG using economical incentives. We formulate it as MPC problem. See Section 8.2.3.

Optimal control decisions are passed from the RD layer to the DCo layer. The RD layer co–optimizes directly controllable units (DCu) and ICU. This way, system flexibility is accounted for and uncertainty associated with the flexible units is incorporated. The DCo layer tracks given input references considering both DCu and ICu with a chosen precision. See Figure 8.2.

8.2.1 System Identification

system identification (ID) techniques such as N4SID ([VD96; Vd93]) allow for online approximation of the underlying system. Several aspects hereby apply:

- As for all data–driven model identification techniques, quality of the obtained data relates to the quality of the identified model
- The gain of additional precision in the obtained model can be connected to an economical cost. This marginal gain in model accuracy can both be economically expensive and operationally desirable ([Hei+18])

The estimated price sensitivity f_c in the currently active cluster c is hereby:

$$f_c(p_k) = \tilde{b}_c + \sum_{i=k}^{N} \tilde{H}_{c,i}\ p_k \qquad (8.1)$$

f_c maps the price offer p_k to the estimated uncertain response. $\tilde{b}_c$ denotes the uncertain baseline interaction, $\tilde{H}_c$ denotes the uncertain impulse response coefficients. Uncertainty is approximated by aggregation and evaluation of model parameters in chosen temporal clusters. See Figure 8.3 as example. We chose in this study daily meta clusters with hourly granularity in consecutive clusters. Identified system response models are then aggregated in these clusters, see Figure 8.4. Aggregation in clusters allows for the approximation of time–varying uncertainty.

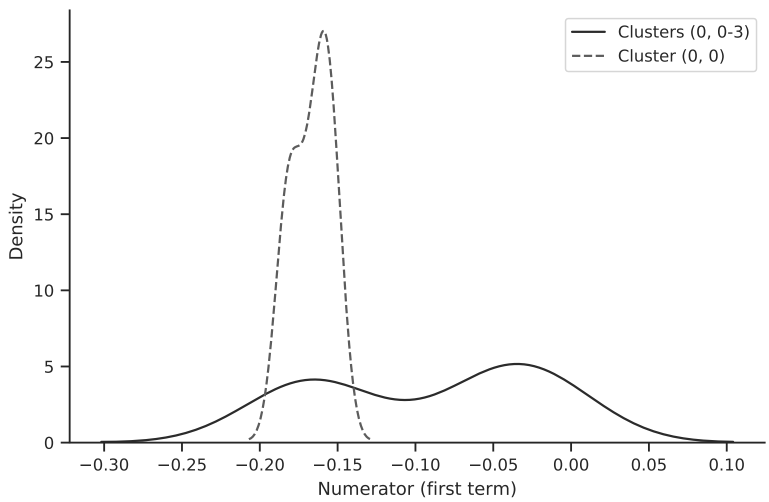

Figure 8.3: Parameter density example: Choice of confidence interval allows for deriving uncertainty estimates for system operation.

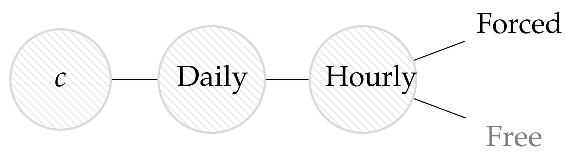

Figure 8.4: Assumed sensitivity function clusters (highlighted). The free system trajectory is recorded for control and evaluation purposes.

8.2.2 Direct Control layer

We consider a classical quadratic regulation objective with input reference tracking term:

$$\min_{\{u_{k+j}\}_{j=0}^{N-1}} \Phi_{\mathrm{DCf}} = \frac{1}{2}\sum_{j=0}^{N-1} ||\Psi||^2_{W_y} + (1-\beta)||\Upsilon||^2_{W_u} \tag{8.2}$$

$$\text{s.t.} \quad \hat{x}_{k+1|k} = A\hat{x}_{k|k} + Bu_k \tag{8.3}$$

$$\hat{x}_{k+1+j|k} = A\hat{x}_{k+j|k} + Bu_{k+j} + G\hat{d}_{k+j}$$

$$j = 1, 2, \ldots, \mathrm{N}-1 \tag{8.4}$$

$$\hat{y}_{k+j|k} = C\hat{x}_{k+j|k} \quad j = 1, 2 \ldots, N \tag{8.5}$$

$$u_{\min} \leq u_{k+j} \leq u_{\max} \tag{8.6}$$

$$\Delta u_{\min} \leq \Delta u_{k+1} \leq \Delta u_{\max} \tag{8.7}$$

$$G_k u_k \leq h_k \tag{8.8}$$

The minimizer $u^\star$ is then denoted as Direct Frequency Control (DCf) layer decision $u^\star_{\mathrm{DCf}}$. Equation 8.8 hereby may include additional system constraints required to obtain sufficient control precision. This can be the case when the sampling rate of upper optimization routines is comparably low. The output reference tracking term is given by

$$\Psi = \hat{y}_{k+1+j|k} - \bar{y}_{k+1+j|k} \tag{8.9}$$

and the input reference tracking term denoted as

$$\Upsilon = u_{k+j} - \bar{u}_{k+j} \tag{8.10}$$

Using an extended state observer (ESO) and the MG internal frequency measurement the unknown residual d is estimated yielding the estimate $\hat{d}$. We account for it using an input disturbance model as outlined in [PR03] — the controller in this form is often in literature referred to as adaptive disturbance rejection controller (ADRC).

This regulator takes input reference sequence $\bar{u}$ from an upper optimization layer into account. Here, this is the RD layer. Given sufficient degrees of freedom the regulator stabilizes system frequency whilst minimizing the deviation from the reference u_{RD}. Lack of freedom in both absolute controllable production capacity and available up–ramp or down–ramp results in system frequency deviations. We neglect a dedicated regularization term acting in the objective when $\beta = 1$; this is due to that we rely on the ESO as means to smooth the control actions. An alternative regulation formulation is formulated in [Ban+18].

The optimal control decision $u^{\star}_{\mathrm{DCf}}$ for this layer includes hereby conventional controllable units as well as the approximated dynamics of the indirectly controllable EVs. The regulator establishes the trade–off between precision in the controlled variable versus the precision in the tracked input references. Consider the following control situation:

- Frequency deviation $\Delta f \neq 0$ (Controlled variable)
- Zero active power contribution reference for the IC units $\bar{u}_{\mathrm{IC}} = 0$
- Saturated directly controlled variables $u_{\mathrm{IC}} = u_{\max}$

The control decision $\bar{u}_{\mathrm{IC}}$ is then utilized to counteract the disturbance acting on the controlled variable.

8.2.3 Indirect Control layer

We state the optimal ICo objective as

$$\min_{\{p_{k+j}\}_{j=0}^{N-1}} \Phi_{\mathrm{IC}} = \frac{1}{2}\sum_{j=0}^{N-1} ||\Psi||_Q^2 + ||\Delta p_{k+j}||_R^2 \tag{8.11}$$

$$\text{s.t.} \quad \hat{x}_{k+1|k} = A\hat{x}_{k|k} + Bp_k \tag{8.12}$$

$$\hat{x}_{k+1+j|k} = A\hat{x}_{k+j|k} + Bp_{k+j}$$

$$j = 1, 2, \ldots, \mathrm{N}-1 \tag{8.13}$$

$$\hat{y}_{k+j|k} = C\hat{x}_{k+j|k} \qquad j = 1, 2 \ldots, N \tag{8.14}$$

$$p_{\min} \leq p_{k+j} \leq p_{\max} \tag{8.15}$$

See for example [JHR11]. An alternative formulation for this setting can be found in [OH11]. Notice that the output reference tracking term is given in Equation 8.9 and equals the formulation for the Direct Control layer.

As for the DCo layer, we again use an ESO to estimate the lumped disturbance. Due to that the underlying system is uncertain, effective uncertainty compensation is hereby fundamental. Notice also that this necessarily leads to situations with poor control performance when the uncertainty is substantial. In these situations, control precision relies on the directly controllable units.

8.3 NUMERICAL RESULTS

We consider a microgrid with one fully controllable unit modeled as first order linear time invariant system and a ramp–rate constraint of $\Delta u_{\text{up}} = .005\ {}^{pu}/_{s}$.

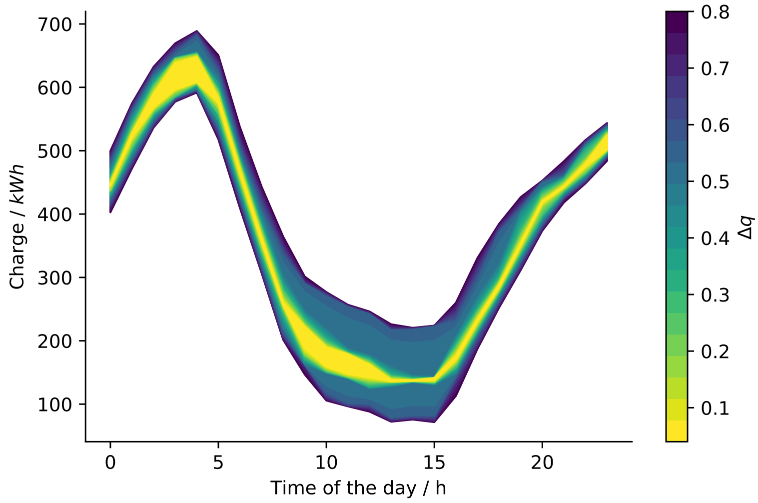

Figure 8.5: Assumed aggregated internal State of Charge of all simulated EVs throughout a day considering 24 hours over 5 days. Δq hereby denotes the quantile range around median.

The load side includes 30 EVs with an assumed individual nominal charge power of 3.6 ± 0.05 kW and individual charge capacity of 24.2 ± 0.05 kWh. The nominal consumption is assumed 216 kW, the EVs account for a fifth of the overall nominal grid power. The active power interaction dynamic $f_{P,n}$ of EV n is assumed as first order system with a time constant of $\tau = 180 \pm .05$ s. $f_{P,n}$ hereby maps the individual EVs active power grid interaction reference to the actual unit active power grid interaction response. The grid interaction reference is given by a stochastic behavioral model denoted in Table 8.1.

Table 8.1: Behavioral clusters with nested time–depending behavior probabilities. The driving P_{driving} probability only applies to EVs after application of $P_{\text{available}}$.

Cluster	Start/End	$P_{\text{available}}$	P_{driving}
Day	6-17	20%	90%
Evening	17-25	70%	50%
Night	0-6	90%	50%

In non–excited mode (price offer $p = 0$) the EVs expose the internal charge pattern over 24 hours and 7 days as illustrated in Figure 8.5: The highest overall State of Charge is in this example reached in the early morning hours whilst the lowest State of Charge is reached in the afternoon. Time delays in the price–control path are neglected.

8.3.0.1 Consumer side price response

The price mapping function equation 8.16 depicts the aggregated reduction in demand for a given price. This is a relationship chosen by the price–sensitive EV controllers. We assume a linear relationship with saturated bounds as load flexibility response in steady state, following the approach outlined in [Hal+13]:

$$f_c(p) = -\frac{\bar{r}_c - \underline{r}_c}{\bar{p}_c - \underline{p}_c}(p - \underline{p}) + \bar{r}_c \tag{8.16}$$

The rebound effect hereby remains unaccounted for in this study. Considering the identification pipeline of one single cluster `(0, 0)` (corresponding to 12pm, day 0) and considering multiple clusters `(0, 0-23)` (corresponding to 12pm, day 0 until 23pm, day 1). See Figure 8.6 and Figure 8.7 respectively. As expected given Figure 8.5, the uncertainty is considerable when observing multiple clusters, supporting the necessity to account for the time–varying behavior.

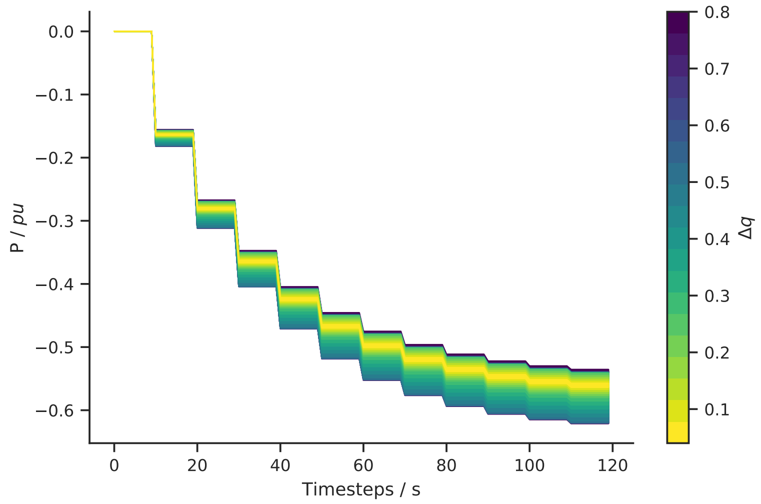

Figure 8.6: Aggregated response when considering one cluster (here: cluster `0, 0`).

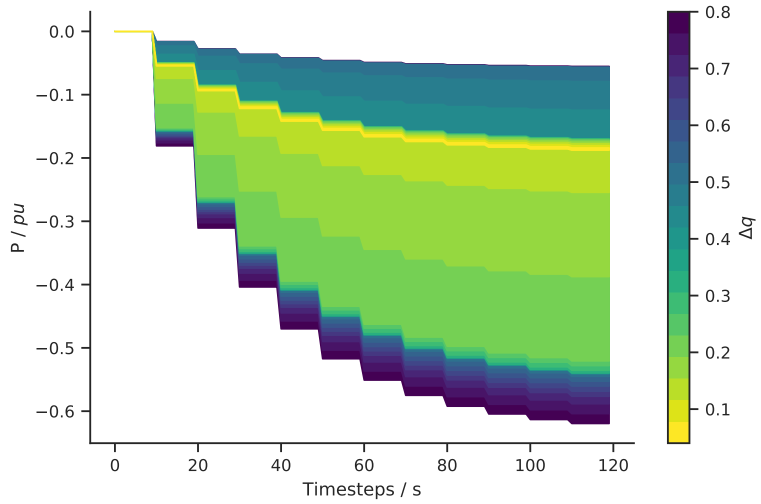

Figure 8.7: Aggregated response when considering multiple clusters, here all hourly clusters of day `0`.

8.3.0.2 Flexibility support

The described RT control hierarchy should support the power balance of the grid in situations where increased need for system flexibility is given. In Figure 8.8, the system frequency is stabilized following an up–ramp of the demand side at timestep `200`. At timestep `210`, ICo is activated in the `DC+IC` scenario. The directly controllable unit saturates at the ramp–rate constraint in the DCo–only scenario. Using ICo the required up–ramp is reduced.

In Figure 8.9 the time cluster $c = 15$ (see Figure 8.5) with only 5 EVs is considered. The experiment depicted in Figure 8.8 is repeated with this altered parameterization. The required up–ramp is comparably reduced in the `DC+IC` scenario. Furthermore, also the variability in the 10 considered experimental timeseries is comparably reduced.

8.4 DISCUSSION AND CONCLUSION

We outlined a control hierarchy enabling for power balance and frequency stability support using EV and ICo. ICo allows for honoring privacy requirements by utilization of system identification techniques used to derive the dynamic price–response relationship. The aggregation of models in temporal clusters enables for the estimation of time–associated uncertainty. Biased forgetting can be used to improve model accuracy and to account for a time–varying underlying system. Simulations show the potential of using EV as price–sensitive system components to support power balancing and frequency stabilization.

Future improvements of the study may include the examination of other price–sensitive flexibility sources, tuning of price–signals,

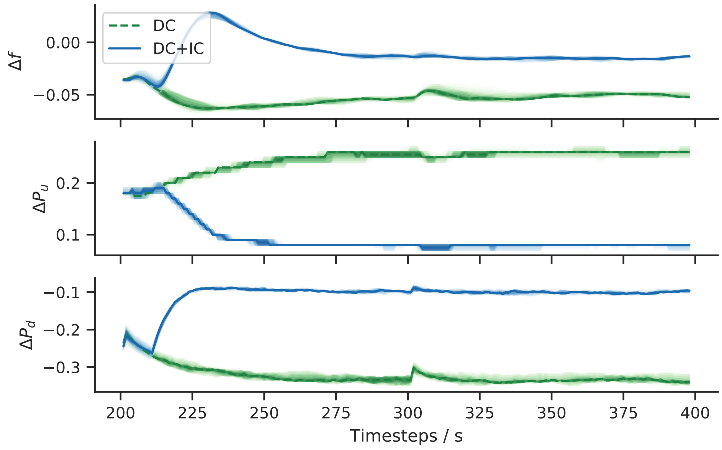

Figure 8.8: Comparison of the controller performance without activated ICo support (`DC` only) and with activated ICo support (`DC+IC`). The disturbance step ΔP_d at timestep `200` is counteracted and active power ΔP_u is reduced. Cluster 1, 30 EVs, 10 stochastic experiments are repeated and illustrated using quantile range steps of 10 steps each, the median is highlighted as dashed line.

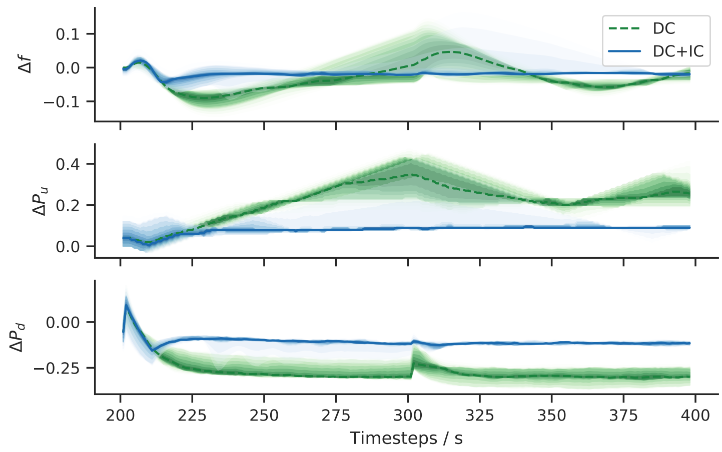

Figure 8.9: Comparison of the controller performance without activated ICo support (`DC` only) and with activated ICo support (`DC+IC`) considering cluster 15 and 5 EVs: The uncertainty in the control situation can be reduced when using DC+IC.10 stochastic experiments are repeated and illustrated using quantile range steps of 10 steps each, the median is highlighted as dashed line.

modeling of rebound effects, alternative system identification methods and support for reactive power control aspects in Microgrids.

This work has been supported by *ENERGINET.DK* under the project microgrid positioning *uGRIP* (77731) and the Innovation Fund Denmark through the *CITIES* research center (no. 1035-0027B).

REFERENCES

[Ban+19] Frederik Banis et al. „Supporting Power Balance in Microgrids with Uncertain Production Using Electric Vehicles and Indirect Control." English. In: *IFAC-PapersOnLine* 52.4 (2019), pp. 371–376. ISSN: 2405-8963. DOI: 10.1016/j.ifacol.2019.08.238.

[Mor+14] Juan M. Morales et al. *Integrating Renewables in Electricity Markets*. Vol. 205. International Series in Operations Research & Management Science. Boston, MA: Springer US, 2014. ISBN: 978-1-4614-9410-2 978-1-4614-9411-9. DOI: 10.1007/978-1-4614-9411-9. URL: http://link.springer.com/10.1007/978-1-4614-9411-9 (visited on 02/08/2018).

[Mad+14] Henrik Madsen et al. „Control of Electricity Loads in Future Electric Energy Systems." English. In: *Handbook of Clean Energy Systems*. Vol. 6. Denmark: Wiley, 2014, pp. 2213–2236. ISBN: 978-1-118-38858-7. URL: http://onlinelibrary.wiley.com/doi/10.1002/9781118991978.hces033/full (visited on 01/24/2017).

[OH11] Olivier Corradi and Henning Ochsenfeld. „Integration of Fluctuating Energy by Electricity Price Control." Master Thesis. Copenhagen: Technical University of Denmark, 2011.

[Flo+16] Caroline Le Flocha et al. „Distributed Optimal Charging of Electric Vehicles for Demand Response and Load Shaping." English. In: *54th IEEE Conference on Decision and Control, CDC 2015*. 2016, p. 7403254. ISBN: 978-1-4799-7886-1. DOI: https://doi.org/10.1109/CDC.2015.7403254.

[Sor+11] E. Sortomme et al. „Coordinated Charging of Plug-In Hybrid Electric Vehicles to Minimize Distribution System Losses." In: *IEEE Transactions on Smart Grid* 2.1 (Mar. 2011), pp. 198–205. ISSN: 1949-3053. DOI: 10.1109/TSG.2010.2090913.

[CHD09] K. Clement, E. Haesen, and J. Driesen. „Coordinated Charging of Multiple Plug-in Hybrid Electric Vehicles in Residential Distribution Grids.“ In: *2009 IEEE/PES Power Systems Conference and Exposition*. Mar. 2009, pp. 1–7. DOI: 10.1109/PSCE.2009.4839973.

[NX17] Nnamdi I. Nwulu and Xiaohua Xia. „Optimal Dispatch for a Microgrid Incorporating Renewables and Demand Response.“ In: *Renewable Energy* 101 (Feb. 2017), pp. 16–28. ISSN: 0960-1481. DOI: 10.1016/j.renene.2016.08.026. URL: http://www.sciencedirect.com/science/article/pii/S0960148116307273 (visited on 08/01/2017).

[SLL13] S. Salinas, M. Li, and P. Li. „Multi-Objective Optimal Energy Consumption Scheduling in Smart Grids.“ In: *IEEE Transactions on Smart Grid* 4.1 (Mar. 2013), pp. 341–348. ISSN: 1949-3053. DOI: 10.1109/TSG.2012.2214068.

[Jin+17] Ming Jin et al. „MOD-DR: Microgrid Optimal Dispatch with Demand Response.“ In: *Applied Energy* 187 (Feb. 2017), pp. 758–776. ISSN: 0306-2619. DOI: 10.1016/j.apenergy.2016.11.093. URL: http://www.sciencedirect.com/science/article/pii/S030626191631724X (visited on 08/01/2017).

[KR15] Michael D. Knudsen and Sergi Rotger-Griful. „Combined Price and Event-Based Demand Response Using Two-Stage Model Predictive Control.“ In: *Smart Grid Communications (SmartGridComm), 2015 IEEE International Conference On*. IEEE, 2015, pp. 344–349. URL: http://ieeexplore.ieee.org/abstract/document/7436324/ (visited on 01/24/2017).

[VD96] Peter Van Overschee and Bart De Moor. „Stochastic Identification.“ en. In: *Subspace Identification for Linear Systems: Theory - Implementation - Applications*. Ed. by Peter Van Overschee and Bart De Moor. Boston, MA: Springer US, 1996, pp. 57–93. ISBN: 978-1-4613-0465-4. DOI: 10.1007/978-1-4613-0465-4_3. URL: https://doi.org/10.1007/978-1-4613-0465-4_3 (visited on 07/15/2019).

[Vd93] P. Van Overschee and B. de Moor. „N4SID: Numerical Algorithms for State Space Subspace System Identification.“ In: *IFAC Proceedings Volumes*. 12th Triennal Wold Congress of the International Federation of Automatic Control. Volume 5 Associated Technologies and Recent Developments, Sydney, Australia, 18-23 July 26.2, Part 5 (July 1993), pp. 55–58. ISSN: 1474-6670. DOI: 10.1016/S1474-6670(17)48221-8. URL: http://www.sciencedirect.com/science/article/pii/S1474667017482218 (visited on 07/15/2019).

[Hei+18] Tor Aksel N. Heirung et al. „Model Predictive Control with Active Learning under Model Uncertainty: Why, When, and How." en. In: *AIChE Journal* 64.8 (2018), pp. 3071–3081. ISSN: 1547-5905. DOI: 10.1002/aic.16180. URL: http://onlinelibrary.wiley.com/doi/abs/10.1002/aic.16180 (visited on 01/04/2019).

[PR03] Gabriele Pannocchia and James B. Rawlings. „Disturbance Models for Offset-Free Model-Predictive Control." In: *AIChE journal* 49.2 (2003), pp. 426–437.

[Ban+18] Frederik Banis et al. „Utilizing Flexibility in Microgrids Using Model Predictive Control." In: *Proceedings of Mediterranean Conference on Power Generation, Transmission, Distribution and Energy Conversion*. IET Control Theory and Applications. Croatia: Institution of Engineering and Technology, Nov. 2018. ISBN: 978-1-83953-133-0. DOI: 10.1049/cp.2018.1856.

[JHR11] John Bagterp Jørgensen, Jakob K. Huusom, and James B. Rawlings. „Finite Horizon MPC for Systems in Innovation Form." In: *Decision and Control and European Control Conference (CDC-ECC), 2011 50th IEEE Conference*. Orlando, USA: IEEE, 2011, pp. 1896–1903.

[Hal+13] Rasmus Halvgaard et al. „Thermal Storage Power Balancing with Model Predictive Control." In: *Control Conference (ECC), 2013 European*. IEEE, 2013, pp. 2567–2572. URL: http://ieeexplore.ieee.org/xpls/abs_all.jsp?arnumber=6669197 (visited on 01/09/2017).

9 PAPER D

Prosumer response estimation using SINDYc in conjunction with Markov-Chain Monte-Carlo sampling

Abstract — *Prosumer response activation is one key ingredient in a smart energy system. Inclusion of prosumers into the system operation leverages flexibility potentials. In order to coordinate prosumers during real–time operation, a control scheme requires knowledge of the dynamics. In this study, we combine the Sparse System Identification of Nonlinear Dynamics with Control (SINDyc) algorithm with Bayesian inference using Markov-Chain Monte-Carlo sampling. By using this combination, we obtain parsimonious models alongside parameter uncertainty estimates. Such models characterize the prosumer response and its uncertainty.*

Authors: Frederik Banis, Henrik Madsen, Niels Kjølstad Poulsen, Daniela Guericke

Submitted for review to the *ENERGIES* journal.

9.1 INTRODUCTION

A prosumer is a unit within the power system that can act both as consumer and producer. Examples are electric vehicles (EVs) with vehicle to grid (V2G) functionality. Such cars can therefore extract and feed–in power from and to the power system [Flo+16].

The activation of prosumers introduces flexibility in the operational scheme which facilitates the integration of higher shares of renewable energy system (RES), thereby contributing to a more sustainable grid operation [Jin+17; NX17]. Furthermore, this may lead to reduced cost of system operation [Sok+12].

System identification Sys-ID techniques are one central building block for achieving long–term reliable real–time (RT) control, see e.g. [Lju99; Nel01; Ngu17]. Identification algorithms such as sub–space methods [Vd93] marked milestones in this area. The sparse system identification of nonlinear dynamics with control (SINDyc) algorithm [BPK16a] is a recent addition in this field, building on sparsity promoting optimization techniques such as the least absolute shrinkage and selection operator (LASSO).

system identification (Sys-ID) techniques enable high control performance in long–time operation as well as data–driven control approaches, such as indirect control (ICo). The application of ICo is one approach to the integration of prosumer response (PR) mechanisms, see [KR15; Cor+13; Hal+12; Hal+13; Mor+14].

The estimated response of prosumers to price–signals is a component or the sole component of the ICo model. In the following, we refer to the prosumer response as PR. An ICo scheme provides economical incentives for a desired system response, such as a reduction of active power consumption [Mor+14; De +18]. PR can in this way alleviate system congestion by introducing additional degrees of freedom in the operational scheme.

A response model derived using SINDyc is sparse in the model coefficients. SINDyc consequently aims for an accurate model with a low number of active terms selected from a candidate model structure.

The PR is potentially uncertain [MVA13; Bru+18]. It is therefore beneficial to represent this uncertainty in order to be able to account for it. SINDyc does not feature estimation of the uncertainty associated with the derived model as–is. Inference techniques such as markov chain monte carlo (MCMC) sampling however can utilize a SINDyc model as part of the prior probability distribution.

Related approaches can be found in [Fri+13; Fue+19; Zen+12]. [Fri+13] employ a Gaussian process–based state space model and a particle based MCMC (PMCMC) to perform Bayesian inference. They utilize an approach that adjusts the candidate model in an adaptive way, such that model complexity increases alongside available data. [Fue+19] build on [BPK16b], however with focus on using a Bayesian framework building on hierarchical Gaussian prior distributions for the task of parameter inference. [Zen+12] combine stochastic collocation method with MCMC. They report that this reduces the large computational load characteristic for MCMC.

In this paper we combine the SINDyc algorithm with parameter uncertainty inference using MCMC using the probabilistic programming language Stan [Car+17]. SINDyc models have been shown to perform well when facing scarce availability of data [KKB18]. Compared with MCMC, the algorithm is computationally light. Full Bayesian inference using MCMC explores a large parameter space. It can therefore adjust and augment a given SINDyc model given sufficient amounts of data. The combination of sparse dynamical system models with MCMC can yield models that generalize well and provide uncertainty estimates with respect to its parameters.

This paper is organized as follows. In Section 9.2, we state the considered prosumer flexibility estimation problem. In Section 9.3 we outline the SINDyc algorithm as introduced by [BPK16a] and discuss Bayesian inference including a SINDyc model as part of the prior. In Section 9.4 we consider a simplified PR estimation example in order to illustrate the described combination of SINDyc and MCMC. We close the paper by concluding in Section 9.6.

9.2 PROBLEM STATEMENT

In order to integrate prosumers into smart–grid operation, a system operator requires knowledge of the price–response sensitivity and associated dynamics (prosumer response (PR)). Provided accurate representations of these characteristics, the system operator can design excitation sequences in order to encourage or penalize the prosumer grid interaction. We can formalize such excitation sequences as a dynamic pricing scheme [RA10; De +18; Cor+13; Mor+14]. This control approach is commonly referred to as indirect control (ICo). The PR is hereby controlled via another domain, the dynamic pricing space. By integrating the ICo into existing control hierarchy concepts we can activate flexibility when needed. See [Mad+14] for examples. We may consider a single dynamic price for all prosumers or individual dynamic prices.

The PR is inherently uncertain due to the human behavior being a main driver. Considering active power P of a prosumer exchanged with the grid at node i, P is a functional of a higher order state x and the price signal p:

$$\dot{P}_i = f_i(x, p) \tag{9.1}$$

We aim to estimate f_i.

9.3 METHODOLOGY

Response characteristics are typically obtained by means of system identification experiments, see for example [Jun+18]. One approach to identifying the underlying dynamics is by formulating a model structure alongside corresponding coefficients and employ least–squares minimization in this setting [Lju99; Nel01]. Addition of a regularizing term can then lead to a sparse model. From here on we refer to the prior distribution as *prior*.

9.3.1 A Sparse System Identification Algorithm (SINDyc)

[BPK16a] formulated the so–called sparse system identification of nonlinear dynamics with control (SINDyc) algorithm for the identification of sparse nonlinear models.

We can describe the dynamical system as:

$$\frac{d}{dt}x = f(x,\ p) \tag{9.2}$$

f is consequently governed by free– and forced dynamics and potentially nonlinear. Reformulating leads to

$$\dot{x} = \Xi\Theta^T(x,\ p) \tag{9.3}$$

$\dot{x}$ is hereby approximated using the variation over system identification (Sys-ID) data X. In the simplest form, a one–step shifted version of the input–output observations X subtracted from the original version yields the approximations of the dynamics. The related Dynamic Mode Decomposition (DMD) algorithm [Sch10; Sch11] uses a similar approach, however for the identification of linear system models. $\Theta^T(x,\ p)$ denotes the model structure of terms including the state x, the input p and potentially cross–terms of both x and p.

The choice of model structure is one important design choice [Nel01; Lju99]. A simple assumption is to assume $\Theta^T(x,\ p)$ to resemble the power series up to a chosen degree. [Nel01] outlines drawbacks of this model structure resulting from properties associated with polynomials:

- Structure selection is computationally demanding, especially for high dimensional problems
- Extrapolation capabilities of the power series are sub–optimal
- Polynomial models suffer heavily under the curse of dimensionality

Positive properties include [Nel01]:

- Capability to approximate a broad group of target problems
- Low sensitivity to noise
- Global explanatory capabilities

Referring to discussions on this type of model in [Nel01], we should emphasize that we choose this model type for the purpose of demonstrating the application of the SINDyc algorithm in conjunction with markov chain monte carlo (MCMC). Other applications may require another type of model. As recommended in [Nel01] and in order to limit aforementioned drawbacks, we only consider polynomials up to third order. We here use the model structure given in [BPK16a], a power series including cross–terms. Ξ is obtained using the sequential thresholded least–squares algorithm proposed in [BPK16b]. As outlined in [BPK16a], we have to choose the regularization weight α in order to obtain a sparse model while retaining model accuracy. We here perform a naive sweep over a set of candidate weights $\bar{\alpha}$ as suggested in [BPK16a] whilst evaluating the sparsity alongside a model evaluation function. See Algorithm 2.

Algorithmus 2 : Sparsity sweep using SINDyc.

Input : SINDyc_args, sparsity_threshold, $\bar{\alpha}$, evaluation_function
Output : Xi
Data : X

```
for α in ᾱ do
    // Execute SINDyc on data
    Xi = SINDyc(X, SINDyc_args)
    // Evaluate model performance
    if evaluation_function(Xi) = True then
        nz = count_nonzero(m)
        nval = count_values(m)
        // Evaluate sparsity
        if (nz/nval) < sparsity_threshold then
            return Xi
    else
        continue
```

9.3.2 Probabilistic Model

We may generalize (9.3) to a probabilistic model. The probabilistic model is then:

$$P(\dot{X}|m) = P(\hat{\Xi}|m)\underline{\Theta}^T(X) + \epsilon \tag{9.4a}$$

m denotes the prior which includes the model coefficients $\Xi^\star$ obtained using SINDyc in Algorithm 2:

$$\hat{\Xi} \sim \mathcal{N}(\hat{\Xi}^\star, \sigma_{\Xi}^2) \tag{9.4b}$$

$$\tilde{\epsilon} \sim \mathcal{N}(\mu_\epsilon,\ \sigma_\epsilon^2) \tag{9.4c}$$

Following the Bayesian principle we can flexibly state the prior based on available information. Parts of the prior may be undefined. Such lack of information becomes part of the overall uncertainty in the model. We include weakly informative priors for these parts as recommended in [Gab+19].

9.3.3 Probabilistic Model Inference

The inference process of the probabilistic model (9.4) is formulated as pseudo–code in Algorithm 3.

`XI` is a list in which we aggregate models inferred using Algorithm 2. $\bar{X}$ is a list of individual Sys-ID experiments. For each n –th experimental data X in $\bar{X}$ we call Algorithm 2 and obtain a corresponding candidate model $\Xi(n)$. `select_mMCMC` selects the MCMC candidate model `m_MCMC` based on the collection of candidate models `XI`. `fit_MCMC_function` then performs MCMC on the model `m_MCMC`. `m_MCMC` is a model corresponding to $\hat{X}i^{\star}$ in the model structure. Algorithm 3 returns $\tilde{\Xi}$, the posterior probability density function (PDF) of the model coefficients.

Algorithmus 3 : Probabilistic model inference using a candidate structure and candidate model derived using SINDYc in Algorithm 2.

Input : fit_MCMC_function, MCMC_args,
select_mMCMC_function, SINDyc_args,
sparsity_threshold, $\bar{\alpha}$, evaluation_function

Output : $\tilde{\Xi}$

Data : $\bar{X}$

```
// Setup container XI for candidate models
XI = list()
for n, X in enumerate(X̄) do
    // Identify sparse system models using Algorithm 2
    Ξ(n) = Algorithm 1(X, SINDyc_args, sparsity_threshold, ᾱ,
        evaluation_function)
    // Collect candidate models
    append(XI, Ξ(n))
// Select the MCMC model based on the collection of candidate
    models XI
m_MCMC = select_mMCMC_function(XI)
// Fit MCMC model using XI
Ξ̃ = fit_MCMC_function(m_MCMC, XI)
return Ξ̃
```

9.3.4 Excitation Model

We use the software package Stan for performing MCMC [Car+17]. Stan requires an ordinary differential equation (ODE) with modeled forcing for the inference of the dynamics subject to forcing. We therefore augment the system in (9.3) with a forcing model which approximates the excitation signal. We restrict the excitation model to a third order polynomial as recommended in [Nel01].

9.4 A SIMULATION EXAMPLE

Consider a system of two prosumers. The first prosumer dynamics are nonlinear; the second prosumer dynamics are linear. w is the noise in the dynamics. The scalar p is the price–signal sent to the prosumers.

We sample the system with $T_s = 1s$. We consider two clusters of data, referred to as `c0` and `c1` in the following.

$$\frac{d}{dt}x = \alpha_m \begin{bmatrix} x_0^2 \\ x_1 \end{bmatrix} + \beta p + w \tag{9.5a}$$

We observe the system response through the measurements y subject to white noise v as

$$y = x + v \tag{9.5b}$$

We hereby draw the system dynamics from random distributions:

$$\alpha_m \sim -\log\mathcal{N}(\log \begin{bmatrix} 0.2 \\ 0.1 \end{bmatrix}, 1e-3) \tag{9.5c}$$

$$\beta \sim \log\mathcal{N}(\log \begin{bmatrix} 0.07 \\ 0.2 \end{bmatrix}, 1e-2) \tag{9.5d}$$

$$w \sim \mathcal{N}(0, .005) \tag{9.5e}$$

$$v \sim \mathcal{N}(0, .005) \tag{9.5f}$$

In cluster $c0$ and $c1$, we have the following number of observations:

$$n_{\text{meas},c0} = 50 \tag{9.5g}$$

$$n_{\text{meas},c1} = 5 \tag{9.5h}$$

While this is a simple model, it should suffice to outline the modeling approaches described in the following.

As for Sys-ID in general, the choice of excitation signal is fundamental for the quality of the system approximation [Nel01; Lju99]. The excitation signal should correspond to the magnitude and frequency range in which we aim to use the model [Nel01]. Whether the excitation signal is adequate to extract sufficient information is to be checked in relation to the considered system and its operating condition.

Here we choose a double–sinusoidal excitation signal applied on top of an assumed constant controller signal $u = 0.5$. For a different operating point we may design a different excitation signal such that we collect sufficient information from the system. The constant signal excites the balanced system throughout a burn–in period, such that the system approaches a new equilibrium prior to the start of the system identification period.

$$e_i = \sin(f) \tag{9.6a}$$

where

$$f \sim \ln\mathcal{N}(-2, 0.05) \tag{9.6b}$$

9.4.1 SINDyc — Polynomial prediction model

We aim for a low order model as simplest candidate model without drift term, such that the system remains in equilibrium when undisturbed or unexcited. The chosen candidate model structure is

$$\frac{d}{dt}y_t = \xi_1 y_t + \xi_2 p_t + \xi_3 y_t^2 + \xi_4 y_t p_t + \xi_5 p_t^2 \tag{9.7}$$

For the SINDyc algorithm, we choose a homogeneous range of 100 candidate regularization coefficients α within the sweep bounds $[5e-4,\ 1e-1]$. See Algorithm 2.

Identifying models using Algorithm 2 for cluster 0, we obtain the coefficient distributions illustrated in Figure 9.1. The uncertainty in the dynamics α and β lead to uncertainty in the magnitudes of the model coefficients. `Model 0` is correctly associated with nonlinear dynamics and the linear `Model 1` is correctly associated with linear dynamics. Examination of the sparsity of the identified model provides information about the success of the identification. The convergence of the algorithm is assured only when the identified model is sparse in the coefficients.

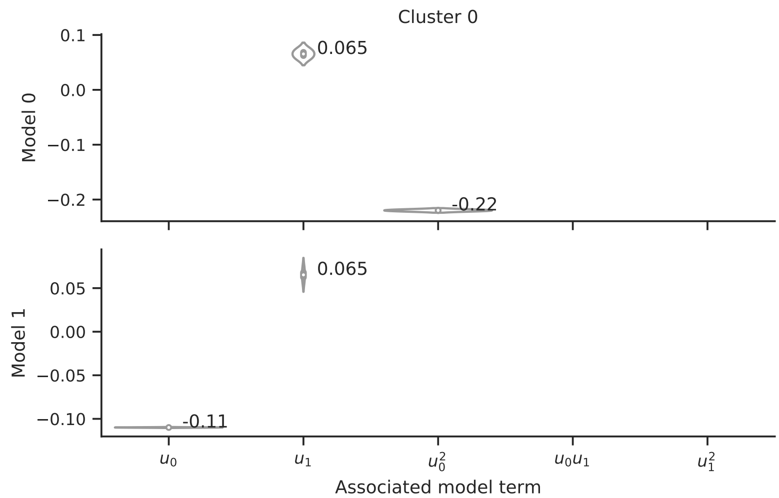

Figure 9.1: Coefficient magnitudes for a low order SINDyc model based on 50 system trajectories, sweep–bounds α set to $[5e-4,\ 1e-1]$ and number of model evaluations set to 50. `u0` corresponds to the state x, `u1` corresponds to the system input u. The mean coefficient magnitudes are depicted next to the violinplots for each associated model term.

The model of the first PR approximates the true system for both the identification data and when considering an out–of–sample experiment. See Figure 9.2.

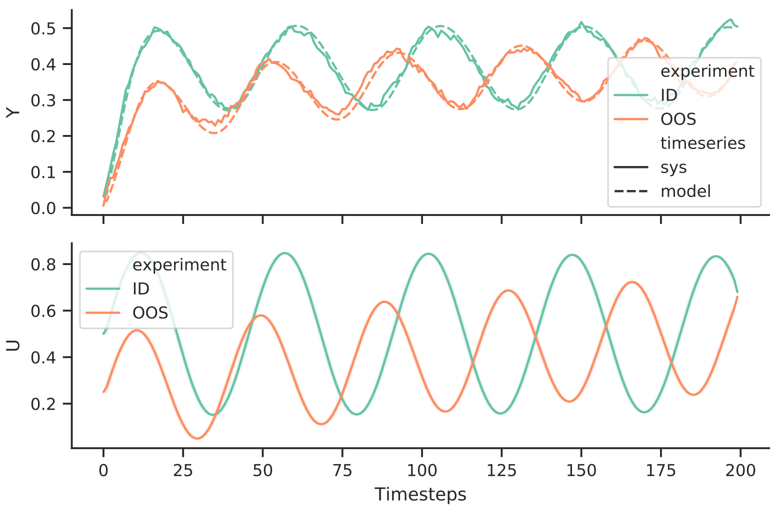

Figure 9.2: System and fitted model response excited by the excitation signal `U`. Identification experiment `ID`, out–of–sample experiment `OOS`.

We can visually examine the quality of the fit by comparing the one–step prediction surfaces of both the true system and the deduced model. See Figure 9.3.

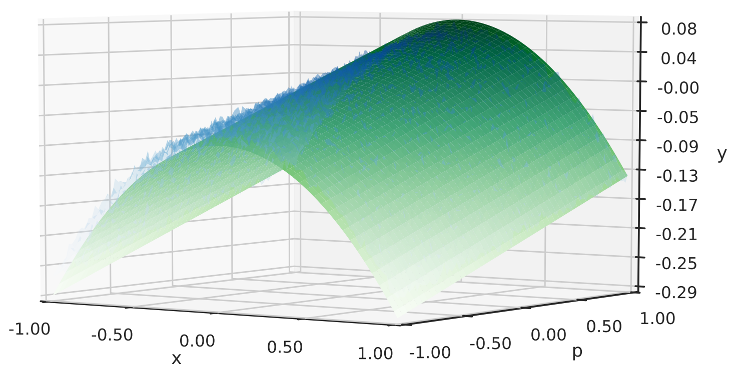

Figure 9.3: One–step prediction comparison of the test system (blue) and fitted model (green).

9.4.2 Model Coefficient Distribution Inference using MCMC

We now aim to obtain a probabilistic dynamic system model of the first prosumer based on the identified candidate depicted in Figure 9.1. The candidate model is $\Xi^{\star}$, $\Theta^{T,\star}(X)$, where:

$$\Xi_{c0}^{T,\star} = [0.06, -0.202] \tag{9.8a}$$
$$\Theta_{c0}^{\star}(X) = [x,\ p] \tag{9.8b}$$

Notice that `u0` and `u1` in Figure 9.1 correspond to the output y and system input p respectively. We neglect all zero–terms in the candidate model structure in (9.7) such that the inference through MCMC uses only the candidate model as stated in (9.8).

We describe the observation z through the model output y with normally distributed measurement error with variance σ_y^2:

$$y \sim \mathcal{N}(z, \sigma_y^2) \tag{9.9a}$$

For the prior for σ_y^2 we assume a log–normal distribution with mean $\log(\sigma_{y0}^2)$, the logarithm of the variance of the observations in the burn–in period. Please notice that for the parameter values chosen here the Gaussian prior model for σ^2 is appropriate, but for some other prior uncertainty ranges for σ^2 it could be more appropriate to use the natural conjugated prior, namely the inverse Gamma distribution. See [MT10] for examples.

$$\sigma_y^2 \sim \ln(\log(\sigma_{y0}^2), 1) \tag{9.9b}$$

The prior for the model coefficients Ξ we assume normally distributed around $Xi_{c0}^{\star}$, the coefficients inferred using the SINDyc algorithm:

$$\hat{\Xi} \sim \mathcal{N}(\Xi_{c0}^{\star}, \sigma_{\Xi}^2) \tag{9.9c}$$

Standard deviation σ_{Ξ} we choose based on the distribution in Ξ_{c0}. Notice that the latter is only proper when the sample size Ξ_{c0} is considered significant:

$$\sigma_{\Xi}^2 \sim \ln(\log(\sigma_{\Xi}), 1) \tag{9.9d}$$

Lack of information in the formulation of this prior we may express through statements of weakly informative priors [Gab+19].

Furthermore, we consider the following posterior predictive check for evaluation of the accuracy of the inference:

$$\hat{y}_{N,n} = \mathcal{N}(z_{N,n}, \sigma_y^2) \tag{9.10}$$

Stan [Car+17] solves the ODEs considered here using the Runge–Kutta–45 method. For MCMC, we choose 1000 iterations per chain, four chains, 500 burn–in or warm–up iterations, no thinning and a seed of 101.

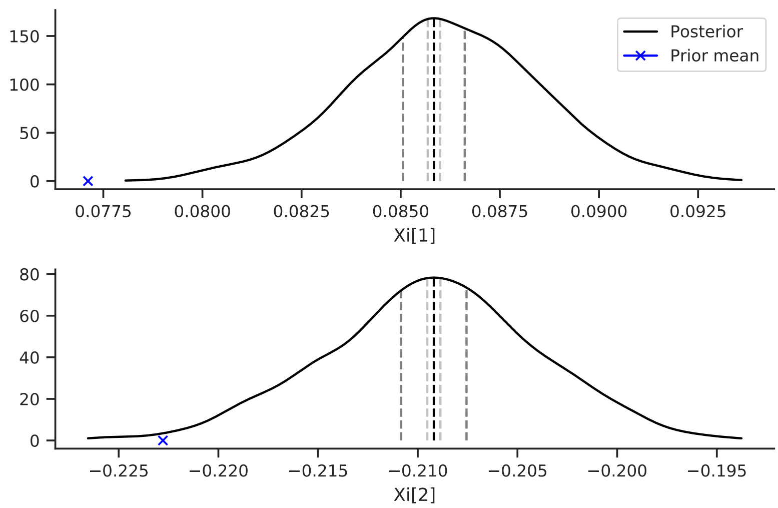

Figure 9.4: Inferred coefficient uncertainties $\hat{\Xi}$ through MCMC (via Stan [Car+17]) given a candidate model derived using SINDyc for cluster 0. Crosses mark the prior means based on the SINDyc model. The maximum of the posterior distribution marked with black dashed line. 95% confidence interval marked using dark grey dashed lines, 99% confidence interval marked using light–grey dashed lines.

As kernel density estimation bandwidth we use Scott's rule as given in [Sco15]. The approximated posterior distributions $\hat{\Xi}_{c0}$ are depicted in Figure 9.4. The coefficient priors chosen by SINDyc are marked using crosses. We can observe that the posterior distribution deviates from these priors.

Improving the prior optimizes the sampling space for a new MCMC sampling. This can lead to shorter computation time for future sampling of the model.

Examining the posterior predictive check illustrated in Figure 9.5 reveals that the model approximates the observed output sub–optimally, yet captures the general trend in the data.

By means of random draws from the posterior samples we can obtain a probabilistic model. Here we draw 100 random samples from the inferred coefficients depicted in Figure 9.4 and from the inferred measurement variance. Out–of–sample co–simulation of this model alongside the 5 samples of the true system is depicted in Figure 9.6.

9.4.3 Low Availability of System Identification Data

Cluster `c1` contains 5 observations. We now repeat the model fitting for this cluster and test the ability of the derived model to predict future observations.

We obtain the sparse coefficient magnitudes illustrated in Figure 9.7. As for `cluster 0`, the nonlinearity in the first PR is correctly identified.

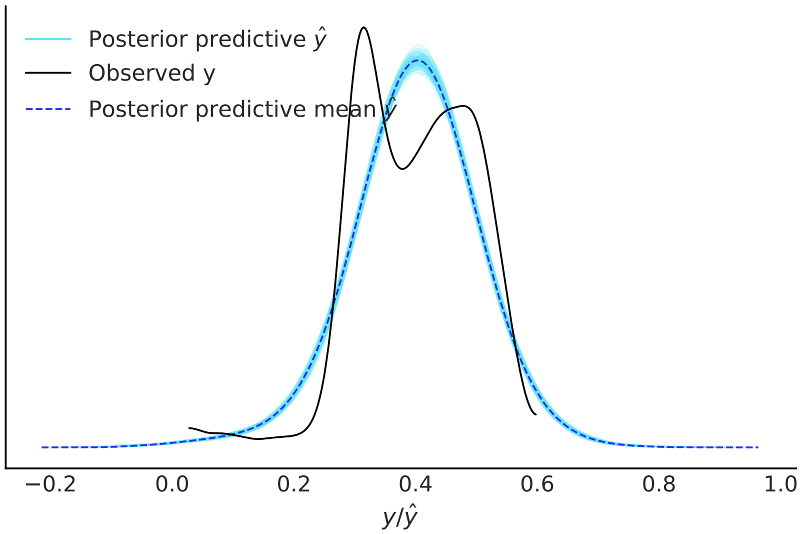

Figure 9.5: Posterior predictive check of the model output prediction $\hat{y}$ with 200 samples drawn from the posterior distribution. Plot generated using ArviZ library [Kum+19].

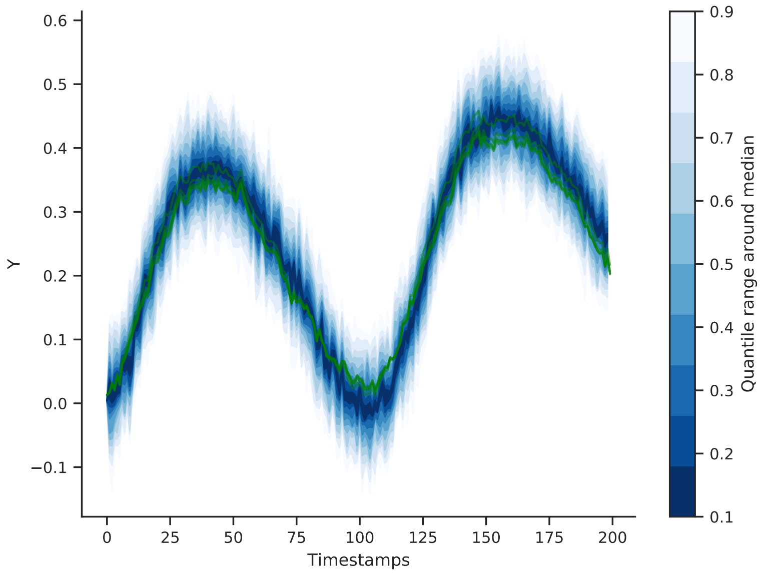

Figure 9.6: Out-of-sample simulation of 5 system realizations and the inferred Stan model (cluster 0).

Uncertainty in the coefficient magnitudes is comparably higher for `cluster 1`.

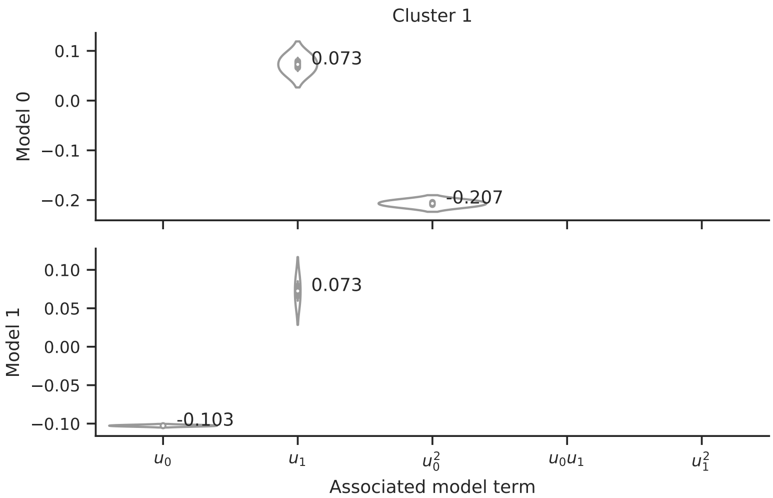

Figure 9.7: Coefficient magnitudes for a linear SINDyc model based on 5 system trajectories, sweep–bounds set to $[5e-4,\ 1e-1]$ and number of model evaluations set to 100. 95% confidence interval (dark grey), 99% confidence interval (light grey).

Co–simulation and out–of–sample simulation is depicted in Figure 9.8.

We repeat the inference using Stan described in Section 9.4.2. The approximated posterior distributions $\hat{\Xi}_{c1}$ are depicted in Figure 9.9. The priors chosen by SINDyc are marked using crosses. Comparing to `cluster 0`, we obtain a posterior distribution closer to the SINDyc prior.

The posterior predictive check illustrated in Figure 9.10 indicates a similar result as for `cluster 0`.

Out–of–sample co–simulation of this model alongside the 5 samples of the true system indicates is depicted in Figure 9.11.

9.5 DISCUSSION

Activation of system flexibility through demand response (DR) and prosumer response (PR) schemes such as indirect control (ICo) are increasingly relevant in relation to power system operation. See [Old+15] for an example. The combination of sparse system identification algorithms such as the sparse system identification of nonlinear dynamics with control (SINDyc) algorithm and markov chain monte carlo (MCMC) enables the inference of model parameters alongside parameter probability estimates. Bayesian approaches are computationally complex [Fri+13]. As shown in the related publications

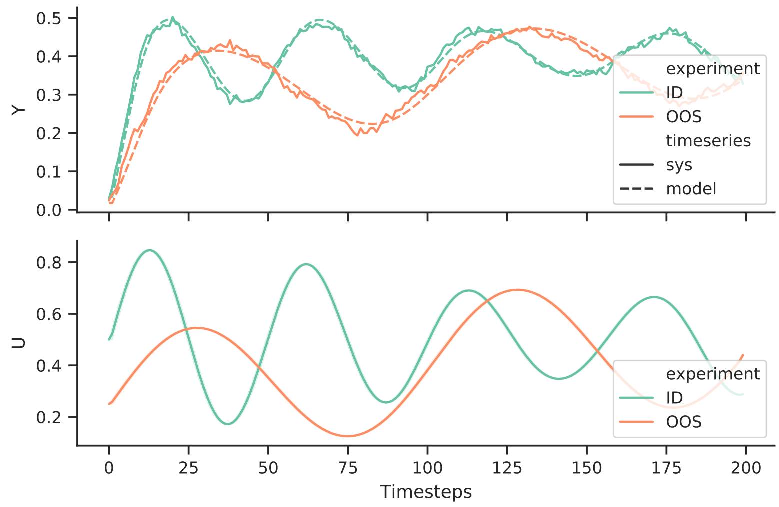

Figure 9.8: Cosimulation of one test system and one identified model using this observation.

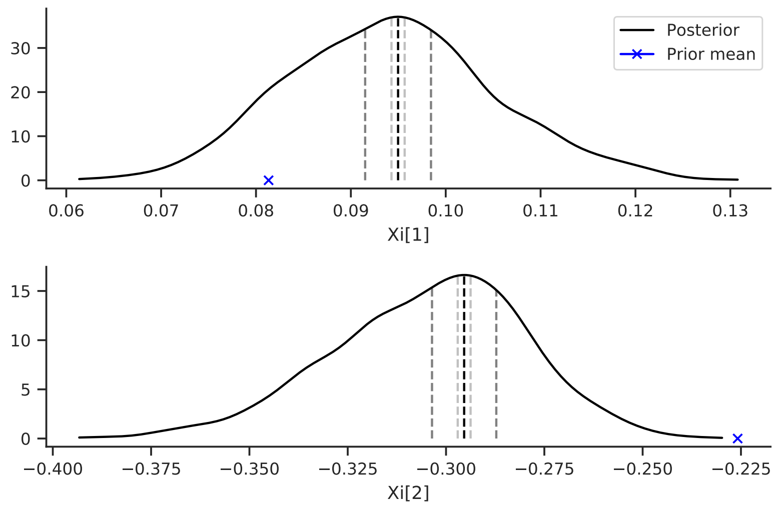

Figure 9.9: Inferred coefficient uncertainties using MCMC (using Stan [Car+17]) given a single candidate model derived using SINDyc for cluster 1. Prior means based on the SINDyc model marked with crosses. The maximum of the posterior distribution is marked with a black dashed line. The 5% confidence interval is marked using dark grey dashed lines, the 1% confidence interval is marked using light–grey dashed lines.

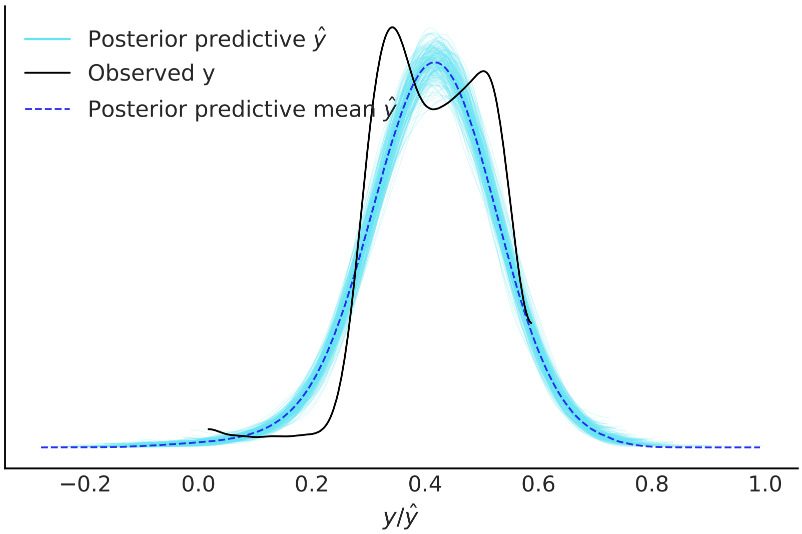

Figure 9.10: Posterior predictive check of the model output prediction $\hat{y}$ with 200 samples drawn from the posterior distribution. The plot is generated using the ArviZ library [Kum+19].

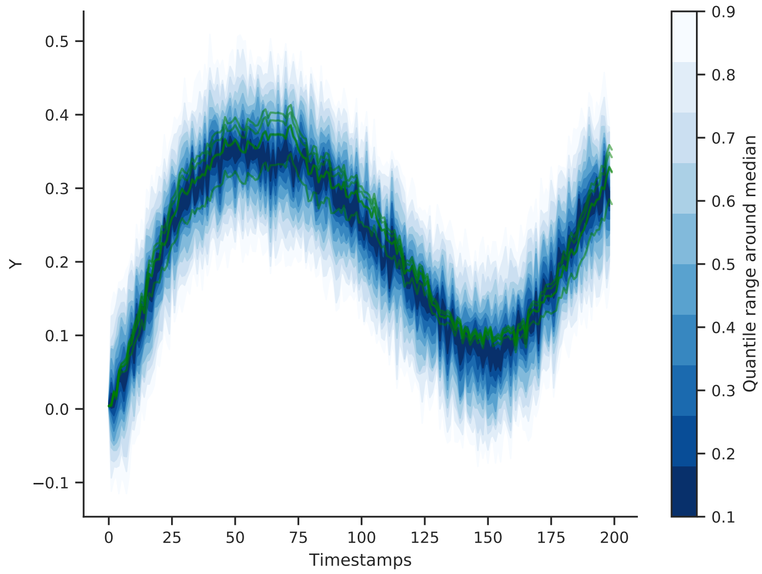

Figure 9.11: Cluster 1: Response modeling with limited data (5 observations) versus revealing additional 45 observations.

[Fri+13; Fue+19; Zen+12], Bayesian inference techniques may benefit from sparsity promoting modeling approaches. The focus on a viable candidate model and associated parameter spaces reduces the problem size. Aside of this, parsimonious candidate model can be a desirable goal in the modeling process [BPK16b].

Similarly as described in [Fue+19], SINDyc models provide information on whether nonlinearities are present in the data when provided with a reasonable library of candidate models. Automatized system identification (Sys-ID) pipelines can benefit from such information.

For future improvements, we may replace the polynomial excitation model described in Section 9.3.4 with an alternative candidate model structure. The goal should be to achieve a high accuracy representation of the excitation signal while maintaining a high performance of the sampling process within the MCMC framework.

Furthermore, the pipeline should be evaluated on a broad range of problems. This should entail the evaluation of required adjustments. When aiming for automatized Sys-ID, robustness and associated issues are to be investigated and potential solutions to be examined.

9.6 CONCLUSIONS

In this paper, we have presented a combination of the sparse system identification of nonlinear dynamics with control (SINDyc) algorithm and markov chain monte carlo (MCMC) using the software package Stan, in context of prosumer response estimation. While SINDyc identifies sparse and potentially nonlinear dynamic system models, MCMC enables for the estimation of rich posterior distributions. MCMC can use a sparse system model identified using SINDyc and benefit from its sparsity property. Probabilistic dynamical system models enable the application of stochastic model predictive controllers, a core–ingredient when aiming to activate prosumer dynamics based on informative grounds.

This work has been supported by Innovation Fund Denmark through the *CITIES* research center (no. 1035-0027B) and by *ENERGINET.DK* under the project microgrid positioning — *uGRIP* (77731).

REFERENCES

[Flo+16] Caroline Le Flocha et al. „Distributed Optimal Charging of Electric Vehicles for Demand Response and Load Shaping." English. In: *54th IEEE Conference on Decision and Control, CDC 2015*. 2016, p. 7403254. ISBN: 978-1-4799-7886-1. DOI: https://doi.org/10.1109/CDC.2015.7403254.

[Jin+17] Ming Jin et al. „MOD-DR: Microgrid Optimal Dispatch with Demand Response." In: *Applied Energy* 187 (Feb. 2017), pp. 758–776. ISSN: 0306-2619. DOI: 10.1016/j.apenergy.2016.11.093. URL: http://www.sciencedirect.com/science/article/pii/S030626191631724X (visited on 08/01/2017).

[NX17] Nnamdi I. Nwulu and Xiaohua Xia. „Optimal Dispatch for a Microgrid Incorporating Renewables and Demand Response." In: *Renewable Energy* 101 (Feb. 2017), pp. 16–28. ISSN: 0960-1481. DOI: 10.1016/j.renene.2016.08.026. URL: http://www.sciencedirect.com/science/article/pii/S0960148116307273 (visited on 08/01/2017).

[Sok+12] Leo Emil Sokoler et al. „Real-Time Optimization for Economic Model Predictive Control." In: *10th European Workshop on Advanced Control and Diagnosis*. 2012. URL: http://orbit.dtu.dk/fedora/objects/orbit:115908/datastreams/file_be97c55b-c4fe-4e65-83a7-c78fb6709d89/content (visited on 01/25/2017).

[Lju99] L. Ljung. *System Identification: Theory for the User*. Prentice Hall Information and System Sciences Series. Prentice Hall PTR, 1999. ISBN: 978-0-13-656695-3. URL: https://books.google.dk/books?id=nHFoQgAACAAJ.

[Nel01] Oliver Nelles. *Nonlinear System Identification*. en. Berlin, Heidelberg: Springer Berlin Heidelberg, 2001. ISBN: 978-3-642-08674-8 978-3-662-04323-3. DOI: 10.1007/978-3-662-04323-3. URL: http://link.springer.com/10.1007/978-3-662-04323-3 (visited on 03/06/2020).

[Ngu17] Nhan T. Nguyen. *Model-Reference Adaptive Control*. en. New York, NY: Springer Berlin Heidelberg, 2017. ISBN: 978-3-319-56392-3.

[Vd93] P. Van Overschee and B. de Moor. „N4SID: Numerical Algorithms for State Space Subspace System Identification." In: *IFAC Proceedings Volumes*. 12th Triennal Wold Congress of the International Federation of Automatic Control. Volume 5 Associated Technologies and Recent Developments, Sydney, Australia, 18-23 July 26.2, Part 5 (July 1993), pp. 55–58. ISSN: 1474-6670. DOI: 10.1016/S1474-6670(17)48221-8. URL: http://www.sciencedirect.com/science/article/pii/S1474667017482218 (visited on 07/15/2019).

[BPK16a] Steven L. Brunton, Joshua L. Proctor, and J. Nathan Kutz. „Sparse Identification of Nonlinear Dynamics with Control (SINDYc)." In: *arXiv:1605.06682 [math]* (May 2016). arXiv: 1605.06682 [math]. URL: http://arxiv.org/abs/1605.06682 (visited on 05/24/2019).

[KR15] Michael D. Knudsen and Sergi Rotger-Griful. „Combined Price and Event-Based Demand Response Using Two-Stage Model Predictive Control." In: *Smart Grid Communications (SmartGridComm), 2015 IEEE International Conference On*. IEEE, 2015, pp. 344–349. URL: http://ieeexplore.ieee.org/abstract/document/7436324/ (visited on 01/24/2017).

[Cor+13] O. Corradi et al. „Controlling Electricity Consumption by Forecasting Its Response to Varying Prices." In: *IEEE Transactions on Power Systems* 28.1 (Feb. 2013), pp. 421–429. ISSN: 0885-8950. DOI: 10.1109/TPWRS.2012.2197027.

[Hal+12] Rasmus Halvgaard et al. „Economic Model Predictive Control for Building Climate Control in a Smart Grid." In: *Innovative Smart Grid Technologies (ISGT), 2012 IEEE PES*. IEEE, 2012, pp. 1–6. URL: http://ieeexplore.ieee.org/abstract/document/6175631/ (visited on 04/02/2017).

[Hal+13] Rasmus Halvgaard et al. „Thermal Storage Power Balancing with Model Predictive Control." In: *Control Conference (ECC), 2013 European*. IEEE, 2013, pp. 2567–2572. URL: http://ieeexplore.ieee.org/xpls/abs_all.jsp?arnumber=6669197 (visited on 01/09/2017).

[Mor+14] Juan M. Morales et al. *Integrating Renewables in Electricity Markets*. Vol. 205. International Series in Operations Research & Management Science. Boston, MA: Springer US, 2014. ISBN: 978-1-4614-9410-2 978-1-4614-9411-9. DOI: 10.1007/978-1-4614-9411-9. URL: http://link.springer.com/10.1007/978-1-4614-9411-9 (visited on 02/08/2018).

[De +18] Giulia De Zotti et al. „Ancillary Services 4.0: A Top-to-Bottom Control-Based Approach for Solving Ancillary Services Problems in Smart Grids." en. In: *IEEE Access* 6 (2018), pp. 11694–11706. ISSN: 2169-3536. DOI: 10.1109/ACCESS.2018.2805330. URL: http://ieeexplore.ieee.org/document/8290690/ (visited on 08/06/2019).

[MVA13] Johanna L. Mathieu, Marina González Vayá, and Göran Andersson. „Uncertainty in the Flexibility of Aggregations of Demand Response Resources." In: *IECON 2013 - 39th Annual Conference of the IEEE Industrial Electronics Society*. Nov. 2013, pp. 8052–8057. DOI: 10.1109/IECON.2013.6700479.

[Bru+18] K. Bruninx et al. „On Controllability of Demand Response Resources Amp; Aggregators' Bidding Strategies." In: *2018 Power Systems Computation Conference (PSCC)*. June 2018, pp. 1–7. DOI: 10.23919/PSCC.2018.8442877.

[Fri+13] Roger Frigola et al. „Bayesian Inference and Learning in Gaussian Process State-Space Models with Particle MCMC." en. In: *arXiv:1306.2861 [cs, stat]* (Dec. 2013). DOI: 10.1.1.766.1321. arXiv: 1306.2861 [cs, stat]. URL: http://arxiv.org/abs/1306.2861 (visited on 03/28/2020).

[Fue+19] R. Fuentes et al. „Efficient Parameter Identification and Model Selection in Nonlinear Dynamical Systems via Sparse Bayesian Learning." en. In: *Journal of Physics: Conference Series* 1264 (July 2019), p. 012050. ISSN: 1742-6588, 1742-6596. DOI: 10.1088/1742-6596/1264/1/012050. URL: https://iopscience.iop.org/article/10.1088/1742-6596/1264/1/012050 (visited on 03/28/2020).

[Zen+12] Lingzao Zeng et al. „A Sparse Grid Based Bayesian Method for Contaminant Source Identification." en. In: *Advances in Water Resources* 37 (Mar. 2012), pp. 1–9. ISSN: 03091708. DOI: 10.1016/j.advwatres.2011.09.011. URL: https://linkinghub.elsevier.com/retrieve/pii/S0309170811001783 (visited on 03/28/2020).

[BPK16b] Steven L. Brunton, Joshua L. Proctor, and J. Nathan Kutz. „Discovering Governing Equations from Data by Sparse Identification of Nonlinear Dynamical Systems." en. In: *Proceedings of the National Academy of Sciences* 113.15 (Apr. 2016), pp. 3932–3937. ISSN: 0027-8424, 1091-6490. DOI: 10.1073/pnas.1517384113. URL: http://www.pnas.org/lookup/doi/10.1073/pnas.1517384113 (visited on 01/12/2020).

[Car+17] Bob Carpenter et al. „Stan: A Probabilistic Programming Language." In: *Journal of Statistical Software* 76.1 (Jan. 2017). DOI: 10.18637/jss.v076.i01. URL: https://www.jstatsoft.org/article/view/v076i01.

[KKB18] Eurika Kaiser, J. Nathan Kutz, and Steven L. Brunton. „Sparse Identification of Nonlinear Dynamics for Model Predictive Control in the Low-Data Limit." In: *Proceedings of the Royal Society A: Mathematical, Physical and Engineering Sciences* 474.2219 (Nov. 2018), p. 20180335. ISSN: 1364-5021, 1471-2946. DOI: 10.1098/rspa.2018.0335. arXiv: 1711.05501. URL: http://arxiv.org/abs/1711.05501 (visited on 05/31/2019).

[RA10] A.J. Roscoe and G. Ault. „Supporting High Penetrations of Renewable Generation via Implementation of Real-Time Electricity Pricing and Demand Response." en. In: *IET Renewable Power Generation* 4.4 (2010), p. 369. ISSN: 17521416. DOI: 10.1049/iet-rpg.2009.0212. URL: https://digital-library.theiet.org/content/journals/10.1049/iet-rpg.2009.0212 (visited on 03/21/2020).

[Mad+14] Henrik Madsen et al. „Control of Electricity Loads in Future Electric Energy Systems.“ English. In: *Handbook of Clean Energy Systems*. Vol. 6. Denmark: Wiley, 2014, pp. 2213–2236. ISBN: 978-1-118-38858-7. URL: http://onlinelibrary.wiley.com/doi/10.1002/9781118991978.hces033/full (visited on 01/24/2017).

[Jun+18] Rune Grønborg Junker et al. „Characterizing the Energy Flexibility of Buildings and Districts.“ In: *Applied Energy* 225 (Sept. 2018), pp. 175–182. ISSN: 0306-2619. DOI: 10.1016/j.apenergy.2018.05.037. URL: http://www.sciencedirect.com/science/article/pii/S030626191830730X (visited on 11/01/2018).

[Sch10] Peter J. Schmid. „Dynamic Mode Decomposition of Numerical and Experimental Data.“ en. In: *Journal of Fluid Mechanics* 656 (Aug. 2010), pp. 5–28. ISSN: 1469-7645, 0022-1120. DOI: 10.1017/S0022112010001217. URL: https://www-cambridge-org.proxy.findit.dtu.dk/core/journals/journal-of-fluid-mechanics/article/dynamic-mode-decomposition-of-numerical-and-experimental-data/AA4C763B525515AD4521A6CC5E10DBD4%5C# (visited on 09/01/2019).

[Sch11] P. J. Schmid. „Applications of the Dynamic Mode Decomposition.“ In: *Theoretical and Computational Fluid Dynamics* 25.1-4 (2011), pp. 249–259. ISSN: 09354964. DOI: 10.1007/s00162-010-0203-9.

[Gab+19] Jonah Gabry et al. „Visualization in Bayesian Workflow.“ en. In: *Journal of the Royal Statistical Society: Series A (Statistics in Society)* 182.2 (Feb. 2019), pp. 389–402. ISSN: 09641998. DOI: 10.1111/rssa.12378. URL: http://doi.wiley.com/10.1111/rssa.12378 (visited on 01/09/2020).

[MT10] Henrik Madsen and Poul Thyregod. *Introduction to General and Generalized Linear Models*. en. Texts in Statistical Science. Chapman & Hall, 2010.

[Sco15] D.W. Scott. *Multivariate Density Estimation: Theory, Practice, and Visualization*. Wiley Series in Probability and Statistics. Wiley, 2015. ISBN: 978-0-471-69755-8. URL: https://books.google.dk/books?id=pIAZBwAAQBAJ.

[Kum+19] Ravin Kumar et al. „ArviZ a Unified Library for Exploratory Analysis of Bayesian Models in Python.“ en. In: *Journal of Open Source Software* 4.33 (Jan. 2019), p. 1143. ISSN: 2475-9066. DOI: 10.21105/joss.01143. URL: http://joss.theoj.org/papers/10.21105/joss.01143 (visited on 01/09/2020).

[Old+15] Frauke Oldewurtel et al. „Adaptively Constrained Stochastic Model Predictive Control Applied to Security Constrained Optimal Power Flow." In: IEEE, July 2015, pp. 931–936. ISBN: 978-1-4799-8684-2. DOI: 10.1109/ACC.2015.7170853. URL: http://ieeexplore.ieee.org/document/7170853/ (visited on 02/01/2017).

10 PAPER E

Three–level Hierarchical Microgrid Control — Model Development and Laboratory Implementation

Abstract — *This paper presents a three–level hierarchical control approach for microgrids in both grid–connected and islanded mode. The first level optimizes microgrid operation in the long–run with the goal of minimizing microgrid's operating costs. The second level takes part in frequency control in grid-connected microgrids or takes full control over frequency stability in isolated microgrids. It utilizes a Model Predictive Controller and Kalman Filter based on available frequency measurements in the microgrid. The third level is the plant level, in which classical controllers are used for tracking optimal set points received from upper two control layers. The developed control scheme is applied to the Smart Grid Lab (SGLab) at the University of Zagreb Faculty of Electrical Engineering and Computing. The findings from this close-to-real-world application are also presented.*

Authors: Mateo Beus, Frederik Banis, Hrvoje Pandžić, Niels Kjølstad Poulsen

Submitted for consideration to the *Power Systems Computation Conference (PSCC) 2020* in Porto, Portugal. Given acceptance, it will be published in the associated conference proceedings and the *Journal of Electric Power Systems Research (EPSR)*. Notice that this is the preprint version.

10.1 INTRODUCTION

The need to satisfy electricity consumption in a sustainable way has led to an increased share of electricity produced from renewable energy system (RES). The power system dominated by the RES generation leads to a reduced use of conventional power plants that were essential to secure the required flexibility by adapting their production levels. This approach cannot be applied in case of power system with high share of RES due to their intermittent nature. Therefore, it is essential to find new sources of flexibility in power systems. As potential solutions to ensure the necessary flexibility in power systems with high share of RES are the use of demand response (DR) and generally the flexibility available in the distribution network. So far, the distribution networks were observed as a set of passive consumers able only to withdraw electricity from the transmission network. The increased share of different types of **DGs!s** (**DGs!s**) caused a paradigm change in the distribution network due to bi-directional power flows. In other words, electricity can also be injected from the distribution to the transmission network. Since **DGs!s** usually does not have sufficient installed capacity to participate independently in the electricity market, it is essential to establish a mechanism that will allow multiple distributed generation (DG) units to participate in electricity markets. A possible way to group a multiple DG units into one entity from the grid perspective is to apply a concept of a microgrid (MG). Furthermore, application of this concept reduces the impact of DGs on the distribution network and thus allows integration of large quantities of DGs in the distribution network [UOZ11]. Although a unique definition of MG does not exist, it is generally accepted that a *microgrid is an integrated energy system consisting of interconnected loads and different types of DGs, which as an integrated system connected to the grid through the point of common coupling (PCC) can operate in parallel with the grid or in islanded mode* [LP04], [Hat+07]. A typical MG can consists of:

- energy storage, e.g. batteries;
- dispatchable DGs, e.g.small–scale hydro power plants, biogas plants, diesel plants, combined heat and power plant (CHP);
- non-dispatchable RES, e.g. solar power plants, wind power plants;
- dispatchable and non-dispatchable loads.

The main intention of this paper is to develop and validate in the laboratory environment MG hierarchical control scheme that can serve as a basis for further MG integration in electricity markets.

The proposed hierarchical control scheme consists of three levels. The responsibility of the first level is to minimize MG operating cost. The second level optimizes real–time (RT) control problems on an aggregated level, while the third level is based on classical controllers and serves only for tracking optimal set points received from the upper two control levels. This control level will not be further analyzed in this paper.

The layout of the paper is as follows. Review of the publications related to the optimization of MG operation is elaborated in Section [[id:c7ed6838-de38-4ca3-9e16-129175e0564b]]. Hierarchical control scheme is introduced in Section [[id:818f6bc6-a1bc-4873-99f3-c5718a55eed4]], while the laboratory setup used to validate the proposed control scheme and simulation results are presented in Section [[id:109c9a14-bee8-44cb-9e5e-4046f2151802]]. The paper is concluded in Section [[id:2663016d-6a4d-47d0-9155-80f8fc1d1bfe]].

10.2 LITERATURE REVIEW

A considerable amount of literature can be found on optimization problem formulation for MG energy management.

In [Che+13] and [Mar+13], the authors formulate mixed integer nonlinear optimization problem (MINLP) used in the context of optimal MG operating strategy. In both cases, MINLP optimization problems are used as energy management system (EMS) control tools with the main goal of performing optimal operation and scheduling of MGs. In [ZYH10], a coordinated two-layer control approach is developed for MG management. Both control layers are based on the receding horizon concept. The main task of the lower control layer is to maintain the power output from the RES constant during short periods. On the other hand, the upper control layer is used to mitigate severe fluctuations of the power output from convectional generators caused by balancing the output of intermittent sources. In order to fulfill their tasks, both control layers rely on the use of battery storage.

Numerous examples in the literature can be found where model predictive control (MPC) is used as a control approach in power system operation problems. In this context, MPC algorithm is usually formed in a way that typical unit commitment or dynamic economic dispatch problem is extended with the receding horizon approach. In [PRG14] and [Par+14], the authors apply an MPC approach based on mixed integer linear problem (MILP) to the problem of efficiently optimizing MG operations while satisfying time-varying requests and operation constraints. In [XI09], the authors use an MPC approach to solve a multi-objective economic/environmental dispatch problem in a power system with high share of RES. The conclusion is that the MPC algorithm is able to minimize the generation costs by directly dispatching the generator output from RES in order to compensate temporal load variations over time horizon. Further, in [XZE09], the authors apply an MPC algorithm to solve a dynamic economic dispatch problem with the main goal of minimizing the MG operating costs. In addition, the difference in formulations between the optimal control dynamic dispatch based on control theory and the dynamic economic dispatch based on optimization theory is demonstrated. In [Qi+11] and [QLC12], a supervisory control system based on an MPC algorithm is developed for optimal management and operation of a hybrid wind-solar power plant. The MPC algorithm calculates optimal power set points for the solar and wind subsystems at each sampling time while minimizing the cost function. These set points are then sent to two local controllers responsible for tracking optimal set points received from the supervisory control system.

Microgrids (MGs) are considered to be complex energy systems since their control requirements involve different control approaches and different time scales. For instance, voltage and frequency control tasks have the time scales of seconds, while MG unit commitment problems have the time scale of hours. In that regard, it is reasonable to apply hierarchical control approach to MG operation problems. In [BD12], the authors review the hierarchical control strategies applied to MGs. The hierarchical control structure introduced in this paper consists of primary, secondary and tertiary control levels. The goal of the primary control level is to stabilize the voltage and frequency, the secondary control level is responsible for compensating voltage and frequency variations caused by the primary control, while the third level is responsible for power flow control through PCC and optimal operation in grid-connected and islanded operating mode. In a similar fashion, in [Van+13] the authors analyze a three-level hierarchical control structure that can be implemented in islanded MGs. In addition, this paper provides an overview of the control strategies related to the reserve provision by DG units, loads, and storage. In [Fen+17], the authors provide a comprehensive comparison between hierarchical control structures and distributed control structures for MGs. The main advantage of hierarchical control compared to the distributed on is the provision of optimal solution since it can integrate a centralized EMS. This implies that in the case of hierarchical control, computational complexity is higher due to the use of more advanced optimization algorithms compared to the distributed control. The main disadvantage of this is that hardware platform in the hierarchical approach requires more powerful computers. Although the communication network is important for both control approaches, the main advantage of the distributed approach is that any single point failure in the communication of the control system would not have severe impact on the normal system operation.

10.3 HIERARCHICAL CONTROL FORMULATION

The hierarchical control approach designed in this paper consists of three levels illustrated in Fig. 10.1. The first-level controller is responsible for the long-term behavior of the MG and it is not influenced by the transient behavior of the fast dynamics. The second-level controller is in charge of frequency stability provision in the MG, while the third level controllers are responsible for tracking set points received from the upper two control levels.

10.3.1 Upper Optimization Level – EMS

Here, we introduce the dynamic economic dispatch formulation used in the first control level. Parameters and variables used in the formulation are described in Table 10.1. The main goal of this control level

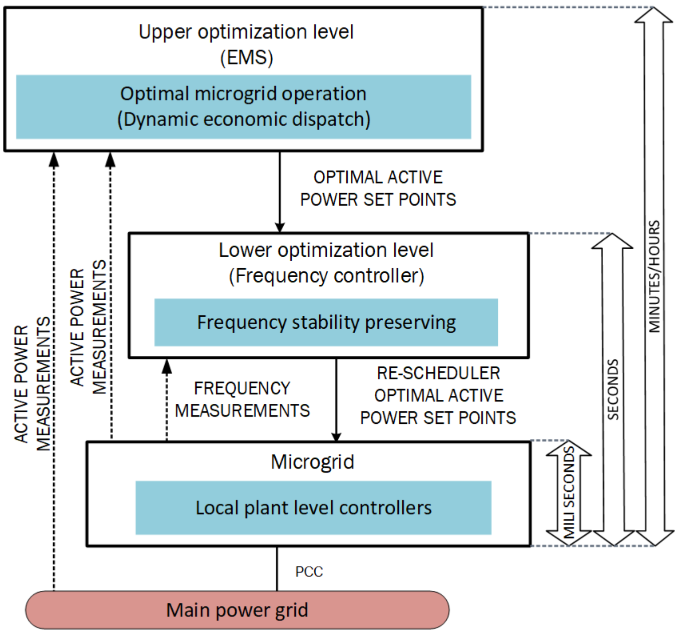

Figure 10.1: Proposed hierarchical control levels of a MG (Paper E).

is to minimize the total operating costs while satisfying the demand and other technical constraints.

10.3.2 Cost Function

The goal is to optimize the following cost function:

$$\min \sum_{t=1}^{T} \sum_{g=1}^{N_g} c_1 p_g(t) + c_2 s(t) \tag{10.1}$$

where the first term represents the cost associated with energy production from DGs and the second term represents cost/profit from the interaction with the utility grid. In addition, t is a time instant and T is the length of the prediction horizon.

10.3.2.1 *Operational Constraints*

Balance between the production and the consumption must be satisfied at each sampling instant t, so the following equality constraint is defined:

$$\sum_{g=1}^{N_g} p_g(t) + p^{\mathrm{RES}} \geq \sum_{l=1}^{L_c} D_l(t) + BL(t) \tag{10.2}$$

where the first term represents production level from the controllable DGs at time instant t and the second term represents total production level from non-controllable RES units in the MG for the entire prediction horizon. The first term on the right-hand side of constraint (10.2) represents consumption level of non-critical controllable loads at time instant t, while the second term represents consumption level of critical non-controllable loads at time instant t.

In addition, each DG unit needs to satisfy the following technical constraints:

Table 10.1: Parameters and variables in the upper optimization level (Paper E).

Parameters	Description
N_g	Number of DG units
N_l	Number of controllable loads
BL	Total consumption level of non–controllable loads [kW]
P_gMIN	Minimum power level of a DG unit [kW]
P_gMAX	Maximum power level of a DG unit [kW]
RU_gMAX	Ramp up limit of a DG unit [kW/h]
RD_gMAX	Ramp down limit of a DG unit [kW/h]
P_{RES}	Total power production from RES [kW]
L_l	Forecasted power level of a controllable load [kW]
p_gINIT	Active power measurements of DG units [kW]
c_1	Production cost [EUR/kWh]
c_2	Energy price [EUR/kWh]

Variables	Description
D_l	Controllable load consumption level [kW]
p_g	Power level of a DG unit [kW]
s	Power exchanged with the utility grid [kW]

$$p_{g,t}^{\mathrm{MIN}} \leq p_{g,t} \leq p_{g,t}^{\mathrm{MAX}} \tag{10.3}$$

$$p_{g,t+1} - p_{g,t} \leq RU_g^{\mathrm{MAX}} \tag{10.4}$$

$$p_{g,t_1} - p_g^{\mathrm{INIT}} \leq RU_g^{\mathrm{MAX}} \tag{10.5}$$

$$p_{g,t-1} - p_{g,t} \leq RD_g^{\mathrm{MAX}} \tag{10.6}$$

$$p_g^{\mathrm{INIT}} - p_{g,t_1} \leq RD_g^{\mathrm{MAX}} \tag{10.7}$$

with g=1,...,N_g. Terms (10.3)–(10.7) constrain production level, $p_{g,t}$, by minimum and maximum output limits, $p_{g,t}^{\mathrm{MIN}}$ and $p_{g,t}^{\mathrm{MAX}}$, as well as ramp up and ramp down rates, RU_g^{MAX} and RD_g^{MAX}, of the DG units. Parameter p_g^{INIT} represents the power output at t=0.

Since controllable loads have the possibility to provide DR, an additional constraint is introduced below to ensure that the total energy of the consumer does not change over the operating horizon.

$$\sum_{t=1}^{T} \sum_{l=1}^{L_c} D_{l,t} = \sum_{t=1}^{T} \sum_{l=1}^{L_c} L_{l,t} \tag{10.8}$$

In (10.8), $L_{l,t}$ represents forecasted load profiles for each load, while $D_{l,t}$ represents set points sent to local load controllers.

10.3.3 Lower Optimization Level – Frequency Controller

10.3.3.1 Controller model

The frequency control problem at the aggregated system level is commonly stated using the swing equation as means to describe the inertia of the system [Kun94; Bev14]. In the linear approximation it can be stated as:

$$\frac{d}{dt}\Delta f_t = -\frac{D}{2H}\Delta f_t + \frac{1}{2H}\Delta P_t^{\mathrm{m}} \tag{10.9}$$

where Δf is the frequency deviation from the nominal frequency. H is the inertia based supply time, D the load damping coefficient. ΔP^{m} is the mechanical power balance within the considered grid.

$$\Delta P_t^{\mathrm{m}} = P_t^{+} - P_t^{-} \tag{10.10}$$

The power injections P_t^{+} and extractions P_t^{-} are nonlinear functions. The overall system can be linearized around a chocen stationary point and discretized using zero–order hold approach. The linearized discrete time system models can then be stated as given in [KMJ04]:

$$\frac{\mathrm{d}x_{t|j}}{\mathrm{d}t} = f_0 + A(x_t - x_j) + B(u_t - u_j) + G(d_t - d_j) + w_t \quad (10.11)$$

$$y_t = Cx_t + e_t \quad (10.12)$$

where u_t is the control input at time t and u_j the corresponding input at the point of linearization. Further, x_t is the system state, d are system disturbances, w is the process noise, e is the measurement noise, and y_t is the output. In the simplest form, y_t equals the state of the swing equation. Then, this is a multiple–inputs single–output (MISO) system.

The swing equation expresses the approximated inertia with respect to a single center of gravity. The parameters of this model are both uncertain and time-varying.

10.3.3.2 Model Predictive Controller

The quadratic controller objective is stated as:

$$\min_{u,\,k} J = J_0 + J_1 \quad (10.13)$$

$$\text{s.t.} \quad u_k^{\min} \leq u_k \leq u_k^{\max} \quad (10.14)$$

$$\Delta u_k^{\min} \leq \Delta u_k \leq \Delta u_k^{\max} \quad (10.15)$$

$$G_k\, u_k \leq h_k \quad (10.16)$$

with the objective terms given as:

$$J_0 = \quad ||\Phi_x \hat{x}_{k|k} + \Gamma_u u_k + \Gamma_d \hat{d}_{k|k} - \tilde{y}_k||^2_{W_z}$$

$$J_1 = \quad \beta||u_k||^2_{W_{\Delta u}} + (1-\beta)||u_k - \bar{u}_{k|k}||^2_{W_{\bar{u}}}$$

Φ_x are Markov parameters of the free system response and Γ_u, Γ_d are Markov parameters of the forced system response with respect to the control decisions and system disturbances respectively. These Markov parameters implement the linear predictive model. For incorporation into the hierarchy of control and optimization routines, the objective includes an input reference tracking term. Notice that Γ_d not only entails disturbance related process knowledge, but always knowledge upon the residual disturbance process. State of this residual process is estimated using a state observer as denoted in (10.19) below. The tuning parameter β is used to switch input reference tracking of the controller. The input reference $\bar{u}$ given $\beta = 0$ is tracked with a precision tuned using the penalization term $W_{\bar{u}}$. Note that both the system state and disturbance are estimates, denoted $\hat{x}$ and $\hat{d}$ respectively. $\hat{d}$ here includes the lumped filtered disturbance estimate. For asymptotic convergence in Δf, the integrated estimated output error ϵ can be feedback in form of an output reference adjustment:

$$\tilde{y}_{k|k} = \hat{y}_{k|k} - \bar{y}_k \tag{10.17}$$

$$\epsilon_{k+1|k} = \epsilon_{k|k} + \hat{y}_{k|k} - \bar{y}_k \tag{10.18}$$

In this case, the frequency deviation reference is $\tilde{y} = 0$ and $\Delta f \to \tilde{y}$. The output reference $\bar{y}$ in grid-connected mode (GCM) is to be chosen in relation to the observed frequency. This includes the necessity to decide how the controller should aim to stabilize the grid frequency. For $\bar{y} = 0$, the controller does not follow given inputs references well if the observed frequency deviates considerably from this reference. Consequently, a frequency control goal is to be chosen that is both feasible and desirable for the system. In islanded mode (IM), $\bar{y} = 0$ is chosen, and consequently $f \to 50$.

$\hat{x}$ and $\hat{d}$ are estimated using a state observer as stated below, using formulations given in [PR03; PR01]:

$$\begin{bmatrix} \hat{x}_{k+1|k} \\ \hat{d}_{k+1|k} \end{bmatrix} = \begin{bmatrix} A & B_d \\ 0 & I \end{bmatrix} \begin{bmatrix} \hat{x}_{k|k-1} \\ \hat{d}_{k|k-1} \end{bmatrix} + \begin{bmatrix} B \\ 0 \end{bmatrix} u_k + \begin{bmatrix} L_x \\ L_d \end{bmatrix} (y_{m,k} - C\hat{x}_{k|k-1} - C_d\hat{d}_{k|k-1}) \tag{10.19}$$

Alternatively to (10.19), a dynamic Kalman filter can be utilized. The uncertainty associated with $\hat{d}$ can then be estimated and used to further improve control performance. Consider [KMJ04] for examples.

10.4 IMPLEMENTATION OF HIERARCHICAL CONTROL FOR EXPERIMENTAL MICROGRID

10.4.1 Laboratory Setup

The MG test site consists of the following units:

- Hydro power plant – total rated power of the plant is 11.8 kW and power factor is 0.5. The plant represents a DG in the simulation;
- Solar power plant – total installed capacity of the solar power plant is 10 kW. The plant is connected to the AC part of the MG using a three-phase inverter;
- Load bank of resistors – maximum power of 8 kW equally distributed in three phases. The load is non-controllable and represents critical load in the simulation;
- Bi-directional converter – rated power of 20 kW and it is used to couple the AC and DC parts of the MG;

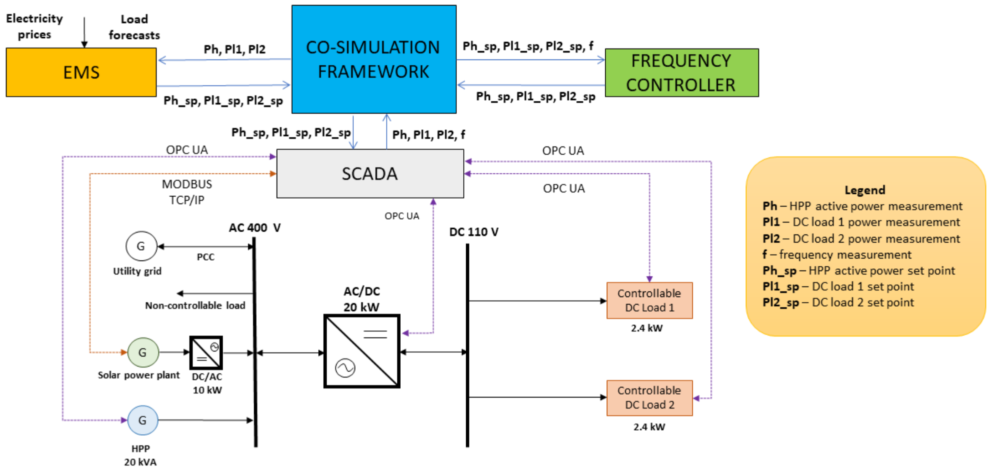

Figure 10.2: Structure of the MG in the SGLab (Paper E).

- Two DC electronic loads – each has rated power of 2.4 kW and the loads are fully controllable.

In Fig. 10.2 it is visible that all the components of the MG are integrated into a supervisory control and data acquisition (SCADA) called PROZA NET [kon]. Although this SCADA system supports different types of communication protocols, i.e. international electrotechnical commission (IEC) 104, IEC 61850, Modbus remote terminal unit (RTU) and transmission control protocol (TCP)/internet protocol (IP), open platform communication (OPC), in this setup only OPC unified architecture (UA) and Modbus TCP/IP communication protocols were used to integrate the MG components. Further, a central component that couples all three control levels is a flexible smart grid co-simulation framework MOSAIK [SSS12], whose main goals are to coordinate execution of all controllers and to control data exchange between controllers.

EMS and Frequency controller are being directly connected through MOSAIK, while the local plant level controllers are integrated into the hierarchical control structure through SCADA that is connected with MOSAIK using a gateway based on TCP client-server communication. In that regard, MOSAIK represents a TCP client and SCADA is a TCP server.

Working principle of the hierarchical control approach is illustrated in Fig. 10.3. The entire operating procedure consists of six steps. Step 1 is conducted every 15 minutes. In this step, MOSAIK initializes and executes the EMS algorithm in general algebraic modeling system (GAMS). Results of the EMS are optimal active power set points for each controllable unit for the next 15 minutes. In Step 2, MOSAIK sends optimal active power set points to the Frequency controller. In Step 3, MOSAIK reads frequency and current active power measurements of all MG components from SCADA and forwards those measurements to the frequency controller. In Step 4, MOSAIK calls the Frequency controller to execute. In Step 5, if frequency measurement does not deviate from the nominal frequency, Frequency controller will send through SCADA optimal active power set points received from MOSAIK in Step 2 to the local plant-level controllers. In case of frequency deviations, Frequency controller will sent re-scheduled optimal active power set points to the local plant-level controllers in order to stabilize the frequency in the IM of operation or to provide primary reserve in the GCM. In addition, Steps 3–6 are cyclically executed every 300 ms.

10.4.2 Simulation Results

In this section we present two deterministic simulation experiments demonstrating the functionality of the proposed MG hierarchical control setup. In both experiments the MG operates in the GCM. The MG topology shown in Fig. 10.2 is used.

During both experiments, the MG is operated with the same forecasted consumption profiles of the controllable loads. The controllable loads in both experiments have the ability to provide, DR which is modeled in a way that the total energy consumption does not change over the operating horizon. Table 10.2 shows load profiles for controllable loads.

The presented experiments differ in the choice of input reference deviation penalization:

EXPERIMENT 1 $\tilde{W}_{\Delta u} = \begin{bmatrix} 1 & 0 & 0 \\ 0 & 5 & 0 \\ 0 & 0 & 5 \end{bmatrix}$

EXPERIMENT 2 $\tilde{W}_{\Delta u} = \begin{bmatrix} 4 & 0 & 0 \\ 0 & 5 & 0 \\ 0 & 0 & 5 \end{bmatrix}$

$\tilde{W}_{\Delta u}$ is hereby a single distinct element in the overall deviation penalization matrix $W_{\Delta u}$. Consequently, the hydro power plant is given higher degrees of freedom in terms of deviations away from the input reference than the two controllable loads. This is true for both experiments, however in *Experiment 1* deviations of the hydro power plant are penalized less.

Both experiments are conducted with a 15-minute prediction horizon and a time step of 1 minute, while the MG controller uses 20-seconds prediction horizon. Since the MG in both experiments operates in the GCM, the main goal of EMS is to minimize power flows to/from the utility grid, while the main purpose of Frequency controller is to provide primary reserve. Hydro power plant, as the only controllable DGs in both experiments, has ramp up/down limit 1.5

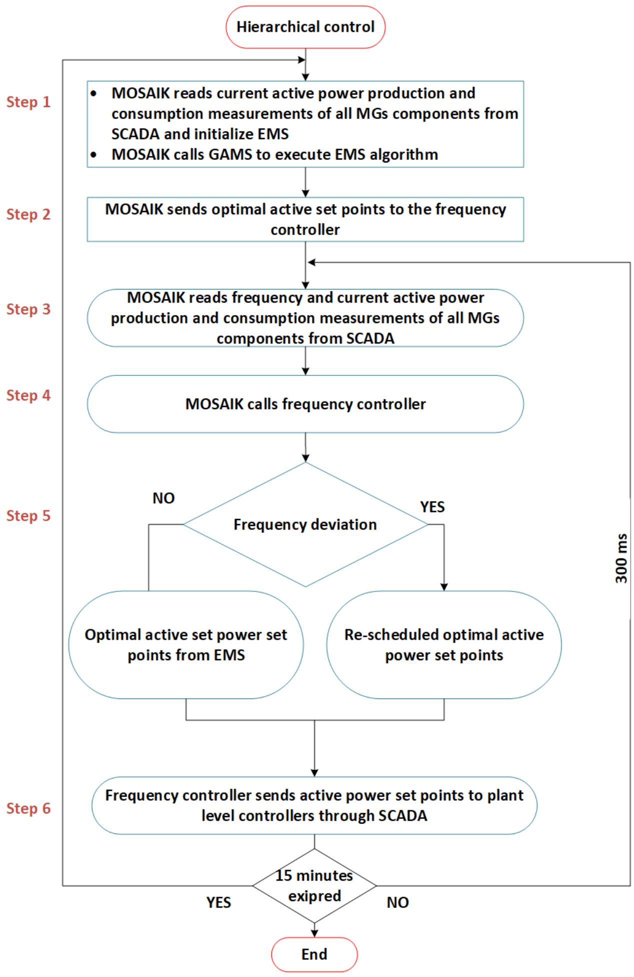

Figure 10.3: Hierarchical control flowchart (Paper E).

kW/min, maximum power 11.5 kW and minimum production level 1 kW. Base load value in both experiments is set to 3 kW. The cost of electricity generated by the hydro power is c_1=0.25 EUR/kWh [IRE], while the electricity price c_2 is 0.31 EUR/kWh during the first seven minutes and 0.21 EUR/kWh during the rest of the simulation time [Eur]. During the first experiment, solar power plant production level was 6.28 kW, while during the second experiment solar power plant production level was 2.98 kW.

Simulation results of both experiments are shown in Figs. 10.4 and 10.5. Frequency controller in both cases follows the set points received from the EMS. In *Experiment 1*, the lower reference penalization value for the hydro power plant causes the hydro power plant references generated by the Frequency controller to deviate more from the references given by the EMS as compared to the second experiment. In Figs. 10.4 and 10.5 the dashed lines in the input space represent Frequency controller references, while the solid lines represent the references received from the EMS. U_0 represents the hydro power plant reference, U_1 represents reference for the controllable load 1 and U_2 for control-

Table 10.2: Load profiles (Paper E).

Time	L_1[kW]	L_2[kW]
t_1	0.4	1.1
t_2	0.7	1.2
t_3	0.8	0.8
t_4	0.8	0.5
t_5	0.6	1.1
t_6	1.0	1.0
t_7	0.9	0.7
t_8	1.2	1.0
t_9	1.2	1.0
t_{10}	0.8	0.8
t_{11}	1.5	0.6
t_{12}	1.7	0.5
t_{13}	1.2	0.5
t_{14}	1.0	0.5
t_{15}	0.4	1.3

lable load 2. Further, y_m represents frequency measurements, while $\hat{y}$ represents frequency estimations. In the lower graph in Fig. 10.4, the largest deviation occurred at time 16:10 when, instead of reducing the output of the hydro power plant (blue line) the Frequency controller actually increased the power (dashed red line). This is because the negative frequency deviation at the same time (see the first graph in Fig. 10.4 caused the Frequency regulator to increase the output of the hydro power plant in order to increase the frequency (input reference deviation penalization equal to 1). On the other hand, the flexible loads (U_1 and U_2) strictly follow the given set points from the EMS as they do not take part in frequency regulation (input reference deviation penalization equal to 5). In Fig. 10.5, which shows the result for *Experiment 2*, the hydro power plant output deviates much less because its input reference deviation penalization is increased to 4, while the loads behave the same way as in *Experiment 1*.

10.5 CONCLUSIONS

The main idea of this paper was to present a three-level hierarchical control approach that can be applied to MGs. The first control level is based on dynamic economic dispatch algorithm and its main purpose is to optimize MG operation in the long-run with the goal of minimizing MG operating costs. The second control level optimizes

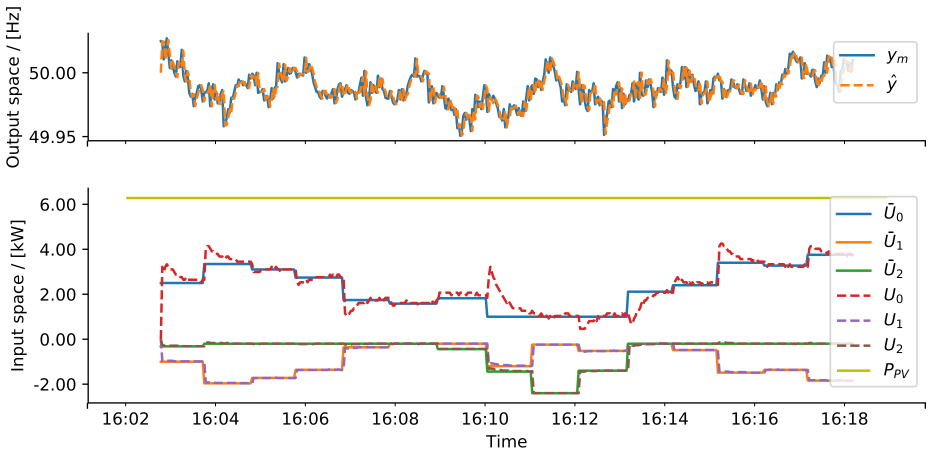

Figure 10.4: Results of *Experiment 1* (deviations of the hydro power plant are penalized less compared to *Experiment 2*) (Paper E).

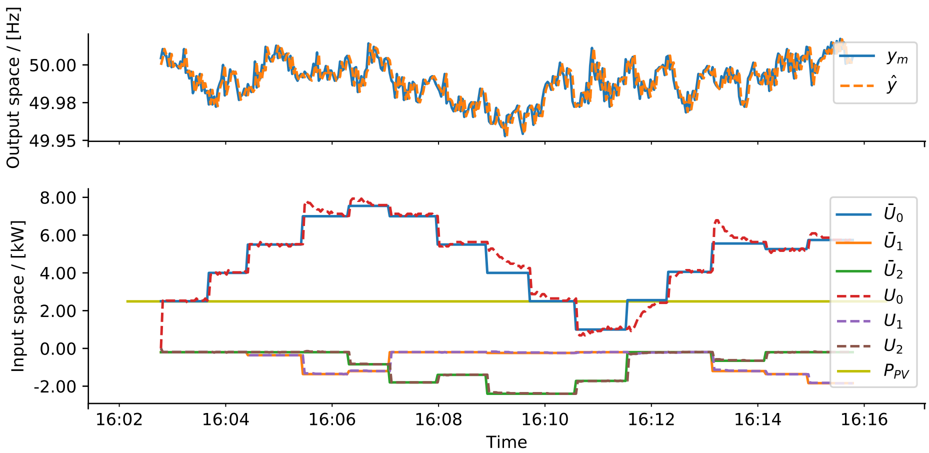

Figure 10.5: Results of *Experiment 2* (deviations of the hydro power plant are penalized more compared to *Experiment 1*) (Paper E).

the aggregated system frequency control problem. Using a model predictive controls (MPCs) formulation and extended Kalman filter, both the constraints and the unknown disturbances are accounted for based on frequency measurement in the MG. The third level is the plant level, in which classical controllers are used for tracking optimal set points received from upper two control layers.

The functionality of this control approach has been tested on the laboratory MG at the SGLab at the University of Zagreb Faculty of Electrical Engineering and Computing. Experimental results have shown the effectiveness of this control approach in the GCM.

Further research will be focused on the experimental validation of the proposed approach in the IM. In that regard, additional components will be included in the MG, such as battery storage or additional photovoltaic capacity.

ACKNOWLEDGMENT

This work is one of the results of the H2020 ERA Net Smart Grids+ project "microGRId Positioning - uGRIP".

REFERENCES

[UOZ11] Taha Selim Ustun, Cagil Ozansoy, and Aladin Zayegh. „Recent Developments in Microgrids and Example Cases around the World—A Review.“ en. In: *Renewable and Sustainable Energy Reviews* 15.8 (Oct. 2011), pp. 4030–4041. ISSN: 13640321. DOI: 10.1016/j.rser.2011.07.033. URL: https://linkinghub.elsevier.com/retrieve/pii/S1364032111002735 (visited on 04/01/2020).

[LP04] R.H. Lasseter and P. Paigi. „Microgrid: A Conceptual Solution.“ en. In: *2004 IEEE 35th Annual Power Electronics Specialists Conference (IEEE Cat. No.04CH37551)*. Aachen, Germany: IEEE, 2004, pp. 4285–4290. ISBN: 978-0-7803-8399-9. DOI: 10.1109/PESC.2004.1354758. URL: http://ieeexplore.ieee.org/document/1354758/ (visited on 04/01/2020).

[Hat+07] Nikos Hatziargyriou et al. „Microgrids.“ In: *IEEE Power and Energy Magazine* 5.4 (July 2007), pp. 78–94. ISSN: 1558-4216. DOI: 10.1109/MPAE.2007.376583.

[Che+13] Yen-Haw Chen et al. „Economic Analysis and Optimal Energy Management Models for Microgrid Systems: A Case Study in Taiwan.“ en. In: *Applied Energy* 103 (Mar. 2013), pp. 145–154. ISSN: 03062619. DOI: 10.1016/j.ap energy.2012.09.023. URL: https://linkinghub.elsevier.com/retrieve/pii/S0306261912006642 (visited on 04/01/2020).

[Mar+13] Mousa Marzband et al. „Experimental Validation of a Real Time Energy Management System for Microgrids in Islanded Mode Using a Local Day-Ahead Electricity Market and MINLP." en. In: *Energy Conversion and Management* 76 (Dec. 2013), pp. 314–322. ISSN: 01968904. DOI: 10.1016/j.enconman.2013.07.053. URL: https://linkinghub.elsevier.com/retrieve/pii/S019689041300424X (visited on 04/01/2020).

[ZYH10] Dinghuan Zhu, Rui Yang, and Gabriela Hug-Glanzmann. „Managing Microgrids with Intermittent Resources: A Two-Layer Multi-Step Optimal Control Approach." In: *North American Power Symposium 2010*. Sept. 2010, pp. 1–8. DOI: 10.1109/NAPS.2010.5619594.

[PRG14] Alessandra Parisio, Evangelos Rikos, and Luigi Glielmo. „A Model Predictive Control Approach to Microgrid Operation Optimization." In: *IEEE Transactions on Control Systems Technology* 22.5 (Sept. 2014), pp. 1813–1827. ISSN: 1558-0865. DOI: 10.1109/TCST.2013.2295737.

[Par+14] Alessandra Parisio et al. „Use of Model Predictive Control for Experimental Microgrid Optimization." en. In: *Applied Energy* 115 (Feb. 2014), pp. 37–46. ISSN: 03062619. DOI: 10.1016/j.apenergy.2013.10.027. URL: http://linkinghub.elsevier.com/retrieve/pii/S0306261913008477 (visited on 02/01/2018).

[XI09] Le Xie and Marija D. Ilic. „Model Predictive Economic/Environmental Dispatch of Power Systems with Intermittent Resources." In: *2009 IEEE Power Energy Society General Meeting*. July 2009, pp. 1–6. DOI: 10.1109/PES.2009.5275940.

[XZE09] Xiaohua Xia, Jiangfeng Zhang, and Ahmed Elaiw. „A Model Predictive Control Approach to Dynamic Economic Dispatch Problem." In: *2009 IEEE Bucharest PowerTech*. June 2009, pp. 1–7. DOI: 10.1109/PTC.2009.5282270.

[Qi+11] Wei Qi et al. „Supervisory Predictive Control of Standalone Wind/Solar Energy Generation Systems." In: *IEEE Transactions on Control Systems Technology* 19.1 (Jan. 2011), pp. 199–207. ISSN: 1558-0865. DOI: 10.1109/TCST.2010.2041930.

[QLC12] Wei Qi, Jinfeng Liu, and Panagiotis D. Christofides. „Supervisory Predictive Control for Long-Term Scheduling of an Integrated Wind/Solar Energy Generation and Water Desalination System.“ In: *IEEE Transactions on Control Systems Technology* 20.2 (Mar. 2012), pp. 504–512. ISSN: 1558-0865. DOI: 10.1109/TCST.2011.2119318.

[BD12] Ali Bidram and Ali Davoudi. „Hierarchical Structure of Microgrids Control System.“ In: *IEEE Transactions on Smart Grid* 3.4 (Dec. 2012), pp. 1963–1976. ISSN: 1949-3061. DOI: 10.1109/TSG.2012.2197425.

[Van+13] Tine L. Vandoorn et al. „Microgrids: Hierarchical Control and an Overview of the Control and Reserve Management Strategies.“ In: *IEEE Industrial Electronics Magazine* 7.4 (Dec. 2013), pp. 42–55. ISSN: 1941-0115. DOI: 10.1109/MIE.2013.2279306.

[Fen+17] Xianyong Feng et al. „Comparison of Hierarchical Control and Distributed Control for Microgrid.“ In: *Electric Power Components and Systems* 45.10 (June 2017). _eprint: https://doi.org/10.1080/15325008.2017.1318982, pp. 1043–1056. ISSN: 1532-5008. DOI: 10.1080/15325008.2017.1318982. URL: https://doi.org/10.1080/15325008.2017.1318982 (visited on 04/01/2020).

[Kun94] Kundur. *Power System Stability And Control*. en. The Epri Power System Engineering. India: McGraw-Hill, 1994. ISBN: 978-0-07-063515-9.

[Bev14] Hassan Bevrani. *Robust Power System Frequency Control*. Power Electronics and Power Systems. Cham: Springer International Publishing, 2014. ISBN: 978-3-319-07277-7 978-3-319-07278-4. DOI: 10.1007/978-3-319-07278-4. URL: http://link.springer.com/10.1007/978-3-319-07278-4 (visited on 09/27/2017).

[KMJ04] Niels Rode Kristensen, Henrik Madsen, and Sten Bay Jørgensen. „Parameter Estimation in Stochastic Grey-Box Models.“ en. In: *Automatica* 40.2 (Feb. 2004), pp. 225–237. ISSN: 00051098. DOI: 10.1016/j.automatica.2003.10.001. URL: https://linkinghub.elsevier.com/retrieve/pii/S000510980300298X (visited on 08/06/2019).

[PR03] Gabriele Pannocchia and James B. Rawlings. „Disturbance Models for Offset-Free Model-Predictive Control.“ In: *AIChE journal* 49.2 (2003), pp. 426–437.

[PR01] Gabriele Pannocchia and James B. Rawlings. *Robustness of MPC and Disturbance Models for Multivariable Ill-Conditioned Processes*. English. Tech. rep. 2001-02. USA: TWMCC, Texas-Wisconsin Modeling and Control Consortium, 2001.

[kon] koncar-ket. *PROZA NET*. URL: www.koncar-ket.en/control_systems/scada.

[SSS12] Steffen Schütte, Stefan Scherfke, and Michael Sonnenschein. „Mosaik-Smart Grid Simulation API." In: *Proceedings of SMARTGREENS* (2012), pp. 14–24. URL: https://mosaik.offis.de/downloads/mosaik_SimAPI_SmartGreens2012.pdf (visited on 12/31/2016).

[IRE] IRENA. *Renewable Energy Technologies: Cost Analysis Series - Hydropower*. URL: https://www.irena.org/documentdownloads/publications/re_technologies_cost_analysis-hydropower.pdf.

[Eur] Eurostat. *Electricity Prices for Household Consumers*. URL: https://ec.europa.eu/eurostat/statistics-explained/index.php/Electricity_price_statistics%5C#Electricity_prices_for_household_consumers.

11 | PAPER F

Optimal coordinated bidding of a profit–maximizing EV aggregator under uncertainty

Abstract — *An aggregator acts as a middlemen between the small customers and the system operator (SO) offering a mutually beneficial agreement to trade electric power, where each market player (system operator, aggregator and EV owner) has its own economic incentives. The EV aggregator aims to maximize its profit while trading energy and providing balancing power in wholesale markets. This paper develops a stochastic and dynamic mixed integer linear program (SD-MILP) for optimal coordinated bidding of an EV aggregator to maximize its profit from participating in competitive day-ahead and real-time markets. Under uncertain day-ahead, real-time market prices as well as fleet mobility, the proposed SD-MILP model finds optimal EV charging/discharging plans at per device level. The degradation costs of EV batteries are precisely modeled. To reflect the continuous clearing nature of the real-time market, rolling planning is applied which allows re-forecasting and re- dispatching. The proposed SD-MILP is used to derive a bidding curve of an aggregator managing 1000 EVs.*

Authors: Yelena Vardanyan, Frederik Banis, Seyyed Ali Pourmousavi Kani, Henrik Madsen

Presented by Dr. Yelena Vardanyan at the *2018 IEEE International Energy Conference (ENERGYCON)*.

Optimal coordinated bidding of a profit-maximizing EV aggregator under uncertainty

Yelena Vardanyan
DTU Compute
Email: yeva@dtu.dk

Frederik Banis
DTU Compute
Email: freba@dtu.dk

Seyyed Ali Pourmousavi Kani
Global Change Institute
Email: a.pour@uq.edu.au

Henrik Madsen
DTU Compute
Email: hmad@dtu.dk

***Abstract*—An aggregator acts as a middlemen between the small customers and the system operator (SO) offering a mutually beneficial agreement to trade electric power, where each market player (system operator, aggregator and EV owner) has its own economic incentives. The EV aggregator aims to maximize its profit while trading energy and providing balancing power in wholesale markets. This paper develops a stochastic and dynamic mixed integer linear program (SD-MILP) for optimal coordinated bidding of an EV aggregator to maximize its profit from participating in competitive day-ahead and real-time markets. Under uncertain day-ahead, real-time market prices as well as fleet mobility, the proposed SD-MILP model finds optimal EV charging/discharging plans at per device level. The degradation costs of EV batteries are precisely modeled. To reflect the continuous clearing nature of the real-time market, rolling planning is applied which allows re-forecasting and re-dispatching. The proposed SD-MILP is used to derive a bidding curve of an aggregator managing 1000 EVs.**

I. Nomenclature

A. Indices

k	index for storages, $k = 1, \dots, K$;
t	planning periods, $t = 1, \dots, T$;
s	scenarios, $s = 1, \dots, S$;
i	index for possible bid prices $i = 1, \dots, I$;

B. Parameters

ω_s	Probabilities associated with the scenarios;
$\overline{P}_k$	Max. storage rate of discharge, charge [kW];
$\underline{P}_k$	Min. storage rate of discharge, charge [kW];
$\overline{E}_k$	Max. capacity of a storage [kWh];
$\overline{\gamma}_k$	Scalar to calculate max SoC;
$\underline{\gamma}_k$	Scalar to calculate min SoC;
$\eta_k^{ch/dch}$	Charge, discharge efficiency of a storage;
$SoC^B_{k,t=0}$	Starting storage level [kWh];
$SoC^{Bend}_{k,}$	End storage level [kWh];
$\lambda_{s,t}$	Day-ahead market price scenarios [€/MWh];
$\lambda^{up/dn}_{s,t}$	Real-time market price scenarios [€/MWh];
ρ_i	Fixed bid price for day-ah. market [€/MWh];
$\rho_i^{up/dn}$	Fixed bid price for real-time market [€/MWh];
c_t	Aggregator's offer to storage owner [€];
c_k^{cap}	Capital cost of a storage [€];
μ_k	The slope of the linear approximation of the battery life as a function of the cycles;
$A_{s,k,t}$	Availability matrix indicating whether EV is available or not;
D_k	Average hourly driving distance of an EV [km];
η_k^{dr}	driving efficiency of an EV;
Γ_1, Γ_2	Sufficiently big constant;

C. Variables

$p^{DAch}_{s,k,t}$	Charging dispatch level for *k* storage in day-ahead market [kWh];
$p^{DAdch}_{s,k,t}$	Discharging dispatch level for *k* storage in day-ahead market [kWh];
$p^{Bch}_{s,k,t}$	Charging dispatch level for *k* storage in real-time market [kWh];
$p^{Bdch}_{s,k,t}$	Discharging dispatch level for *k* storage in real-time market [kWh];
$\mathbb{P}^{DAch}_{s,t}$	Energy as day-ahead buying position [kWh];
$\mathbb{P}^{DAdch}_{s,t}$	Energy as day-ahead selling position [kWh];
$\mathbb{P}^{Bch}_{s,t}$	Down-regulating volume in real-time market [kWh];
$\mathbb{P}^{Bdch}_{s,t}$	Up-regulating volume in real-time market [kWh];
$C\mathbb{P}^{DAch}_{s,t}$	Total cost of charging in day-ahead market [€];
$C\mathbb{P}^{DAdch}_{s,t}$	Total cost of discharging in day-ahead market [€];
$C\mathbb{P}^{Bch}_{s,t}$	Total cost of charging in real-time market [€];
$C\mathbb{P}^{Bdch}_{s,t}$	Total cost of discharging in real-time market [€];
$x^{DAch}_{i,t}$	Charging bid volume in day-ahead market [kWh];
$x^{DAdch}_{i,t}$	Discharging bid volume in day-ahead [kWh];
$x^{Bch}_{i,t}$	Charging bid volume in real-time market [kWh];
$x^{Bdch}_{i,t}$	Discharging bid volume in real-time market [kWh];
$SoC^B_{s,k,t}$	Storage level at the end of time step *t* [kWh];
$\hat{\alpha}_{s,t,i}$	binary variable;
$\hat{\alpha}^{up/dn}_{s,t,i}$	binary variable;

II. INTRODUCTION

According to [1] worldwide EV penetration is assumed to increase up to 20 million by 2020. Therefore, there is a huge potential using EV batteries to assist the electric power grid [2]. However, the single EV can not enter to electricity market to trade their energy for the following two reasons: 1) the available trading power of individual EV is below the required threshold to participate in electricity markets [3], and 2) The participation of individual EVs will increase the number of market actors which will increase the difficulty of managing electricity markets. Therefore a new market entity, an aggregator, will be required in order to enable smooth cooperation between EV owners and SO.

The main target of the aggregator, as a market entity, is to buy the electric power at the lowest possible cost to satisfy driving needs of its fleet of EVs [2] and [4]. Meanwhile, the economic incentive of the aggregator is to increase its revenue by performing energy arbitrage [5], [6], [7] and [8]. With the vehicle-to-grid (V2G) capability of EVs, the idea of using EVs as a electric power source to provide balancing power attracted many researchers in the field. Having a flexible power source, EV aggregator can provide reserve power and increase its profit. The possibilities of using EVs as a resource for real-time balancing and system reserves by providing ancillary services are studied in [9], [10], [11], [12] and [13].

The EV interaction with the grid can be categorized as unidirectional and bidirectional. The problem of bidding regulation and spinning reserves for unidirectional EV interaction is explored in [10]. However, the bidirectional mode offers higher flexibility and profits. Bidirectional EV interaction with the grid is modeled in [11] and [13]. However, using the batteries as storage devices for grid purposes reduces their lifetime [14] and [13]. Thus, EV owners must be compensated for the lost utility of their batteries due to degradation when providing services.

Taking into consideration the uncertain nature of market conditions and fleet characteristics, stochastic approaches fit better to the aggregators optimal bidding problem. In [9] and [12] the authors develop the optimal bidding strategy of an EV aggregator participating in day-ahead energy and regulation markets using stochastic optimization.

This paper develops an optimal bidding strategy model for an EV aggregator who participates in the day-ahead and real-time markets considering the uncertain nature of market conditions and fleet characteristics. Unlike previous formulations [9], [12] and [13], this formulation accounts dynamically clearing nature of the real-time market while deriving optimal bids to day-ahead and real-time markets. In order to benefit from the released information over time, the rolling planing is employed to update the scenario tree of real-time prices within the planning day. In addition the developed model enables the aggregator to manage both stationary storages and EVs. The main contributions of the paper are:

- The development of a stochastic and dynamic mixed-integer linear program (SD-MILP) for an aggregator who manages big number of stationary storages and EVs to obtain the optimal coordinated bidding in two-settlement markets.
- The derivation of optimal coordinated charge (discharge) bids for day-ahead and real-time markets with moderate computation time when applying scenario-reduction techniques.
- The inclusion of uncertainty in both market prices as well as EV mobility parameters.

The paper is structured as follows. Section III describes the mathematical model formulation of an aggregator. Section IV provides case-study results and Section V provides the conclusion.

III. MATHEMATICAL PROBLEM FORMULATION

The mathematical formulation of an EV aggregator interacting with day-ahead and real-time markets is stated below.

A. Stochastic optimal strategy of an EV Aggregator

The stochastic optimization problem stated in (1) aims at the maximization of scenario-weighted expected profits from day-ahead energy trading $\Pi^{DA}_{s,t}$ and real-time power exchange $\Pi^{B}_{s,t}$.

$$\text{Maximize}_{\Phi}\ \mathbb{E}[\Pi^{Tot}] = \sum_{s} \omega_s (\sum_{t=1}^{T} (\Pi^{DA}_{s,t} + \Pi^{B}_{s,t})) \tag{1}$$

where $\Pi^{DA}_{s,t}$ and $\Pi^{B}_{s,t}$ are expressed as in (2) and (3) correspondingly.

$$\Pi^{DA}_{s,t} = \lambda_{s,t}\mathbb{P}^{DAdch}_{s,t} - C\mathbb{P}^{DAdch}_{s,t} - \lambda_{s,t}\mathbb{P}^{DAch}_{s,t} + C\mathbb{P}^{DAch}_{s,t} \tag{2}$$

$$\Pi^{B}_{s,t} = \lambda^{up}_{s,t}\mathbb{P}^{Bdch}_{s,t} - C\mathbb{P}^{Bdch}_{s,t} - \lambda^{dn}_{s,t}\mathbb{P}^{Bch}_{s,t} + C\mathbb{P}^{Bch}_{s,t} \tag{3}$$

The different components in (2) and (3) break down as follows:

$$\mathbb{P}^{DAdch/ch}_{s,t} = \sum_{k} p^{DAdch/ch}_{s,k,t}, \quad \mathbb{P}^{Bdch/ch}_{s,t} = \sum_{k} p^{Bdch/ch}_{s,k,t} \tag{4}$$

$$C\mathbb{P}^{DAdch}_{s,t} = \sum_{k} (c_t \frac{p^{DAdch}_{s,k,t}}{\eta^{dch}_{k}} + \left|\frac{\mu_k}{100}\right| \frac{c^{cap}_{k}}{\overline{E}_k} p^{DAdch}_{s,k,t}) \tag{5}$$

$$C\mathbb{P}^{DAch}_{s,t} = \sum_{k} (c_t p^{DAch}_{s,k,t} \eta^{dch}_{k} + \left|\frac{\mu_k}{100}\right| \frac{c^{cap}_{k}}{\overline{E}_k} p^{DAch}_{s,k,t}) \tag{6}$$

$$C\mathbb{P}^{Bdch}_{s,t} = \sum_{k} (c_t \frac{p^{Bdch}_{s,k,t}}{\eta^{dch}_{k}} + \left|\frac{\mu_k}{100}\right| \frac{c^{cap}_{k}}{\overline{E}_k} p^{Bdch}_{s,k,t}) \tag{7}$$

$$C\mathbb{P}^{Bch}_{s,t} = \sum_{k} (c_t p^{Bch}_{s,k,t} \eta^{dch}_{k} + \left|\frac{\mu_k}{100}\right| \frac{c^{cap}_{k}}{\overline{E}_k} p^{Bch}_{s,k,t}) \tag{8}$$

It is obvious that the equations (2) and (3) express the aggregator's revenue minus cost while providing optimal discharge/charge bids in day-ahead and real-time markets respectively. The constraint (4) provides the aggregated charge/discharge bids in both markets. The aggregator's cost in both markets while providing charging/discharging optimal bids is set out in constraints (5)-(8), where the first term is the aggregator's payment to the EV owner and the second term is the battery degradation cost.

To derive the step-function bidding curve for hour t of the day-ahead market, we first fix the parameters ρ_1, ρ_2, ..., ρ_I at I arbitrary prices. The unknown variables x_1, x_2, ..., x_I of the step function are derived as follows:

$$\mathbb{P}_{s,t}^{DAch/DAdch} = \sum_{l=0}^{i} x_{i-l,t}^{DAch/DAdch} \quad if \quad \rho_i \leq \lambda_{s,t} \leq \rho_{i+1} \tag{9}$$

Using binary variable $\hat{\alpha}_{s,t,i}^{ch/dch}$ and a large enough constant Γ_1, (9) can be reformulated as constraints (10)-(12):

$$\rho_i - \Gamma_1(1-\hat{\alpha}_{s,t,i}^{ch/dch}) \leq \lambda_{s,t} \leq \rho_{i+1} + \Gamma_1(1-\hat{\alpha}_{s,t,i}^{ch/dch}) \tag{10}$$

$$\sum_{l=0}^{i} x_{i-l,t}^{DAch/DAdch} - \Gamma_1(1-\hat{\alpha}_{s,t,i}^{ch/dch}) \leq \mathbb{P}_{s,t}^{DAch/DAdch}$$
$$\leq \sum_{l=0}^{i} x_{i-l,t}^{DAch/DAdch} + \Gamma_1(1-\hat{\alpha}_{s,t,i}^{ch/dch}) \tag{11}$$

$$\sum_{i=1}^{I} \hat{\alpha}_{s,t,i}^{ch/dch} = 1 \tag{12}$$

The up- and down-regulating bids to real-time market are expressed in (13).

$$\mathbb{P}_{s,t}^{Bch/Bdch} = \sum_{l=0}^{i} x_{i-l,t}^{Bch/Bdch}$$
$$if \quad \rho_i^{up/down} \leq \lambda_{s,t}^{up/dn} \leq \rho_{i+1}^{up/down} \tag{13}$$

In the similar way, using binary variables $\hat{\alpha}_{s,t,i}^{dn/up}$ and a large enough constant Γ_2 (13) can be reformulated as:

$$\rho_i^{dn/up} - \Gamma_2(1-\hat{\alpha}_{s,t,i}^{dn/up}) \leq \lambda_{s,t}^{dn/up} \leq \rho_{i+1}^{dn/up}$$
$$+ \Gamma_2(1-\hat{\alpha}_{s,t,i}^{dn/up}) \tag{14}$$

$$\sum_{l=0}^{i} x_{i-l,t}^{Bch/Bdch} - \Gamma_2(1-\hat{\alpha}_{s,t,i}^{dn/up}) \leq \mathbb{P}_{s,t}^{Bch/Bdch}$$
$$\leq \sum_{l=0}^{i} x_{i-l,t}^{Bch/Bdch} + \Gamma_2(1-\hat{\alpha}_{s,t,i}^{dn/up}) \tag{15}$$

$$\sum_{i=1}^{I} \hat{\alpha}_{s,t,i}^{dn/up} = 1 \tag{16}$$

Constants Γ_1 and Γ_2 must be selected carefully to avoid introducing extra bounds or ill-conditioning in the optimization problem. The state of charge balance constraint can be modeled as:

$$SoC_{s,k,t}^{B} = SoC_{s,k,t-1}^{B} + [p_{k,t}^{ch}\eta_k^{ch} - \frac{p_{k,t}^{dch}}{\eta_k^{dch}} + p_{s,k,t}^{Bch}\eta_k^{ch}$$
$$- \frac{p_{s,k,t}^{Bdch}}{\eta_k^{dch}}]A_{s,k,t} - D_k\eta_k^{dr}(1-A_{s,k,t}) \tag{17}$$

Constraint (17) states that for each hour the new content of the storage is equal to its old content plus energy inflow minus energy outflow. Please note that, the equation (17) allows to model both stationary and mobile (EV) storages. For stationary storages $A_{s,k,t}$ availability matrix is always 1; hence the last term which is energy spend on driving purposes vanishes. For EVs the availability matrix is either 0 or 1 depending on weather the EV is available or on the trip. The storage level is bounded by its minimum and maximum levels (18).

$$\underline{\gamma}_k^{min}\overline{E}_k \leq SoC_{s,k,t}^{B} \leq \overline{\gamma}_k\overline{E}_k \tag{18}$$

The constraints (19) prevents discharging/charging in the periods of unavailability. Finally the constraint (20) states the end SoC condition.

$$A_{s,k,t}\underline{P}_k \leq p_{s,k,t}^{DAdch} - p_{s,k,t}^{DAch} + p_{s,k,t}^{Bdch} - p_{s,k,t}^{Bch} \leq A_{s,k,t}\overline{P}_k \tag{19}$$

$$SoC_{s,k,T}^{B} \geq SoC_k^{Bend} \tag{20}$$

The day-ahead market is cleared at noon the day before delivery day while the real-time market is continuous, hourly market. This means the EV aggregator has new price information realized after the day-ahead market clearing and before the real-time market closure. In order to benefit from the released information over time, the scenario tree of real-time prices can be updated within the planning day using the rolling planning. Let $\Omega_{[t,T]}$ be the scenario tree predicted for hours t to T using the historical prices up to hour t. In the rolling planning, $\Omega_{[t,T]}$ is dynamically updated by real-time prices revealed until hour t. The ideal case would be to update the $\Omega_{[t,T]}$ on the hourly bases. However, the solution time to solve the stochastic model dynamically increases exponentially. Thus, in order to keep the model computationally tractable, $\Omega_{[t,T]}$ is updated every few hours which is called 'iteration'. For each iteration, new scenario tree is used which contains the updated forecasts for real-time market prices.

The stochastic and dynamic optimal bidding strategy for deriving the coordinated bidding curves in day-ahead and real-time markets follows as:

$$\text{Maximize}_{\Phi} \quad \sum_{s=1}^{|\Omega_{[t,T]}|} \omega_s(\sum_{t=1}^{T}(\Pi_{s,t}^{DA} + \Pi_{s,t}^{B})) \tag{21}$$

subject to :

$$(2),(3),(4),(5)-(8),(10)-(12),(14)-(16),(17)-(20) \tag{22}$$

IV. CASE STUDY

In order to study the applicability of the developed SD-MILP optimal bidding strategy both charging and discharging modes are studied. The developed approach is applied to derive a bidding discharge/charge curve of an aggregator managing a fleet of 1000 EVs.

A. data input

1) Market data acquisition: The historical price data, for both day-ahead and real-time markets, are taken from the Nordic electricity market website, from March 10, 2012 to March 10, 2013 [15].

2) Market price scenario generation and reduction: The modeling and forecasting of electricity prices are very challenging due to its complex structure. Its stochastic behavior is typically mean-reverting and spiky with high volatility [16]. The existing dynamics between day-ahead and real-time markets make the price forecasting even more complicated. Substantial amount of work has been done on modeling and forecasting of day-ahead market prices [17]. However, the existing references on real-time price modeling and forecasting is very limited [18], [19] and [20]. This section develops the Markov-based HW model for modeling and predicting the day-ahead and real-time prices. The proposed model has the following steps.

a) Step 1: Estimate the parameters of the HW model: Reference [21] presents the HW model for a time series with unique seasonal pattern. The HW model is applied to forecast the electricity demand and imbalance cost in [22] and [23]. The standard HW model for a time series of prices $\{\lambda_t\}_{t=1}^{T}$ is as follows [24]:

$$\gamma_t = \alpha(\lambda_t / I_{t-\Xi}) + (1-\alpha)(\gamma_{t-1} + T_{t-1}) \tag{23}$$

$$T_t = \beta(\gamma_t - \gamma_{t-1}) + (1-\beta)T_{t-1} \tag{24}$$

$$I_t = \sigma(\lambda_t / \gamma_t) + (1-\sigma)I_{t-\Xi} \tag{25}$$

$$\tilde{p}_t(h) = (\gamma_t + hT_t)I_{t-\Xi+h} \tag{26}$$

where γ_t is the exponential component, T_t is the trend and I_t is the seasonal component with period Ξ. α, β, and σ are smoothing parameters which belong to the interval (0,1]. $\tilde{p}_t(h)$ is the h-hour ahead forecast.

b) Step 2: Estimate the transition probability matrix of Markov model for different states of real-time market prices: The magnitude of day-ahead and real-time electricity prices can be estimated using the HW technique. However, the real-time market prices have discrete mode meaning that in addition to price magnitudes, the price states need to be forecasted. In each bidding interval *t*, the real-time market price may have one of the following four states: (1) No up- or down-regulating price exists, (2) Only down-regulating price exists, (3) Only up-regulating price exists, and (4) Both up- and down-regulating prices exist. The state of real-time market prices can be modeled using a four-state Markov process.

The probabilities of the transition matrix for real-time Markov model are estimated using historical real-time market prices. Based on the real-time prices, for each bidding period *t*, the binary pair (b_t^{up}, b_t^{dn}) is defined as follows.

$$b_t^{up(dn)} = \begin{cases} 1 & \text{if an up-(down-regulating) price exists} \\ 0 & \text{Otherwise} \end{cases} \tag{27}$$

We define o_t as the parameter which shows the state of the real-time price at time t.

$$o_t^{Real-time} = \begin{cases} 1 & \text{if} \quad (b_t^{up}, b_t^{dn}) = (0,0) \\ 2 & \text{if} \quad (b_t^{up}, b_t^{dn}) = (0,1) \\ 3 & \text{if} \quad (b_t^{up}, b_t^{dn}) = (1,0) \\ 4 & \text{if} \quad (b_t^{up}, b_t^{dn}) = (1,1) \end{cases} \quad t = 1, 2...T \tag{28}$$

Let $O_{ij} = \{o_t^{Real-time} : o_t^{Real-time} = j, o_{t-1}^{Real-time} = i, t = 1, ..., T\}$, then element (i,j) of transition probability matrix pr_{ij} for $i, j = 1, ..., 4$ can be calculated as:

$$pr_{ij} = \frac{Card(O_{ij})}{\sum_{n=1}^{4} Card(O_{i,n})} \quad i, j = 1, ...4 \tag{29}$$

c) Step 3: The day-ahead and real-time price scenarios: The prediction technique explained in step 1 is applied to forecast the day-ahead market price magnitude. Then, using the expected values and the variances of day-ahead market prices and assuming normal distribution the day-ahead market price scenarios are generated. However, both price magnitude and direction have to be forecasted for real-time market. To predict real-time market price magnitude the real-time market hystorical prices are collected and processed. Then the forecasting tool in step 1 is applied. The Markov model provided in step 2 is employed to capture the price direction for the real-time market. Again, the real-time market price scenarios are generated using the predicted price magnitude, direction and assuming normal distribution. For day-ahead and real-time markets various price scenarios are generated for each planning hour. The backward reduction algorithm is used to reduce the number of price scenarios. This is done in a way that the statistical information in prices is maintained in the best possible way [25]. Using the forecasted prices, 1000 price scenarios with equal probabilities are generated and they are reduced to 10 price scenarios. These preserved price scenarios will be used for calculating the optimal bidding curve of the EV aggregator.

3) Availability simulation: A Monte Carlo simulation tool is used to produce mobility scenarios for imitating the uncertain driving behavior. Then, discrete cumulative distribution functions (cdf) is employed, which is derived considering i) the probability of travel on a specific day, ii) the probability that a trip starts in a specific hour, and iii) the probability that a trip covers a certain distance. It is assumed mutually independent distributions [12]. Finally, 10 equally probable mobility scenarios are produced and integrated with the 10 price scenarios prepared in Step 3.

4) General parameters: The EV driving patterns are according to the reference [26]. The maximum battery capacity is taken 50 KWh [26], while the battery level is bounded by its minimum of 20 % and maximum of 100 % of the maximum capacity [27]. Both the charging and discharging power rate is taken 6 kW. Finally, the charging and discharging efficiency is set to 90 $\%$ and 93 $\%$ respectively [28]. For every scenario the target state of charge level is equal to the initial state of charge level and is taken 60 $\%$ of the maximum capacity. The capital cost for EV battery is set to 200 $€/MWh$ and the slope μ_k=-[0.0013] according to [13].

B. Simulations results

A three-level step function with ρ_1=15$€/MWh$, ρ_2=50$€/MWh$, and ρ_3 =75$€/MWh$ is considered for bidding curves. The proposed Markov-based HW model, scenario backward reduction algorithm and the Monte Carlo simulation tool to produce mobility patterns are coded in Matlab. The SD-MILP is coded in GAMS platform and solved using Cplex solver. All optimization problems are solved with optimality gap of 0%. The whole simulation is run on a computer with 2.66 GHz processor and 4 GB RAM. The objective function values together with the computation time for a fleet of 1000 EVs and all iterations are stated in Table I. According to Table I the computation time is highest for the first iteration. Moreover, the computation time for the second iteration is lowest, then it is slightly increasing in the third and the fourth iterations. Possible answer to this is the application of rolling planning in the SD-MILP optimization model. After the first iteration all variables for the day-ahead market is fixed to their optimal values. In addition, for the real-time market and for every iteration the information related to previous hours is kept and the information related to remaining hours is updated. The resulting optimization problem becomes tighter, therefore the solver takes longer time to solve.

TABLE I: Model solution report for a fleet of 1000 EVs, It: Itertaion

	It. 1	It. 2	It. 3	It. 4
$\mathbb{E}[\Pi^{Tot}]$(€)	200.35	168.8	167.35	130.24
Comp. time (second)	28.64	15.2	18.3	19

The optimal coordinated bids of the hydropower producer in two markets is set out in Table II. The bid volumes to day-ahead market remain the same for all iterations (the first and the second columns in Table II). In contrast Table II shows that real-time bid volumes (up/down regulation) are changing when time evolves and new price information reveals over time. According to Table II, the EV aggregator is actively participating in day-ahead market offering discharging bids and in real-time market providing down-regulation bids.

The day-ahead and real-time bidding curves for hours 2 and 3 are shown in Figures 1 and 2. According to the Figure 1 the model offers to enter directly to real-time market providing up- and down-regulating bids. However, Figure 2 shows that, for the hour 3 the model yields an incentive to offer discharging bid to day-ahead market and charging bid to real-time market.

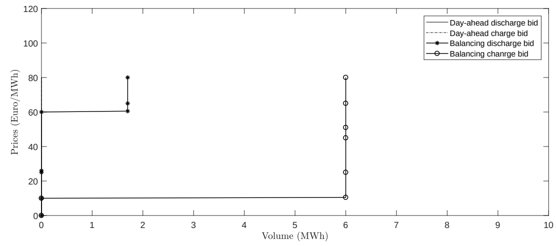

Fig. 1: The bidding curves for hour 2.

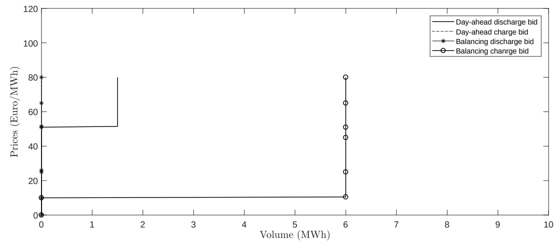

Fig. 2: The bidding curves for hour 3.

V. Conclusion

The aggregators are required business entities, who enable smooth cooperation of large fleets of EVs and the SO while maximizing their own profit. This paper proposes a SD-MILP for deriving optimal coordinated bidding in day-ahead and real-time markets for a profit-maximizing EV aggregator. The prices in these market places are modeled and predicted using a proposed Markov-based HW model. The HW model predicts the magnitude of day-ahead and real-time market prices. The direction of real-time market prices are predicted using Markov model. The scenario tree is also updated with arrival of new information for real-time market prices. This has been done by implementing the rolling planning in the SD-MILP. The developed procedure is tested using a fleet of 1000 EVs. Results show that EVs can provide a new collection of services to the power system. However, the degradation of the batteries should be accounted precisely in order to motivate the EVs' participation in day-ahead and real-time markets. The current paper can be extended by modeling also intra-day market.

Acknowledgements

This work has been curried out in the context of the Smart-Net project, funded by the European Commission under the Horizon 2020 LCE-6-2015 Research and Innovation Action on Transmission Grids and Wholesale Markets (http://smartnet-project.eu).

References

[1] "Global EV outlook: Understanding the electric vehicle landscape to 2020," International Energy Agency, Tech. Rep., 2013. [Online]. Available: http://www.iea.org/publications/globalevoutlook_2013.pdf

TABLE II: The optimal coordinated bidding in day-ahead and real-time markets for four iterations of rolling planning

	Day-ahead market		Up-regulation (discharge)				Down-regulation (charge)			
	discharge	charge	real-time market				real-time market			
Hours	All It.	All It.	It. 1	It. 2	It. 3	It. 4	It. 1	It. 2	It.3	It. 4
1	0	0	0	0	0	0	6	6	6	6
2	0	0	1.7	1.7	1.7	1.7	6	6	6	6
3	1.5	0	0	0	0	0	6	6	6	6
4	6	0	0	0	0	0	6	6	6	6
5	0	0	0	0	0	0	6	6	6	6
6	0	0	0	0	0	0	6	6	6	6
7	0	0	0	0	0	0	0	0	0	0
8	0	0	0	0	0	0	0	0	0	0
9	0	0	0	0	0	0	0	0	0	0
10	1.5	0	0	0	0	0	6	6	6	6
11	0	0	0	0	0	0	6	6	6	6
12	0	0	6	0	0	0	6	6	6	6
13	0	0	0	0	0	0	6	6	2.7	2.7
14	6	0	6	0	0	0	6	6	6	6
15	6	0	0	0	0	0	6	6	6	6
16	0	0	0	0	0	0	6	6	6	6
17	0	0	0	0	0	0	0	0	0	0
18	0	0	0	0	0	0	0	0	0	0
19	0	0	0	0	0	0	6	6	6	6
20	0.5	0	0	0	0	0	6	6	6	6
21	0	0	0	0	0	0	6	6	6	6
22	0	0	6	6	6	0.25	6	6	6	6
23	6	0	0	0	0	0	6	6	6	6
24	6	0	0	0	0	0	6	6	6	6

[2] M. A. Ortega-Vazquez, F. Bouffard, and V. Silva, "Electric vehicle aggregator/system operator coordination for charging scheduling and services procurement," *IEEE Transactions on Power Systems*, vol. 28, no. 2, pp. 1806–1815, Nov. 2013.

[3] "Demand response-PJM," Tech. Rep., 2013. [Online]. Available: http://www.pjm.com//media/markets-ops/dsr/end-use-customer-fact-sheet.ashx

[4] J. A. P. Lopes, F. J. Soares, and P. M. R. Almeida, "Integration of electric vehicles in the electric power system," *Proc. IEEE*, vol. 99, no. 1, pp. 168–183, Jan 2011.

[5] R. J. Bessa, M. A. Matos, F. J. Soares, and J. A. P. Lopes, "Optimized bidding of a EV aggregation agent in the electricity market," *IEEE Trans. Smart Grid*, vol. 3, no. 1, p. 443452, March 2012.

[6] M. Sarker, M. Ortega-Vazquez, and D. Kirschen, "Optimal coordination and scheduling of demand response via monetary incentives," *IEEE Trans. Smart Grid*, vol. 6, no. 3, p. 13411352, May 2015.

[7] R. J. Bessa and M. A. Matos, "Global against divided optimization for the participation of an ev aggregator in the day-ahead electricity market. part i: Theory," *Elect. Power Syst. Res*, vol. 95, pp. 309–318, Feb. 2013.

[8] ——, "Global against divided optimization for the participation of an ev aggregator in the day-ahead electricity market. part ii: Numerical analysis," *Elect. Power Syst. Res*, vol. 95, p. 319329, Feb 2013.

[9] S. I. Vagropoulos and A. G. Bakirtzis, "Optimal bidding strategy for electric vehicle aggregators in electricity markets," *IEEE Transactions on Power Systems*, vol. 28, no. 4, pp. 4031–4041, Nov. 2013.

[10] E. Sortomme and M. A. El-Sharkawi, "Optimal combined bidding of vehicle-to-grid ancillary services," *IEEE Trans. Smart Grid*, vol. 3, no. 1, pp. 70–79, March 2012.

[11] ——, "Optimal scheduling of vehicle-to-grid energy and ancillary services," *IEEE Trans. Smart Grid*, vol. 3, no. 1, pp. 351–359, March 2012.

[12] I. Momber, A. Siddiqui, T. G. San Román, and L. Söder, L., "Risk averse scheduling by a pev aggregator under uncertainty," *IEEE Transactions on Power Systems*, vol. 30, no. 2, pp. 882–891, March 2015.

[13] M. R. Sarker, Y. Dvorkin, and M. A. Ortega-Vazquez, "Optimal participation of an electric vehicle aggregator in day-ahead energy and reserve markets," *IEEE Transactions on Power Systems*, vol. 31, no. 5, pp. 3506–3515, Nov. 2016.

[14] M. A. Ortega-Vazquez, "optimal scheduling of electric vehicle charging and vehicle-to-grid services at household level including battery degradation and price uncertainty," *IET Gener., Transm., Distrib.*, vol. 8, no. 6, pp. 1007–1016, Jan. 2014.

[15] Nord Pool database http://www.nordpoolspot.com/.

[16] S. Fiorenzani, *Quantitative methods for electricity trading and risk management*. Palgrave macmillan, 2006.

[17] K. S. Aggarwal, M. Saini, and A. Kumar, "Electricity price forecasting in deregulated markets: A review and evaluation," *Electrical Power and Energy Systems*, vol. 31, no. 1, pp. 13–22, January 2009.

[18] K. Skytte, "The regulating power market on the Nordic power exchange Nord Pool: an econometric analysis," *Energy Economics*, vol. 21, 1999.

[19] M. Olsson and L. Söder, "Modeling real-time balancing power market prices using combined SARIMA and Markov processes," *IEEE Transactions on Power Systems*, vol. 23, no. 2, pp. 443–450, April 2008.

[20] S. Jaehnert, H. Farahmand, and G. L. Doorman, "Modelling of Prices Using the Volume in the Norwegian Regulating Power Market," in *IEEE Power Tech Conference*, 2009.

[21] P. Winters, "Forecasting sales by exponentially weighted moving averages," *Management Science*, vol. 6, no. 3, pp. 324–342, April 1960.

[22] V. Lepojevic and M. Andelkovic-Pesic, "Forecasting electricity consumption by using holt-winters and seasonal regression models," *Economics and Organization*, vol. 8, no. 4, pp. 421–431, 2011.

[23] T. Jonsson, P. Pinson, A. H. Nielsen, and H. Medsen, "Exponential smoothing approaches for prediction in real-time markets," *Energies*, vol. 7, no. 6, pp. 3710–3732, June 2014.

[24] J. W. Taylor, "Short-term electricity demand forecasting using double seasonal exponential smoothing." *Journal of the Operations Research Society*, vol. 54, no. 8, pp. 799–805, August 2003.

[25] N. Gröwe-Kuska, H. Heitsch, and W. Römisch, "Scenario reduction and scenario tree construction for power management problems," in *Proc. IEEE Bologna Power Tech*, vol. 3, 2003.

[26] O. Sundström and C. Binding, "Flexible charging optimization for electric vehicles considering distribution grid constraints," *IEEE Trans. Smart Grid*, vol. 3, no. 1, pp. 26–37, March 2012.

[27] A. Pesaran and et. al., "Battery requirements for plug-in hybrid electric vehicles - analysis and rationale," in *23rd International Electric Vehicle Symposium*, Dec. 2007.

[28] J. Van Roy and et. al., "An availability analysis and energy consumption model for a flemish fleet of electric vehicles," in *EEVC European Electric Vehicle Congress*, Oct. 2011.

12 PAPER G

Reactive Power Control in Microgrids using Target Adjusted Model Predictive Control

Abstract — *We examine target adjusted Optimal Controllers (OCs) and target adjusted Model Predictive Controllers (MPCs) and compare them to classical OC and MPC formulations for coordinated perturbed voltage regulation in microgrids (MGs). The voltage regulation problem considered hereby is a tracking problem of the perturbed voltage regulation problem.*

Authors: Frederik Banis, Kamal Jafarian Dehkordi, Henrik Madsen, Niels Kjølstad Poulsen, Daniela Guericke

Technical report.

12.1 INTRODUCTION

Voltage control is a fundamental control problem in power systems [Kun94]. In contrast to frequency control or frequency stabilization, voltage control is a control problem to be solved locally with respect to the controlled variables. Nodal reactive power injections affect the bus voltages, subsequent bus voltage levels hereby expose sensitivity to control decisions at all nodes within relevant electrical distance. Consequently, the system is potentially highly dynamic and nonlinear [HP14].

We can approach reactive power control at different levels of aggregation, sampling resolution and associated feasible problem size [LD14].

Therefore, this problem is historically addressed by means of a control hierarchy [Kun94; Bev14; Sch78]. Solutions to complex and computationally demanding optimization problems are then used as input to the computationally lighter control problems at lower levels in the hierarchy. This results from the aspect that problem complexity in the planning problem defining the operating point and operating region of the system is considerably higher compared to real–time control problems. Control problems are tailored to the requirements at given level in the hierarchy [MC].

Alternatively, distributed control approaches enable for relative improvements in terms of privacy, computational load and as consequence, increased problem size that can be addressed [Mol+17; Sch+16].

At the highest level, an optimal power flow (OPF) problem is to be solved in order to account for fundamental system requirements [Fau+18] .

For the real–time (RT) control problem at aggregated system level, optimal control (OC) and model predictive control (MPC) techniques are commonly proposed [VC13]. In the case of MPC, this is due to its well–known capability to account for system constraints within the optimization step in combination with its large research base.

For retaining a light system model, linearization techniques are proposed that provide approximations to the power flow equations which can be used in MPC based strategies [MMD18]. Methods for examination of the sensitivity within the system are available [Lek+18].

The control performance of MPC relies on a good model of the system. For the aggregated voltage control problem, retrieval of such model can be hard to accomplish. Extremum Seeking Control techniques pose the problem such that convergence to stable system operating points can be guaranteed even with little knowledge of the underlying system, see [Joh+18] as example. Once sufficient data of the system has been collected, sparse regression techniques can be applied in order to retrieve parsimonious models that avoid over–fitting, see [BPK16].

Adaptive control approaches allow for enhanced robustness with respect to disturbance and model uncertainties [Ngu17]. Dong. et. al. [Don18] discuss aspects of the setup of a control structure for load frequency control (LFC) and voltage stabilization using adaptive disturbance rejection controller (ADRC) Control approaches. ADRC is claimed to be robust with respect to disturbances and model uncertainties. Other approaches to the RT control problem include adaptive learning strategies. [VBV06] propose usage of such learning technique based on available historical data in order to infer optimized decisions.

In this paper we compare alternative OC and MPC formulations for the aggregated voltage control problem. These target adjusted formulations have been previously proposed for the LFC problem [Ban+19].

We compare these controller variations the integrated squared errors (ISEs) of the mean voltage deviation magnitude. Furthermore we examine their robustness towards a range of selected uncertainties.

The paper is organized as follows. In Section 12.2.1 the considered operational objective is stated, it follows the description of used models in 12.2.2 and formulation of the state observer in Section 12.2.3. Considered OC approaches are outlined in 12.2.4, MPC approaches in 12.2.6. Numerical results are presented in 12.3. Results are discussed in 12.4 and the paper closes with the conclusions 12.5.

12.2 METHODOLOGY

We aim to design RT OCs and MPCs for the aggregated voltage control problem. This control layer should therefore track references provided by a higher layer controller. Such layer typically solves the alternating current optimal power flow (AC-OPF) problem. The RT layer then provides modified control decisions provided to the lower level controllers. It can be therefore denoted as coordinated RT control layer, leveraging the overall system for the rejection of disturbances.

Consider the nomenclature stated in Table 12.1 and acronyms in Table 12.2.

12.2.1 Operational Objective and Performance Metric

We can formulate the control objective as to

- maintain voltages close to their references
- maintain the average voltage excursion from the reference value close to zero

The former objective is relevant as this aggregated control layer should operate with respect to operating points provided by a higher layer optimization routine. Such routine solves, for example, the AC-OPF problem. The latter objective is relevant as we aim to achieve power sharing while maintaining the first objective. This entails that we aim to reject disturbances and compensate uncertainty. Furthermore, we may aim for higher accuracy at certain nodes in the grid. The reduced degrees of freedom at such node are then to be compensated by higher control effort at other nodes.

The mean integrated squared error (ISE) is chosen here as evaluation metric for the stated objective. It can be formulated as:

$$\mathrm{ISE} = \int_k^j \left(\frac{y - \bar{y}}{n_y}\right)^2 \tag{12.1}$$

Notice that a higher optimization layer defines $\bar{y}$, the desired voltage magnitude at all nodes within the control zone.

12.2.2 Models

We consider an aggregated dynamical multiple–input multiple–output (MIMO) system where the inputs are reactive power injections and the outputs are bus voltage levels. The system may be partly based on first–principles, partly based on secondary–principles. First principles entails knowledge of the system based on physical insights. Secondary principles refer to data–driven modeling techniques, see for example [Nel01; Lju99].

Table 12.1: Nomenclature. </> denotes not specified units.

Symbol	Description	Unit
Variables		
$u^\star$	Optimal input sequence (Control variables)	pu
$\bar{u}$	Input reference trajectory	pu
x	System state	/
$\hat{x}$	One–step prediction of x	/
$\underline{x}$	State target	/
$\underline{u}$	Control target	/
$\hat{d}$	Disturbance estimate	pu
$\hat{d}_r$	Residual disturbance estimate	pu
$\hat{d}_{r,e}$	Sum of residual disturbance estimate and output residual ϵ_y	/
y	Voltage deviation (Controlled variable)	pu
$\hat{y}$	One–step prediction of y	pu
y_m	Grid voltage measurement	pu
ϵ_y	Integrated output error	pu
$\epsilon_A, \epsilon_B, \epsilon_{B_d}$	Multiplicative model–plant errors w.r.t. corresponding model parameters	/
$\underline{p}$	System equilibrium	/
w	State error: Wiener process	/
v	Measurement error: White noise process	pu
θ	Model parameter vector	/
σ, h	Nonlinear model functions	/
ω	Standard Wiener process	/
T_s	Controller sampling time	s
N	Prediction horizon	/
$L_x,\ L_d$	Kalman gain w.r.t. states and w.r.t. disturbance	/
$A,\ B,\ B_d,\ G,\ E,\ C, D$	State Space System matrices	/
Φ_x	Free Markov parameters	/
Γ_u	Forced Markov parameters (controlled)	/
Γ_d	Forced Markov parameters (uncontrolled)	/
G, h	Objective inequality coefficients, bounds	/
K	Optimal Control feedback gain	/
K_∞	Lumped deduced disturbance gain	/
$K_{u,\infty}$	Disturbance gain to the system inputs (subset of K_∞)	pu
$K_{x,\infty}$	Disturbance gain to the system states (subset of K_∞)	/
Δv	Voltage deviation with respect to nominal voltage	pu
W_z	Output space precision penalization	/
$W_{\Delta u}$	Rate of movement penalization	/
$W_{\bar{u}}$	Input reference tracking penalization	/
β	Tuning term: Input reference tracking	/

Table 12.2: Acronyms

AC-OPF	alternating current optimal power flow
ADRC	adaptive disturbance rejection controller
DARE	discrete time algebraic riccati equation
DER	distributed energy resource
DLQR	discrete time linear quadratic regulator
IRC	impulse response coefficients
ISE	integrated squared error
LFC	load frequency control
MG	microgrid
MIMO	multiple–input multiple–output
MISO	multiple–inputs single–output
MPC	model predictive control
OC	optimal control
OPF	optimal power flow
PCC	point of common coupling
RES	renewable energy system
RT	real–time
SDE	stochastic differential equation
Sys-ID	system identification

The plant models are typically nonlinear and can be stated as stochastic differential equations (SDEs) such as formulated for example in [KMJ04]:

$$dx_t = f(x_t, u_t, t, \theta)dt + \sigma(u_t, t, \theta)d\omega_t \tag{12.2a}$$

$$y_k = h(x_k, u_k, t_k, \theta) + v_k \tag{12.2b}$$

where t is the time variable; t_k are sampling instants; x_t is a vector of system states with the main state being the voltage deviations from the nominal voltage levels Δv; u_t is a vector of input variables (reactive power injections); y_k is the single output variable and equals the main state Δv; θ is a vector of parameters; f, σ and h are nonlinear functions; ω_t is a standard Wiener process and v_k is a white noise process with $v_k \in \mathcal{N}(0, S(u_k, t_k, \theta))$. See [KMJ04] for further clarifications and details of this formulation.

Using the notation and formulation given in [MMD18], the reactive power flow in a line (l, m) modeled as symmetrical π –model is given by

$$q_{lm} = -(b_{lm} + b_{sh,lm}/2)v_l^2 + b_{lm}v_l v_m \cos(\theta_l - \theta_m) - g_{lm}v_l v_m \sin(\theta_l - \theta_m) \tag{12.3}$$

The set of model spaces consists of the buses $i \in \mathcal{B}$ and the lines $(l, m) \in \mathcal{L}$. Real and reactive power injections and extractions are denoted p_i and q_i respectively, voltages and phasor angles v_i and θ_i respectively. We may assume that the angle reference for the MG is set at PCC and is therefore $\theta_{\text{ref}} = \theta_{\text{PCC}} = 0°$. See [MMD18] further details upon notation.

The linearized system model may then be represented in relation to a point of linearization as stated below.

$$\frac{dx_{t|j}}{dt} = f_0 + A(x_t - x_j) + B(u_t - u_j) + G(d_t - d_j) + w_t \tag{12.4a}$$

$$y_t = Cx_t + e_t \tag{12.4b}$$

x is the system state; u the controlled system input, d the uncontrolled system input (disturbance). w and e are process and measurement noise respectively. This is a multiple–inputs single–output (MISO) system if more than one unit in the MG are considered.

12.2.3 State Estimation

The residual $\hat{d}$ can be estimated using an augmented Kalman filter following the formulations given in [PR01; PR03]. The augmented system model with integrating input disturbance is

$$A_a = \begin{bmatrix} A & B_d \\ 0 & I \end{bmatrix} \tag{12.5a}$$

$$B_a = \begin{bmatrix} B \\ 0 \end{bmatrix} \tag{12.5b}$$

$$x_a = \begin{bmatrix} x \\ d \end{bmatrix} \tag{12.5c}$$

Using the augmented system equations stated in equation (12.5) on the facing page, the dynamic filter equations consist of the prediction step

$$\hat{x}_{a,k|k-1} = A_a \hat{x}_{a,k-1|k-1} + B_a u_{k-1} \tag{12.6a}$$

$$P_{k|k-1} = A_a P_{k-1|k-2} A_a^T + Q_{k|k} \tag{12.6b}$$

and following update step

$$K_{k+1|k} = P_{k|k-1} C^T (C P_{k|k-1} C^T + R_{k|k-1})^{-1} \tag{12.6c}$$

$$P_{k+1|k} = (I - K_{k+1|k} C) P_{k|k-1} \tag{12.6d}$$

$$\begin{aligned} \hat{x}_{k+1|k} = {} & \hat{x}_{a,k|k-1} + \\ & K_{k+1|k}(y_{m,k|k} - C\hat{x}_{a,k|k-1} - C_d \hat{d}_{r,k|k-1}) \end{aligned} \tag{12.6e}$$

See for example [Joh05; KMJ04].

$y_{m,k}$ is the vector of measured nodal voltage level deviations from the point of linearization. This is the one–step predictor of both estimated state $\hat{x}$ and disturbance residual $\hat{d}$.

12.2.4 Target Adjusted Stationary DLQR

The classical stationary discrete time linear quadratic regulator (DLQR) control law can be stated as

$$u_k^\star = -K\hat{x}_{k|k} \tag{12.7}$$

By offsetting with the target $\underline{p}$ we can derive the target adjusted stationary DLQR as

$$u_k^\star = \underline{u}_{k|k} - K(\hat{x}_{k|k} - \underline{x}_{k|k}) \tag{12.8}$$

The controller gain K for both formulations we find as solution to the discrete time algebraic riccati equation (DARE) [Van81; Lau78], where $\underline{p} = \{\underline{x}\ ,\underline{u}\}$ is a system equilibrium. We model it as linear relationship to the estimated disturbance residual $\hat{d}_r$:

$$\underline{p}_{k|k} = K_\infty \hat{d}_{r,k|k} \tag{12.9}$$

K_∞ hereby is a gain from a unit disturbance to one corresponding system equilibrium point. When $\hat{d}_r$ is based on future information, the controller is enabled to act proactively. Equation 12.9 recovers a system equilibrium corresponding to $\hat{d}_r$.

We can only approximate the inverse of M for the considered system. In consequence, we obtain K_∞ by using a least–squares approximation:

$$\overbrace{\begin{bmatrix} A-I & B \\ C & 0 \end{bmatrix}}^{M} \overbrace{\begin{bmatrix} K_{x,\infty} \\ K_{u,\infty} \end{bmatrix}}^{K_\infty} = \begin{bmatrix} B_d \\ 0 \end{bmatrix} \tag{12.10}$$

This approach is outlined in [MR93; PR03] and related methods have been applied e.g. in [Huu+10]. Notice that the system of equations stated in Equation 12.10 has to be solved once for each model formulation in order to recover the corresponding gain K_∞. B_d here denotes the modeled residual disturbance dynamics. These dynamics are unknown and have to be approximated. Mismatch of B_d related to the plant dynamics degrade the controller performance. This loss of performance is then to be compensated for by application of appropriate robustness and adaptive control strategies which are not subject of this paper.

See [Ban+19] for a corresponding formulation in the context of LFC.

For the stationary DLQR denoted in Equation 12.7, feedback of the estimated output residual ϵ_y can lead to offset free control:

$$u_k^\star = -K\hat{x}_{k|k} - \epsilon_{y,k|k} \tag{12.11}$$

$$\epsilon_{y,k+1|k} = \epsilon_{y,k|k-1} + \hat{y}_{k+1|k} - \bar{y}_k \tag{12.12}$$

$\bar{y}$ is hereby the output reference (reference nodal voltage deviations) and $\hat{y}$ is the estimated one–step output prediction (estimated one–step nodal voltage deviations). In the simplest case, $\bar{y}$ resembles a vector of zeroes, given that the controller shall drive nodal voltage deviations towards their values at point of linearization of the underlying system. The feedback of the output residual as outlined above is a simple compensation for the stationary output tracking offset. It can reduce closed–loop stability and increase sensitivity to model–plant errors. For the chosen exemplary system model described in Section 12.3, this is the case. Consequently, Equation 12.11 remains unused for the stationary DLQR. For the target adjusted stationary DLQR, no further adjustments are included and offset free control is achieved.

12.2.5 Classical MPC

The classical quadratic input–output reference tracking objective can be stated as such:

$$
\begin{aligned}
\min_{u,\,k} J_0 = {} & ||\Phi_x \hat{x}_{k|k} + \Gamma_u u_k + \Gamma_d \hat{d}_{k|k} - \underline{y}_k||^2_{W_z} \\
& + \beta ||u_k||^2_{W_{\Delta u}} \\
& + (1-\beta)||u_k - \bar{u}_{k|k}||^2_{W_{\bar{u}}}
\end{aligned} \tag{12.13}
$$

Φ_x, Γ_u and Γ_d are impulse response coefficients (IRC) of the linearized system model. Φ_x are IRC with respect to the states, Γ_u are IRC with respect to the inputs and Γ_d are IRC with respect to the disturbances.

If no output residual error feedback is used, $\underline{y} = \bar{y}$. For reduced offset for the predictive controller stated in 12.13, Equation 12.12 in the simplest implementation is used over the whole prediction horizon. If the reference $\bar{y}$ changes throughout the prediction horizon, a dynamic variation of $\bar{y}$ can be used within 12.12.

β denotes a tuning term used to switch the controller from regulatory action without input reference tracking to regulatory action with input reference tracking.

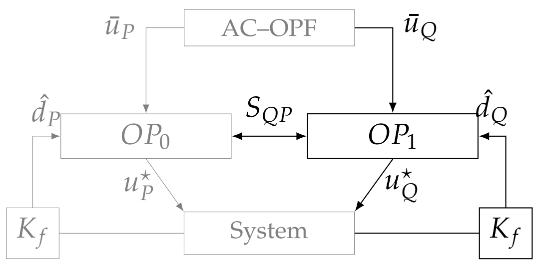

Figure 12.1: Minimal exemplary aggregated operational control scheme consisting of an upper layer with a precise system model — here represented in form of an AC–OPF — and lower layer maintaining system stability and achievemnt towards RT control objectives. Voltage controls OP_1 receive control input references $\bar{u}_Q$ and pass the modified solution $u_Q^\star$ to the system controls.

12.2.6 Target Adjusted MPC

The target adjusted approach discussed in Section 12.2.4 can be applied in the MPC framework using

$$
\begin{aligned}
\min_{u,\,k} J_1 \quad & ||\Phi_x(\hat{x}_{k|k} - \underline{x}_{k|k}) + \Gamma_u(u_k - \underline{u}_{k|k}) - \bar{y}_k||^2_{W_z} \\
& + \beta ||u_k - u^\star_{k-1}||^2_{W_{\Delta u}} \\
& + (1-\beta)||u_k - \bar{u}_{k|k}||^2_{W_{\bar{u}}}
\end{aligned} \tag{12.14}
$$

Again β is used to switch the controller from regulatory behavior without input reference tracking to regulatory behavior with input reference tracking. A similar regulator implementation in the LFC context can be found in [Ban+19].

We can achieve offset free control for the target adjusted MPC Equation 12.14 via adjustment of the control target $\underline{p}$:

$$\underline{p}_{\epsilon} = K_{\infty}\hat{d}_{\epsilon,k|k} \tag{12.15}$$

where

$$\hat{d}_{\epsilon,k|k} = \hat{d}_{k|k} + \epsilon_{y,k|k} \tag{12.16}$$

$\underline{p}_{\epsilon}$ is hereby the adjusted control target. Alternatively, the objective 12.14 can be augmented with the output residual error as stated in 12.12.

12.2.7 Constraints

Hard input constraints and ramp–rate constraints for both MPCs can be stated as

$$u_{\min,k} \leq u_k \leq u_{\max,k} \tag{12.17}$$
$$\Delta u_{\min,k} \leq \Delta u_k \leq \Delta u_{\max,k} \tag{12.18}$$
$$G_k\, u_k \leq h_k \tag{12.19}$$

12.3 NUMERICAL RESULTS

Consider the test system presented in Figure 12.2.

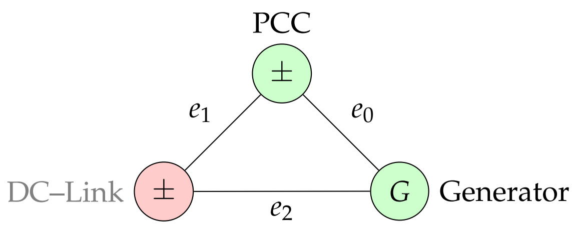

Figure 12.2: Considered test–network. Actors PCC and Generator, disturbance DC–link. The edge e_2 is identified as critical edge within the network in terms of controller stability.

It consists of two actors $\{G, \text{ PCC}\}$ and one disturbance $\{\text{DC–link}\}$.

The edge e_2 is identified as critical edge within the network in terms of controller stability. Linearized dynamics of the actors and disturbance are considered as

$$G = \frac{s + 17.01}{s^2 + 10.7s + 3.135} \tag{12.20a}$$

$$\mathrm{PCC} = \frac{1}{6s + 1} \tag{12.20b}$$

$$\text{DC–link} = \frac{1}{6s + 1} \tag{12.20c}$$

Actors and disturbance connect to the grid via nodes n_i. Edges e_j connect these nodes. Node and edge groups expose the group–specific linearized dynamics given by

$$n_i = \frac{1}{s + 1} \tag{12.21a}$$

$$e_j = \frac{1}{\tau_{ej} + 1} \qquad \mid \tau_{eJ} = 2s \tag{12.21b}$$

The system consisting of actors, disturbance, nodes and edges is discretized using zero–order hold approximation with sampling rate of 2 seconds.

This test–system should provide qualitative insights for a three node test system, quantitative results depend on the specific system parameterization.

For the disturbance, two disturbance sequences are used as input throughout this paper, a sequence `d0` with noise and a sequence `d1` without noise, see Figure 12.3 below. Noise in `d0` remains hereby constant throughout all simulations. For proactive action and predictions of the controllers, the disturbance sequence reveals N steps ahead of time.

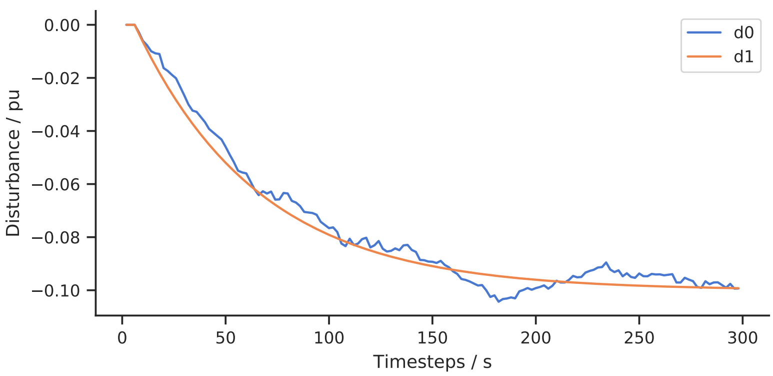

Figure 12.3: Disturbance trajectory used in the following simulations.

A prediction horizon of $N = 10$ is used. The static gain K is obtained by solution to DARE parameterized with $R_c = 0.05$. All units are initialized as resting at the point of linearization without initial excitation. The state observer is initialized with augmented state associated uncertainty $P = \frac{1}{1e^{-5}}$ and DARE parameterized with $R_o = 0.05$. The DARE is solved using the algorithm outlined in [Van81] and implemented in [JOP+01].

Diagonal elements $w_z = 1.0$, $w_{\bar{u}} = 0.1$, $w_{\Delta u} = 0.05$ are chosen for the penalization matrices W_z, $W_{\bar{u}}$, $W_{\Delta u}$. The input disturbance model dynamics are chosen as $\tau_{\text{dist}} = 1.0$.

The controllers listed in Table 12.3 are considered throughout this section. The optimal controllers `OC1`, `OC2` are considered with and without proactive action. All listed MPCs are considered with and without the inclusion of predictive action. Perfect knowledge is assumed in both cases for the disturbance predictions. All MPCs are considered without active constraints.

Table 12.3: Examined control laws and objective functions.

Controller label	Control law equation / objective function	Error compensation
`OC0`	Classical stationary DLQR 12.7	-
`OC1`	Target adjusted DLQR 12.8	-
`OC2`	Target adjusted DLQR 12.8	12.11
`MPC0`	Classical MPC 12.13	12.12
`MPC1`	Target adjusted MPC 12.14	12.15
`MPC2`	Target adjusted MPC 12.14	12.12

12.3.1 Comparison of Optimal Controllers

We compare three OCs, two of which without and with proactive action:

- `OC0`: Classical implementation, no output residual feedback
- `OC1`: Target adjusted implementation (non–proactive / proactive), no output residual feedback
- `OC2`: Target adjusted implementation (non–proactive / proactive), output residual feedback via control target

In Figure 12.4, the summed nodal ISE is depicted over the simulation samples. Accumulated summed nodal ISE at the end of the simulation period is depicted with bar charts at the bottom. Notice that we consider here the summed ISE over all three nodes, as described in Section 12.2.1. `OC0` achieves the worst ISE. `OC1` performs notably better. The best ISE in this simulation is achieved by `OC2`. Proactive capabilities does not improve the performance.

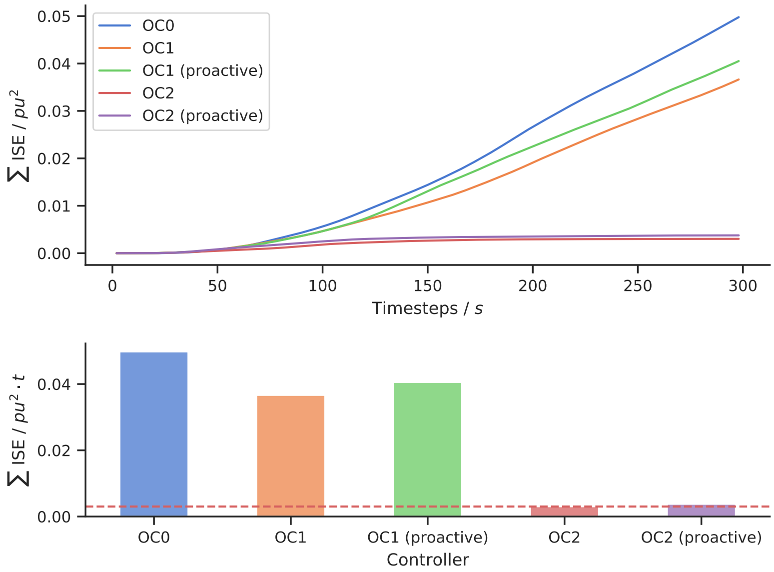

Figure 12.4: OC comparison: ISE of aggregated outputs and aggregated system controls.

12.3.2 Comparison of Model Predictive Controllers

Three MPCs are compared:

- `MPC0`: Classical implementation, output residual feedback via output control goal adjustment
- `MPC1`: Target adjusted MPC, output residual feedback via control target
- `MPC2`: Target adjusted MPC, output residual feedback via output control goal adjustment

In Figure 12.5, the experiment illustrated in Figure 12.4 of the previous Section 12.3.1 is repeated with the listed MPCs. Again, the summed nodal ISE is shown, as well as the accumulated ISE at the end of the simulation period.

`MPC0` performs best both without and with predictions.

12.3.3 Parametric System Model Mismatch

We examine the Model–Plant dynamics mismatch, errors ϵ_A, ϵ_B and ϵ_{B_d} are hereby factors applied to the model. That is, the first two errors render the model slower than the actual plant, owing to that the opposite examination leads to instability.

`OC0` and `OC1` expose offset when facing parametric model mismatch, see Figure 12.6. Sensitivity to mismatch in both free system dynamics

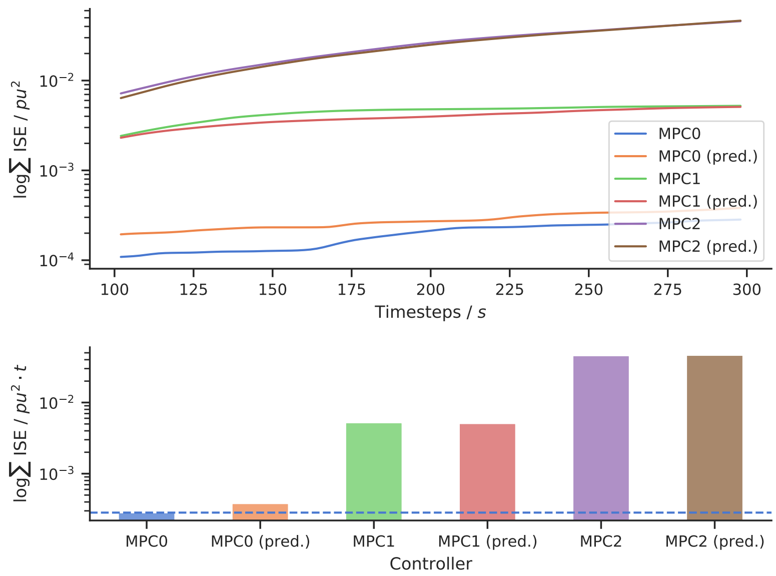

Figure 12.5: MPC comparison: ISE of aggregated outputs and aggregated system controls. For longer simulation durations, `MPC0 (pred.)` outperforms its non–predictive counterpart `MPC0`.

A and forced system dynamics B is more pronounced for the classical stationary DLQR `OC0`. Only two distinct convergence points are observed for mismatch in the lumped disturbance dynamics B_d for these controllers. `OC2` is robust regarding the examined mismatches in terms of offset. Response characteristics however degrade strongest for mismatch in B_d for this controller.

The classical MPC `MPC0` exposes minor offset for all simulations depicted in Figure 12.3.3. `MPC1` converges towards zero–offset with slightly damped response characteristics with increasing mismatch in A. This controller drives the summed voltage excursions to zero robustly in all experiments. `MPC2` exhibits performance degradation for both mismatches ϵ_A and ϵ_B. Steady state sensitivity regarding mismatch in the lumped disturbance dynamics B_d remains small for `MPC0` and `MPC1`. Controller responses become faster when model–internal dynamics $B_{d,m}$ are faster than plant–internal dynamics $B_{d,p}$. For errors ϵ_{B_d}, sensitivity is the least for `MPC2` in comparison to the two other controllers.

The considered multiplicative errors ϵ_A, ϵ_B and ϵ_{B_d} are only one class of model–plant mismatch, the parametric mismatch. Given that an uncertainty measure is estimated alongside the derived model, this measure can be used to narrow ϵ_A, ϵ_B and ϵ_{B_d} down to probabilistic intervals. This knowledge enables informed decisions regarding which controller to choose given the current operating regime.

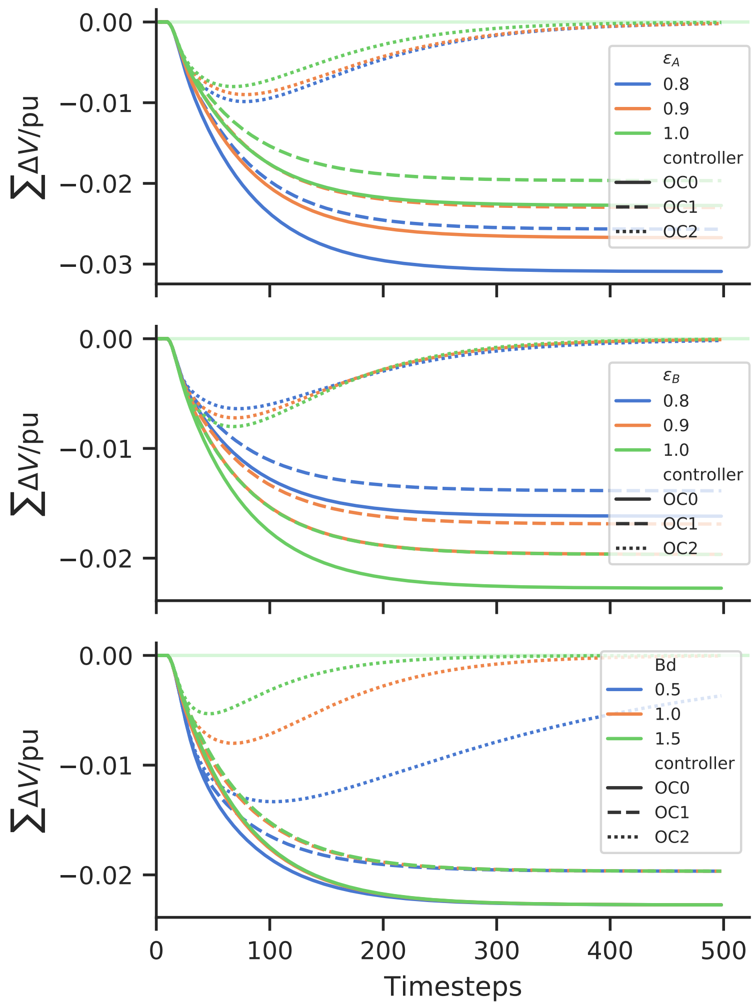

Figure 12.6: Comparison of the performance of the considered OCs for multiplicative parametric mismatches of the free system response coefficients A (ϵ_A), forced system response coefficients B (ϵ_B) and lumped filter disturbance response coefficients B_d (ϵ_{B_d}).

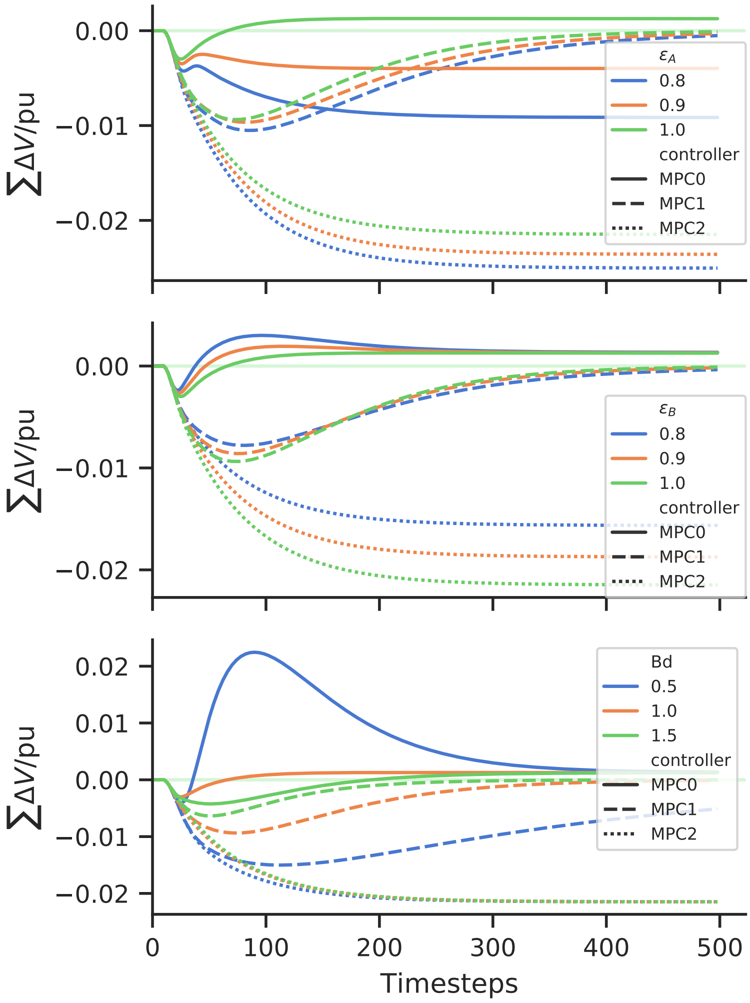

Figure 12.7: Comparison of the performance of the considered MPCs for multiplicative parametric mismatches of the free system response coefficients A (ϵ_A), forced system response coefficients B (ϵ_B) and lumped filter disturbance response coefficients B_d (ϵ_{B_d}).

12.3.4 Robustness

In Figure 12.8 and Figure 12.9, the numerator dynamics parameter τ_{e2} of the critical edge e2 is altered from the nominal value of $\tau_{e2} = 2s$, see Equation 12.21b, to values of $\{1.5, 1.07, 0.630.2\}s$. This leads to instability of OC2 and MPC1 for $\tau_{e2} = 0.2s$ and $\tau_{e2} = 0.63s$, that is, when τ_{e2} is faster than the real edge. MPC2 exposes offset. The other controllers remain stable for the chosen range of numerator dynamics τ_{e2}.

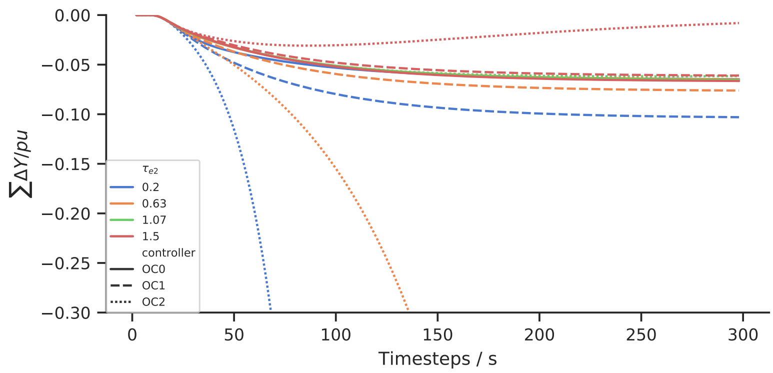

Figure 12.8: Instability issues with controller OC2.

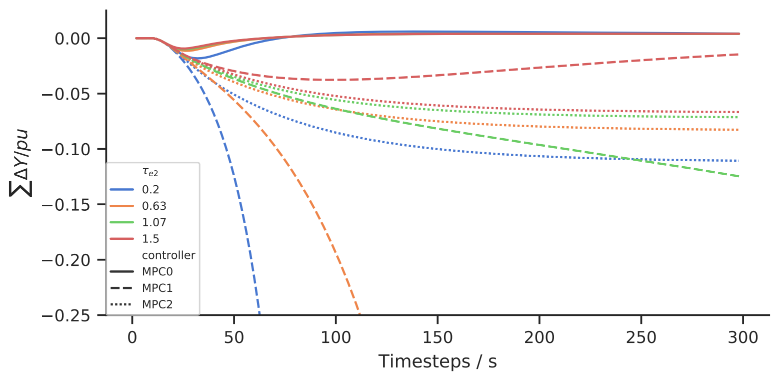

Figure 12.9: Instability issues with controller MPC1.

12.4 DISCUSSION

The control decisions of both OCs and MPCs depend on the quality of the available model. The compared controllers expose different properties, such as robustness and control performance evaluated in terms of ISE.

Different means of incorporating output residual feedback do exist. However, this implementation does reduce robustness towards critical dynamics. An improvement to this issue is to establish the mapping from output space to disturbance space.

The target adjusted OC formulations `OC1` and `OC2` perform better on the chosen problem in terms of ISE and stationary offset resulting from balanced parametric model–plant mismatch. `OC2` performs best in this comparison. However, performance of these controllers degrades stronger, including instability issues, when the critical edge in the chosen model exposes faster dynamics than in the initially chosen set of system parameterizations. Proactive action with the target adjusted controllers does not offer a benefit in terms of ISE. The target adjusted MPC formulation `MPC2` performs worse in terms of ISE compared to the classical implementation `MPC1`, while exposing non–ideal response characteristics. Performance of `MPC2` furthermore degrades stronger when facing balanced parametric model–plant mismatch.

12.5 CONCLUSIONS

We examine three optimal controllers (OCs) and three model predictive controllers (MPCs) when applied to a voltage level control problem. Two controllers of each category are stated as target adjusted controllers, which are then compared to the classical implementations for the chosen control problem. The latter is given as aggregated system model with interleaved dynamics.

The examined system model is chosen arbitrarily and partly based on system identification (Sys-ID) experiments. For real applications and more useful results, we should examine system models approximated at multiple operating and linearization points for the examined system. The considered target adjusted OCs and MPCs do offer alternative solution approaches to the control problem. While the target adjusted OCs enables for the inclusion of proactive action, this does not offer a performance benefit in the considered scenario. One target adjusted OC formulation outperforms the classical implementation in terms of ISE. The target adjusted MPCs perform worse than the classical MPCs implementation.. The MPCs facilitate integration into existing control hierarchy concepts by enabling input reference tracking. They can consequently be readily applied in test facilities.

REFERENCES

[Kun94] Kundur. *Power System Stability And Control*. en. The Epri Power System Engineering. India: McGraw-Hill, 1994. ISBN: 978-0-07-063515-9.

[HP14] Jahangir Hossain and Hemanshu Roy Pota. „Power System Voltage Stability and Models of Devices." In: *Ro-*

bust Control for Grid Voltage Stability: High Penetration of Renewable Energy. Singapore: Springer Singapore, 2014, pp. 19–59. ISBN: 978-981-287-115-2 978-981-287-116-9. DOI: 10.1007/978-981-287-116-9_2. URL: http://link.springer.com/10.1007/978-981-287-116-9_2 (visited on 09/18/2017).

[LD14] Ling Luo and Sairaj V. Dhople. „Spatiotemporal Model Reduction of Inverter-Based Islanded Microgrids." In: *IEEE Transactions on Energy Conversion* 29.4 (Dec. 2014), pp. 823–832. ISSN: 1558-0059. DOI: 10.1109/TEC.2014.2348716.

[Bev14] Hassan Bevrani. *Robust Power System Frequency Control*. Power Electronics and Power Systems. Cham: Springer International Publishing, 2014. ISBN: 978-3-319-07277-7 978-3-319-07278-4. DOI: 10.1007/978-3-319-07278-4. URL: http://link.springer.com/10.1007/978-3-319-07278-4 (visited on 09/27/2017).

[Sch78] F. C. Schweppe. „Power Systems '2000': Hierarchical Control Strategies." In: *IEEE Spectrum* 15.7 (July 1978), pp. 42–47. ISSN: 0018-9235. DOI: 10.1109/MSPEC.1978.6367813.

[MC] Omid Alizadeh Mousavi and Rachid Cherkaoui. *1 Literature Survey on Fundamental Issues of Voltage and Reactive Power Control Literature Survey*.

[Mol+17] Daniel K. Molzahn et al. „A Survey of Distributed Optimization and Control Algorithms for Electric Power Systems." en. In: *IEEE Transactions on Smart Grid* 8.6 (Nov. 2017), pp. 2941–2962. ISSN: 1949-3053, 1949-3061. DOI: 10.1109/TSG.2017.2720471. URL: http://ieeexplore.ieee.org/document/7990560/ (visited on 03/05/2020).

[Sch+16] Johannes Schiffer et al. „Voltage Stability and Reactive Power Sharing in Inverter-Based Microgrids With Consensus-Based Distributed Voltage Control." en. In: *IEEE Transactions on Control Systems Technology* 24.1 (Jan. 2016), pp. 96–109. ISSN: 1063-6536, 1558-0865. DOI: 10.1109/TCST.2015.2420622. URL: http://ieeexplore.ieee.org/document/7097655/ (visited on 03/05/2020).

[Fau+18] Timm Faulwasser et al. „Optimal Power Flow: An Introduction to Predictive, Distributed and Stochastic Control Challenges." en. In: *at - Automatisierungstechnik* 66.7 (July 2018), pp. 573–589. ISSN: 2196-677X, 0178-2312. DOI: 10.1515/auto-2018-0040. arXiv: 1811.01163. URL: http://arxiv.org/abs/1811.01163 (visited on 11/05/2019).

[VC13] G. Valverde and T. Van Cutsem. „Model Predictive Control of Voltages in Active Distribution Networks.“ In: *IEEE Transactions on Smart Grid* 4.4 (Dec. 2013), pp. 2152–2161. ISSN: 1949-3053. DOI: 10.1109/TSG.2013.2246199.

[MMD18] S. Misra, D. K. Molzahn, and K. Dvijotham. „Optimal Adaptive Linearizations of the AC Power Flow Equations.“ In: *2018 Power Systems Computation Conference (PSCC)*. June 2018, pp. 1–7. DOI: 10.23919/PSCC.2018.8442547.

[Lek+18] S. Leksawat et al. „Decoupled Voltage Sensitivity Analysis for Decentralized Smart Grid Operation.“ In: *2018 International Symposium on Power Electronics, Electrical Drives, Automation and Motion (SPEEDAM)*. June 2018, pp. 1184–1189. DOI: 10.1109/SPEEDAM.2018.8445216.

[Joh+18] J. Johnson et al. „Distribution Voltage Regulation Using Extremum Seeking Control With Power Hardware-in-the-Loop.“ In: *IEEE Journal of Photovoltaics* 8.6 (Nov. 2018), pp. 1824–1832. ISSN: 2156-3381. DOI: 10.1109/JPHOTOV.2018.2869758.

[BPK16] Steven L. Brunton, Joshua L. Proctor, and J. Nathan Kutz. „Sparse Identification of Nonlinear Dynamics with Control (SINDYc).“ In: *arXiv:1605.06682 [math]* (May 2016). arXiv: 1605.06682 [math]. URL: http://arxiv.org/abs/1605.06682 (visited on 05/24/2019).

[Ngu17] Nhan T. Nguyen. *Model-Reference Adaptive Control*. en. New York, NY: Springer Berlin Heidelberg, 2017. ISBN: 978-3-319-56392-3.

[Don18] Lili Dong. „Active Disturbance Rejection Based Load Frequency Control and Voltage Regulation in Power Systems.“ In: *Control Theory and Technology* 16.4 (2018), pp. 336–350. ISSN: 20956983. DOI: 10.1007/s11768-018-8112-3.

[VBV06] D. Villacci, G. Bontempi, and A. Vaccaro. „An Adaptive Local Learning-Based Methodology for Voltage Regulation in Distribution Networks With Dispersed Generation.“ en. In: *IEEE Transactions on Power Systems* 21.3 (Aug. 2006), pp. 1131–1140. ISSN: 0885-8950. DOI: 10.1109/TPWRS.2006.876691. URL: http://ieeexplore.ieee.org/document/1664947/ (visited on 09/21/2019).

[Ban+19] Frederik Banis et al. „Load Frequency Control in Microgrids Using Target Adjusted Model Predictive Control.“ English. In: *IET Renewable Power Generation* (2019). ISSN: 17521424 and 17521416. DOI: 10.1049/iet-rpg.2019.0487.

[Nel01] Oliver Nelles. *Nonlinear System Identification*. en. Berlin, Heidelberg: Springer Berlin Heidelberg, 2001. ISBN: 978-3-642-08674-8 978-3-662-04323-3. DOI: 10.1007/978-3-662-04323-3. URL: http://link.springer.com/10.1007/978-3-662-04323-3 (visited on 03/06/2020).

[Lju99] L. Ljung. *System Identification: Theory for the User*. Prentice Hall Information and System Sciences Series. Prentice Hall PTR, 1999. ISBN: 978-0-13-656695-3. URL: https://books.google.dk/books?id=nHFoQgAACAAJ.

[KMJ04] Niels Rode Kristensen, Henrik Madsen, and Sten Bay Jørgensen. „Parameter Estimation in Stochastic Grey-Box Models." en. In: *Automatica* 40.2 (Feb. 2004), pp. 225–237. ISSN: 00051098. DOI: 10.1016/j.automatica.2003.10.001. URL: https://linkinghub.elsevier.com/retrieve/pii/S000510980300298X (visited on 08/06/2019).

[PR01] Gabriele Pannocchia and James B. Rawlings. *Robustness of MPC and Disturbance Models for Multivariable Ill-Conditioned Processes*. English. Tech. rep. 2001-02. USA: TWMCC, Texas-Wisconsin Modeling and Control Consortium, 2001.

[PR03] Gabriele Pannocchia and James B. Rawlings. „Disturbance Models for Offset-Free Model-Predictive Control." In: *AIChE journal* 49.2 (2003), pp. 426–437.

[Joh05] John Bagterp Jorgensen. „Efficient Numerical Implementation of the Continuous-Discrete Extended Kalman Filter." In: (Aug. 2005). URL: https://cn.inside.dtu.dk/cnnet/filesharing/SADownload.aspx?FileId=4620177%5C&FolderId=1089171%5C&ElementId=552305 (visited on 11/16/2017).

[Van81] P. Van Dooren. „A Generalized Eigenvalue Approach for Solving Riccati Equations." In: *SIAM Journal on Scientific and Statistical Computing* 2.2 (June 1981), pp. 121–135. ISSN: 0196-5204. DOI: 10.1137/0902010. URL: http://epubs.siam.org/doi/abs/10.1137/0902010 (visited on 07/26/2019).

[Lau78] Alan J. Laub. *A Schur Method for Solving Algebraic Riccati Equations*. eng. Tech. rep. USA: Massachusetts Institute of Technology, Laboratory for Information and Decision Systems, 1978, pp. 44–46. URL: https://dspace.mit.edu/handle/1721.1/1301 (visited on 07/26/2019).

[MR93] Kenneth R. Muske and James B. Rawlings. „Model Predictive Control with Linear Models." en. In: *AIChE Journal* 39.2 (1993), pp. 262–287. ISSN: 1547-5905. DOI: 10.1002/aic.690390208. URL: http://aiche.onlinelibrary.

wiley.com/doi/abs/10.1002/aic.690390208 (visited on 07/30/2019).

[Huu+10] J. K. Huusom et al. „Tuning of Methods for Offset Free MPC Based on ARX Model Representations.“ In: *Proceedings of the 2010 American Control Conference*. USA, June 2010, pp. 2355–2360. DOI: 10.1109/ACC.2010.5530560.

[JOP+01] Eric Jones, Travis Oliphant, Pearu Peterson, et al. „SciPy: Open Source Scientific Tools for Python.“ In: (2001). [Online; accessed ¡today¿]. URL: http://www.scipy.org/.

Part III

APPENDIX

This appendix contains an overview over software and tools used throughout this Ph.D. and furthermore, an overview over the *uGRIP* project.

12.6 THE UGRIP PROJECT

From the first annual uGRIP project status report (The uGRIP team):

"This project aims to develop a full-scale microgrid that consists of distributed generators, both renewable and controllable, storage units and flexible loads at FER-UNIZG laboratory. A structure of the local, distribution–level market will be defined and demonstrated within the project. The complex interactions among the microgrid, distribution network, transmission network, wholesale electricity market and local distribution market will be investigated and viable operation mechanism will be proposed." [ERA15].

Table 12.4: Project partners within the uGRIP project.

Participating organizations	Name of organizations	Country
Lead partner	University of Zagreb Faculty of Electrical Engineering and Computing – FER-UNIZG	Croatia
Project partner	Technical University of Denmark - DTU	Denmark
Project partner	Institute for Information Technology - OFFIS	Germany
Associate partner	KONCAR Power Plant and Electric Traction Engineering Inc. – KONCAR-KET	Croatia
Associate partner	Croatian Power Utility – HEP Inc.	Croatia

"The growing share of intermittent and partly predictable renewable energy system (RES) requires a more flexible operation of the power system. Flexibility is a key to maximize the utilization of RES, while minimizing the negative impact of their associated variability and uncertainty." [ERA15]

In addition to this disruptive trend, we can observe other developments leading to increasing requirements on electricity grids. An example is the electrification of the mobility sector. These trends add up to a need for adapting how we distribute and transform electric energy. See for example [Mei+13; Eur12].

In this regard:

"An effective way of increasing system flexibility is the integration of price-responsive microgrids." [ERA15]

and:

"A [. . .] microgrid may perform arbitrage, provide flexibility thus increasing the utilization of RES, take part in corrective actions, provide voltage support, and defer investments in power lines and (distributed) generation." [ERA15]

The research goals of the uGrip project are:

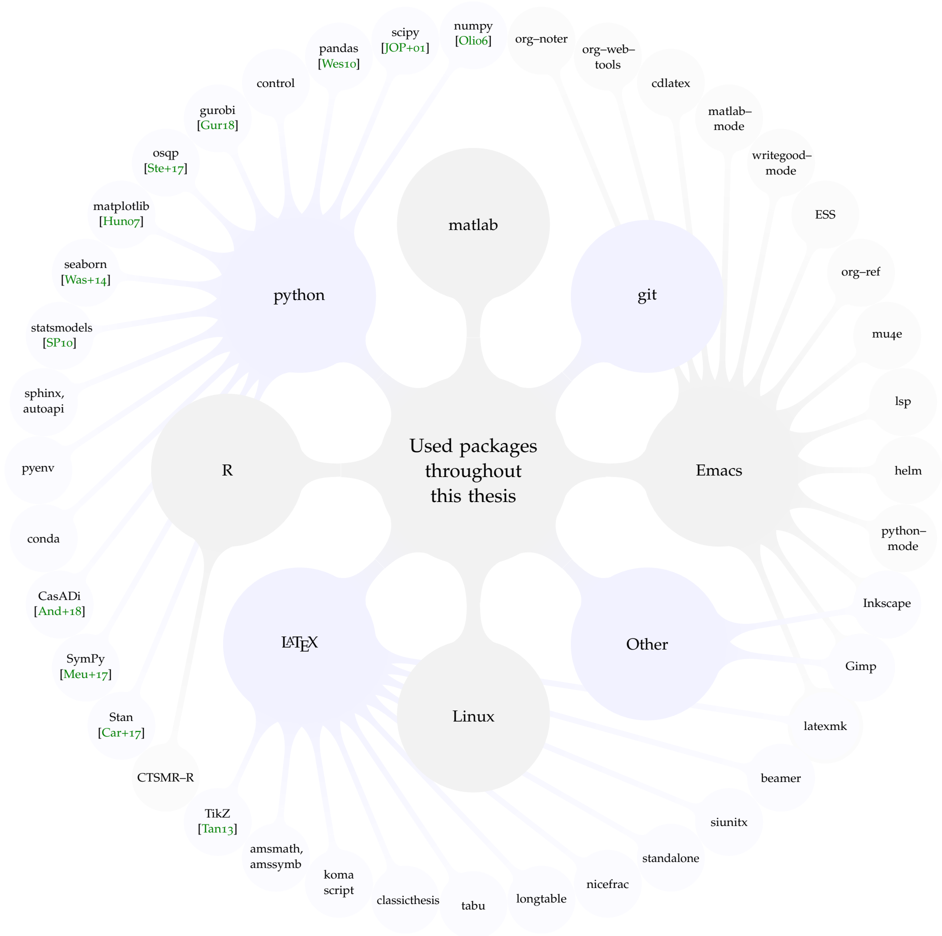

Figure 12.10: Software and tools used throughout this Ph.D.

- Assessment of microgrid business cases for different countries, e. g. Croatia, based on their grid codes and incentive policies
- Development of a robust framework that optimizes the scheduling process of a microgrid while actively participating in electricity markets
- Development and definition of standardized communication protocols used between microgrid elements
- Development of a microgrid at the FER-UNZIG laboratory
- Design and development of a local market to manage the microgrid at the FER-UNZIG laboratory
- Developing and executing simulation scenarios integrating the available hardware components (microgrid elements) and software models with the co-simulation framework MOSAIK

Source: Presentation of the uGRIP project at the ERA-NET Smart Energy Systems Meeting, Fraunhofer IFF, Magdeburg (Germany). September 2018.

12.7 FER-UNIZG LABORATORY

The microgrid (MG) test system considered within the *uGRIP* project consists of an alternating current (AC)–side and a direct current (DC)–side. Within the AC–side, the following components have been available throughout the case studies:

POINT OF COMMON COUPLING The laboratory AC–side can be operated in islanded modes (IMs) or grid-connected modes (GCMs) mode. For the latter, the MG internal frequency is synchronized to the main grid's frequency.

HYDRAULIC POWER PLANT This is a small–scale Pelton turbine, driven by hydraulic pressure established by a pump. This unit acts as prime–mover within the system. See also [BP18] and Table 12.5.

Within the DC–side, the following components have been available:

CONTROLLABLE LOADS enable simulating consumers at the DC–side.

CONTROLLABLE ACCUMULATORS enable simulating both consumption and production at the DC–side.

SOLAR PANELS at the building roof.

Throughout experiments, focus has been the hydraulic power plant as main MG actor. By means of Sys-ID, we derived models used in MPCs. In context of the project, project partners at FER–UNIZG derived an MPC for the hydraulic power plant [BP18], whereas DTU focused on aggregated system model predictive control (MPC).

An important consideration for case studies was the combination of software products: interfacing and orchestration of supervisory control and data acquisition (SCADA), NEPLAN, Python, general algebraic modeling system (GAMS) and other libraries was required. The co–simulation library MOSAIK [SSS12] has been used as to this end. Throughout the project, project partner *OFFIS* developed interfaces for the listed software products.

Table 12.5: Laboratory hydro power plant: Specifications (with curtesy of FER–UNIZG Smart Grids laboratory).

Turbine type	Pelton
Number of units	1
Sn	20 kVA
Un	380 V
Rated power factor	0.5
Rated speed	1000 RPM
Synchronous reactance	0.8 p.u.
Transient reactance	0.093 p.u.
Subtransient reactance	0.093 p.u.
Negative sequence reactance	0.13 p.u.
Zero sequence reactance	0.04 p.u.
Penstock length	3 m
Penstock diameter	0.15 m

Co-simulation

An MG consists of subsystems. Sub–systems require inputs and provide outputs at heterogeneous sampling rates, using potentially incompatible communication standards. Consequently, a challenge in such coupled system's simulation is to establish a level of integration that enables the testing of operational scenarios. A co–simulation setup, therefore, established missing links in–between subsystem enabling for simulation of the coupled and integrated system.